



**SAPIENZA**  
UNIVERSITÀ DI ROMA

# New methodological and modeling approaches for the environmental monitoring through the Nitrogen isotopic signatures of algal primary producers

**Department of Environmental Biology**  
**XXXII° Doctoral Program in Environmental and Evolutionary Biology**  
**Curriculum: Ecological Sciences**

**Federico Fiorentino**  
**1235513**

Tutor  
Prof.ssa Maria Letizia Costantini

A.A. 2019-2020



## Table of Contents

### Abstract

<b>Introduction</b> .....	<b>1</b>
---------------------------	----------

<b>Chapter 1:</b> Epilithon $\delta^{15}\text{N}$ signatures indicate the origins of nitrogen loading and its seasonal dynamics in a volcanic lake (published in Ecological Indicators).....	<b>8</b>
--	----------

<b>Chapter 2:</b> Lake water quality for human use and tourism in central Italy (Rome) (published in WIT Transactions in Ecology and the Environment) .....	<b>18</b>
---	-----------

<b>Chapter 3:</b> Nitrogen and metal pollution in the Southern Caspian Sea: a multiple approach to biomonitoring (Submitted to Environmental Science and Pollution Research). .....	<b>27</b>
---	-----------

<b>Chapter 4:</b> Isotopic biomonitoring of N pollution in rivers embedded in complex human landscapes (published in Science of the Total Environment). .....	<b>56</b>
---	-----------

<b>Chapter 5:</b> New analytical protocol for the classification of nitrogen inputs in lakes based on epilithic $\delta^{15}\text{N}$ indicator (submitted to Ecological Indicators). .....	<b>66</b>
---	-----------

<b>Discussion</b> .....	<b>116</b>
-------------------------	------------

<b>References</b> .....	<b>119</b>
-------------------------	------------

## **Abstract**

Aquatic ecosystems represent unreplaceable sources of ecosystem services. On the other hand, the exploitation of water resources and the influx of human activity-related pollutants in the water bodies undermine the structure and function of these ecosystems, until the inability of all their use. Despite the efforts in environmental monitoring and inputs management, around the 28% of the European water bodies is nowadays affected by nutrient pollution. Among the anthropic nutrient inputs, Nitrogen loadings are spreading with human-related loads. The expected increase of climate change can exacerbate the negative effects of these inputs on the aquatic environment. Unfortunately, the environmental monitoring of the anthropic Nitrogen inputs is constrained by three main factors: the dilution process in the aquatic medium, the assimilation by different compartments and the identifiability of their organic/inorganic origins. To overcome all the previously cited constraints, the Nitrogen isotopic signature of macroalgae and epilithic association is nowadays widely used. Firstly, the Nitrogen signature of a macroalgal/epilithic sample is the result of the assimilation process of Nitrogen from the surrounding water, solving both assimilation and dilution issues. Lastly, the value of the macroalgal/epilithic Nitrogen signature is highly dependent by the origin of the uptaken Nitrogen, solving the third issue. However, while for marine ecosystems a wide scientific Nitrogen isotopic signature literature is available, for freshwater and land locked ecosystems there is a large lack of information about method applicability for the environmental monitoring. This dissertation investigates the changes of the epilithic association and macroalgal Nitrogen signatures to different Nitrogen inputs affecting, three rivers (Itri, Capodacqua Santa Croce and Garigliano) and one lake (Lake Bracciano), in Central Italy, and the Iranian Caspian Sea littoral zones. The results confirm the applicability of the method in land locked and fluvial ecosystems regardless the several differences between the aquatic ecosystems considered. Both epilithic association and macroalgal Nitrogen signatures discriminate the origin of the various Nitrogen inputs, changing according to the spatial and temporal variability of the anthropic activities, and provide a robust determination of four well separated Nitrogen impact classes.

## Introduction

Water is a key factor for all the life forms, and for human beings, is also fundamental for the development and flourishing of their various activities, from the primary sector to the tertiary sector (Hadwen et al., 2005; Pimentel et al., 2004). By exploiting the water resource ecosystem services, humanity benefits. On the other hand, the exploitation of such services exposes the aquatic environment to potential discharges of various form of pollutants, threatening this key factor (Vörösmarty et al., 2010). The decrease of the water quality because of the lack of or poor human management policies, is both detrimental for the aquatic community and for the human health and interest (Xu et al., 2010). In the worst-case scenario, pollution can lead to the complete disruption of the ecosystem structure and functioning and to the inability of all human-related water uses with consequent adverse effects.

The excess of human-derived nutrients, or cultural eutrophication, is a form of pollution (Bhagowati et al., 2019; Le Moal et al., 2019) tightly related with the intensification of the agricultural and industrial activities as well as the urban development (Maberly et al., 2002; Paerl et al., 2014). Phosphorus has been one of the first macronutrient monitored, due to its involvement, when no more limiting, in the increase of the primary productivity in freshwater ecosystems (Dodds and Smith, 2016). However, several studies highlighted the role of another macronutrient, Nitrogen, in limiting and/or co-limiting the algal blooms both in freshwater and marine ecosystems (Paerl et al., 2016; Yao et al., 2018).

Biological reactive Nitrogen derived by natural process is estimated to range between  $300 - 500 \text{ Tg (N) * year}^{-1}$ . Since 2000, Nitrogen derived by industrial fixation, mainly for agriculture (Smith 2003), was estimated to be  $\approx 165 \text{ Tg (N) * year}^{-1}$ , accounting for  $\approx 33-55\%$  of the Nitrogen global increase (Howart, 2008). According to Glibert (2017 and literature cited), around  $60 \text{ Tg (N) * year}^{-1}$  are released by rivers in other water bodies. The removal of Nitrogen limitation promotes algal primary productivity and can give rise to the algal blooms. Some of them are toxic for the aquatic biota and for humans (Yao et al., 2018) and known as harmful algal blooms (HABs). Independently by the degree of toxicity of the algal blooms, this phenomenon ‘triggers’ waterfall effects that lead to a complete impairment of all the aquatic ecosystem compartments, loss of ecosystem services and earnings (Le Moal et al., 2019; Paerl et al., 2016). For example, despite the scientific evidences, the ethical or strictly anthropocentric interests and the efforts in managing the P and N inputs, more than the 40% of the worldwide

lakes are affected by human-induced algal blooms (Vinçon-Leite and Casenave, 2019). The causes of these percentages are manifold, spanning from the intrinsic difficulties in nutrient input identifiability to the illegal discharges (Jones et al., 2001). Moreover, climate change can amplify the negative effects of Nitrogen inputs on aquatic environment and ‘boosts’ the algal blooms (Delpla et al., 2009; Paerl 2017). In some geographic areas, like the Mediterranean, the increase in the frequency of long-lasting droughts is expected (Spinoni et al., 2018). Due to the absence of rainfalls for long periods, inputs do not immediately reach the water bodies and are accumulated in the soil, potentially explaining the decrease of their concentrations in water column (Greaver et al., 2016; Hayes et al., 2015; van Vliet and Zwolsman, 2008). However, when huge rainfalls arrive, they are released in notable amounts (Delpla et al., 2009; Hayes et al., 2015), potentially overcoming the buffering activity of riparian vegetation (Dong et al., 2014; Kosten et al., 2009) and N removal capacity of the water body (Greaver et al., 2016). On the other hand, in the case of agricultural and/or wastewater loadings that eventually enter in the water body despite the low rainfalls, drought can potentially lead to their concentrations decreasing the water level (Brusewitz et al., 2017; van Vliet and Zwolsman, 2008).

The first attempts in the environmental trophic status assessment were focused on the chemical analysis of nutrient concentrations in the water column, associated with other physicochemical and biological variables (Gartner et al., 2002). This approach has advantages and drawbacks. On one hand, the chemical determination of nutrient concentrations is highly precise, on the other, this kind of analysis is limited in space and time due to the diffusion in the aquatic medium, as well as by the biotic assimilation (Dailer et al., 2010; Gartner et al., 2002; Hadwen et al., 2005; Kaminski et al., 2018). In Europe, the Water Frame Directive (WFD, 2000/60/EC) represents the attempt to standardize the environmental monitoring protocol of the aquatic ecosystems for all the European countries, with the declared aim to reach the ‘good status’ for all the water bodies by 2015. For the surface water bodies, the ‘good status’ is a combination of the ‘good ecological status’ and the ‘good chemical status’. The ‘ecological status’ integrates the physicochemical analysis, the hydrological analysis and the analysis of the biotic components of the aquatic ecosystems. The ‘good chemical status’ is obtained when all the quality standards for chemical substances are met. Despite its importance, the WFD shows practical difficulties. For the complete assessment of the ecological status, a ‘reference’ per water body typology is required, as well as the ‘typical’ undisturbed community (Voulvoulis et al., 2017). Even assuming if these prerequisites are met, the status estimate

is not ‘difficulties free’, as reported by Carré et al. (2017). Moreover, at the present state, the ecological status determination has been inferred even if one, or more, of its components were missing (Carré et al., 2017). Despite the objective of bringing all the surficial water bodies to a ‘good ecological status’, for the 60% of them this goal has not been achieved (Carvalho et al., 2019). As a result, a substantial number of water bodies ( $\approx 28\%$ ) are currently affected by nutrient pollution (Carvalho et al., 2019). One of the possible causes of this phenomenon is, as previously stated, the identifiability of the input origins. Human derived Nitrogen inputs can be roughly classified in two main groups (Kendall et al., 2007): the ‘inorganic’ one (like the industrial chemical fertilizers obtained without the biological  $N_2$ -fixation pathway) and the ‘organic’ one (like the wastewaters and manures, where Nitrogen therein has followed a biological pathway). Once known the origin of the ‘dominant’ input, especially in heterogenous contexts, it is likely that the subsequent management actions will be more specifically addressed. Moreover, this kind of information can be used as an ‘early warning’ ecological indicator, i.e. an environmental monitoring tool able to detect the occurrence of a specific anthropic Nitrogen input even when it was a space and/or time isolated event and before it can produce a recognizable detrimental effect on the community structure (Dale and Bayeler, 2001).

In the context of the environmental monitoring of the Nitrogen inputs, the stable isotopes analysis (SIA) represents a flexible tool for discriminating the origin of such inputs in terms of their isotopic signatures,  $\delta^{15}N$  (‰), i.e. as deviation in parts per thousand from the international standard (atmospheric air  $^{15}N:^{14}N = 0.0036765$ , Sulzman 2007). The SIA is based on the difference between ‘light’ and ‘heavy’ isotope physical properties. In fact, even if the chemical properties of the light and heavy isotopes are identical, the higher energy required for breaking molecular bounds in presence of heavy isotopes determines their ‘accumulation’ in the biotic sample, whereas light isotopes tend to be more easily removed (Sulzman, 2007). Nitrogen, in particular, shows a notable increase (from +2.6‰ up to +3.4‰), known as fractionation or trophic enrichment factor (TEF), from a trophic level to the following one (Careddu et al., 2015). Therefore, compared to the international standard, if a source of a Nitrogen input derives from excreta or dead organic matter (‘organic pathway’), it is ‘enriched’ in heavy isotopes (Jona-Lasinio et al., 2015), whereas if the Nitrogen input derives from the industrial atmospheric  $N_2$  fixation (atmospheric  $^{15}N$  percentage  $\approx 0.37\%$ , Table 13.1 Katzemberg, 2008), without the involvement of  $N_2$ -fixers (‘inorganic pathway’), light Nitrogen isotopes are ‘preferentially’ fixed and the resulting molecules are ‘depleted’ in heavy isotopes

(Wang et al., 2016). The major advantage of this approach is the possibility to analyze not the human-derived input itself, but the Nitrogen isotopic signature of biological samples that have assimilated it, bypassing the dilution of the input in the water medium (Gartner et al., 2002; Kaminski et al., 2018).

Among the various components of aquatic food webs, the macroalgae and the epilithic associations (Orlandi et al., 2014; Pastor et al., 2014), respectively in marine and freshwater ecosystems, show some ideal characteristics for the environmental monitoring thought the SIA: **1**) are sessile, **2**) directly uptake Nitrogen from the water column (Jones et al., 2004), **3**) their fractionation is small or null (Dailer et al., 2010; Orlandi et al., 2017) and **4**) the lag time between input exposure and isotopic signature acquisition is relatively short (Orlandi et al., 2014). The distinction between ‘inorganic’ ( $-3‰ \leq \delta^{15}\text{N} \leq +3‰$ , Cole et al., 2004; Lapointe and Bedford, 2007), and ‘organic’ ( $\delta^{15}\text{N} > +6‰$ , Jona-Lasinio et al., 2015) Nitrogen isotopic signatures is based on the comparison between the macroalgal/epilithic  $\delta^{15}\text{N}$  signatures and the  $\delta^{15}\text{N}$  of potential Nitrogen input sources. The use of macroalgae and epilithic associations has been proven to be successful in identifying the origin of human-derived Nitrogen inputs in marine (Orlandi et al., 2014; Rossi et al., 2018), coastal brackish (Jona-Lasinio et al., 2015) and few fluvial ecosystems (Bentivoglio et al., 2016; Pastor et al., 2014). In scientific literature, no information about method applicability were known for land locked ecosystems.

To demonstrate the applicability of the algal Nitrogen isotopic signature in land locked ecosystems, increase the knowledge of this method on fluvial ecosystems and provide a robust determination for the human-related and ‘non-impacted’ epilithic/macroalgal  $\delta^{15}\text{N}$ , this dissertation focuses on three fluvial ecosystems (Itri, Capodacqua Santa Croce and Garigliano) and on the littoral zones of two deeply different land locked ecosystems (Lake Bracciano and Caspian Sea).

For what concerns the two land locked ecosystems, one is the littoral zone of Lake Bracciano, a volcanic lake in Central Italy, whereas the second is the Southern littoral zone of the Caspian Sea (Iran). Besides the various geographical and morphometric differences, the two land locked ecosystems also differ for their fresh and brackish water ‘identity’ and for the magnitude of the anthropic pressures.

Lake Bracciano is an oligo-mesotrophic freshwater lake (Bolpagni et al., 2016; Mastrantuono et al., 2008), is a regional park and the main drinking water reservoir for the city



of Rome (Rossi et al., 2019). Considering the human population of Bracciano, Anguillara Sabazia, Trevignano Romano and Manziana towns, the lake has  $\approx 52,000$  inhabitants (ISTAT, 2018). Along its perimeter ( $\approx 32$  Km, Rossi et al., 2019) are recognizable human activities related to tourism, agriculture and fishery. A wastewater collecting system prevents the inlet of the inputs into the water body, but local human-related nutrient inputs were recorded (Mastrantuono and Mancinelli, 2005). The lake is particularly prone to be affected by climatic variations (Taviani and Henriksen, 2015), as demonstrated by the water level decreases occurred in recent years (Mastrantuono et al., 2008; Rossi et al., 2019). In particular, the recent 2017 drought caused significant damages to the agricultural activities in the Latium Region and in Lake Bracciano surroundings as well. Also the leisure activities around the lake were indirectly and negatively affected by the drought. Such decrease of the water level produced significant reductions of the aquatic vegetation, changes in associated invertebrate community (Mastrantuono et al., 2008), and, coupled with the previously mentioned anthropic derived nutrient inputs, threatened the endemic species *Isoëtes sabatina* (Baccetti et al., 2017; Troia and Azzella, 2013). Moreover, the fishery activity is seriously affected by the presence of the invasive species *Micropterus salmoides*, which invasive success is dependent, among the other physical and biotic drivers, by the low coverage of aquatic vegetation (Costantini et al., 2018).

The Caspian Sea is the largest brackish water lake in the world, and it is completely land locked (de Mora et al. 2004). The Iranian region of the Caspian Sea (Southern zone), has a population of  $\approx 7,000,000$  inhabitants and 10 million of tourist presences (Abadi et al., 2018). Recent researches reported an increase of its trophic state (Sadeghi et al., 2013), due to the insufficient presence of wastewater treatment plants (Abadi et al., 2018) and the high agricultural input discharges. Such inputs, in the Anzali wetlands, promoted the spread of the fast-growing invasive species *Azolla filiculoides*, that nowadays covers a quarter of these wetlands (Sadeghi et al., 2013, 2017). Moreover, water, sediment and biota quality and 'healthiness' are threatened by metal pollution (Dadar et al., 2016; de Mora et al., 2004; Hosseini et al., 2013; Irankhah et al., 2016), related especially to the oil extraction, industrial and mining activities (Jelodar et al., 2012; Sohrabi et al., 2010). In Southern Caspian Sea, the metal pollution, in particular, caused a significant reduction of the population of the Caspian kutum (*Rutilus frisii kutum*), which accounts for  $\approx 70\%$  of the fish caught (Dadar et al., 2016), and high level of Hg were found by Hosseini et al. (2013) in caviar of Persian sturgeon (*Acipenser persicus*).

The three fluvial ecosystems are all located in Central Italy. Both Itri and Capodacqua Santa Croce (hereafter referred as ‘Santa Croce’) rivers originate by the Aurunci mountains, and are, respectively,  $\approx 14$  Km and  $\approx 10$  Km long. Itri river crosses the Itri town and flows close to Vindicio (Formia). Its daily flow is influenced by the presence of a wastewater treatment plant. Santa Croce river crosses the towns of Spigno Saturnia, Minturno and flows close to Formia. A secondary branch, ( $\approx 3.5$  Km), which drains an agricultural dominated area, merges into the main channel at its upstream. The last one, Garigliano, originated by the merging of the Liri and Gari rivers. It is 158 Km long and the main source of freshwater, organic matter and nutrient inputs in the Gaeta Gulf. These inlets affect the water quality, the biodiversity and the food web structures of the gulf coastal zone (Careddu et al., 2015, 2017; Cicala et al., 2019; Rossi et al., 2018). All the three rivers cross anthropized areas that potentially cause organic and/or inorganic Nitrogen inputs in the water bodies. Around the sampling sites, Itri river is mainly characterized by wooded natural surface, whereas Santa Croce and Garigliano are mainly characterized by agricultural activities surrounding the water bodies. For all the three rivers, urban area coverages are less than or equal to 5% of the whole land covers.

The chapters of this dissertation will cover the epilithic association and macroalgal  $\delta^{15}\text{N}$  ability to discriminate the origins (‘inorganic’, ‘non-impacted’, ‘moderate organic’ and ‘high organic’) of the human-derived Nitrogen inputs that affect the Lake Bracciano and Southern Caspian Sea littoral zone and the three Central Italy rivers. In particular:

**Chapter 1** is focused on the response of the epilithic  $\delta^{15}\text{N}$  at narrow (4 days) and wide (seasonal) time scales, highlights how the epilithic  $\delta^{15}\text{N}$  changes along the entire lake perimeter (GAM estimates) in function of the magnitude of the human activities and proposes a classification of the Nitrogen inputs on the bases of four monodimensional ranges of the epilithic  $\delta^{15}\text{N}$  signatures (‘inorganic’, ‘non-impacted’, ‘moderate organic’ and ‘high organic’). To exclude potential effects of the specific epilithic association composition on the observed  $\delta^{15}\text{N}$  signatures, a translocation experiment of the epilithon was performed.

**Chapter 2** estimates the Lake Bracciano epilithic  $\delta^{15}\text{N}$  signatures related to the touristic activities in the May-August period. According to the results of Chapter 1, this was the period therein the tourism had the maximum organic impact, in terms of high  $\delta^{15}\text{N}$  signatures, especially in the Western areas of Lake Bracciano.

**Chapter 3** is focused on the littoral zone of the Southern Caspian Sea and explores the ability of the macroalgae  $\delta^{15}\text{N}$  signatures to detect the different human derived Nitrogen inputs

in potentially metal pollution exposed sediment and biota (macroalgae) compartments. The effects of the cultural eutrophication of the Iranian Caspian Sea littoral zone were highlighted by the decreasing linear relationship between the water dissolved Oxygen and the macroalgal  $\delta^{15}\text{N}$  signatures, as well by the increasing linear trend between the macroalgal  $\delta^{15}\text{N}$  signatures and water dissolved inorganic Nitrogen. Moreover, both macroalgal and sediment samples showed, for different metals, even high level of pollution, not related with the Nitrogen signatures of macroalgae samples.

**Chapter 4** applies the monodimensional epilithic  $\delta^{15}\text{N}$  signature ranges classification approach to highlight the sources of human-related Nitrogen inputs in three rivers. For these rivers, the dominant sources of Nitrogen are the ‘moderate’ and ‘high organic’ inputs. These two classes of human-related inputs affect most of the investigated areas and show a linear relationship with the  $\text{NO}_3^-$  concentrations in the water samples. In general, to the increase of Nitrogen pollution corresponds the decrease of Gastropoda diversity and abundance.

**Chapter 5** extends the research on the Lake Bracciano epilithic  $\delta^{15}\text{N}$ . A new protocol for the epilithic  $\delta^{15}\text{N}$  analysis is proposed. Four Gaussian distributions were estimated, by Bayesian Gaussian Mixture Model, from epilithic  $\delta^{15}\text{N}$  field data of Chapter 1 and new epilithic  $\delta^{15}\text{N}$  field data. Each distribution characterizes a Nitrogen input class (recognized in Chapter 1). This approach solved the critical issue of the robust assignment of an epilithic  $\delta^{15}\text{N}$  to the most appropriate class. This classification approach of the epilithic  $\delta^{15}\text{N}$  highlighted the class shifts occurred before the drought (2015-2016, Chapter 1) and ongoing the drought (2017-2019), at different spatial scales (sampling site and GAM estimates on the entire lake perimeter) and time scales (among vernal seasons and among years). Moreover, the class changes of the epilithic  $\delta^{15}\text{N}$  signatures reflected the negative effects of the drought on agricultural and touristic activities.

## Chapter 1

**Epilithon  $\delta^{15}\text{N}$  signatures indicate the origins of nitrogen loading and its seasonal dynamics in a volcanic Lake.**

**Fiorentino, Federico<sup>a</sup>**, Cicala, Davide<sup>a</sup>, Careddu, Giulio<sup>a</sup>, Calizza, Edoardo<sup>a</sup>, Jona-Lasinio, Giovanna<sup>c</sup>, Rossi, Loreto<sup>a,b,\*</sup>, Costantini, Maria Letizia<sup>a,b</sup>.

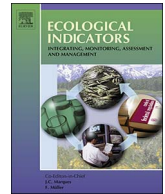
<sup>a</sup> Department of Environmental Biology, Sapienza University of Rome, Via dei Sardi 70, 00185 Rome, Italy

<sup>b</sup> CoNISMa, Piazzale Flaminio 9, 00100 Rome, Italy

<sup>c</sup> Department of Statistical Sciences, Sapienza University of Rome, P.le Aldo Moro 5, 00185 Rome, Italy

**Corresponding Author:** loreto.rossi@uniroma1.it (L. Rossi).

Manuscript published in *Ecological Indicators*



# Epilithon $\delta^{15}\text{N}$ signatures indicate the origins of nitrogen loading and its seasonal dynamics in a volcanic Lake



Federico Fiorentino<sup>a</sup>, Davide Cicala<sup>a</sup>, Giulio Careddu<sup>a</sup>, Edoardo Calizza<sup>a</sup>, Giovanna Jona-Lasinio<sup>c</sup>, Loreto Rossi<sup>a,b,\*</sup>, Maria Letizia Costantini<sup>a,b</sup>

<sup>a</sup> Department of Environmental Biology, Sapienza University of Rome, Via dei Sardi 70, 00185 Rome, Italy

<sup>b</sup> CoNISMa, Piazzale Flaminio 9, 00100 Rome, Italy

<sup>c</sup> Department of Statistical Sciences, Sapienza University of Rome, P.le Aldo Moro 5, 00185 Rome, Italy

## ARTICLE INFO

### Keywords:

Environmental monitoring  
Stable isotopes  
Water pollution  
Tourism  
Bioindicator  
Freshwater

## ABSTRACT

The intensification of agricultural land use and urbanisation has increased nutrient loads in aquatic ecosystems. Nitrogen loads can alter ecosystem structure and functioning, resulting in increased algal productivity, algal blooms and eutrophication. The principal aim of the present paper is to extend the use of epilithic  $\delta^{15}\text{N}$  signatures to a lake ecosystem in order to evaluate the potential impact of anthropogenic nitrogen discharges (organic and inorganic) that can also reach coastal waters.

Epilithic associations were collected from volcanic rocks in different seasons in shallow water along the entire perimeter of Lake Bracciano and analysed for their nitrogen stable isotope signatures. Furthermore, some stones were moved from an unpolluted site to a polluted one in order to verify the effect on the nitrogen signature of the epilithic association. The epilithon's  $\delta^{15}\text{N}$  signatures provided strong evidence of the space-time variability of N inputs. The differing quality of nitrogen loads was reflected in high isotopic variation within the lake, especially at the beginning of summer ( $1.7\text{‰} \leq \delta^{15}\text{N} \leq 13.3\text{‰}$ ), while in winter, when anthropogenic pressure was lowest, the  $\delta^{15}\text{N}$  signature variation was less accentuated ( $3.1\text{‰} \leq \delta^{15}\text{N} \leq 7.6\text{‰}$ ). At all sampling times, spatial variability was found to be related to the various human activities along the lake shore (especially tourism and agriculture), while seasonal variation at all sampling sites was related to the intensity of anthropogenic pressures (higher in summer and lower in winter).

Our results showed that epilithic algal associations and the physicochemical properties of the water did not influence the  $\delta^{15}\text{N}$  signature, which in contrast was strongly related to the site-specific effect of human activities around the lake. Thus, the distribution of  $\delta^{15}\text{N}$  across space and time can be used to direct nutrient reduction strategies in the region and can assist in monitoring the effectiveness of environmental protection measures.

## 1. Introduction

Inland waters account for only 2% of the Earth's surface (Wetzel, 2001) but provide several ecosystem services of importance to human communities (Page et al., 2012; Pimentel et al., 2004; Smith, 2003). On the other hand, the intensification of agricultural land use, industrial activity and urbanisation has caused an increase in nitrogen loads in aquatic ecosystems (Derse et al., 2007; di Lascio et al., 2013; Galloway et al., 2003; Matson et al., 1997; Vilmi et al., 2015; Vitousek et al., 1997). Associated with phosphorus, nitrogen inputs can alter ecosystem structure and functioning, resulting in increased algal productivity and algal blooms (Dodds et al., 1989; Maberly et al., 2002; Page et al., 2012). Physicochemical environmental monitoring methods only provide snapshots of ecosystem trophic conditions, and therefore several

sampling times are required, although even then, pulse inputs are likely to be missed (Danilov and Ekelund, 2001; DeNicola et al., 2004; Gartner et al., 2002; Vilmi et al., 2015). There is a need therefore for improved and integrated management of N pollution in fresh waters.

Isotope analysis is widely employed in trophic ecology, microbial ecology and nutrient cycling studies (Calizza et al., 2013a,b; Careddu et al., 2015; Costantini et al., 2014; di Lascio et al., 2013; Mancinelli et al., 2013; Rossi et al., 2007). In addition, the nitrogen isotopic signature,  $\delta^{15}\text{N}$ , has been successfully used to monitor coastal marine habitats by determining the type of nitrogen input (Orlandi et al., 2014). Inorganic fertilisers have a  $\delta^{15}\text{N}$  range of  $-4\text{‰}$  to  $+4\text{‰}$ , while for organic fertilisers and organic waste (including compost and animal excretion)  $\delta^{15}\text{N}$  can range from  $+6\text{‰}$  to  $+38\text{‰}$  in exceptional cases (Cole et al., 2004; Dailer et al., 2010; Derse et al., 2007; Jona-Lasinio

\* Corresponding author at: Department of Environmental Biology, Sapienza University of Rome, Via dei Sardi 70, Rome 00185, Italy.  
E-mail address: [loreto.rossi@uniroma1.it](mailto:loreto.rossi@uniroma1.it) (L. Rossi).

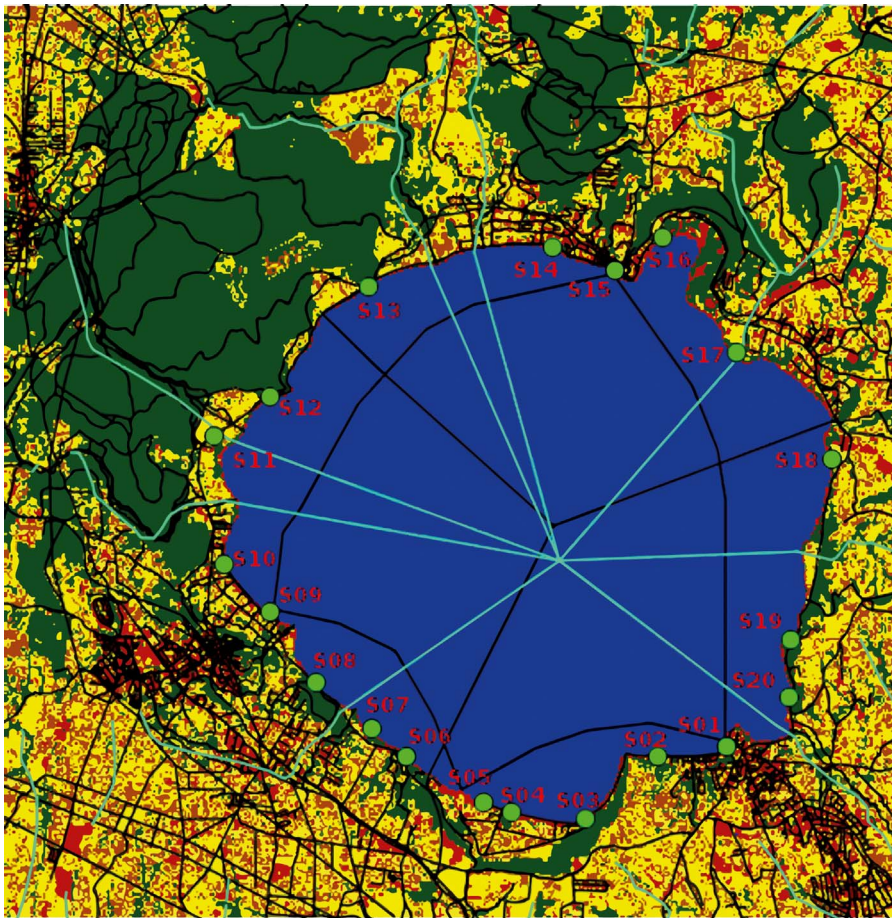


Fig 1. Bracciano (RM) land cover based on Corine Land Cover second level. Legend: green = vegetation, yellow = crops, blue = lake, red = built up, brown = soil, black = roads, light blue = streams. Green points indicate the sampling sites.

et al., 2015; Kendall et al., 2007).

Given their ability to assimilate and store N inputs in their tissues, macroalgae (in marine ecosystems) and epilithon (in river ecosystems) can provide information on anthropogenic N loadings based on changes in their isotopic signatures (Cejudo et al., 2014; Cole et al., 2004; Costanzo et al., 2005; Jones et al., 2004; Pastor et al., 2014; Schiller et al., 2009; Yokoyama and Ishihi, 2006), even on short time scales (Orlandi et al., 2014), reflecting space-time variability in N availability (Jona-Lasinio et al., 2015; Vizzini et al., 2005). Several studies have been performed on macroalgal  $\delta^{15}\text{N}$  signatures in marine coastal ecosystems (Cole et al., 2004; Dailer et al., 2010; Gartner et al., 2002; Titlyanov et al., 2011) and coastal brackish lakes (Jona-Lasinio et al., 2015) and lagoons (Vizzini et al., 2005). Recent studies have applied stable isotope analysis to epilithic  $\delta^{15}\text{N}$  signatures to evaluate the effect of anthropic land use on rivers (Bentivoglio et al., 2016; Cejudo et al., 2014; Pastor et al., 2013, 2014; Peipoch et al., 2012; Schiller et al., 2009). However, in spite of its widespread presence, epilithon is poorly understood as an ecological indicator of nitrogen pollution.

Epilithon is defined as an association of non-planktonic algae, fungi and bacteria immersed in a polysaccharide matrix able to colonise stones on the bottom of lakes (Burns and Ryder, 2001; Castenholz, 1960, Harrison, 1998; Kahlert et al., 2002). Its abundance and composition are probably related to light (Watkins et al., 2001), temperature and nutrient availability (Maberly et al., 2002). Epilithic algal growth reaches its maximum in spring and its minimum in summer, with a second slightly smaller growth peak in late summer in stratifying lakes (Castenholz, 1960; Harrison, 1998).

Epilithon is a potentially interesting biological resource for monitoring aquatic ecosystems thanks to its high ability to colonise diverse substrates in all freshwater ecosystems and the ease of collection in littoral areas (Round, 1991; Sabanci, 2011), which allows more rapid

sampling procedures than those required for phytoplankton and surface sediments (DeNicola et al., 2004). The littoral zone is a key habitat for primary and secondary productivity (Mancinelli et al., 2007; Vilmi et al., 2015), while epilithic associations contribute significantly to the productivity of the system as a whole and represent a trophic resource for benthic invertebrates (Fink et al., 2006; di Lascio et al., 2011; Hawes and Smith, 1994; Rossi et al., 2010), providing a key link between allochthonous nutrient inputs and aquatic consumers (Bentivoglio et al., 2016).

Our study focused on the Bracciano volcanic lake in the Central Italian Volcanic Lake District (CIVOILD; Costantini et al., 2012; Mazza et al., 2015), because of its high diversity of anthropic activities. A regional park since 1999, it is the main drinking water reservoir for the city of Rome, with direct water extraction (ACEA Sustainability Report, 2015). Previous research assessed the lake as oligo-mesotrophic (Ferrara et al., 2002; Margaritora et al., 2003; Mastrantuono et al., 2008). Moreover, in order to prevent anthropic discharges into the basin, in the early 80s, a centralised system was created to collect urban waste waters for a population of up to 40,000 inhabitants. Nevertheless, the present-day population of the CO.B.I.S. (the area served by the system, comprising the municipalities of Anguillara-Sabazia, Bracciano, Manziana, Oriolo-Romano and Trevignano Romano) is around 49,000 (ISTAT, 2016), which rises further in summer due to tourism, exceeding the system's capacity.

The aim of this study was to extend the use of epilithic  $\delta^{15}\text{N}$  signatures to space-time monitoring of a tourism-oriented lacustrine ecosystem. We considered anthropogenic nitrogen input type and its variation across seasons, related to the intensity of tourism and agricultural activities in the littoral zone, on both short (i.e. week-end) and long (i.e. season) time scales. Specifically, we tested the hypothesis that (i) variations in organic and inorganic N inputs were reflected in increased or



decreased  $\delta^{15}\text{N}$  in epilithon, and (ii) the tourism-driven summer increase in anthropogenic pressure was reflected in a seasonal increase in isotopic signatures in tourism-impacted sites that was not seen in sites unaffected by tourism.

## 2. Materials and methods

### 2.1. Study area

Lake Bracciano (42°07'16"N; 12°13'55"E) is a volcanic lake located in central Italy, 32 km northwest of Rome (Lazio, Italy). It has a surface area of 57 km<sup>2</sup> and a perimeter of about 31.5 km. Its elevation is 164 m a.s.l. and its maximum depth is 165 m. The lake is oligo-mesotrophic, and warm monomictic from May to October and homothermic from November to February (Ferrara et al., 2002). It has a theoretical renewal time of 137 years, and is used as a drinking water reservoir for the city of Rome and the Vatican State. The combined action of climate change and water extraction produces dangerous water level variations that drastically change the shape of the shoreline and inshore bathymetry, causing substantial loss of areas where denitrification can take place as a result of the dry conditions during the frequently prolonged periods of minimum depth. Land use in the surrounding area is highly heterogeneous (Fig. 1), with the following types recorded:

- Vegetation: broadleaf woods, shrub-herbaceous vegetation, semi-natural areas
- Crops: annual crops, mixed crops, permanent crops, orchards
- Built up: the towns of Trevignano Romano (42°09'N; 12°15'E), Anguillara Sabazia (42°05'18"N; 12°16'39"E), Vigna di Valle (42°04'34"N; 12°12'28"E) and Bracciano (42°06'N; 12°11'E), as well as greenhouses, campsites and beach resorts
- Soil
- Roads
- Streams

Since 1999, the lake and its surroundings have been part of the regional park of Bracciano Martignano.

So as to cover the whole perimeter of the lake (Fig. 1), twenty collection sites were selected in the littoral zone. The sites were located:

- In and near the towns (site 1–site 3, site 7, site 9, site 10, site 14, site 15, site 20)
- Close to tourism structures directly on the lake shore (campsites, beach resorts, garages etc.) (site 4, site 5, site 8, site 11, site 17)
- Cultivated fields (site 16 and site 18)
- Naturally vegetated areas (site 6, site 12, site 13, site 19)

A class was assigned to each sampling site in accordance with the dominant type of potential impact and its associated nitrogen input, on the basis of the human activities observed in the immediate vicinity (Table 1). We expected 'organic' inputs for those sites seasonally affected by tourism during summer; 'organic/inorganic' for those sites characterised by agricultural activity (as the type of fertiliser used was unknown) and 'non-impacted' for sites in naturally vegetated areas and in or near the towns. We expected sites in towns to be in the 'non-impacted' category given that the waste waters of urban areas in the catchment are directly channelled to the centralised collection system and discharged downstream. In addition to the catchment land-use classification, given that the lake is not directly served by a railway, we considered the cash earned by parking meters in parking areas on the lake shore used by non-residents ( $n = 6$ ) to be a proxy for tourism pressure. Earnings were measured weekly from the beginning of May to the end of August. The parking meters do not operate from October to March. The number of non-resident cars per week in late March, April, and September was roughly the same as the May value, while from October to early March it was about half (COBIS, personal

**Table 1**

Expected and observed impact classes for each sampling site. The expected impacts were assigned before sampling in accordance with the human activities in the immediate vicinity of each sampling site. We considered the expected impact to be organic if it was related to tourism, "organic/inorganic" if it was related to agriculture. The observed impacts refer to the  $\delta^{15}\text{N}$  measured at each site.

Site	IMPACT	
	Expected	Observed
1	Non-impacted	Non-impacted
2	Non-impacted	Non-impacted
3	Non-impacted	Moderate organic
4	Organic	Non-impacted
5	Organic	Moderate organic
6	Non-impacted	Non-impacted
7	Organic	Moderate organic
8	Organic	Moderate organic
9	Organic	Moderate organic
10	Organic	High organic
11	Organic	Moderate organic
12	Non-impacted	High organic
13	Non-impacted	Non-impacted
14	Non-impacted	Non-impacted
15	Non-impacted	Non-impacted
16	Organic/Inorganic	Inorganic
17	Organic	Non-impacted
18	Organic/Inorganic	Inorganic
19	Non-impacted	Non-impacted
20	Non-impacted	Moderate organic

communication). The cost of parking is €1 per hour per car. To relate the number of non-resident cars to tourism pressure, one car was considered equivalent to 2.5 tourists (i.e. non-residents) as a mean value. The number of tourists was converted into g of N per day considering: 1 tourist = 6.16 g N/day (1 day = 24 h) (Pagnotta and Barbiero, 2003). Parking meters used by non-residents further away from the lake shore ( $n = 4$ ) were also considered and compared with parking meters near the lake shore to confirm that the increase in car numbers was directly related to the increase in tourism-driven pressure on the lake.

### 2.2. Field procedures

We sampled at six times, from June 2015 to March 2016. Specifically, two samplings were conducted at the end of June (June 26: early summer 1, and June 30: early summer 2). Early summer 2 followed a public holiday for the entire municipality of Rome (June 29) after a weekend (June 27–28) during which tourism peaked in the lake area. Other samplings were conducted on July 28 (summer), September 23 (autumn), December 15 (winter) and March 31 (spring, 2016). At each site epilithon was sampled by scraping smooth volcanic rocks (size approximately 30 × 15 × 7 cm) in the littoral zone using single-edge sterilised razors. Two 5 × 5 cm patches were collected from each of

three rocks sampled at each site, the rocks being 25 m apart along sampling transects parallel to the lake shore. The epilithon samples were stored in plastic Petri dishes and conserved on ice for transport to the laboratory. The temperature (°C), pH, total dissolved solids (ppm) and oxygen concentration (mg/l) and saturation (%) were recorded at each sampling site by multi-parameter probe (Hanna instruments HI 9829).

Following field samplings and data analysis, a transplant experiment was performed. We moved rocks from one site to another in order to test for site-specific effects on the epilithic  $\delta^{15}\text{N}$  signature. Two rocks, duly labelled, from a site with non-impacted  $\delta^{15}\text{N}$  signatures (site 3, as determined during previous samplings), were carefully moved to the site with the highest observed  $\delta^{15}\text{N}$  (site 10, 9.9 km from site 3). Rocks of the same size and smoothness as those used for field sampling were chosen. At the same time, two rocks from site 10 were moved to site 3 and labelled. During translocation, which took less than 30 min, rocks were maintained right side up in water collected at their site of origin. Unfortunately, rocks moved from site 10 to site 3 were removed by persons unknown. In October 2015 (T0 in the translocation experiment), epilithon was sampled by scraping three replicate patches (5 × 5 cm each) per rock. Half of the total surface of the two rocks was then scrubbed clean and the rocks were moved to site 10. After 30 days, in November 2015 (T1 in the translocation experiment), the epilithic associations were re-sampled from the same two rocks moved to site 10 (three patches per rock), taking samples from both the unscraped surfaces (the epilithon left intact at T0 and hence belonging to site 3) and from the regrown surfaces (the epilithon that had regrown on the surfaces scraped bare at T0, and hence belonging to site 10). Moreover, at T1, three epilithic replicates from three rocks in site 10 were sampled to obtain a reference  $\delta^{15}\text{N}$  value for epilithon growing naturally at that site. The samples were stored in plastic Petri dishes and conserved on ice for transport to the laboratory.

### 2.3. Laboratory procedures

Epilithic samples were conserved at  $-80\text{ }^\circ\text{C}$  before being freeze-dried for 24 h and ground to a fine homogeneous powder using a ball mill (Fritsch Mini-Mill Pulverisette 23 with a zirconium oxide ball).

For each epilithic sample, two replicates ( $2.0 \pm 0.2\text{ mg}$ ) were subsampled and pressed into ultra-pure tin capsules and analysed using an Elementar Vario Micro-Cube elemental analyser (Elementar Analysensysteme GmbH, Germany) coupled with an IsoPrime100 isotope mass ratio spectrometer (Isoprime Ltd., Cheadle Hulme, UK). The obtained nitrogen (N) stable isotope ratios ( $^{15}\text{N}:^{14}\text{N}$ ) were expressed in  $\delta$  units, i.e. parts per thousand deviations from international standards (atmospheric  $\text{N}_2$ ), in accordance with the following equations:  $\delta\text{R}(\text{‰}) = [(R_{\text{SAMPLE}} - R_{\text{STANDARD}})/R_{\text{STANDARD}}] * 10^3$  (Ponsard and Arditi, 2000), where R is the heavy-to-light isotope ratio of the element. The internal laboratory standard was IAEA-600 Caffeine. Measurement errors were found to be typically smaller than  $\pm 0.05\text{‰}$ . In accordance with Cole et al. (2004), Derse et al. (2007) and Kendall et al. (2007), four impact classes, based on observed epilithic  $\delta^{15}\text{N}$  signatures, were identified: ‘inorganic input’ ( $\delta^{15}\text{N} < 3\text{‰}$ ), ‘non-impacted’ ( $3\text{‰} \leq \delta^{15}\text{N} \leq 6\text{‰}$ ), ‘moderate organic input’ ( $6\text{‰} < \delta^{15}\text{N} \leq 9\text{‰}$ ) and ‘high organic input’ ( $\delta^{15}\text{N} > 9\text{‰}$ ).

### 2.4. Statistical analysis

The entire data-set includes 287  $\delta^{15}\text{N}$  observations.

Two-way ANOVA was applied to test for the effect of impact class (i.e. non-impacted, moderate organic, highly organic, inorganic) and season on epilithic  $\delta^{15}\text{N}$  values. In addition, the Kruskal-Wallis test for repeated measures was used in order to test for differences between mean values of impact classes for the study period as a whole. In this case, sampling times were considered to be repeated measures. Each site was assigned to a certain impact class in accordance with its  $\delta^{15}\text{N}$

value at the early summer 2 sampling time. This sampling occurred after a public holiday for the entire Municipality of Rome (the nearest major city to the lake, 4.3 million inhabitants), and was the time when tourism pressure and the mean and range of nitrogen isotopic signatures across sites were all at their highest.

Due to the presence of non-linear relationships among  $\delta^{15}\text{N}$  signatures and/or sampling sites/time, we used a Generalised Additive Model (GAM) (significance level  $\alpha = 0.05$ ). GAM can be considered a semi-parametric generalisation of linear regression and Generalised Linear Models. It is able to deal with non-linear relationships (Zuur et al., 2007, 2009) and to take account of space-time variability (Ciannelli et al., 2008; Colloca et al., 2014; Pastor et al., 2014). Therefore we considered the observed  $\delta^{15}\text{N}$  epilithic signatures as a function of space (longitude and latitude coordinates of the sampling site) and time (sampling time). This allowed us to interpolate the  $\delta^{15}\text{N}$  values along the entire lake perimeter at each sampling time. A Mantel test was applied to determine whether differences in  $\delta^{15}\text{N}$  (in ‰) between site pairs were related to the distance (in km) between sites.

All statistical analyses were performed using open-source R software.

## 3. Results

### 3.1. Field sampling

Nitrogen isotope statistics are shown in Table 2 and physicochemical parameters are shown in Table S1 in the online supplementary material. Epilithic  $\delta^{15}\text{N}$  was not found to be related to physicochemical parameters (pH:  $R^2 = 0.04$ ,  $p = 0.51$ ; T:  $R^2 = 0.00$ ,  $p = 0.99$ ; TDS:  $R^2 = 0.14$ ,  $p = 0.18$ ;  $\text{O}_2$  mg/l:  $R^2 = 0.01$ ,  $p = 0.71$ ;  $\text{O}_2\text{‰}$ :  $R^2 = 0.01$ ,  $p = 0.68$ ). Similarly, we found no significant correlation between  $\delta^{15}\text{N}$  and  $\text{‰N}$ , either at individual sampling times or considering the study period as a whole ( $p$  always  $> 0.05$ ). Distance between site pairs explained less than 5% of the observed epilithic isotopic variation between sites (Mantel Test,  $R^2 = 0.04$ ,  $t = 2.53$ ,  $p > 0.05$ ). As an example, sites 1 and 13 were 8.8 km apart but their  $\delta^{15}\text{N}$  signatures differed by only 0.3‰. At the opposite extreme, sites 15 and 16 were only 0.9 km apart but their  $\delta^{15}\text{N}$  signatures differed by 3.3‰. The lowest average  $\delta^{15}\text{N}$  value was observed at site 16, near greenhouses and crops. The highest value was observed at site 10, near the tourism lakeside of Bracciano town. The range (i.e. max-min) of  $\delta^{15}\text{N}$  values across sites was greatest in early summer 2 and lowest in winter (Table 2). Based on the observed  $\delta^{15}\text{N}$  values, 9 sites were classed as non-impacted, 7 as moderate organic, 2 as high organic, and 2 as inorganic (Table 1).

Considering the mean value of all sites within each class, epilithic  $\delta^{15}\text{N}$  varied among both impact classes and sampling times (Two-way ANOVA, impact class:  $F = 5.4$ ,  $p < 0.001$ ; sampling time:  $F = 20.6$ ,  $p < 0.0001$ ; interaction between impact class and sampling time:  $F = 0.8$ ,  $p > 0.05$ ). When considering the sampling times as repeated observations, all pairwise comparisons between impact classes showed significant differences (Kruskal-Wallis test for repeated measures,  $H_c = 18.9$ ,  $p < 0.001$ ; Mann-Whitney pairwise comparisons between impact classes,  $p$  always  $< 0.05$ ) (Fig. 2). Generalised additive models (GAM) made it possible to observe significant differences in  $\delta^{15}\text{N}$  between sites at all times ( $p < 0.05$ ) (Table S2 in the online supplementary material). GAM also made it possible to include latitudinal and longitudinal variations in  $\delta^{15}\text{N}$  signatures, to interpolate  $\delta^{15}\text{N}$  across sites, and hence to produce an isotopic map of the lake littoral belt (Fig. 3). In early summer 1, there were diffuse moderate organic inputs along all the western side of the lake, whereas high organic impact was detected only at site 10, near the tourism lakeside of Bracciano town. Site 10 retained its high organic impact status in early summer 2 and summer, and then decreased to moderate organic between autumn and spring. Inorganic N input was evident in the East-North East (near greenhouses and crops) in early summer 1, autumn and spring, while it



**Table 2**

Epilithic  $\delta^{15}\text{N}$  signatures for each site (rows) and sampling time (columns). In each cell, the average isotopic signature and its standard error are reported. The last column shows the average isotopic signature, standard error and range ( $\Delta$ , as max–min) for each sampling site. The last row shows the range (max–min across all sites) at each sampling time.

Site	early summer 1	early summer 2	summer	autumn	winter	spring	mean $\pm$ S.E. ( $\Delta$ )
01	4.67 $\pm$ 0.32	4.66 $\pm$ 0.29	4.37 $\pm$ 1.17	3.76 $\pm$ 0.52	4.17 $\pm$ 0.94	6.52 $\pm$ 0.28	4.69 $\pm$ 0.32 (2.76)
02	5.23 $\pm$ 0.22	5.48 $\pm$ 0.36	3.36 $\pm$ 0.33	2.68 $\pm$ 0.42	3.10 $\pm$ 0.47	2.67 $\pm$ 0.05	3.75 $\pm$ 0.52 (2.81)
03	5.28 $\pm$ 0.33	6.23 $\pm$ 0.14	6.86 $\pm$ 0.67	5.44 $\pm$ 0.63	3.19 $\pm$ 0.03	2.46 $\pm$ 0.32	4.91 $\pm$ 0.41 (4.4)
04	6.06 $\pm$ 0.29	5.35 $\pm$ 1.05	4.30 $\pm$ 0.45	4.04 $\pm$ 0.38	6.32 $\pm$ 0.32	3.70 $\pm$ 0.52	4.96 $\pm$ 0.31 (2.62)
05	6.29 $\pm$ 0.51	6.57 $\pm$ 0.51	7.29 $\pm$ 0.63	10.08 $\pm$ 0.61	5.49 $\pm$ 1.02	4.30 $\pm$ 0.97	6.67 $\pm$ 0.50 (5.78)
06	6.22 $\pm$ 0.26	6.28 $\pm$ 0.27	3.66 $\pm$ 0.02	2.41 $\pm$ 0.06	3.69 $\pm$ 0.18	1.65 $\pm$ 0.39	3.98 $\pm$ 0.43 (4.63)
07	7.58 $\pm$ 0.23	–	7.67 $\pm$ 1.48	5.99 $\pm$ 0.21	4.12 $\pm$ 0.23	4.59 $\pm$ 0.52	5.99 $\pm$ 0.48 (3.55)
08	7.08 $\pm$ 0.46	6.88 $\pm$ 0.16	1.88 $\pm$ 0.32	7.99 $\pm$ 1.04	6.20 $\pm$ 0.11	4.30 $\pm$ 0.29	5.72 $\pm$ 0.51 (6.11)
09	8.32 $\pm$ 0.15	8.48 $\pm$ 0.19	8.49 $\pm$ 0.31	7.71 $\pm$ 0.53	7.19 $\pm$ 0.23	7.37 $\pm$ 0.52	7.93 $\pm$ 0.18 (1.3)
10	10.86 $\pm$ 0.56	13.33 $\pm$ 0.42	11.35 $\pm$ 1.20	8.74 $\pm$ 0.27	7.60 $\pm$ 1.02	8.55 $\pm$ 0.17	10.07 $\pm$ 0.53 (5.73)
11	–	–	6.85 $\pm$ 0.46	–	–	–	–
12	8.46 $\pm$ 0.74	11.31 $\pm$ 1.63	9.75 $\pm$ 0.72	6.33 $\pm$ 0.45	4.70 $\pm$ 0.46	6.15 $\pm$ 0.05	7.78 $\pm$ 0.62 (6.61)
13	5.59 $\pm$ 0.75	8.05 $\pm$ 0.04	4.32 $\pm$ 0.27	3.37 $\pm$ 0.17	3.52 $\pm$ 0.59	–	4.97 $\pm$ 0.49 (4.68)
14	7.43 $\pm$ 0.42	6.19 $\pm$ 0.12	3.87 $\pm$ 1.48	6.15 $\pm$ 0.38	6.70 $\pm$ 1.68	4.56 $\pm$ 0.41	5.82 $\pm$ 0.44 (3.56)
15	–	7.38 $\pm$ 0.50	4.77 $\pm$ 0.48	3.90 $\pm$ 0.89	–	7.00 $\pm$ 0.53	5.76 $\pm$ 0.52 (3.48)
16	2.15 $\pm$ 0.20	1.67 $\pm$ 0.09	2.73 $\pm$ 1.37	1.35 $\pm$ 0.89	4.42 $\pm$ 0.25	2.37 $\pm$ 0.56	2.45 $\pm$ 0.34 (3.07)
17	–	5.14 $\pm$ 0.10	–	3.57 $\pm$ 0.81	–	–	4.35 $\pm$ 0.51 (1.57)
18	–	–	–	2.17 $\pm$ 0.36	–	–	–
19	–	5.14 $\pm$ 0.10	1.72 $\pm$ 0.39	3.57 $\pm$ 0.81	7.25 $\pm$ 1.94	2.24 $\pm$ 0.33	3.98 $\pm$ 0.65 (5.53)
20	–	6.4 $\pm$ 0.23	–	–	–	3.26 $\pm$ 0.82	4.58 $\pm$ 0.87 (3.14)
mean	6.52 $\pm$ 0.32	6.73 $\pm$ 0.37	5.48 $\pm$ 0.44	4.96 $\pm$ 0.35	5.18 $\pm$ 0.29	4.48 $\pm$ 0.52	5.48 $\pm$ 0.42
$\Delta$ (max–min)	8.71	11.66	9.63	8.73	4.5	6.9	7.62

was reduced in early summer and summer and was absent in winter. Regardless of season, sites near the towns of Trevignano Romano and Anguillara Sabazia had isotopic signatures of 3‰ to 6‰.

Earnings from parking meters near tourism structures and the lake shore increased from May to August, whereas earnings from parking meters further away from tourism structures and the lake shore were lower and did not vary in this period (Fig. 4 and Fig. S1 in the online supplementary material). Rainfall in the drainage basin of the lake varied between sampling times, being highest in autumn and lowest in winter (Fig. 4). The mean  $\delta^{15}\text{N}$  of sites assigned to the ‘high organic impact’ class was directly related to earnings from parking meters near tourism structures (Fig. 4) but was not related to rainfall ( $R^2 = 0.001$ ,  $p > 0.05$ ). In non-impacted sites it was related to neither earnings from parking meters nor rainfall (Fig. 4). Similarly, in moderate organic and inorganic impacted sites it was not related to earnings from parking meters ( $p$  always  $> 0.05$ ). On the other hand, in inorganic impacted sites  $\delta^{15}\text{N}$  decreased with increasing rainfall (Fig. 4) and was not related to earnings from parking meters ( $R^2 = 0.01$ ,  $p > 0.05$ ). Rainfall was not related to  $\delta^{15}\text{N}$  in non-impacted, moderate and high organic impacted sites ( $p$  always  $> 0.05$ ). Independently by the impact class,

$\delta^{15}\text{N}$  was never related with earnings from parking meters away from the shore ( $p$  always  $> 0.05$ ). Based on the linear regression between earnings from parking and  $\delta^{15}\text{N}$  in impacted sites (Table S3), we were able to determine thresholds in terms of the number of tourists and g of N per day that are expected to increase pollution levels in tourism sites from non-impacted to moderate organic and high organic impact (Fig. S2, on-line supplementary material).

**3.2. Translocation experiment**

The  $\delta^{15}\text{N}$  of epilithon collected on rocks moved from site 3 (a non-impacted site) to site 10 (high-organic impact) varied during the 30 days of the experiment (one-way ANOVA and Tukey post-hoc comparisons, Rock 1:  $F = 18.8$ ,  $p < 0.001$ ; Rock 2:  $F = 72.5$ ,  $p < 0.001$ ) (Fig. 5). For both rocks, the  $\delta^{15}\text{N}$  of epilithon that grew back on the scraped patches (R) did not differ from that of epilithon growing on rocks naturally present at site 10 (R vs. site 10, Rock 1:  $p = 0.22$ ; Rock 2:  $p = 0.11$ ), while it was higher than epilithic  $\delta^{15}\text{N}$  measured at site 3 before translocation (T0) (R vs. T0, Rock 1:  $p = 0.02$ ; Rock 2:  $p < 0.001$ ). The  $\delta^{15}\text{N}$  of the unscraped epilithon

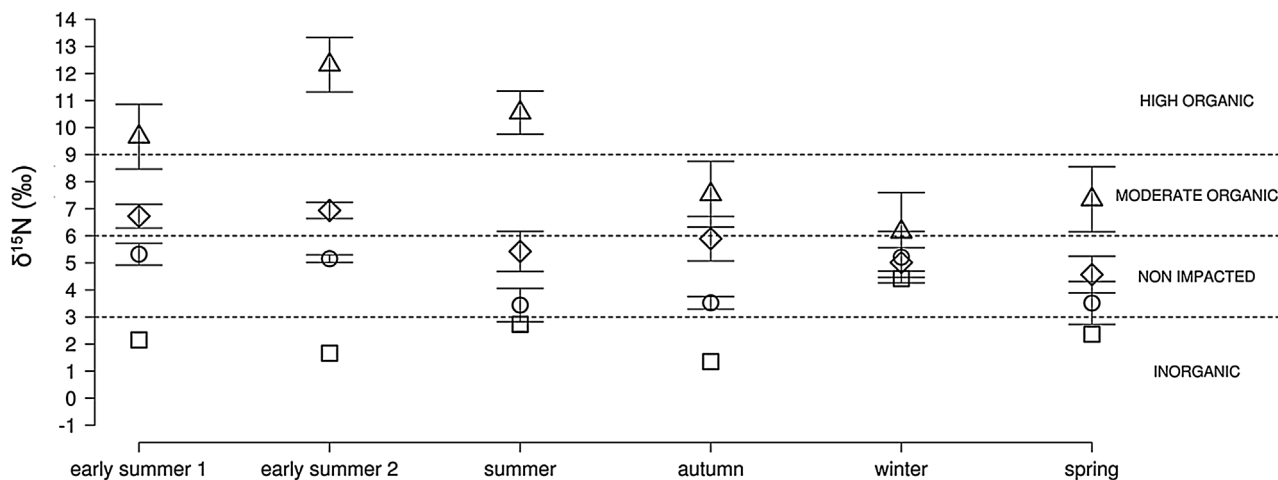


**Fig. 2.** Plot of the four impact class averages ( $\pm$  S.E.) at each sampling time. Legend: triangle = high organic signature, rhombus = moderate organic signature, circle = non-impacted signature, square = inorganic signature.

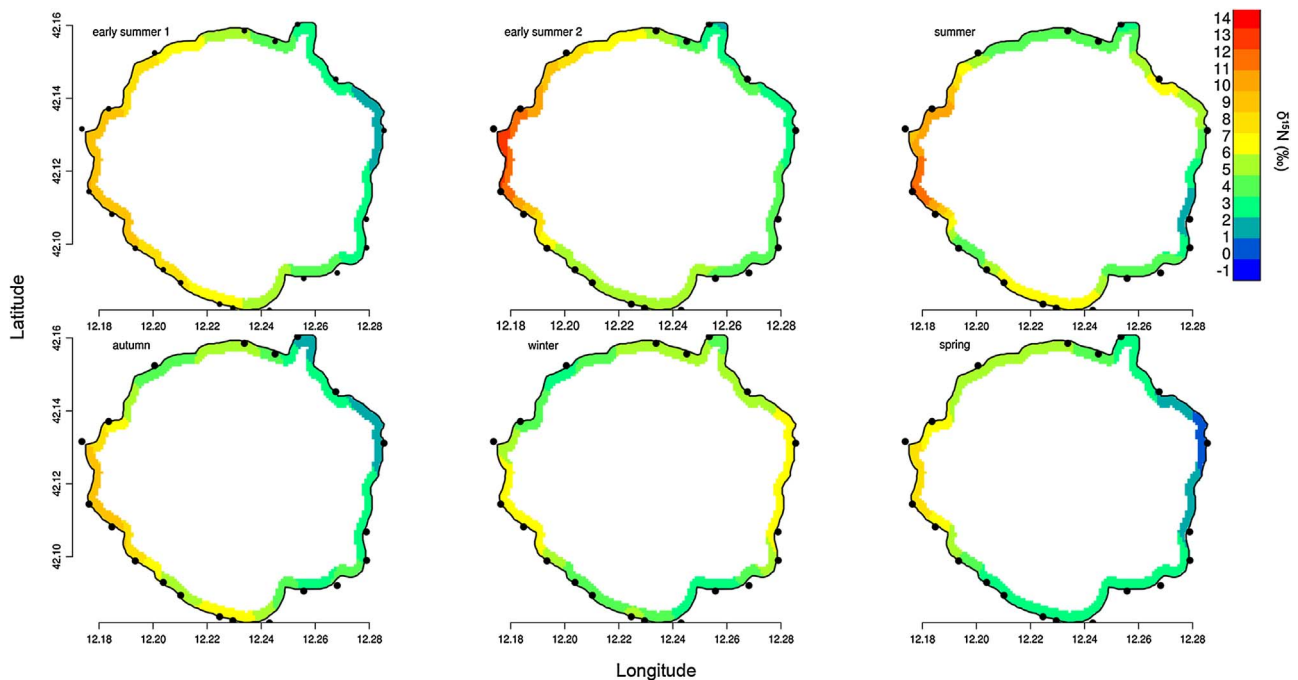


Fig. 3. Plot of GAM-predicted epilithic  $\delta^{15}\text{N}$  signatures along the littoral belt at all sampling times. Inorganic input range (blue)  $\delta^{15}\text{N} < 3\text{‰}$ , Non-impacted input range (green)  $3 \leq \delta^{15}\text{N} \leq 6\text{‰}$ , Moderate organic impacted range (yellow)  $6 < \delta^{15}\text{N} \leq 9\text{‰}$ , High organic impacted range (red)  $\delta^{15}\text{N} > 9\text{‰}$ .

taken from site 3 but left exposed to site 10 for one month (T1) also increased after translocation (T0 vs. T1, Rock 1:  $p = 0.03$ ; Rock 2:  $p < 0.001$ ) and was similar to the  $\delta^{15}\text{N}$  of epilithon that grew back on scraped patches (R vs. T1, Rock 1:  $p = 0.08$ ; Rock 2:  $p = 0.14$ ). Lastly, there was no difference between the  $\delta^{15}\text{N}$  of the epilithon that grew back on the two translocated rocks ( $p = 0.35$ ).

#### 4. Discussion

Our results indicate that epilithic  $\delta^{15}\text{N}$  signature represents a powerful tool in lacustrine environmental monitoring due to its ability to detect and record different types of anthropogenic nitrogen input in the water body. Indeed, consistent with our expectations and with previous research into macroalgal and epilithic  $\delta^{15}\text{N}$  signatures in several non-lacustrine aquatic ecosystems (Bentivoglio et al., 2016; Cejudo et al., 2014; Dailer et al., 2010; Jona-Lasinio et al., 2015; Pastor et al., 2014), we found that the magnitude and type of input reaching the lake littoral zone varied strongly in space and time. Accordingly, the  $\delta^{15}\text{N}$  values associated with these inputs were found to vary across sites and seasonally. It was shown how, for a lake affected by a variety of anthropic activities, especially tourism and agriculture, epilithic  $\delta^{15}\text{N}$  was able to describe both pulsed and more persistent inputs to the coastal waters. Based on  $\delta^{15}\text{N}$ , we were able to distinguish between N loadings of organic origin associated with short-term and seasonal pressures generated by tourism (on public holidays and in summer) and those of inorganic origin resulting from agricultural practices, which were dependent on runoff from agricultural areas.

Our sampling design, with six sampling times and a dense sampling grid with sites along the whole of the lake perimeter, enabled us to identify and describe potential sources of nitrogen in a space-time framework. Early summer was the period of greatest pressure from tourism, with agricultural inputs also being detected. This produced a broad range of epilithic  $\delta^{15}\text{N}$  signatures across sites. In the period of lowest human presence (winter), it was possible to recognise a decrease in the  $\delta^{15}\text{N}$  values of tourism-impacted sites and in the variability of  $\delta^{15}\text{N}$  along the lake perimeter. Indeed, tourism sites belonging to the high-organic impact class in early summer and summer approached non-impacted or moderate-organic impacted conditions in autumn and

winter. This suggests a meta-stable dynamics of tourism-related N pollution in the lake and the ability of the lake to recover on a seasonal temporal scale. In addition, the results obtained at site 10 in early summer 2 emphasise the presence of hidden inputs of nutrients. Inputs of nitrogen and phosphorous were also found in this part of the lake by Catalani et al. (2006). As in studies of benthic macroalgal  $\delta^{15}\text{N}$  (Orlandi et al., 2014) and river epilithic  $\delta^{15}\text{N}$  (Schiller et al., 2009), our study also had fine temporal resolution. Indeed, in sites with high organic impact,  $\delta^{15}\text{N}$  increased by 2.6‰ between early summer 1 and 2, in association with a 40% increase in tourism pressure (as measured by earnings from parking meters), suggesting that even short-term, pulsed inputs of anthropogenic N can be detected by means of isotopic analysis of epilithon. As expected with an efficient basin-wide wastewater collection system, the towns of Anguillara Sabazia in the South and Trevignano Romano (except after the public holiday) in the North remained in the non-impacted range. Lastly, anthropogenic inorganic N inputs were observed in the East-North East near greenhouses and crops. These inputs were evident in early summer 1, autumn and spring, suggesting that N inputs from agriculture are of a highly pulsed nature linked to discharge of fertiliser-derived N after rainfall. As for organic inputs, inorganic loadings were “absorbed” by the lake over a seasonal temporal scale and were completely absent in winter, when the agricultural activity in the lake basin drops.

The absence of a linear correlation between epilithic  $\delta^{15}\text{N}$  and nitrogen content was explained by the contrasting types of nitrogen input to the water body. Indeed, we would expect a positive linear correlation between  $\delta^{15}\text{N}$  and %N if the sole nitrogen input was organic, and a negative linear correlation if the sole nitrogen input was inorganic. Due to the fact that Lake Bracciano received two distinct kinds of input there was no evidence, at any of our sampling times, that high/low isotopic signatures were reflected in high/low epilithic nitrogen content.

Another advantage of epilithic  $\delta^{15}\text{N}$  signature, which arises from our translocation experiment, is the independence of isotopic values from the site-specific composition of the epilithon (MacLeod and Barton, 1998), meaning that the signatures were purely a function of local N inputs affecting the sampling site at different sampling times. While our translocation experiment was based on only two sites, this result is supported by the independence of  $\delta^{15}\text{N}$  from physicochemical

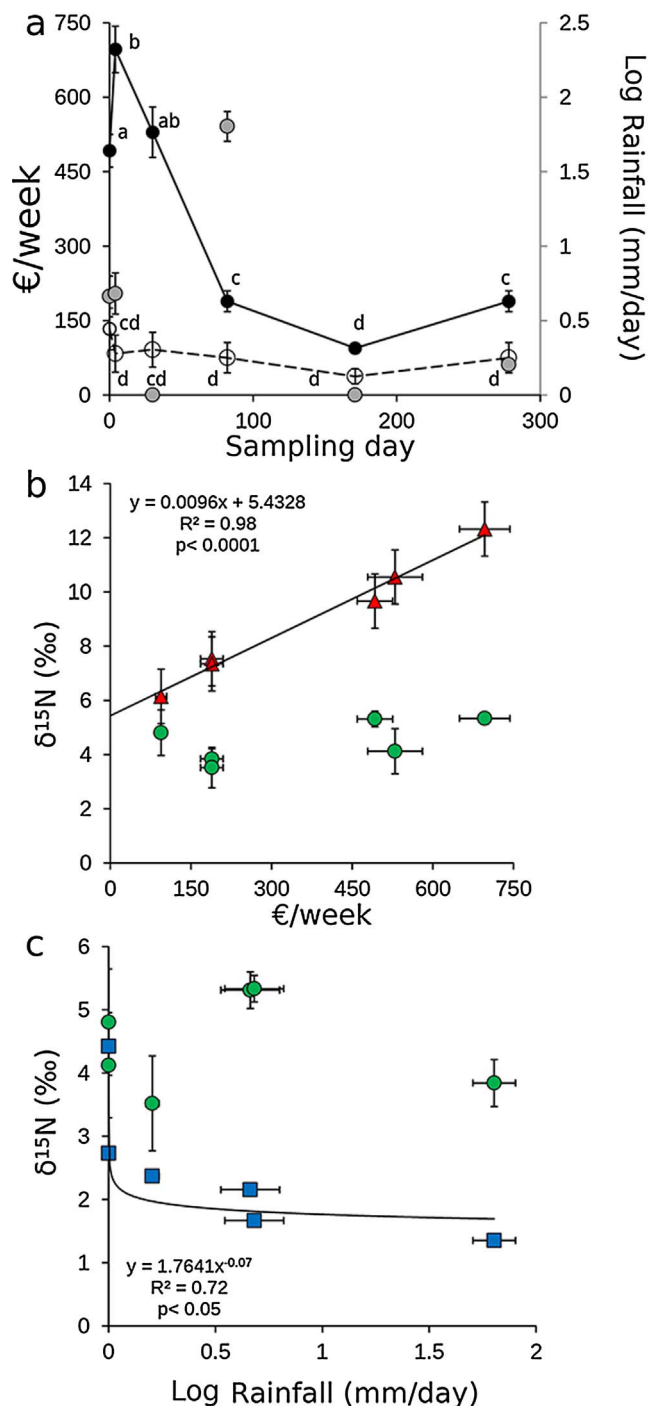


**Fig. 4.** Anthropogenic pressure, rainfall and  $\delta^{15}\text{N}$  in epilithon. **a:** Rainfall (as mean mm/day during the week preceding each sampling date, grey symbols), earnings from parking meters close to tourism structures on the lake shore (black symbols) and away from the lake shore (empty symbols). All parking meters are for non-residents. Different letters indicate a significant difference between sampling times (from day 0: early summer 1, to day 278: spring) and/or parking meter locations (two-way ANOVA and Tukey post-hoc comparisons,  $p < 0.05$ ). **b:** Relationship between earnings from parking meters close to tourism structures on the lake shore and  $\delta^{15}\text{N}$  in sites with high-organic impact (triangles) and in non-impacted sites (circles). **c:** Relationship between rainfall and  $\delta^{15}\text{N}$  in sites with inorganic impact (squares) and in non-impacted sites (circles). Linear regression is not shown when not significant ( $p > 0.05$ ).

parameters and distance between site pairs. It is also consistent with previous observations by MacLeod and Barton (1998), who found no effect of epilithic composition on its  $\delta^{15}\text{N}$  signature. This suggests that using epilithon to monitor N pollution does not necessarily require its

taxonomic identification, resulting in a less time-consuming and more practical technique.

## 5. Conclusions

Freshwater ecosystems provide indispensable ecosystem services (Page et al., 2012; Pimentel et al., 2004; Smith, 2003) but these same services expose them to various forms of anthropic disturbance, especially nitrogen loads derived from agriculture and sewage (Dodds et al., 1989; Matson et al., 1997; Vitousek et al., 1997). There is a strong need therefore for an accurate, practical and fast environmental monitoring tool. In marine, coastal, transitional water and lotic ecosystems, macroalgal and epilithic  $\delta^{15}\text{N}$  signatures have proved to be successful in determining the types and space-time variability of nitrogen loads (Bentivoglio et al., 2016; Cejudo et al., 2014; Cole et al., 2004; Dailer et al., 2010; Gartner et al., 2002; Jona-Lasinio et al., 2015; Orlandi et al., 2014; Pastor et al., 2013, 2014; Peipoch et al., 2012; Schiller et al., 2009; Titlyanov et al., 2011; Vizzini et al., 2005), while in lacustrine ecosystems there is a lack of knowledge concerning epilithic  $\delta^{15}\text{N}$  signatures.

Our study demonstrates that epilithic  $\delta^{15}\text{N}$  signatures fully satisfy the requirements for nitrogen input monitoring. Specifically, epilithic  $\delta^{15}\text{N}$  signatures can detect the source of the inputs, their nature (inorganic vs. organic, reflecting anthropic activities) and their temporal variation, with a temporal resolution of as little as four days. In greater detail, epilithic  $\delta^{15}\text{N}$  identified the critical season for each type of input, together with the main drivers linking N loading to anthropic activities in the lake basin. We were able to recognise the greatest and most persistent loads of organic nitrogen (from tourism) and inorganic nitrogen (from greenhouses and crops, transported by run-off) affecting the lake, although nutrient concentrations in water are below legal limits and the lake is classified as oligo-mesotrophic (Ferrara et al., 2002). This suggests that isotopic signatures are able to detect anthropogenic N inputs even at low concentrations, providing a monitoring tool that can detect early signs of ecological risk affecting the lake ecosystem. The independence of  $\delta^{15}\text{N}$  from epilithic composition and water physicochemical parameters, together with the widespread presence of epilithon in freshwater ecosystems, suggests that the proposed method is of potentially broad application. Therefore, even in cases where epilithon is absent, impacted or potentially impacted sites can still be monitored by using samples obtained elsewhere.

The results of our experiment suggest that epilithic isotopic signals represent a highly efficient and rapid method of monitoring a lake's nitrogen loads and that, when isotopic variation can be quantitatively related to anthropogenic pressure, as measured here with reference to earnings from parking meters, isotopic thresholds can be directly translated into practical management information for decision makers. The results of this study indicate the need for improvement of sewage treatment facilities (with an emphasis on organic nitrogen removal), implementation of wastewater re-use protocols, and the conservation or recovery of healthy littoral belts of the lake ecosystem that are able to absorb agricultural N inputs after rainy periods.

## Acknowledgements

We thank two anonymous Reviewers for their comments, which substantially improved the manuscript, and George Metcalf for revising the English text. We also thank the municipality of Trevignano Romano for its collaboration. This research was supported by Sapienza Starting Grants ("Avvio alla Ricerca") 2015-E. Calizza, PNRA 2013-L. Rossi and PNRA 2015-M.L. Costantini.

## Appendix A. Supplementary data

Supplementary data associated with this article can be found, in the online version, at <http://dx.doi.org/10.1016/j.ecolind.2017.04.007>.

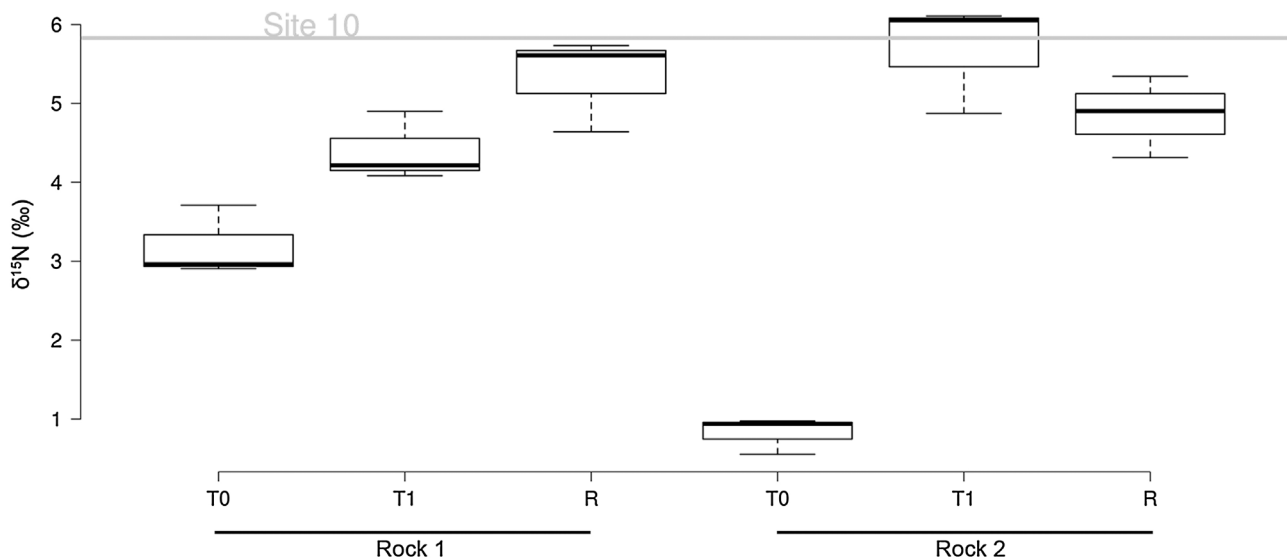


Fig. 5. Boxplot of transplant experiment. T0 = first sampling time, October, before the shift from site 3 to site 10. T1 = second sampling time, November, 30 days after the shift. R = regrown (on scraped patch) epilithic community. Rock 1 = first epilithic community. Rock 2 = second epilithic community. The grey line represents the autochthonous epilithic  $\delta^{15}\text{N}$  signature of site 10.

## References

- ACEA. Sustainability Report, 2015. <http://annualreport2015.acea.it/sustainability/download-area/>.
- Bentivoglio, F., Calizza, E., Rossi, D., Carlino, P., Careddu, G., Rossi, L., Costantini, M.L., 2016. Site-scale isotopic variations along a river course help localize drainage basin influence on river food webs. *Hydrobiologia* 770, 257–272. <http://dx.doi.org/10.1007/s10750-015-2597-2>.
- Burns, A., Ryder, D.S., 2001. Potential for biofilms as biological indicators in Australian riverine systems. *Ecol. Manage. Restor.* 2, 53–64. <http://dx.doi.org/10.1046/j.1442-8903.2001.00069.x>.
- Calizza, E., Rossi, L., Costantini, M.L., 2013a. Predators and resources influence phosphorus transfer along an invertebrate food web through changes in prey behaviour. *PLoS One* 8, e65186.
- Calizza, E., Costantini, M.L., Carlino, P., Bentivoglio, F., Orlandi, L., Rossi, L., 2013b. *Posidonia oceanica* habitat loss and changes in litter-associated biodiversity organization: a stable isotope-based preliminary study. *Estuar. Coast. Shelf. Sci.* 135, 137–145. <http://dx.doi.org/10.1016/j.ecss.2013.07.019>.
- Careddu, G., Costantini, M.L., Calizza, E., Carlino, P., Bentivoglio, F., Orlandi, L., Rossi, L., 2015. Effects of terrestrial input on macrobenthic food webs of coastal sea are detected by stable isotope analysis in Gaeta Gulf. *Estuar. Coast. Shelf. Sci.* 154, 158–168. <http://dx.doi.org/10.1016/j.ecss.2015.01.013>.
- Castenholz, R.W., 1960. Seasonal changes in the attached algae of freshwater and saline lakes in the Lower Grand Coulee, Washington. *Limnol. Oceanogr.* 5, 1–28. <http://dx.doi.org/10.4319/lo.1960.5.1.0001>.
- Catalani, A., Medici, F., Rinaldi, G., 2006. Bracciano's Lake waters: an experimental survey on the surface layer pollution. *Ann. Chim.* 96, 743–750.
- Cejudo, E., Schiff, S.L., Aravena, R.O., 2014. Epilithon isotope composition as an environmental archive in rivers receiving wastewater: the case of the Grand River, Ontario, Canada. *J. Water Sci.* 27, 213–219. <http://dx.doi.org/10.7202/1027807ar>.
- Ciannelli, L., Fauchald, P., Chan, K.S., Agostini, V.N., Dingsør, G.E., 2008. Spatial fisheries ecology: recent progress and future prospects. *J. Mar. Syst.* 71, 223–236. <http://dx.doi.org/10.1016/j.jmarsys.2007.02.031>.
- Cole, M.L., Valiela, I., Kroeger, K.D., Tomasky, G.L., Cebrian, J., Wigand, C., McKenney, R.A., Grady, S.P., Carvalho da Silva, M.H., 2004. Assessment of a  $\delta^{15}\text{N}$  isotopic method to indicate anthropogenic eutrophication in aquatic ecosystems. *J. Environ. Qual.* 33, 124–132. <http://dx.doi.org/10.2134/jeq2004.1240>.
- Colloca, F., Mastrantonio, G., Jona-Lasinio, G., Ligas, A., Sartor, P., 2014. *Parapenaeus longirostris* (Lucas, 1846) an early warning indicator species of global warming in the central Mediterranean Sea. *J. Mar. Syst.* 138, 29–39. <http://dx.doi.org/10.1016/j.jmarsys.2013.10.007>.
- Costantini, M.L., Zaccarelli, N., Mandrone, S., Rossi, D., Calizza, E., Rossi, L., 2012. NDVI spatial pattern and the potential fragility of mixed forested areas in volcanic lake watersheds. *For. Ecol. Manage.* 285, 133–141. <http://dx.doi.org/10.1016/j.foreco.2012.08.029>.
- Costantini, M.L., Calizza, E., Rossi, L., 2014. Stable isotope variation during fungal colonisation of leaf detritus in aquatic environments. *Fungal Ecol.* 11, 154–163. <http://dx.doi.org/10.1016/j.funeco.2014.05.008>.
- Costanzo, S.D., Udy, J., Longstaff, B., Jones, A., 2005. Using nitrogen stable isotope ratios ( $\delta^{15}\text{N}$ ) of macroalgae to determine the effectiveness of sewage upgrades: changes in the extent of sewage plumes over four years in Moreton Bay, Australia. *Mar. Pollut. Bull.* 51, 212–217. <http://dx.doi.org/10.1016/j.marpolbul.2004.10.018>.
- Dailer, M.L., Knox, R.S., Smith, J.E., Napier, M., Smith, C.M., 2010. Using  $\delta^{15}\text{N}$  values in algal tissue to map locations and potential sources of anthropogenic nutrient inputs on the island of Maui, Hawaii, USA. *Mar. Pollut. Bull.* 60, 655–671. <http://dx.doi.org/10.1016/j.marpolbul.2009.12.021>.
- Danilov, R.A., Ekelund, N.G.A., 2001. Comparison of usefulness of three types of artificial substrata (glass, wood and plastic) when studying settlement patterns of periphyton in lakes of different trophic status. *J. Microbiol. Meth.* 45, 167–170. [http://dx.doi.org/10.1016/S0167-7012\(01\)00247-0](http://dx.doi.org/10.1016/S0167-7012(01)00247-0).
- DeNicola, D.M., Eyto, E.D., Wemaere, A., Irvine, K., 2004. Using epilithic algal communities to assess trophic status in Irish lakes. *J. Phycol.* 40, 481–495. <http://dx.doi.org/10.1111/j.1529-8817.2004.03147.x>.
- Derse, E., Kneel, K.L., Wankel, S.D., Kendall, C., Berg, C.J., Paytan, A., 2007. Identifying sources of nitrogen to Hanalei Bay, Kauai, utilizing the nitrogen isotope signature of macroalgae. *Environ. Sci. Technol.* 41, 5217–5223. <http://dx.doi.org/10.1021/es0700449>.
- di Lascio, A., Rossi, L., Costantini, M.L., 2011. Different temperature tolerance of northern and southern European populations of a freshwater Isopod Crustacean species (*Asellus aquaticus* L.). *Foundam. Appl. Limnol.* 179, 193–201.
- di Lascio, A., Rossi, L., Carlino, P., Calizza, E., Rossi, D., Costantini, M.L., 2013. Stable isotope variation in macroinvertebrates indicates anthropogenic disturbance along an urban stretch of the river Tiber (Rome, Italy). *Ecol. Indic.* 28, 107–114. <http://dx.doi.org/10.1016/j.ecolind.2012.04.006>.
- Dodds, W.K., Johnson, K.R., Priscu, J.C., 1989. Simultaneous nitrogen and phosphorus deficiency in natural phytoplankton assemblages: theory, empirical evidence, and implications for lake management. *Lake Reserv. Manag.* 5, 21–26. <http://dx.doi.org/10.1080/07438148909354677>.
- Ferrara, O., Vagagnini, D., Margaritora, F.G., 2002. Zooplankton abundance and diversity in lake Bracciano, Latium, Italy. *J. Limnol.* 61, 169–175. <http://dx.doi.org/10.4081/jlimnol.2002.169>.
- Fink, P., Peters, L., Von Elert, E., 2006. Stoichiometric mismatch between littoral invertebrates and their periphyton food. *Arch. Hydrobiol.* 165, 145–165. <http://dx.doi.org/10.1127/0003-9136/2006/0165-0145>.
- Galloway, J.N., Aber, J.D., Erisman, J.W., Seitzinger, S.P., Howarth, R.W., Cowling, E.B., Cosby, B.J., 2003. The nitrogen cascade. *Bioscience* 53, 341–356.
- Gartner, A., Lavery, P., Smit, A.J., 2002. Use of  $\delta^{15}\text{N}$  signatures of different functional forms of macroalgae and filter-feeders to reveal temporal and spatial patterns in sewage dispersal. *Mar. Ecol. Prog. Ser.* 235, 63–73. <http://dx.doi.org/10.3354/meps235063>.
- Harrison, S.S.C., 1998. Patterns in the epilithic community of a lake littoral. *Freshw. Biol.* 39, 477–492. <http://dx.doi.org/10.1046/j.1365-2427.1998.00296.x>.
- Hawes, I., Smith, R., 1994. Seasonal dynamics of epilithic periphyton in oligotrophic Lake Taupo, New Zealand. *N. Z. J. Mar. Freshw. Res.* 28, 1–12. <http://dx.doi.org/10.1080/00288330.1994.9516592>.
- ISTAT, 2016. <http://demo.istat.it/index.html>.
- Jona-Lasinio, G., Costantini, M.L., Calizza, E., Pollice, A., Bentivoglio, F., Orlandi, L., Careddu, G., Rossi, L., 2015. Stable isotope-based statistical tools as ecological indicator of pollution sources in Mediterranean transitional water ecosystems. *Ecol. Indic.* 55, 23–31. <http://dx.doi.org/10.1016/j.ecolind.2015.03.006>.
- Jones, R.I., King, L., Dent, M.M., Maberly, S.C., Gibson, C.E., 2004. Nitrogen stable isotope ratios in surface sediments, epilithon and macrophytes from upland lakes with differing nutrient status. *Freshw. Biol.* 49, 382–391. <http://dx.doi.org/10.1111/j.1365-2427.2004.01194.x>.
- Kahlert, M., Hasselrot, A.T., Hillebrand, H., Pettersson, K., 2002. Spatial and temporal variation in the biomass and nutrient status of epilithic algae in Lake Erken, Sweden. *Freshw. Biol.* 47, 1191–1215. <http://dx.doi.org/10.1046/j.1365-2427.2002.00844.x>.
- Kendall, C., Elliott, E.M., Wankel, S.D., 2007. Tracing anthropogenic inputs of nitrogen to ecosystems. In: Michener, R.H., Lajtha, K. (Eds.), *Stable Isotopes in Ecology and*



- Environmental Science. Blackwell Publishing, pp. 375–449 Chapter 12.
- Maberly, S.C., King, L., Dent, M.M., Jones, R.I., Gibson, C.E., 2002. Nutrient limitation of phytoplankton and periphyton growth in upland lakes. *Freshw. Biol.* 47, 2136–2152. <http://dx.doi.org/10.1046/j.1365-2427.2002.00962.x>.
- MacLeod, N.A., Barton, D.R., 1998. Effects of light intensity, water velocity, and species composition on carbon and nitrogen stable isotope ratios in periphyton. *Can. J. Fish. Aquat. Sci.* 55, 1919–1925. <http://dx.doi.org/10.1139/f98-075>.
- Mancinelli, G., Costantini, M.L., Rossi, L., 2007. Top-down control of reed detritus processing in a lake littoral zone: experimental evidence of a seasonal compensation between fish and invertebrate predation. *Int. Rev. Hydrobiol.* 2007 (92), 117–134. <http://dx.doi.org/10.1002/iroh.200510962>.
- Mancinelli, G., Carrozzo, L., Costantini, M.L., Rossi, L., Marini, G., Pinna, M., 2013. Occurrence of the Atlantic blue crab *Callinectes sapidus* Rathbun, 1896 in two Mediterranean coastal habitats: temporary visitor or permanent resident? *Estuar. Coast. Shelf. Sci.* 135, 46–56. <http://dx.doi.org/10.1016/j.ecss.2013.06.008>.
- Margaritora, F.G., Bazzanti, M., Ferrara, O., Mastrantuono, L., Seminara, M., Vagaggini, D., 2003. Classification of the ecological status of volcanic lakes in Central Italy. *J. Limnol.* 62, 49–59. <http://dx.doi.org/10.4081/jlimnol.2003.s1.49>.
- Mastrantuono, L., Solimini, A.G., Nôges, P., Bazzanti, M., 2008. Plant-associated invertebrates and hydrological balance in the large volcanic Lake Bracciano (Central Italy) during two years with different water levels. *Hydrobiologia* 599, 143–152. <http://dx.doi.org/10.1007/s10750-007-9196-9>.
- Matson, P.A., Parton, W.J., Power, A.G., Swift, M.J., 1997. Agricultural intensification and ecosystem properties. *Science* 277, 504–509. <http://dx.doi.org/10.1126/science.277.5325.504>.
- Mazza, R., Taviani, S., Capelli, G., De Benedetti, A.A., Giordano, G., 2015. Quantitative hydrogeology of volcanic lakes: examples from the central Italy volcanic lake district. In: Rouwet, D., Christenson, B., Tassi, F., Vandemeulebrouck, J. (Eds.), *Volcanic Lakes*. Springer, Berlin, Heidelberg, pp. 355–377. <http://dx.doi.org/10.1007/978-3-642-36833-2>. Chapter 15.
- Orlandi, L., Bentivoglio, F., Carlino, P., Calizza, E., Rossi, D., Costantini, M.L., Rossi, L., 2014.  $\delta^{15}\text{N}$  variation in *Ulva lactuca* as a proxy for anthropogenic nitrogen inputs in coastal areas of Gulf of Gaeta (Mediterranean Sea). *Mar. Pollut. Bull.* 84, 76–82. <http://dx.doi.org/10.1016/j.marpolbul.2014.05.036>.
- Page, T., Heathwaite, A.L., Moss, B., Reynolds, C., Beven, K.J., Pope, L., Willows, R., 2012. Managing the impacts of nutrient enrichment on river systems: dealing with complex uncertainties in risk analyses. *Freshw. Biol.* 57, 108–123. <http://dx.doi.org/10.1111/j.1365-2427.2012.02756.x>.
- Pagnotta, R., Barbiero, G., 2003. Stima dei carichi inquinanti nell'ambiente marino-costiero. *Ann. Ist. Sup. Sanità* 39, 3–10.
- Pastor, A., Peipoch, M., Cañas, L., Chappuis, E., Ribot, M., Gacia, E., Riera, J.L., Marty, E., Sabater, F., 2013. Nitrogen stable isotopes in primary uptake compartments across streams differing in nutrient availability. *Environ. Sci. Technol.* 47, 10155–10162. <http://dx.doi.org/10.1021/es400726e>.
- Pastor, A., Riera, J.L., Peipoch, M., Cañas, L., Ribot, M., Gacia, E., Martí, E., Sabater, F., 2014. Temporal variability of nitrogen stable isotopes in primary uptake compartments in four streams differing in human impacts. *Environ. Sci. Technol.* 48, 6612–6619. <http://dx.doi.org/10.1021/es405493k>.
- Peipoch, M., Martí, E., Gacia, E., 2012. Variability in  $\delta^{15}\text{N}$  natural abundance of basal resources in fluvial ecosystems: a meta-analysis. *Freshw. Sci.* 31, 1003–1015. <http://dx.doi.org/10.1899/11-157.1>.
- Pimentel, D., Berger, B., Filiberto, D., Newton, M., Wolfe, B., Karabinakis, E., Clark, S., Poon, E., Abbott, E., Nandagopal, S., 2004. Water resources: agricultural and environmental issues. *Bioscience* 54, 909–918.
- Ponsard, S., Ardití, R., 2000. What can stable isotopes ( $\delta^{15}\text{N}$  and  $\delta^{13}\text{C}$ ) tell about the food web of soil macro-invertebrates? *Ecology* 81, 852–864.
- Rossi, L., Costantini, M.L., Brilli, M., 2007. Does stable isotope analysis separate transgenic and traditional corn (*Zea mays* L.) detritus and their consumers? *Appl. Soil. Ecol.* 35, 449–453. <http://dx.doi.org/10.1016/j.apsoil.2006.09.001>.
- Rossi, L., Costantini, M.L., Carlino, P., Di Lascio, A., Rossi, D., 2010. Autochthonous and allochthonous plant contributions to coastal benthic detritus deposits: a dual-stable isotope study in a volcanic lake. *Aquat. Sci.* 72, 227–236. <http://dx.doi.org/10.1007/s00027-009-0125-z>.
- Round, F.E., 1991. Diatoms in river water-monitoring studies. *J. Appl. Phycol.* 3, 129–145. <http://dx.doi.org/10.1007/BF00003695>.
- Sabancı, F.Ç., 2011. Relationship of epilithic diatom communities to environmental variables in Homa lagoon (Izmir, Turkey). *Aquat. Biol.* 13, 233–241.
- Schiller, D.V., Martí, E., Riera, J.L., 2009. Nitrate retention and removal in Mediterranean streams bordered by contrasting land uses: a  $^{15}\text{N}$  tracer study. *Biogeosciences* 6, 181–196. <http://dx.doi.org/10.5194/bg-6-181-2009>.
- Smith, V.H., 2003. Eutrophication of freshwater and coastal marine ecosystems a global problem. *Environ. Sci. Poll. Res.* 10, 126–139. <http://dx.doi.org/10.1065/espr2002.12.142>.
- Titlyanov, E.A., Kiyashko, S.I., Titlyanova, T.V., Huyen, P.V., Yakovleva, I.M., 2011. Identifying nitrogen sources for macroalgal growth in variously polluted coastal areas of southern Vietnam. *Bot. Mar.* 54, 367–376. <http://dx.doi.org/10.1515/bot.2011.041>.
- Vilmi, A., Karjalainen, S.M., Landeiro, V.L., Heino, J., 2015. Freshwater diatoms as environmental indicators: evaluating the effects of eutrophication using species morphology and biological indices. *Environ. Monit. Assess.* 187, 243–252. <http://dx.doi.org/10.1007/s10661-015-4485-7>.
- Vitousek, P.M., Aber, J.D., Howarth, R.W., Likens, G.E., Matson, P.A., Schindler, D.W., Schlesinger, W.H., Tilman, D.G., 1997. Human alteration of the global nitrogen cycle: sources and consequences. *Ecol. Appl.* 7, 737–750. [http://dx.doi.org/10.1890/1051-0761\(1997\)007\[0737:HAOTGN\]2.0.CO;2](http://dx.doi.org/10.1890/1051-0761(1997)007[0737:HAOTGN]2.0.CO;2).
- Vizzini, S., Savona, B., Do Chi, T., Mazzola, A., 2005. Spatial variability of stable carbon and nitrogen isotope ratios in a Mediterranean coastal lagoon. *Hydrobiologia* 550, 73–82. <http://dx.doi.org/10.1007/s10750-005-4364-2>.
- Watkins, E.M., Schindler, D.W., Turner, M.A., Findlay, D., 2001. Effects of solar ultraviolet radiation on epilithic metabolism, and nutrient and community composition in a clear-water boreal lake. *Can. J. Fish. Aquat. Sci.* 58, 2059–2070. <http://dx.doi.org/10.1139/f01-150>.
- Wetzel, R.G., 2001. Rivers and lakes. Their distribution, origins and forms. In: Wetzel, R.G. (Ed.), *Limnology: Lake and River Ecosystems*. Gulf Professional Publishing, pp. 15–42 Chapter 3.
- Yokoyama, H., Ishihi, Y., 2006. Seasonal variation in  $\delta^{13}\text{C}$  and  $\delta^{15}\text{N}$  of epilithic microalgae in Gokasho Bay. *Plankton Benthos Res.* 1, 208–213. <http://dx.doi.org/10.3800/pbr.1.208>.
- Zuur, A., Ieno, E.N., Smith, G.M., 2007. Beginner's guide to GAM with R. In: Zuur, A., Ieno, E.N., Smith, G.M. (Eds.), *Analyzing Ecological Data*. Springer, Science & Business Media, pp. 97–124. <http://dx.doi.org/10.1007/978-0-387-45972-1>. Chapter 7.
- Zuur, A.F., Ieno, E.N., Walker, N.J., Saveliev, A.A., Smith, G.M., 2009. Things are not always linear; additive modelling, chapter 3. In: Zuur, A., Ieno, E.N., Walker, N., Saveliev, A.A., Smith, G.M. (Eds.), *Mixed Effects Models and Extensions in Ecology with R*. Springer, New York, pp. 35–69. <http://dx.doi.org/10.1007/978-0-387-87458-6>.

## Chapter 2

### **Lake water quality for human use and tourism in Central Italy (Rome).**

Calizza, Edoardo<sup>1</sup>, **Fiorentino, Federico**<sup>1</sup>, Careddu, Giulio<sup>1</sup>, Rossi, Loreto<sup>1,2,\*</sup>, Costantini, Maria Letizia<sup>1,2</sup>.

<sup>1</sup> Department of Environmental Biology, Sapienza University of Rome, Via dei Sardi 70, 00185 Rome, Italy

<sup>2</sup> CoNISMa, Piazzale Flaminio 9, 00100 Rome, Italy

**Corresponding Author:** loreto.rossi@uniroma1.it (L. Rossi).

Manuscript published in *WIT Transactions on Ecology and the Environment*

# LAKE WATER QUALITY FOR HUMAN USE AND TOURISM IN CENTRAL ITALY (ROME)

EDOARDO CALIZZA<sup>1</sup>, FEDERICO FIORENTINO<sup>1</sup>, GIULIO CAREDDU<sup>1</sup>,  
LORETO ROSSI<sup>1,2</sup> & MARIA LETIZIA COSTANTINI<sup>1,2</sup>

<sup>1</sup>Department of Environmental Biology, Sapienza University of Rome, Italy

<sup>2</sup>CoNISMa, Italy

## ABSTRACT

The lakes in the Italian region of Lazio, and in particular Lake Bracciano, have suffered due to reduced rainfall during the most recent years (1264.8 mm in 2014 vs 308.4 mm in 2015 and 883.6 mm in 2016 in Lake Bracciano). Moreover, Lake Bracciano exhibits both a direct water withdrawal (as drinkable water for the city of Rome and several other towns), and an indirect one, by the groundwaters, for agriculture. The 1.5 m water reduction, never observed in the last two decades, bared over 10 m of the littoral zone with the consequent exposition of gravel shores, trashes and reduction of the bottom areas involved in the denitrification process. This condition poses a threat to the ecosystem and to the human profits in term of eutrophication, healthy water loss, ship handling difficulties, touristic boats included, and tourism decline. In a previous investigation, we sampled the epilithic algae in the littoral zone of Lake Bracciano and estimated their nitrogen isotopic signature ( $\delta^{15}\text{N}$ ). We highlighted the presence of diffuse organic and inorganic nitrogen inputs not intercepted by the wastewater collection system. These inputs, in synergy with water-level reduction, are able to undermine the ecosystem structure and health. In this paper, we show the nitrogen isotopic signatures, and their sources, as euros gained by parking meters for non-residents. We highlight the role of the touristic pressure not intercepted by the wastewater treatment plant in terms of  $\delta^{15}\text{N}$  increase during the most critical season (i.e. summer). The results show strong increases of euros gained and consequent  $\delta^{15}\text{N}$  signature increases ( $9\% < \delta^{15}\text{N} < 17\%$ ) from the end of June to the middle of August. We provide evidence supporting the need to adopt management policies to preserve the ecosystem services and related human health and earnings.

*Keywords: Epilithon, nitrogen inputs,  $\delta^{15}\text{N}$ , volcanic lake.*

## 1 INTRODUCTION

Lake ecosystems represent impressive and irreplaceable sources of ecosystem services, including drinkable water, irrigation water for agriculture, fishing and leisure activities [1]–[3]. On the other hand, human activities can determine nutrient inputs, especially nitrogen and phosphorus, in the water body [4]–[9] and turn them to pressures. In lacustrine ecosystems nitrogen enrichment can enhance algal blooms with severe consequences for ecosystem, human health and profits [10]–[12]. Therefore, the identification of the organic/inorganic origin and seasonal dynamics of inputs is essential in order to establish the proper management initiatives.

Lake Bracciano [13]–[16], located north of Rome in the Central Italian Volcanic Lake District (CIVOILD), represents an interesting case of study since it: (1) is a regional park since 1999, (2) exhibits several human activities (from agriculture and fisheries to recreation and tourism especially in Summer), (3) is the water source for the CO.B.I.S. (Consorzio del Bacino Idrico Sabatino, which includes the towns of Anguillara-Sabazia, Bracciano, Manziana, Oriolo-Romano and Trevignano Romano) population and (4) is the main drinking water reservoir for the city of Rome, by direct water extraction [17]. The latter two points are particularly crucial. As a matter of fact, direct (as drinkable water) and indirect (for agriculture) withdrawals together with rainfall reductions (1264.8 mm in 2014 vs. 308.4 mm in 2015 and 883.6 mm in 2016), produced an alarming water level decline, never observed



in the last decades [18]. In fact, the water level has reduced by 1.5 meters, thus exposing 10 meters of bare littoral zone [19]. This alarming condition of the hydrological balance can affect the benthic community [20] and the denitrification processes [21] with consequent nitrogen accumulation, which, in turn, can promote algal blooms [22] and boost the deterioration of water quality and ecosystem services.

In a previous work [23], we were able to identify the different types of nitrogen inputs (both organic and inorganic) affecting the Lake Bracciano littoral zone and their space-time dynamics (related to the different human activity magnitudes along the whole perimeter in a yearlong monitoring study), by the nitrogen isotopic signature of the epilithic association,  $\delta^{15}\text{N}$ . Epilithic  $\delta^{15}\text{N}$  turned out to be a very flexible, easy to collect and manipulate, and species-specific independent monitoring tool [23]. Using the  $\delta^{15}\text{N}$  values, we were able to identify the organic impacted area in the western littoral side of the lake. This side, in summer, was characterized by a high touristic pressure, partially not intercepted by the wastewater collection system, reflected by  $\delta^{15}\text{N}$  values over the threshold of the 6‰ and 9‰ and therefore classifiable, respectively, as moderate organic and highly organic impacted [23].

Aims of this paper are to quantify the relationship between organic  $\delta^{15}\text{N}$  and tourism activities in this zone (in terms of parking meters earnings), to estimate the  $\delta^{15}\text{N}$  values especially in July and August and to provide reasonable evidence for the pressing needs for management policies of Lake Bracciano especially during the summer season.

## 2 MATERIALS AND METHODS

Lake Bracciano (42°07'16"N; 12°13'55"E) is a volcanic lake located in central Italy, 32 km northwest of Rome (Lazio, Italy). It has a surface area of 57 km<sup>2</sup> and a perimeter of about 31.5 km. Its elevation is 164 m a.s.l. and its maximum depth is 165 m. The lake is oligo-mesotrophic, and warm monomictic from May to October and homothermic from November to February [13]. It has a theoretical renewal time of 137 years, and is used as a drinking water reservoir for the city of Rome and the Vatican State. To prevent the local urban wastewater discharges in the water body a centralized collection system was built in the early 80s. This collection system is able to serve 40,000 inhabitants, but the present-day CO.B.I.S. population is around 49,000 inhabitants and increases in summer [24].

The combined action of climate change and water extraction produces dangerous water level variations that drastically change the shape of the shoreline and inshore bathymetry. Since 1999, the lake and its surroundings have been part of the regional park of Bracciano Martignano. Due the presence of a high touristic enterprise concentration [23] we chose three sampling sites (namely, A, B and C; Fig. 1) in the western side of the lake, characterized by a high level of anthropic activities on the lakeshore (bar, restaurants, beach resorts etc.). Moreover, we considered the earnings of four parking meters, in parking areas on the lakeshore used by non-residents, to be a proxy for tourism pressure. Earnings were measured weekly from the beginning of May to the end of August. The cost of parking was €1 per hour per car. The parking meters do not operate from October to March.

### 2.1 Field procedures

Samplings were performed from June 2015 to March 2016 (six sampling dates). In each sampling date and at each sampling site (three sites: A, B and C), three small patches (5 × 5 cm) of epilithic association were carefully scraped with a single-edge razor from three similar and smooth volcanic rocks (approximately 30 × 15 × 7 cm) from shallow waters. Samples were stored in Petri plates and conserved in ice for transport in laboratory.







Figure 1: Location of the three sampling sites (A, B, C) in Lake Bracciano.

## 2.2 Laboratory procedures

Samples were conserved at  $-80^{\circ}\text{C}$  before freeze-drying for 24 hours and ground to a fine homogenous powder using a ball mill (Fritsch Mini-Mill Pulverisette 23 with a zirconium oxide ball). For each epilithic sample, two replicates ( $2.0 \pm 0.2$  mg) were sub-sampled and pressed into ultra-pure tin capsules and analysed using an Elementar Vario Micro-Cube elemental analyser (Elementar Analysensysteme GmbH, Germany) coupled with an IsoPrime100 isotope mass ratio spectrometer (Isoprime Ltd., Cheadle Hulme, UK). The obtained nitrogen (N) stable isotope ratios ( $^{15}\text{N}:^{14}\text{N}$ ) were expressed in  $\delta$  units, as parts per thousand deviations from international standards (atmospheric  $\text{N}_2$ ), in accordance with the following equations:  $\delta R(\text{‰}) = [(R_{\text{SAMPLE}} - R_{\text{STANDARD}}) / (R_{\text{STANDARD}}) * 10^3]$  [25], where R is the heavy-to-light isotope ratio of the element. The internal laboratory standard was IAEA-600 Caffeine. Measurement errors were found to be typically smaller than  $\pm 0.05\text{‰}$ . In accordance with Cole et al. [26], Derse et al. [27] and Kendall et al. [28], four impact classes were identified: ‘inorganic input’ ( $\delta^{15}\text{N} < 3\text{‰}$ ), ‘non-impacted’ ( $3\text{‰} \leq \delta^{15}\text{N} \leq 6\text{‰}$ ), ‘moderate organic input’ ( $6\text{‰} < \delta^{15}\text{N} \leq 9\text{‰}$ ) and ‘high organic input’ ( $\delta^{15}\text{N} > 9\text{‰}$ ).

## 2.3 Statistical analysis

An ANOVA (significance level  $\alpha = 0.05$ ) was applied to test the presence of significant differences in euro earnings of the parking meters between May, June, July and August, followed by a Tukey post-hoc test. We then performed a linear regression between the earnings of the parking meters and the days from starting date. The records had a time lag of 7 days, so we considered the first record as day 0 and the last one as day 119 (18 weeks). We therefore estimated the  $\delta^{15}\text{N}$  values during the whole study period as a function of average euros earned according with our previous study [23].

### 3 RESULTS

Results show an increasing anthropic presence in the lake during summer as indicated by the increasing amount of the euro earnings (Fig. 2(a) and (b); ANOVA,  $F = 41.94$ ,  $p < 0.001$ ) and a consequent increase of organic N input as indicated by the estimated  $\delta^{15}\text{N}$  values. In particular, the anthropic pressure abruptly increased at the end of June (during a public holiday for the entire municipality of Rome, 29<sup>th</sup> June) and July, and remained high in August with a peak on 15<sup>th</sup> August (a national public holiday; Fig. 2(a) at day 105). The Tukey post-hoc test (Fig. 2(b)) found statistically significant differences ( $p < 0.001$ ) between May/June and July/August, but not between May and June and between July and August. The linear regression between the euros earnings and the days from the beginning of records showed a strong linear increasing (Fig. 3(a);  $t = 6.083$ ,  $p < 0.001$ ,  $R^2 = 0.68$ ) with a slope of  $7.04 (\pm 1.16)$  euros\*day and an intercept of  $105.21 (\pm 80.68)$ . Estimated  $\delta^{15}\text{N}$  signatures from the 56<sup>th</sup> day (end of June) to the 119<sup>th</sup> day (end of August), were always over the threshold of 9‰, and then classifiable as typically high organic input signatures (Fig. 3(b)).

### 4 DISCUSSION

It is widely recognized that tourism represents a strong pressure for various aquatic ecosystems, both marine [29], [30] and freshwater [5], [6], [10]. On the other hand, a lack of knowledge of its effect in lacustrine ecosystems persists and the lake littoral zone might be a useful zone to sample in order to intercept the touristic pressure [31], [32]. Moreover, physicochemical environmental monitoring methods only provide snapshots of ecosystem trophic conditions, and therefore several sampling dates are required and pulse inputs, like the first nitrogen isotopic peak observed in our study, are likely to be missed [33] especially if they occur during holidays. On the contrary stable isotopes analysis is a flexible and reliable tool employed in trophic ecology and environmental monitoring since the stable nitrogen isotope ratio ( $\delta^{15}\text{N}$ ), as sensitive indicator of N sources in many ecosystems, is rapidly integrated, similarly to the radioisotopes, in fast growing organisms and algae and, thus, in the benthic food webs [34]–[41].

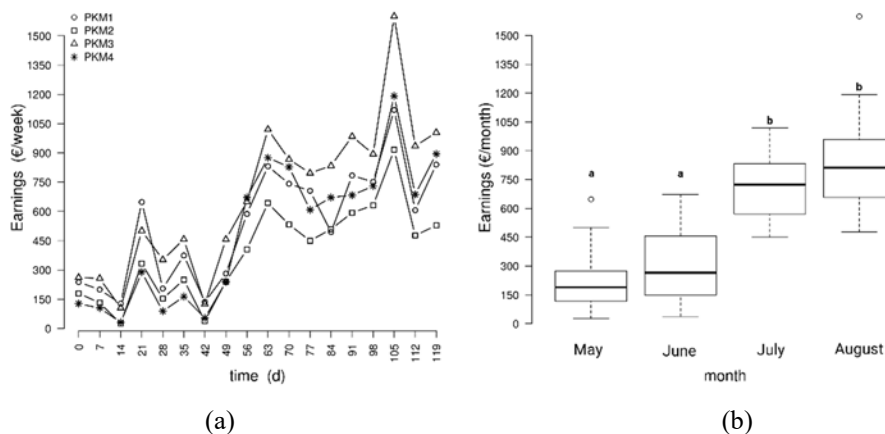


Figure 2: Euros earned by parking meters. (a) The lines represent the euro amounts earned by each parking meters, PKM1, PKM2, PKM3, PKM4, for non-residents from May (day 0) to August (day 119); (b) Box plots of the earnings of parking meters during the observed months. Different letters above the box plot indicate significant differences between months (Tukey post hoc test,  $\alpha = 0.05$ ).

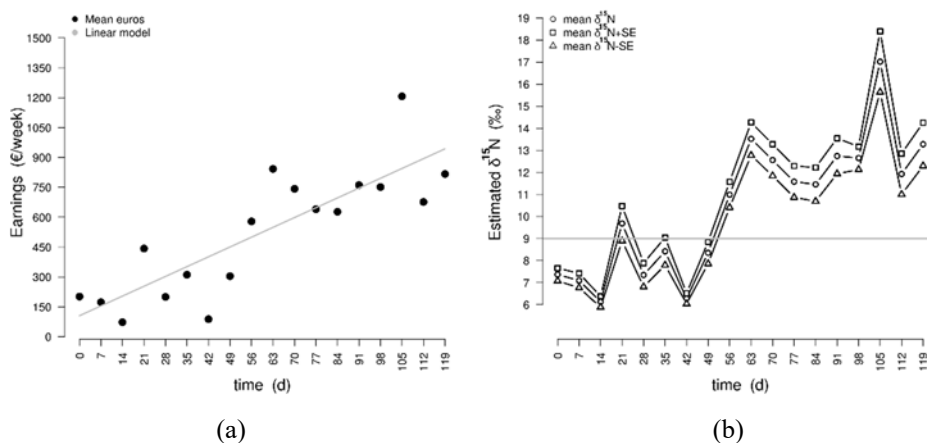


Figure 3: Euros and estimated  $\delta^{15}\text{N}$  (‰) trends. (a) Plot of linear model, significance level  $\alpha = 0.05$ , between mean euros earned by the four parking meters and days; (b) Plot of estimated mean  $\delta^{15}\text{N}$  (‰): circle = mean  $\delta^{15}\text{N}$  signatures, square = mean  $\delta^{15}\text{N} + \text{standard error (SE)}$ , triangle = mean  $\delta^{15}\text{N} - \text{standard error (SE)}$ . The high organic signature threshold (9‰) is reported.

Our results indicate that summer is a critical season, in terms of organic nitrogen inputs, for Lake Bracciano. As a matter of fact, from the beginning of May to the end of June the parking meters for the non-residents earned similar amounts, and, from the end of June to the end of August, globally showed a linear increasing trend in their incomes. Moreover, in the period considered, there were two peaks characterized by abrupt increases of anthropic pressure on the lake shores both related to public holidays (29<sup>th</sup> July and 15<sup>th</sup> August). As a consequence of the higher human pressure, in May and June the estimated  $\delta^{15}\text{N}$  signatures were above the non-impacted range whereas during the summer season (late June, July and August), the estimated  $\delta^{15}\text{N}$  signatures were in the high organic input range, with a maximum  $\delta^{15}\text{N}$  value comprised between  $15.64\text{‰} < \delta^{15}\text{N} < 18.39\text{‰}$ . Such nitrogen isotopic signatures can be considered as the worst case, assuming a high response degree of  $\delta^{15}\text{N}$  signatures to increasing parking meter earnings (i.e. a high response degree of nitrogen isotopic signatures and touristic pressure). Similar isotopic values, associated with tourism, had been detected in surface sediments of eutrophic lakes [42] and in marine macroalgae [29], [43], [44], therefore providing a proxy of the effects of tourism on water bodies.

## 5 CONCLUSIONS

Lake Bracciano already suffers from the effect of climate change and direct water extraction and our results indicated that, during the late summer season (July and August), the non-residents anthropic pressure on Lake Bracciano shores rapidly increased, threatening the water healthiness and ecosystem health. The high estimated  $\delta^{15}\text{N}$  signatures were over the threshold of high organic inputs in late June, July and August, in accordance with our previous work [23].

For its high naturalistic, social and economic values, there is the necessity of management policies adoption and, primarily, an “upgrade” of the wastewater treatment plant compared to the current and inadequate 40,000 units, especially where the concentration of touristic



activities is high, and especially during the public holidays, when the touristic pressure and related  $\delta^{15}\text{N}$  signatures reached their respective peaks.

#### ACKNOWLEDGEMENTS

This research was supported by Sapienza Starting Grants (“Avvio alla Ricerca”) 2015-E. Calizza, PRNA 2013-L. Rossi and PNRA 2015-M.L. Costantini, ATENEO 2015 Costantini.

#### REFERENCES

- [1] Page, T., Heathwaite, A.L., Moss, B., Reynolds, C., Beven, K.J., Pope, L. & Willows, R., Managing the impacts of nutrient enrichment on river systems: Dealing with complex uncertainties in risk analyses. *Freshwater Biology*, **57**(s1), pp. 108–123, 2012.
- [2] Pimentel, D., Berger, B., Filiberto, D., Newton, M., Wolfe, B., Karabinakis, E., Clark, S., Poon, E., Abbett, E. & Nandagopal, S., Water resources: Agricultural and environmental issues. *BioScience*, **54**(10), pp. 909–918, 2004.
- [3] Smith, V.H., Eutrophication of freshwater and coastal marine ecosystems a global problem. *Environmental Science and Pollution Research*, **10**(2), pp. 126–139, 2003.
- [4] Derse, E., Knee, K.L., Wankel, S.D., Kendall, C., Berg, C.J. & Paytan, A., Identifying sources of nitrogen to Hanalei Bay, Kauai, utilizing the nitrogen isotope signature of macroalgae. *Environmental Science & Technology*, **41**(15), pp. 5217–5223, 2007.
- [5] di Lascio, A., Rossi, L., Carlino, P., Calizza, E., Rossi, D. & Costantini, M.L., Stable isotope variation in macroinvertebrates indicates anthropogenic disturbance along an urban stretch of the river Tiber (Rome, Italy). *Ecological Indicators*, **28**, pp. 107–114, 2013.
- [6] Galloway, J.N., Aber, J.D., Erisman, J.W., Seitzinger, S.P., Howarth, R.W., Cowling, E.B. & Cosby, B.J., The nitrogen cascade. *Bioscience*, **53**(4), pp. 341–356, 2003.
- [7] Matson, P.A., Parton, W.J., Power, A.G. & Swift, M.J., Agricultural intensification and ecosystem properties. *Science*, **277**(5325), pp. 504–509, 1997.
- [8] Vilmi, A., Karjalainen, S.M., Landeiro, V.L. & Heino, J., Freshwater diatoms as environmental indicators: Evaluating the effects of eutrophication using species morphology and biological indices. *Environmental Monitoring and Assessment*, **187**(5), pp. 1–10, 2015.
- [9] Vitousek, P.M., Aber, J.D., Howarth, R.W., Likens, G.E., Matson, P.A., Schindler, D.W., Schlesinger, W.H. & Tilman, D.G., Human alteration of the global nitrogen cycle: Sources and consequences. *Ecological Applications*, **7**(3), pp. 737–750, 1997.
- [10] Xu, H., Paerl, H.W., Qin, B., Zhu, G. & Gao, G., Nitrogen and phosphorus inputs control phytoplankton growth in eutrophic Lake Taihu, China. *Limnology and Oceanography*, **55**(1), pp. 420–432, 2010.
- [11] Jankowski, K., Schindler, D.E. & Holtgrieve, G.W., Assessing nonpoint-source nitrogen loading and nitrogen fixation in lakes using  $\delta^{15}\text{N}$  and nutrient stoichiometry. *Limnology and Oceanography*, **57**(3), pp. 671–683, 2012.
- [12] Hadwen, W.L., Bunn, S.E., Arthington, A.H. & Mosisch, T.D., Within-lake detection of the effects of tourist activities in the littoral zone of oligotrophic dune lakes. *Aquatic Ecosystem Health & Management*, **8**(2), pp. 159–173, 2005.
- [13] Ferrara, O., Vagaggini, D. & Margaritora, F.G., Zooplankton abundance and diversity in Lake Bracciano, Latium, Italy. *Journal of Limnology*, **61**(2), pp. 169–175, 2002.
- [14] Margaritora, F.G., Bazzanti, M., Ferrara, O., Mastrantuono, L., Seminara, M. & Vagaggini, D., Classification of the ecological status of volcanic lakes in Central Italy. *Journal of Limnology*, **62**(1s), pp. 49–59, 2003.



- [15] Rossi, L., Costantini, M.L., Carlino, P., di Lascio, A. & Rossi, D., Autochthonous and allochthonous plant contributions to coastal benthic detritus deposits: A dual-stable isotope study in a volcanic lake. *Aquatic Science*, **72**(2), pp. 227–230, 2010.
- [16] Costantini, M.L., Zaccarelli, N., Mandrone, S., Rossi, D., Calizza, E. & Rossi, L., NDVI spatial pattern and the potential fragility of mixed forested areas in volcanic lake watersheds. *Forest Ecology and Management*, **285**, pp. 133–141, 2012.
- [17] ACEA, Sustainability Report. [www.annualreport2015.acea.it/sustainability/download-area/](http://www.annualreport2015.acea.it/sustainability/download-area/). Accessed on: 28 Apr. 2017.
- [18] Osservatorio Meteorologico di Anguillara-Sabazia, <http://www.anguillara-meteo.com/noaa/NOAA.php>. Accessed on: 28 Apr. 2017.
- [19] Rossi, D., Variazioni della linea di costa del lago di Bracciano in relazione al nuovo modello 3D bati-morfologico del fondale. *Proceedings of the Sixteenth Meeting of the Italian Society of Ecology*, 2006.
- [20] Wantzen, K.M., Rothhaupt, K.O., Mörtl, M., Cantonati, M., László, G. & Fischer, P., Ecological effects of water-level fluctuations in lakes: An urgent issue. *Ecological Effects of Water-Level Fluctuations in Lakes*, ed. Springer Netherlands, pp. 1–4, 2008.
- [21] Strosnider, W.H., Hitchcock, D.R., Burke, M.K. & Lewitus, A.J., Predicting hydrology in wetlands designed for coastal stormwater management. *ASABE*, paper no. 077084, pp. 1–17, 2007.
- [22] Paerl, H.W., Hall, N.S. & Calandrino, E.S., Controlling harmful cyanobacterial blooms in a world experiencing anthropogenic and climatic-induced change. *Science of the Total Environment*, **409**(10), pp. 1739–1745, 2011.
- [23] Fiorentino, F., Cicala, D., Careddu, G., Calizza, C., Jona-Lasinio, G., Rossi, L. & Costantini, M.L., Epilithon  $\delta^{15}\text{N}$  signatures indicate the origins of nitrogen loading and its seasonal dynamics in a volcanic Lake. *Ecological Indicators*, **79**, pp. 19–27, 2017.
- [24] ISTAT, 2016. <http://demo.istat.it/index.html>. Accessed on: 28 Apr. 2017.
- [25] Ponsard, S. & Arditì, R., What can stable isotopes ( $\delta^{15}\text{N}$  and  $\delta^{13}\text{C}$ ) tell about the food web of soil macro-invertebrates? *Ecology*, **81**(3), pp. 852–864, 2000.
- [26] Cole, M.L., Valiela, I., Kroeger, K.D., Tomasky, G.L., Cebrian, J., Wigand, C., McKenney, R.A., Grady, S.P. & Carvalho da Silva, M.H., Assessment of a  $\delta^{15}\text{N}$  isotopic method to indicate anthropogenic eutrophication in aquatic ecosystems. *Journal of Environmental Quality*, **33**(1), pp. 124–132, 2004. <http://dx.doi.org/10.2134/jeq2004.1240>
- [27] Derse, E., Knee, K.L., Wankel, S.D., Kendall, C., Berg, C.J. & Paytan, A., Identifying sources of nitrogen to Hanalei Bay, Kauai, utilizing the nitrogen isotope signature of macroalgae. *Environmental Science & Technology*, **41**(15), pp. 5217–5223, 2007.
- [28] Kendall, C., Elliott, E.M. & Wankel, S.D., Tracing anthropogenic inputs of nitrogen to ecosystems. *Stable Isotopes in Ecology and Environmental Science*, Blackwell Publishing, pp. 375–449, 2007.
- [29] Mwaura, J., Umezawa, Y., Nakamura, T. & Kamau, J., Evidence of chronic anthropogenic nutrient within coastal lagoon reefs adjacent to urban and tourism centers, Kenya: A stable isotope approach. *Marine Pollution Bulletin*, forthcoming.
- [30] Orlandi, L., Bentivoglio, F., Carlino, P., Calizza, E., Rossi, D., Costantini, M.L. & Rossi, L.,  $\delta^{15}\text{N}$  variation in *Ulva lactuca* as a proxy for anthropogenic nitrogen inputs in coastal areas of Gulf of Gaeta (Mediterranean Sea). *Marine Pollution Bulletin*, **84**(1), pp. 76–82, 2014.
- [31] Hadwen, W.L., Bunn, S.E., Arthington, A.H. & Mosisch, T.D., Within-lake detection of the effects of tourist activities in the littoral zone of oligotrophic dune lakes. *Aquatic Ecosystem Health & Management*, **8**(2), pp. 159–173, 2005.



- [32] Mancinelli, G., Costantini, M.L. & Rossi, L., Top-down control of reed detritus processing in a lake littoral zone: experimental evidence of a seasonal compensation between fish and invertebrate predation. *International Review of Hydrobiology*, **92**(2), pp. 117–134, 2007.
- [33] Gartner, A., Lavery, P. & Smit, A.J., Use of  $\delta^{15}\text{N}$  signatures of different functional forms of macroalgae and filter-feeders to reveal temporal and spatial patterns in sewage dispersal. *Marine Ecology Progress Series*, **235**, pp. 63–73, 2002.
- [34] Calizza, E., Rossi, L. & Costantini, M.L., Predators and resources influence phosphorus transfer along an invertebrate food web through changes in prey behaviour. *PLoS One*, **8**(6), e65186, 2013.
- [35] Calizza, E., Costantini, M. L., Carlino, P., Bentivoglio, F., Orlandi, L. & Rossi, L., Posidonia oceanica habitat loss and changes in litter-associated biodiversity organization: A stable isotope-based preliminary study. *Estuarine, Coastal and Shelf Science*, **135**, pp. 137–145, 2013.
- [36] Careddu, G., Costantini, M.L., Calizza, E., Carlino, P., Bentivoglio, F., Orlandi, L. & Rossi, L., Effects of terrestrial input on macrobenthic food webs of coastal sea are detected by stable isotope analysis in Gaeta Gulf. *Estuarine, Coastal and Shelf Science*, **154**, pp. 158–168, 2015.
- [37] Jona-Lasinio, G., Costantini, M.L., Calizza, E., Pollice, A., Bentivoglio, F., Orlandi, L., Careddu, G. & Rossi, L., Stable isotope-based statistical tools as ecological indicator of pollution sources in Mediterranean transitional water ecosystems. *Ecological Indicators*, **55**, pp. 23–31, 2015.
- [38] Rossi, L., Costantini, M.L. & Brillì, M., Does stable isotope analysis separate transgenic and traditional corn (*Zea mays* L.) detritus and their consumers? *Applied Soil Ecology*, **35**(2), pp. 449–453, 2007.
- [39] Costantini, M.L., Calizza, E. & Rossi, L., Stable isotope variation during fungal colonisation of leaf detritus in aquatic environments. *Fungal Ecology*, **11**, pp. 154–163, 2014.
- [40] Mancinelli, G., Carrozzo, L., Costantini, M.L., Rossi, L., Marini, G. & Pinna, M., Occurrence of the Atlantic blue crab *Callinectes sapidus* Rathbun, 1896 in two Mediterranean coastal habitats: Temporary visitor or permanent resident? *Estuarine, Coastal and Shelf Science*, **135**, pp. 46–56, 2013.
- [41] di Lascio, A., Rossi, L. & Costantini, M.L., Different temperature tolerance of northern and southern European populations of a freshwater Isopod Crustacean species (*Asellus aquaticus* L.). *Fundamental and Applied Limnology*, **179**(3), pp. 193–201, 2011.
- [42] Wu, J., Lin, L., Gagan, M.K., Schleser, G.H. & Wang, S., Organic matter stable isotope ( $\delta^{13}\text{C}$ ,  $\delta^{15}\text{N}$ ) response to historical eutrophication of Lake Taihu, China. *Hydrobiologia*, **563**(1), pp. 19–29, 2006.
- [43] Titlyanov, E.A., Kiyashko, S.I., Titlyanova, T.V., Huyen, P.V. & Yakovleva, I.M., Identifying nitrogen sources for macroalgal growth in variously polluted coastal areas of southern Vietnam. *Botanica Marina*, **54**(4), pp. 367–376, 2011.
- [44] Lin, H.J., Wu, C.Y., Kao, S.J., Kao, W.Y. & Meng, P.J., Mapping anthropogenic nitrogen through point sources in coral reefs using  $\delta^{15}\text{N}$  in macroalgae. *Marine Ecology Progress Series*, **335**, pp. 95–109, 2007.



## Chapter 3

### **Nitrogen and metal pollution in the Southern Caspian Sea: a multiple approach to biomonitoring**

Costantini, Maria Letizia<sup>1,2</sup>, Agah, Homira<sup>3</sup>, **Fiorentino, Federico**<sup>1</sup>, Irandoost, Farnaz<sup>1</sup>, Trujillo, Francisco James Leon<sup>4</sup>, Careddu, Giulio<sup>1</sup>, Calizza, Edoardo<sup>1,2,\*</sup>, Rossi, Loreto<sup>1,2</sup>.

<sup>1</sup> Department of Environmental Biology, Sapienza University of Rome, Via dei Sardi 70, 00185, Rome, Italy

<sup>2</sup> National Inter-University Consortium for Marine Sciences (CoNISMa), Piazzale Flaminio 9, 00196, Rome, Italy

<sup>3</sup> Iranian National Institute for Oceanography and Atmospheric Sciences (INIOAS), No. 3, Etemadzadeh St., Fatemi Ave., 1411813389 Tehran, Iran

<sup>4</sup> University of Lima, Av. Javier Prado Este 4600, Santiago de Surco 15023, Perú

**Corresponding Author:** edoardo.calizza@uniroma1.it (E. Calizza)

Manuscript submitted to *Environmental Science and Pollution Research*

# Environmental Science and Pollution Research

## Nitrogen and metal pollution in the Southern Caspian Sea: a multiple approach to biomonitoring --Manuscript Draft--

<b>Manuscript Number:</b>							
<b>Full Title:</b>	Nitrogen and metal pollution in the Southern Caspian Sea: a multiple approach to biomonitoring						
<b>Article Type:</b>	Research Article						
<b>Keywords:</b>	Coastal waters; Environmental monitoring; Macroalgae; Sediment; Nitrogen stable isotopes; Trace elements						
<b>Corresponding Author:</b>	Edoardo Calizza, Ph.D. Sapienza University of Rome Rome, ITALY						
<b>Corresponding Author Secondary Information:</b>							
<b>Corresponding Author's Institution:</b>	Sapienza University of Rome						
<b>Corresponding Author's Secondary Institution:</b>							
<b>First Author:</b>	Maria Letizia Costantini, Associate Professor						
<b>First Author Secondary Information:</b>							
<b>Order of Authors:</b>	Maria Letizia Costantini, Associate Professor Homira Agah, Professor Federico Fiorentino, PhD candidate Farnaz Irandoost, PhD candidate Francisco James Leon Trujillo Giulio Careddu, PhD Edoardo Calizza, Ph.D. Loreto Rossi, Full Professor						
<b>Order of Authors Secondary Information:</b>							
<b>Funding Information:</b>	<table border="1"> <tr> <td>Sapienza Università di Roma (Progetti di Ateneo 2016)</td> <td>Prof. Loreto Rossi</td> </tr> <tr> <td>Programma Nazionale di Ricerche in Antartide (2015/AZ1.01)</td> <td>Prof. Maria Letizia Costantini</td> </tr> <tr> <td>Programma Nazionale di Ricerche in Antartide (2016_00291)</td> <td>Prof. Loreto Rossi</td> </tr> </table>	Sapienza Università di Roma (Progetti di Ateneo 2016)	Prof. Loreto Rossi	Programma Nazionale di Ricerche in Antartide (2015/AZ1.01)	Prof. Maria Letizia Costantini	Programma Nazionale di Ricerche in Antartide (2016_00291)	Prof. Loreto Rossi
Sapienza Università di Roma (Progetti di Ateneo 2016)	Prof. Loreto Rossi						
Programma Nazionale di Ricerche in Antartide (2015/AZ1.01)	Prof. Maria Letizia Costantini						
Programma Nazionale di Ricerche in Antartide (2016_00291)	Prof. Loreto Rossi						
<b>Abstract:</b>	<p>The Caspian Sea hosts areas of high ecological value as well as several productive human activities that dump in the water body different kinds of pollutants. This complexity calls for effective monitoring tools necessary to plan proper water resource management and conservation. Here, we aimed at detecting anthropic sources of Nitrogen inputs, by N stable isotope analysis of macroalgae, and trace metals in macroalgae and sediments along the Iranian coast of the Caspian Sea. <math>\delta^{15}\text{N}</math> values in macroalgae detected both inorganic and organic pollution sources. Inorganic inputs, especially in the eutrophic western waters, were associated with inland agricultural activities, while organic inputs were detected in urbanized and touristic areas in association with high dissolved N and low dissolved O<sub>2</sub>. Metal concentrations ranged from non-impacted to heavily impacted values. Localized peaks of Pb and Zn were observed in an area potentially affected by byproducts of mining activity transported</p>						



	<p>downstream by river discharge. By contrast, Cr and Ni concentrations were high in all sampling sites, thus potentially representing hazardous elements for marine biota. The observed differences in pollution levels suggest that isotopic biomonitoring coupled with metal analysis of sediments and macroalgae can represent an effective approach for determining the origin and distribution of pollution sources even in complex coastal areas. In particular, the use of macroalgae demonstrated the potential of isotopic analysis for detecting the dominant N source of pollution also at low N concentrations.</p>
<b>Suggested Reviewers:</b>	<p>Alberto Basset, PhD Full Professor, University of Salento alberto.basset@unisalento.it</p> <p>Maurizio Pinna, PhD University of Salento maurizio.pinna@unisalento.it</p> <p>Salvatrice Vizzini University of Palermo salvatrice.vizzini@unipa.it</p>
<b>Opposed Reviewers:</b>	
<b>Additional Information:</b>	
<b>Question</b>	<b>Response</b>
§Are you submitting to a Special Issue?	No

[Click here to view linked References](#)

# Nitrogen and metal pollution in the Southern Caspian Sea: a multiple approach to biomonitoring

Maria Letizia Costantini<sup>1,2</sup>, Homira Agah<sup>3</sup>, Federico Fiorentino<sup>1</sup>, Farnaz Irandoost<sup>1</sup>, Francisco James Leon Trujillo<sup>4</sup>, Giulio Careddu<sup>1</sup>, Edoardo Calizza<sup>1,2,\*</sup>, Loreto Rossi<sup>1,2</sup>.

<sup>1</sup>Department of Environmental Biology, Sapienza University of Rome, Via dei Sardi 70, 00185, Rome, Italy

<sup>2</sup>National Inter-University Consortium for Marine Sciences (CoNISMa), Piazzale Flaminio 9, 00196, Rome, Italy

<sup>3</sup>Iranian National Institute for Oceanography and Atmospheric Sciences (INIOAS), No. 3, Etemadzadeh St., Fatemi Ave., 1411813389 Tehran, Iran

<sup>4</sup>University of Lima, Av. Javier Prado Este 4600, Santiago de Surco 15023, Perú

\*Corresponding Author Email: [edoardo.calizza@uniroma1.it](mailto:edoardo.calizza@uniroma1.it), Telephone: +390649917803

## Abstract

The Caspian Sea hosts areas of high ecological value as well as several productive human activities that dump in the water body different kinds of pollutants. This complexity calls for effective monitoring tools necessary to plan proper water resource management and conservation. Here, we aimed at detecting anthropic sources of Nitrogen inputs, by N stable isotope analysis of macroalgae, and trace metals in macroalgae and sediments along the Iranian coast of the Caspian Sea.  $\delta^{15}\text{N}$  values in macroalgae detected both inorganic and organic pollution sources. Inorganic inputs, especially in the eutrophic western waters, were associated with inland agricultural activities, while organic inputs were detected in urbanized and touristic areas in association with high dissolved N and low dissolved  $\text{O}_2$ . Metal concentrations ranged from non-impacted to heavily impacted values. Localized peaks of Pb and Zn were observed in an area potentially affected by byproducts of mining activity transported downstream by river discharge. By contrast, Cr and Ni concentrations were high in all sampling sites, thus potentially representing hazardous elements for marine biota. The observed differences in pollution levels suggest that isotopic biomonitoring coupled with metal analysis of sediments and macroalgae can represent an effective approach for determining the origin and distribution of pollution sources even in complex coastal areas. In particular, the use of macroalgae demonstrated the potential of isotopic analysis for detecting the dominant N source of pollution also at low N concentrations.

**Keywords:** Coastal waters; Environmental monitoring; Macroalgae; Sediment; Nitrogen stable isotopes; Trace elements

## Acknowledgements

This research was supported by Ateneo-Sapienza 2016 (L. Rossi), Programma Nazionale di Ricerche in Antartide-2015/AZ1.01 (M.L. Costantini), and Programma Nazionale di Ricerche in Antartide-2016\_00291 (L. Rossi).

## Introduction

1 Aquatic systems are often affected by anthropic activities taking place both on land and nearshore (Shahrban  
2 and Etemad-Shahidi 2010; Sohrabi et al. 2010), which poses a threat for the structure and functioning of coastal  
3 ecosystems (Halpern et al. 2008; Paerl et al. 2014). Indeed, industrial and agricultural activities, as well as wastewater  
4 discharges associated with resident population and tourism, dump different types of inputs, notably nutrients (Dailer et  
5 al. 2010; Halpern et al. 2008) and trace metals (Goher et al. 2014; Pekey et al. 2004), which can reduce the water  
6 quality up to the inability of its use. In particular, the release of excess concentration of Nitrogen and Phosphorus can  
7 result in coastal eutrophication (Howarth and Marino 2006; Paerl et al. 2014), and consequent algal blooms, hypoxia  
8 and fish kills (Diaz and Rosenberg 2008; Paerl et al. 2016). In parallel, metals can directly and indirectly affect the  
9 aquatic biota (Adel et al. 2017) and, through biomagnification along food chains (Goher et al. 2014; Saghali et al.  
10 2014), can reach humans with consequent risks for health (Agah et al. 2011; Dadar et al. 2016; Hosseini et al. 2013).

11 Among others, closed seas represent peculiar habitats of high ecological value, which are highly exposed to pollution  
12 impacts due to confinement and a long residence time of their water mass (Bastami et al. 2015; de Mora et al. 2004).  
13 Situated in the western Asia, the Caspian Sea is the largest closed water body on our planet. Due to its long isolation  
14 time, it shows a high level of endemism and offers a wide range of ecological niches (Bastami et al. 2015). On the other  
15 hand, being a land-locked system (Sohrabi et al. 2010), pollutants resulting from human activities persist in the water  
16 body, undermining the water quality and associated ecosystem services (de Mora et al. 2004). Various sources of  
17 pollution, such as river discharge, onshore industrial and municipal wastewater and offshore and onshore oil extraction,  
18 threaten the Caspian Sea. Its water quality is also influenced by the water level fluctuations, which can increase water  
19 pollution from the flooded coastal zones, when water level rises, and can determine strong impacts on coastal  
20 settlements and agriculture. In recent decades the water mass is reducing due to increasing evaporation rate (Chen et al.  
21 2017), mainly affecting the shallow northern side, but having also adverse effects on the southern part of the water body  
22 where the majority of the water mass is dislocated (Chen et al. 2017). This sector hosts areas of high ecological value  
23 (Sadeghi et al. 2012), and represents a crucial area for human activities, including tourism, fish farming, agriculture,  
24 manufacturing and oil extraction (Abadi et al. 2018; Ebadi and Hisoriev 2017, Hasani et al. 2017). In this complex  
25 context, a proper description of potential pollution sources, origin and dispersion is challenging but mandatory to  
26 address management and mitigation actions aimed at preserving the quality of the water resource and the integrity of the  
27 underlying ecological system. Indeed, while long range transport of pollution may represent a major issue for the  
28 management of the water resource in wide and transnational water basins (as it is the case for the Caspian Sea), the  
29 identification of local pollution sources is necessary to achieve an effective management by regional and national  
30 Authorities (Zonn 2005).

31 Recently, Nitrogen stable isotope signature ( $\delta^{15}\text{N}$ ) of primary producers, especially macroalgae in brackish and  
32 marine ecosystems (Orlandi et al. 2014, 2017; Rossi et al. 2018; Jona-Lasinio et al. 2015; Vizzini et al. 2005) and  
33 epilithon in freshwater ecosystems (Bentivoglio et al. 2016; Fiorentino et al. 2017), has been recognized as a robust  
34 technique for the environmental monitoring of organic and inorganic inputs in waters (Dailer et al. 2010; Heaton, 1986;  
35 Korom, 1992; Kreitler and Jones, 1975; Kreitler 1979; Mariotti et al., 1982; Rossi et al. 2018). On the other hand,  
36 macroalgae are widely recognized as a powerful tool for the monitoring of metal pollution in marine ecosystems due to  
37 their ability to bind metals (Astorga-España et al. 2008), leading their concentrations to several orders of magnitude  
38 higher than that measured in waters (Villares et al. 2001). Macroalgae are common in polluted sites and easy to sample  
39 (Astorga-España et al. 2008; Dailer et al. 2010). Their use was thus successful in order to obtain spatial and temporal  
40 information on bioavailability of these pollutants (Chakraborty et al. 2014). However, a complete description of  
41  
42  
43  
44  
45  
46

1 pollution pathways in coastal areas needs to take into account pollutants' concentration in the sediments (Bastami et al.  
2 2017), which are sink for metals released into an environment and provides a stable record of deposition history (Agah  
3 et al. 2012; Bastami et al. 2014; Goher et al. 2014; Villares et al. 2001).

4 Aim of the present study is to test the effectiveness of stable isotope monitoring in algae, combined with  
5 sediment analysis, to locate pollution sources and thus disentangle the complex mosaic of land and marine inputs of  
6 Nitrogen and trace metals affecting heavily anthropised coastal areas. More specifically, in this case study we  
7 investigated the anthropogenic sources of pollution in the southern littoral zone of the Caspian Sea, a unique ecosystem  
8 threatened by multiple anthropogenic stressors (Zonn 2005). We focused on the Gilan province, near the city of Bandar-  
9 e Anzalī, and the Mazandaran province. The first one, with its wetlands, is an important site for migratory birds (Zamani  
10 Hargalani et al. 2014; Sadeghi et al. 2012), while the second one is the most densely populated Iranian province (Ziarati  
11 et al. 2014). We hypothesized that inorganic and organic anthropogenic N inputs were reflected respectively in a  
12 decrease and increase of  $\delta^{15}\text{N}$  values measured in algae (Calizza et al. 2015; Jona-Lasinio et al. 2015; Orlandi et al.  
13 2014; Rossi et al. 2018). In parallel, we measured metal concentrations in algae and sediment in order to (i) compare  
14 pollution levels in these two basal food sources supporting the coastal food web, and (ii) provide a comprehensive  
15 description of anthropogenic pollution affecting the coastal area.  
16  
17  
18  
19  
20  
21  
22  
23

## 24 **Materials and methods**

### 25 *Study area*

26 The Caspian Sea, denoted as a sea or a lake, is the largest inland water body in the world (de Mora et al. 2004),  
27 with a total surface of  $\approx 371,000 \text{ Km}^2$  and a maximum depth of 1025 m. It accounts for  $\approx 40\text{-}44\%$  of the total lacustrine  
28 waters in the world (Bastami et al. 2015), and it is surrounded by Azerbaijan, Federation of Russia, Islamic Republic of  
29 Iran, Kazakhstan and Turkmenistan.  
30  
31  
32  
33

34 Samplings were carried out between May and June 2016 along the Iranian coast, in the Southern Caspian Sea.  
35 Sampling sites included the city of Bandar-e Anzalī (37°48'07"N and 49°47'15"E) in the Gilan Province, and 4 sites in  
36 the Mazandaran Province (Fig. 1): the urbanized beaches of Hachirud (36°69'11"N and 51°34'54"E), Radio Darya  
37 (36°68'16"N and 51°43'64"E), Nowshahr (36°65'40"N and 51°50'61"E), and the beach of Sisangan (36°58'62"N and  
38 51°79'03"E), located in front of the Sisangan forest National Park. The sampling site at Bandar-e Anzalī (hereafter  
39 Anzali) was located in the sandy shoreline of the city (around 150000 inhabitants) and it was potentially exposed to  
40 wastewater and agricultural inputs, as well as pollution derived by the harbor and local industry (Sadeghi et al. 2012,  
41 2013). This area is affected by the discharge of the Sefid-Rud River (the 'White River'), which is the second river in  
42 Iran, 670 km-long and with a drainage basin of 13450 km<sup>2</sup>. Along its lowland stretch (around 55 km in length), the river  
43 crosses a heavily cultivated area, where crops cover the majority of the drainage basin and reach the river banks.  
44 Hachirud, Radio Darya and Nowshahr were located in the urbanized area of Chalus (around 70000 inhabitants). In this  
45 area, urban aggregates are surrounded by agricultural activities, especially tea and rice fields, which are more abundant  
46 at Hachirud than at Radio Darya and Nowshahr that are popular touristic destinations (Irankhah et al. 2016). The area of  
47 Chalus is affected by the discharge of Chalus River, which is 92 km-long and has a drainage basin of 1710 km<sup>2</sup>. Along  
48 its upstream stretch Chalus River crosses an industrial area. Here, the Sorb Dona mine is dedicated to mineral extraction  
49 and represents a potential source of metal pollution affecting water quality (Jelodar et al. 2012; Amini Rad et al. 2013).  
50 Sisangan beach was a narrow beach separating the Sisangan National forest from the sea, in the Sisangan National Park,  
51 established in 1965, where human activity is regulated. The sampling site at Sisangan was expected to be the less  
52 affected by direct anthropogenic inputs among all sampling sites.  
53  
54  
55  
56  
57  
58  
59  
60  
61  
62  
63  
64  
65

## Field sampling procedures

For each sampling site, five sampling stations, 50 m apart from each other, were selected. At each station, samples of algae and sediments were collected. Specifically, at each station three samples of *Enteromorpha* spp. were randomly collected by hand, between 0.5 and 1 m depth, and used for the isotopic comparison between sampling sites. Occasionally, *Spirogyra* spp. and *Sargassum* spp. were also found and collected to compare metal concentrations among algal species. After collection, algal samples were placed in clean plastic bags, labelled and carried to laboratory in ice-boxes. Then, samples were washed up to remove mud, clay and salt, and air dried. For the analysis of trace metals, surface sediments (0-5 cm) were collected by using an Ekman grab. After collection, sediment samples were stored in clean polyethylene plastic bottles, labelled and carried to the laboratory in ice-boxes for further treatment. The sediment samples were lyophilized, sieved and fractions smaller than 63  $\mu\text{m}$  were transferred in clean dark glass bottles and kept frozen (at  $-20\text{ }^{\circ}\text{C}$ ) prior to chemical analyses (Wolf-Welling et al. 2002). Water samples were also collected for Nitrogen and Phosphorus analysis. During sampling, the pH, dissolved oxygen (mg/l) and temperature ( $^{\circ}\text{C}$ ) in water were recorded by using portable field probes.

## Laboratory procedures

Dissolved Nitrogen (TN as  $\text{NH}_4^+ + \text{NO}_2^- + \text{NO}_3^-$ , mg/l) and total Phosphorus (TP, mg/l) were determined by a spectrophotometer (DR-2500 Model HACH, USA). Samples of macroalgae were processed and analyzed for stable isotope analysis in the Laboratory of Trophic Ecology, Dept. of Environmental Biology, Sapienza, University of Rome (Italy). After freeze drying, samples were conserved at  $60^{\circ}\text{C}$  in an oven for 72 h and then ground to a fine homogenous powder using a ball mill (Fritsch Mini-Mill Pulverisette 23 with a zirconium oxide ball). For each sample, two sub-replicates ( $2.0 \pm 0.2\text{ mg}$ ) were weighed, pressed into ultra-pure tin capsules and analyzed using an Elementar Vario Micro-Cube elemental analyser (Elementar Analysensysteme GmbH, Germany) coupled with an IsoPrime100 isotope mass ratio spectrometer (Isoprime Ltd., Cheadle Hulme, UK). The Nitrogen stable isotope ratio ( $^{15}\text{N}:^{14}\text{N}$ ) was expressed in  $\delta$  units, i.e. parts per thousand deviations from international standards (atmospheric  $\text{N}_2$ ), in accordance with Ponsard and Arditi (2000) equation (Eq. 1):

$$\delta R(\text{‰}) = \left[ \frac{(R_{\text{sample}} - R_{\text{standard}})}{R_{\text{standard}}} \right] * 10^3 \quad (\text{Eq. 1})$$

Where R is the heavy-to-light isotope ratio of the element. The internal laboratory standard was IAEA-600 Caffeine. Measurement errors were found to be typically smaller than  $\pm 0.5\text{‰}$ .

In accordance with the literature (Calizza et al. 2015; Dailer et al. 2010; Fiorentino et al. 2017; Lapointe and Bedford 2007; Risk et al. 2009; Titlyanov et al. 2011; Wang et al. 2016) we derived four impact classes based on the macroalgal  $\delta^{15}\text{N}$  values, indicative of different N inputs: ‘inorganic input’ ( $\delta^{15}\text{N} < 3\text{‰}$ ), ‘non-impacted’ ( $3\text{‰} \leq \delta^{15}\text{N} \leq 6\text{‰}$ ), ‘moderate organic input’ ( $6\text{‰} < \delta^{15}\text{N} \leq 9\text{‰}$ ) and ‘high organic input’ ( $\delta^{15}\text{N} > 9\text{‰}$ ).

The analysis of metals in sediment and macroalgae were performed by the Institute for Nano Science and Nanotechnology at Sharif University of Technology (Iran). Samples of macroalgae for metal analysis were grinded using a porcelain mortar and kept frozen until analysis. One g-dry sample was digested by 10 ml  $\text{HNO}_3$  and 1 ml  $\text{H}_2\text{O}_2$  (30% Merck, suprapur) for 2 hours at  $90^{\circ}\text{C}$ . The digested samples were cooled at laboratory temperature, filtered through a Whatman filter paper (No. 42) and diluted to 50 ml with distilled deionized water. Metal concentrations were determined by ICP-OES (series No ICAP6000, Spectro Arcos Amatek, Termo Company, England). For each element,

1 the BioSediment Accumulation Factor (BSAF), i.e the bioavailability of the element, was evaluated according to the  
2 following equation (Eq. 2, Alahverdi and Savabieasfahani 2012):  
3

$$4 \quad BSAF = \frac{X_{macroalgae}}{X_{sediment}} \text{ (Eq. 2)}$$

5  
6  
7  
8 Where X is the concentration of a given element.

9  
10 The grain size of sediment was measured using laser (Laser scattering particle size distributor analyzer LS-950  
11 Model by Horiba) and shaker (FRITSCH analysette 3 PRO) instruments for silty-muddy and sandy sediments. 0.5 g of  
12 sediment sample were weighed in a Teflon vessel and digested using HNO<sub>3</sub> (65% Merck suprapur) and HCl (1:3 v/v) at  
13 85 °C for 3 hours (Al-Mur et al. 2017). The acidified samples were cooled for 1 hour at laboratory temperature, filtered  
14 through a Whatman filter paper (No. 42) and diluted to 50 ml with distilled deionized water. For each digestion  
15 program, a ‘blank’ was also prepared.  
16

17  
18 Metals (Al, Ba, Ca, Co, Cr, Cu, Fe, K, Mg, Mn, Na, Ni, Pb, Ti, V and Zn), as well as some other elements (P and S),  
19 were analyzed using inductively coupled plasma optical emission spectrometry ICP-OES after acid digestion.  
20 Quantification of elements was based upon calibration curves obtained from different standard solutions prepared at 2,  
21 20, 200, 500, 1000 and 2000 µg/l (Merck, code No. 1.11355.0100).  
22  
23

24  
25 For Cr, Cu, Ni, Pb and Zn, it was possible to compare the observed concentrations with values proposed by the  
26 sediment Standard Quality Guidelines (SQG, Perin et al. 1997), also utilized by Pekey et al. (2004, Marmara Sea) and  
27 Agah et al. (2011, Caspian Sea). This classification provides threshold values for three different classes of impact: Non-  
28 polluted (NP), Moderately polluted (MP) and Heavily polluted (HP). Observed concentrations were also compared with  
29 the ‘threshold effect level’ (TEL, Long et al. 1998). The TEL provides threshold values which can be related with  
30 potential toxic effects of each metal on the marine biota (Long et al. 1998).  
31  
32  
33  
34  
35

### 36 *Statistical analysis*

37  
38 Data analysis was performed with the open source software R 3.4.2 (R Core Team, 2017) and ade4 R package  
39 (Dray and Dufour 2007). δ<sup>15</sup>N in macroalgae was considered as a dependent variable and analyzed by a linear model  
40 against ‘Site’ as explicative ‘dummy’ variable (James et al. 2013). The confidence level was set at α= 0.05. A principal  
41 component analysis (PCA) was performed to assess the distribution and associations of metals in surface sediments. In  
42 order to explore potential coupling between metal and nutrient inputs in different ecosystem compartments, we also  
43 tested the presence of significant linear correlation between (i) metal concentrations in macroalgae and sediments, and  
44 (ii) δ<sup>15</sup>N and metal concentrations in algae. In order to explore the potential relationships between δ<sup>15</sup>N and dissolved  
45 Nitrogen (hereafter referred as ‘TN’) and between O<sub>2</sub> and δ<sup>15</sup>N, we performed linear regressions (confidence level was  
46 set at α= 0.05).  
47  
48  
49  
50  
51  
52

## 53 **Results**

### 54 *δ<sup>15</sup>N in macroalgae and physico-chemical parameters in water*

55  
56 δ<sup>15</sup>N values of macroalgae detected inorganic and organic N inputs, which affected differently the study areas  
57 (Fig. 2). In the western coast of the southern Caspian Sea (Anzali, Gilan province) Nitrogen signatures fell in the  
58 inorganic range, with a mean δ<sup>15</sup>N (± standard error) of 2.22 ‰ (±0.60). δ<sup>15</sup>N values were higher in the central coast and  
59 in particular in the Chalus county, where they reached the highest values falling in the ‘moderate organic’ and ‘high  
60  
61  
62  
63  
64  
65



1 organic' ranges near the beaches of Hachirud and Radio Darya respectively, with means of 7.30 ‰ (±0.47) and 8.41 ‰  
2 (±0.88) (Fig.2). East of this area, Nitrogen signatures fell in the 'non-impacted' range with means of 5.12 ‰ (±0.19)  
3 and 4.81‰ (±0.64) near Nowshahr and Sisangan (Mazandaran province) respectively. Differences between areas were  
4 statistically significant (F-value= 15.76, p <0.05) and the linear model for the  $\delta^{15}\text{N}$  values of macroalgae explained  $\approx$   
5 70% of the deviance. In particular, the values found in the inorganic impacted site (Anzali) were statistically different  
6 from those of the other sites (Tukey's pairwise comparisons, p always <0.05). Furthermore, values in the two non-  
7 impacted sites were similar (Nowshahr and Sisangan, p>0.05) and significantly different from those of organic  
8 impacted sites (p<0.05 both).  
9

10  
11  $\delta^{15}\text{N}$  values in macroalgae were positively correlated with dissolved Nitrogen (TN) and negatively with  $\text{O}_2$   
12 concentration in waters (Fig. 3).  $\text{O}_2$  concentration did not vary with water temperature (p>0.05), which was rather  
13 constant between sampling sites (Table 1). Total Phosphorus was high in the inorganic and organic impacted sites, and  
14 low in the two non-impacted sites.  
15  
16  
17

### 18 *Metal concentrations in sediments*

19  
20 The sampling locations were all characterized by sandy-silty sediments. Overall, metals ranked with the  
21 following mean concentration (ppm) decreasing pattern: Fe (71929) > Ca (68607) > Al (30488) > Mg (22365) > Ti  
22 (9283) > K (6954) > Na (6517) > Mn (2182) > V (462) > Cr (433) > Ba (186) > Zn (140) > Ni (58) > Pb (42) > Co  
23 (29) > Cu (24). The mean concentration of each element varied across sampling sites (Table 2).  
24  
25  
26

27 The principal component analysis grouped elements in three groups, each of them including positively  
28 correlated elements (Table 3). The first two groups included metals and were separated along the first PCA axis ( $\approx$ 83%  
29 of total variance explained), whereas the non-metal elements (P and S, group III) mainly scattered on the second PCA  
30 axis ( $\approx$ 12% of total variance). Notably, group II included all those metals that are expected to potentially affect marine  
31 biota depending on the concentration (Table 3).  
32  
33  
34

35 According to the SQG (Table 4), high levels of Cr and Ni were present in all sites and TEL was exceeded. In  
36 the inorganic polluted area concentrations of Cu, Pb and Zn were below the level of pollution, whereas in the organic  
37 polluted sites (Hachirud and Radio Darya) high levels of Pb and Zn were found, exceeding the corresponding TEL, and  
38 Cu was in the moderate pollution class (Table 4). Cu exceeded the TEL both in the organic and inorganic polluted sites  
39 (Table 4). Although in Sisangan metals did not reach concentrations as high as those observed in remaining sites, values  
40 fell in the high pollution range for Cr, and in the moderate pollution range for Ni and Zn. Here, Zn concentration was  
41 below TEL.  
42  
43  
44  
45

### 46 *Metal concentrations in macroalgae*

47  
48 On average, element concentrations (in ppm) in macroalgae decreased according to the following order (Table  
49 5): Ca (21025) > Mg (2522) > Fe (1755) > Al (1750) > P (503) > K (427) > Mn (75) > Zn (56) > Ti (38) > Cu (27) > Cr  
50 (3.2) > V (2.7) > Ni (2.6) > Co (0.6).  
51  
52

53 Concentrations of elements differed between macroalgal species (Table 5). Specifically, *Enteromorpha* showed  
54 the highest concentration for Al, Cr, Fe, Ni, P, Ti, V (maximum values observed in Anzali), while Cr and Ni, which were  
55 abundant in the sediments, were present in low concentrations in all the other macroalgal species. The BSAF values  
56 were generally lower than 1, implying that the concentration observed in algae was lower than that observed in  
57 sediment for the corresponding element. No significant linear correlations were found between a specific element in  
58  
59  
60  
61  
62  
63  
64  
65

1 macroalgae and the same element in sediment ( $p$  always  $> 0.05$ ). Furthermore,  $\delta^{15}\text{N}$  and metal concentrations in algae  
2 were not related ( $p$  always  $> 0.05$ ).

3 Among other elements, high Fe concentrations in *Enteromorpha* were found at all sampling sites, and high Cu  
4 levels were found also in front of the Sisangan National Park.  
5

## 6 7 **Discussions**

8 The results from stable isotope and metal analyses show considerable spatial variation of water quality in the study area  
9 that derives from various human activities, carried out both at sea and on land, and that can impair water resources and  
10 human health. Integration of the two techniques was crucial for depicting more fully this anthropic impact complexity.  
11 On one hand, the  $\delta^{15}\text{N}$  analysis of macroalgae was a useful monitoring tool allowing classification of the coastal waters  
12 on the base of the predominant sources of anthropogenic N inputs. On the other hand, analysis of sediments revealed  
13 potentially hazardous elements for marine biota and indicated distinct and spatially variable inputs of natural and  
14 anthropogenic trace metals into the sea.  
15  
16  
17  
18

19 As regards the N inputs into the water body, the low  $\delta^{15}\text{N}$  values of the macroalgae found in the western  
20 Iranian coast (Gilan province) were indicative of anthropogenic inorganic N sources (Dailer et al. 2010; Rossi et al.  
21 2018), seemingly associated with inland agricultural activities (Sadeghi et al. 2012, 2013; Ziarati et al. 2014). Indeed,  
22 this area is affected by the discharge of the second Iranian river, which crosses several kilometers of an intensively  
23 cultivated area before entering the Caspian Sea. In spite of the low levels of dissolved Nitrogen detected in seawater, the  
24 isotopic biomonitoring through macroalgae was able to identify clearly the inorganic dominant N source of pollution in  
25 that area. On the contrary, the higher  $\delta^{15}\text{N}$  values of macroalgae found near the beaches of Hachirud and Radio Darya,  
26 associated with higher dissolved Nitrogen levels in seawaters, indicated respectively moderate and high organic N  
27 pollution in these two central sites (Dailer et al. 2010). Due to urbanization and the importance of this area as touristic  
28 attraction, the N organic inputs can be mainly attributed to tourism and municipal wastewaters (Rossi et al. 2018). East  
29 of this area,  $\delta^{15}\text{N}$  values indicated ‘non-impacted’ conditions, according to current literature classification (Calizza et al.  
30 2015; Dailer et al. 2010; Fiorentino et al. 2017; Lapointe and Bedford 2007; Risk et al. 2009; Titlyanov et al. 2011;  
31 Wang et al. 2016), which are consistent with the site location in front of the Sisagan National Park, where human  
32 activities are strongly regulated.  
33  
34  
35  
36  
37  
38  
39  
40

41 The increasing dissolved N concentration in the southern Caspian Sea coasts was related with increasing  $\delta^{15}\text{N}$   
42 values of macroalgae indicating the organic source of the N pollutants. In such conditions, oxygen concentrations in  
43 water decreased (even close to the hypoxic threshold of 2 mg/l, Jessen et al. 2015), plausibly due to heterotrophic  
44 microbial respiration that is expected to increase with organic matter degradation (Diaz and Rosenberg 2008).  
45  
46

47 As regards metals in sediments, concentrations of Co and Cu were comparable with relatively recent studies in  
48 the area, whereas higher concentrations of Ni, Pb and Zn were found (Sohrabi et al. 2010). According to the SQG  
49 classification, most of the sampling sites fall in the ‘moderately impacted’ and ‘highly impacted’ classes for various  
50 trace metals reflecting the human pressure on the study area (Karbassi et al. 2008; Vesali Naseh et al. 2012; Sohrabi et  
51 al. 2010). As observed for N pollution, the measured variability of most metal concentrations across sites suggests  
52 spatial differences in anthropogenic pollution affecting the southern Caspian Sea, and provides site-specific baseline  
53 values of present conditions for future comparisons. Metals clustered in two sets negatively correlated: one of them  
54 included all those metals that are considered potentially hazardous for the marine biota. This suggests opposite trends  
55 between background (group I) and hazardous (group II) metal sources, and points to independent inputs of these two  
56 types of metals. Notably, the highest concentrations of hazardous metals in sediment (corresponding to highly impacted  
57  
58  
59  
60  
61  
62  
63  
64  
65



1 conditions) were measured in the coastal tract affected by the discharge of Chalus River. In particular, this river is a  
2 potential source of Pb and Zn, due to the presence of the Sorb Dona mine in its upstream sector (Amini Rad et al. 2013;  
3 Jelodar et al. 2012) and data suggest that the upstream industrial activity produced a localized 'footprint' clearly  
4 detectable in the coastal marine ecosystem. Pb and Zn can be transported downstream after absorption by sediment or  
5 suspended particles, mainly due to flood events (Amini Rad et al. 2013; Jelodar et al. 2012), but fast particle  
6 sedimentation rate in the coastal area may explain the detection of high metal concentration only in those sites directly  
7 affected by the river discharge. By contrast, while high concentrations of Ni were found in Anzali, where there is the  
8 most important port in the southern Caspian Sea, and in the two most touristic sites (Hachirud and Radio Darya), high  
9 concentrations of Cr were found in all sampling sites. These two elements are commonly used as anti-fouling agents in  
10 marine paints (Tabari et al. 2010) but they can be also related to oil extraction (Alahverdi and Savabieasfahani 2012;  
11 Naser 2013). Thus, although the exact source of pollution may be difficult to determine, our results suggests that the  
12 intense anthropic activity taking place at sea exposes the coastal waters to high levels of metal pollution even in the area  
13 facing the Sisagan National Park, the expected non-impacted site.

14 No significant relationships were found between metal levels in algae and sediments. Furthermore, concentrations in  
15 algae were lower than those observed in sediment for most of the elements. This indicates a divergent translocation of  
16 metals from water to these two basal compartments of the food web and implies different effects of the herbivore and  
17 the detrital energy pathways on the transfer of these pollutants to upper trophic levels. As regards metals in algae,  
18 marked variations across sites and algal species were observed. Overall, *Enteromorpha* displayed the widest distribution  
19 and the highest concentration for the majority of metals, thus ranking as the best bioindicator among the sampled  
20 macroalgae. Some metal concentrations found in *Enteromorpha* can be considered indicative of impacted conditions  
21 according to literature (Fe: Caliceti et al. 2002, Zn: Villares et al. 2001, Cu: Chakraborty et al. 2014). Together, high  
22 concentrations of Fe, Cu and Zn are usually associated to oil drilling, while Cu inputs can be associated also to  
23 antifouling products (Secrieru and Secrieru 2002; Tabari et al. 2010; Naser 2013). In addition, the lower levels of Cu in  
24 macroalgae and Fe in sediment, sampled between the Sisagan National Park and the Chalus river mouth, suggest that  
25 the high metal concentrations observed in macroalgae at Sisagan are not associated with the transportation of inland  
26 pollutants by the river, further confirming their marine origin.

27 In conclusion, the analyses of nutrient and metal pollutants, affecting two basal resource compartments  
28 (benthic primary producers and sediments) that support coastal food webs, allowed us to classify different areas subject  
29 to various anthropic impacts as well as to describe differences in concentration of metals accumulating in macroalgae  
30 and shallow-water sediments.

31 Nitrogen isotopic signatures of macroalgae detected N inputs of both inorganic and organic origins.  
32 Furthermore, they allowed us to associate the organic impact with the dissolved N values and, thus, with the low values  
33 of dissolved oxygen up to observed hypoxic values critical to the marine life (Jessen et al. 2015). In parallel, the  
34 analysis of potentially hazardous metals showed that sediments were enriched in many elements, and in particular Cr,  
35 Ni, Zn and Pb, in relation with human activities taking place on land or at sea. We found that concentrations of metals  
36 were higher in comparison to relatively recent observations (Sohrabi et al. 2010), suggesting an increasing trend of  
37 pollution in the southern sector of the Caspian Sea. This was particularly evident in correspondence of river mouths and  
38 included elements able to spread along food chains up to fish consumed by man (Agah et al. 2007; Mashroofeh et al.  
39 2013), thus representing a threat for human health (Hosseini et al. 2013; Mashroofeh et al. 2013). This further indicates  
40 the need of a more comprehensive monitoring able to include upper trophic levels and to explicitly take into account the  
41 spatial variability of anthropogenic pressure described in this study.

1 As concluding remarks, the significant differences in pollution levels measured across sampling sites suggest  
2 that biomonitoring at the local scale can represent an effective approach for identifying the dislocation and origin of  
3 local pollution sources even in complex coastal marine areas potentially affected by long-range transport of pollutants,  
4 as it is the case for the Caspian Sea (Zonn 2005). In this perspective, integration between stable isotope analysis and  
5 heavy metal analysis can be very helpful in unraveling the main sources of pollution. The marked differences between  
6 algae and sediment in terms of metal concentrations highlights the need to characterize multiple ecosystem  
7 compartments to achieve a comprehensive monitoring of coastal pollution, a complete description of the anthropic  
8 pressure affecting each area, and its potential effects on the aquatic food web (Signa et al. 2019).  
9  
10  
11  
12

13 **Funding Information:** This research was supported by Ateneo-Sapienza 2016 (L. Rossi), Programma Nazionale di  
14 Ricerche in Antartide-2015/AZ1.01 (M.L. Costantini), and Programma Nazionale di Ricerche in Antartide-2016\_00291  
15 (L. Rossi).  
16  
17  
18  
19  
20  
21

22 **Conflict of interest:** The Authors declare that they have no conflict of interests.  
23  
24  
25  
26  
27  
28  
29  
30  
31  
32  
33  
34  
35  
36  
37  
38  
39  
40  
41  
42  
43  
44  
45  
46  
47  
48  
49  
50  
51  
52  
53  
54  
55  
56  
57  
58  
59  
60  
61  
62  
63  
64  
65

## References

- 1  
2  
3 Abadi M, Zaman A, Parizanganeh A, Khosravi Y, Badiiee H (2018) Heavy metals and arsenic content in water along the  
4 southern Caspian coasts in Iran. *Environ Sci Pollut Res* 25:23725–23735. [https://doi.org/10.1007/s11356-018-](https://doi.org/10.1007/s11356-018-2455-7)  
5  
6 2455-7  
7  
8  
9 Adel M, Saravi HN, Dadar M, Niyazi L, Ley-Quinonez CP (2017) Mercury, lead, and cadmium in tissues of the  
10 Caspian Pond Turtle (*Mauremys caspica*) from the southern basin of Caspian Sea. *Environ Sci Pollut Res*  
11 24:3244–3250. <https://doi.org/10.1007/s11356-015-5905-5>  
12  
13  
14 Agah H, Leermakers M, Elskens M, Fatemi SMR, Baeyens W (2007) Total mercury and methyl mercury concentrations  
15 in fish from the Persian Gulf and the Caspian Sea. *Water Air Soil Pollut* 181: 95-105.  
16  
17 <https://doi.org/10.1007/s11270-006-9281-0>  
18  
19  
20 Agah H, Hashtroudi M, Baeyens W (2011) Trace metals analysis in the sediments of the Southern Caspian Sea. *J*  
21 *Persian Gulf* 2:1–12.  
22  
23  
24 Agah H, Hashtroudi MS, Baeyens W (2012) Trace metals and major elements in sediments of the Northern Persian  
25 Gulf. *J Persian Gulf* 3:45–58.  
26  
27  
28 Alahverdi M, Savabieasfahani M (2012) Metal pollution in seaweed and related sediment of the Persian Gulf, Iran. *Bull*  
29 *Environ Contam Toxicol* 88:939–945. <https://doi.org/10.1007/s00128-012-0586-y>  
30  
31  
32 Al-Mur BA, Quicksall AN, Al-Ansari AMA (2017) Spatial and temporal distribution of heavy metals in coastal core  
33 sediments from the Red Sea, Saudi Arabia. *Oceanologia* 59:262–270.  
34  
35 <https://doi.org/10.1016/j.oceano.2017.03.003>  
36  
37  
38 Amini Rad H, Hasannattaj A, Scholz M, Navayineya B, Weekes L (2013) Generic adsorption coefficients and natural  
39 removal of heavy metals in muddy river water. *Int J Bioassays* 2:1260-1268.  
40  
41  
42 Astorga-España MS, Calisto-Ulloa NC, Guerrero S (2008) Baseline concentrations of trace metals in macroalgae from  
43 the strait of Magellan, Chile. *Bull Environ Contam Toxicol* 80:97–101. [https://doi.org/10.1007/s00128-007-](https://doi.org/10.1007/s00128-007-9323-3)  
44  
45 9323-3  
46  
47  
48 Bastami KD, Bagheri H, Kheirabadi V, Zaferani GG, Teymori MB, Hamzehpoor A, Soltani F, Haghparast S, Harami  
49 SRM, Ghorghani NF, Ganji S (2014) Distribution and ecological risk assessment of heavy metals in surface  
50 sediments along southeast coast of the Caspian Sea. *Mar Pollut Bull* 81: 262–267.  
51  
52 <https://doi.org/10.1016/j.marpolbul.2014.01.029>  
53  
54  
55 Bastami KD, Neyestani MR, Shemirani F, Soltani F, Haghparast S, Akbari A (2015) Heavy metal pollution assessment  
56 in relation to sediment properties in the coastal sediments of the southern Caspian Sea. *Mar Pollut Bull*  
57 92:237–243. <https://doi.org/10.1016/j.marpolbul.2014.12.035>  
58  
59  
60  
61  
62  
63  
64  
65

- 1 Bastami KD, Neyestani MR, Esmailzadeh M, Haghparast S, Alavi C, Fathi S, Nourbakhsh S, Shirzadi EA, Parhizgar R  
2 (2017) Geochemical speciation, bioavailability and source identification of selected metals in surface  
3 sediments of the Southern Caspian Sea. *Mar Pollut Bull* 114:1014–1023.  
4  
5 <https://doi.org/10.1016/j.marpolbul.2016.11.025>  
6  
7 Bentivoglio F, Calizza E, Rossi D, Carlino P, Careddu G, Rossi L, Costantini ML (2016) Site-scale isotopic variations  
8 along a river course help localize drainage basin influence on river food webs. *Hydrobiologia* 770:257–272.  
9  
10 <https://doi.org/10.1007/s10750-015-2597-2>  
11  
12 Caliceti M, Argese E, Sfriso A, Pavoni B (2002) Heavy metal contamination in the seaweeds of the Venice lagoon.  
13  
14 *Chemosphere* 47:443–454. [https://doi.org/10.1016/S0045-6535\(01\)00292-2](https://doi.org/10.1016/S0045-6535(01)00292-2)  
15  
16 Calizza E, Costantini ML, Rossi L (2015) Effect of multiple disturbances on food web vulnerability to biodiversity loss  
17 in detritus-based systems. *Ecosphere* 6:1-20. <https://doi.org/10.1890/ES14-00489.1>  
18  
19 Chakraborty S, Bhattacharya T, Singh G, Maity JP (2014) Benthic macroalgae as biological indicators of heavy metal  
20 pollution in the marine environments: A biomonitoring approach for pollution assessment. *Ecotoxicol Environ*  
21 *Saf* 100:61–68. <https://doi.org/10.1016/j.ecoenv.2013.12.003>  
22  
23 Chen JL, Wilson CR, Tapley BD, Save H, Cretaux JF (2017) Long-term and seasonal Caspian Sea level change from  
24 satellite gravity and altimeter measurements. *J Geophys Res Solid Earth* 122:2274-2290.  
25  
26 <https://doi.org/10.1002/2016JB013595>  
27  
28 Dadar M, Adel M, Saravi HN, Dadar M (2016) A comparative study of trace metals in male and female Caspian kutum  
29 (*Rutilus frisii kutum*) from the southern basin of Caspian Sea. *Environ Sci Pollut Res* 23:24540–24546.  
30  
31 <https://doi.org/10.1007/s11356-016-6871-2>  
32  
33 Dailer ML, Knox RS, Smith JE, Napier M, Smith CM (2010) Using  $\delta^{15}\text{N}$  values in algal tissue to map locations and  
34 potential sources of anthropogenic nutrient inputs on the island of Maui, Hawai‘i, USA. *Mar Pollut Bull*  
35 60:655–671. <https://doi.org/10.1016/j.marpolbul.2009.12.021>  
36  
37 de Mora S, Sheikholeslami MR, Wyse E, Azemard S, Cassi R (2004) An assessment of metal contamination in coastal  
38 sediments of the Caspian Sea. *Mar Pollut Bull* 48:61–77. [https://doi.org/10.1016/S0025-326X\(03\)00285-6](https://doi.org/10.1016/S0025-326X(03)00285-6)  
39  
40 Diaz RJ, Rosenberg R (2008) Spreading dead zones and consequences for marine ecosystems. *Science* 321:926–929.  
41  
42 <https://doi.org/10.1126/science.1156401>  
43  
44 Dray S, Dufour AB (2007) The ade4 Package: implementing the duality diagram for ecologists. *J Stat Softw* 22:1-20.  
45  
46 Ebadi AG, Hisoriev H (2017) The prevalence of heavy metals in *Cladophora glomerata* L. from Farahabad Region of  
47 Caspian Sea – Iran. *Environ Toxicol Chem* 99:883–891. <https://doi.org/10.1080/02772248.2017.1323894>  
48  
49  
50  
51  
52  
53  
54  
55  
56  
57  
58  
59  
60  
61  
62  
63  
64  
65

- 1  
2 indicate the origins of nitrogen loading and its seasonal dynamics in a volcanic Lake. *Ecol Indic* 79:19–27.  
3  
4 <https://doi.org/10.1016/j.ecolind.2017.04.007>
- 5  
6 Goher ME, Farhat HI, Abdo MH, Salem SG (2014) Metal pollution assessment in the surface sediment of Lake Nasser,  
7  
8 Egypt. *Egypt J Aquat Res* 40:213–224. <https://doi.org/10.1016/j.ejar.2014.09.004>
- 9  
10 Halpern BS, Walbridge S, Selkoe KA, Kappel CV, Micheli F, D'Agrosa C, Bruno JF, Casey KS, Ebert C, Fox HE,  
11  
12 Fujita R, Heinemann D, Lenihan HS, Madin EMP, Perry MT, Selig ER, Spalding M, Steneck R, Watson R  
13  
14 (2008) A global map of human impact on marine ecosystems. *Science* 319:948–952.  
15  
16 <https://doi.org/10.1126/science.1149345>
- 17  
18 Hasani M, Sakieh Y, Dezhkam S, Ardakani T, Salmanmahiny A (2017) Environmental monitoring and assessment of  
19  
20 landscape dynamics in southern coast of the Caspian Sea through intensity analysis and imprecise land-use  
21  
22 data. *Environ Monit Assess* 189:1-19. <https://doi.org/10.1007/s10661-017-5883-9>
- 23  
24 Heaton THE (1986) Isotopic studies of nitrogen pollution in the hydrosphere and atmosphere: A review. *Chem Geol*  
25  
26 59:87–102. [https://doi.org/10.1016/0168-9622\(86\)90059-X](https://doi.org/10.1016/0168-9622(86)90059-X)
- 27  
28 Hosseini SM, Sobhanardakani S, Navaei MB, Kariminasab M, Aghilinejad SM, Regenstein JM (2013) Metal content in  
29  
30 caviar of wild Persian sturgeon from the southern Caspian Sea. *Environ Sci Pollut Res* 20:5839-5843.  
31  
32 <https://doi.org/10.1007/s11356-013-1598-9>
- 33  
34 Howarth RW, Marino R (2006) Nitrogen as the limiting nutrient for eutrophication in coastal marine ecosystems:  
35  
36 Evolving views over three decades. *Limnol Oceanogr* 51:364–376.  
37  
38 [https://doi.org/10.4319/lo.2006.51.1\\_part\\_2.0364](https://doi.org/10.4319/lo.2006.51.1_part_2.0364)
- 39  
40 Irankhah S, Soudi MR, Gharavi S (2016) Ex situ study of *Enterococcus faecalis* survival in the recreational waters of  
41  
42 the southern coast of the Caspian Sea. *Iran J Microbiol* 8:101–107.
- 43  
44 James G, Witten D, Hastie T, Tibshirani R (2013) Linear regression. In: James G, Witten D, Hastie T, Tibshirani R  
45  
46 (eds) *An introduction to statistical learning: with applications in R*, Springer-Verlag, New York, pp. 82-86.
- 47  
48 Jelodar AH, Rad HA, Navaiynia B, Zazouli MA (2012) Heavy metal ions adsorption by suspended particle and  
49  
50 sediment of the Chalus River, Iran. *Afr J Biotechnol* 11:628-634. <https://doi.org/10.5897/AJB09.902>
- 51  
52 Jessen C, Bednarz VN, Rix L, Teichberg M, Wild C (2015) Marine eutrophication. In: Harmon RH, Hänninen O (eds),  
53  
54 *Environmental Indicators* Springer, Dordrecht, pp. 177–203.
- 55  
56 Jona-Lasinio G, Costantini ML, Calizza E, Pollice A, Bentivoglio F, Orlandi L, Careddu G, Rossi L (2015) Stable  
57  
58 isotope-based statistical tools as ecological indicator of pollution sources in Mediterranean transitional water  
59  
60 ecosystems. *Ecol Indic* 55:23–31. <https://doi.org/10.1016/j.ecolind.2015.03.006>
- 61  
62  
63  
64  
65

- 1 Karbassi A, Saeedi M, Amirnejad R (2008) Historical changes of heavy metals content and sequential extraction in a  
2 sediment core from the Gorgan Bay, Southeastern Caspian Sea. *Indian J Geomarine Sci* 37:267-272.
- 3  
4 Korom SF (1992) Natural denitrification in the saturated zone: A review. *Water Resour Res* 28:1657–1668.  
5  
6 <https://doi.org/10.1029/92WR00252>
- 7  
8 Kreitler CW, Jones DC (1975) Natural soil nitrate: The cause of the nitrate contamination ground water in Runnels  
9 County, Texas. *Groundwater* 13:53–61. <https://doi.org/10.1111/j.1745-6584.1975.tb03065.x>
- 10  
11 Kreitler CW (1979) Nitrogen-isotope ratio studies of soils and groundwater nitrate from alluvial fan aquifers in Texas. *J*  
12 *Hydrol* 42:147–170. [https://doi.org/10.1016/0022-1694\(79\)90011-8](https://doi.org/10.1016/0022-1694(79)90011-8)
- 13  
14  
15  
16 Lapointe BE, Bedford BJ (2007) Drift rhodophyte blooms emerge in Lee County, Florida, USA: Evidence of escalating  
17 coastal eutrophication. *Harmful Algae* 6:421–437. <https://doi.org/10.1016/j.hal.2006.12.005>
- 18  
19  
20 Long ER, Field LJ, MacDonald DD (1998) Predicting toxicity in marine sediments with numerical sediment quality  
21 guidelines. *Environ Toxicol Chem* 17:714–727. <https://doi.org/10.1002/etc.5620170428>
- 22  
23  
24 Mariotti A, Mariotti F, Champigny ML, Amarger N, Moysse A (1982) Nitrogen isotope fractionation associated with  
25 nitrate reductase and uptake of NO<sub>3</sub><sup>-</sup> by Pearl Millet. *Plant Physiol* 69:880–884.  
26  
27 <https://doi.org/10.1104/pp.69.4.880>
- 28  
29  
30 Mashroofeh A, Bakhtiari AR, Pourkazemi M, Rasouli S (2013) Bioaccumulation of Cd, Pb and Zn in the edible and  
31 inedible tissues of three sturgeon species in the Iranian coastline of the Caspian Sea. *Chemosphere*, 90:573-  
32 580. <https://doi.org/10.1016/j.chemosphere.2012.08.034>
- 33  
34  
35  
36 Naser HA (2013) Assessment and management of heavy metal pollution in the marine environment of the Arabian Gulf:  
37 a review. *Mar Pollut Bull* 72:6-13. <https://doi.org/10.1016/j.marpolbul.2013.04.030>
- 38  
39  
40 Orlandi L, Bentivoglio F, Carlino P, Calizza E, Rossi D, Costantini ML, Rossi L (2014)  $\delta^{15}\text{N}$  variation in *Ulva lactuca*  
41 as a proxy for anthropogenic nitrogen inputs in coastal areas of Gulf of Gaeta (Mediterranean Sea). *Mar Pollut*  
42 *Bull* 84:76–82. <https://doi.org/10.1016/j.marpolbul.2014.05.036>
- 43  
44  
45  
46 Orlandi L, Calizza E, Careddu G, Carlino P, Costantini ML, Rossi L (2017) The effects of nitrogen pollutants on the  
47 isotopic signal ( $\delta^{15}\text{N}$ ) of *Ulva lactuca*: Microcosm experiments. *Mar Pollut Bull* 115:429–435.  
48  
49 <https://doi.org/10.1016/j.marpolbul.2016.12.051>
- 50  
51  
52 Paerl HW, Hall NS, Peierls BL, Rossignol KL (2014) Evolving paradigms and challenges in estuarine and coastal  
53 eutrophication dynamics in a culturally and climatically stressed world. *Estuaries Coast* 37:243–258.  
54  
55 <https://doi.org/10.1007/s12237-014-9773-x>
- 56  
57  
58  
59  
60  
61  
62  
63  
64  
65

- 1 Paerl HW, Gardner WS, Havens KE, Joyner AR, McCarthy MJ, Newell SE, Qin B, Scott JT (2016) Mitigating  
2 cyanobacterial harmful algal blooms in aquatic ecosystems impacted by climate change and anthropogenic  
3 nutrients. *Harmful Algae* 54:213–222. <https://doi.org/10.1016/j.hal.2015.09.009>  
4
- 5 Pekey H, Karakaş D, Ayberk S, Tolun L, Bakoğlu M (2004) Ecological risk assessment using trace elements from  
6 surface sediments of İzmit Bay (Northeastern Marmara Sea) Turkey. *Mar Pollut Bull* 48:946–953.  
7  
8 <https://doi.org/10.1016/j.marpolbul.2003.11.023>  
9
- 10 Perin G, Bonardi M, Fabris R, Simoncini B, Manente S, Tosi L, Scotto S (1997) Heavy metal pollution in Central  
11 Venice Lagoon bottom sediments: Evaluation of the metal bioavailability by geochemical speciation  
12 procedure. *Environ Technol* 18:593–604. <https://doi.org/10.1080/09593331808616577>  
13  
14
- 15 Ponsard S, Arditi R (2000) What can stable isotopes ( $\delta^{15}\text{N}$  and  $\delta^{13}\text{C}$ ) tell about the food web of soil macro  
16 invertebrates? *Ecology* 81:852–864.  
17  
18 [https://doi.org/10.1890/0012-9658\(2000\)081\[0852:WCSINA\]2.0.CO;2](https://doi.org/10.1890/0012-9658(2000)081[0852:WCSINA]2.0.CO;2)  
19  
20
- 21 R Core Team (2017) R: a language and environment for statistical computing.  
22  
23 R Foundation for Statistical Computing, Vienna, Austria. URL <https://www.R-project.org/>  
24
- 25 Risk MJ, Lapointe BE, Sherwood OA, Bedford BJ (2009) The use of  $\delta^{15}\text{N}$  in assessing sewage stress on coral reefs.  
26  
27 *Mar Pollut Bull* 58:793–802. <https://doi.org/10.1016/j.marpolbul.2009.02.008>  
28  
29
- 30 Rossi L, Calizza E, Careddu G, Rossi D, Orlandi L, Jona-Lasinio G, Aguzzi L, Costantini ML (2018) Space-time  
31 monitoring of coastal pollution in the Gulf of Gaeta, Italy, using  $\delta^{15}\text{N}$  values of *Ulva lactuca*, landscape  
32 hydromorphology, and Bayesian Kriging modelling. *Mar Pollut Bull* 126:479–487.  
33  
34 <https://doi.org/10.1016/j.marpolbul.2017.11.063>  
35  
36
- 37 Sadeghi R, Zarkami R, Sabetraftar K, Van Damme P (2012) Use of support vector machines (SVMs) to predict  
38 distribution of an invasive water fern *Azolla filiculoides* (Lam.) in Anzali wetland, southern Caspian Sea, Iran.  
39  
40 *Ecol Modell* 244:117–126. <https://doi.org/10.1016/j.ecolmodel.2012.06.029>  
41  
42
- 43 Sadeghi R, Zarkami R, Sabetraftar K, Van Damme P (2013) Application of genetic algorithm and greedy stepwise to  
44 select input variables in classification tree models for the prediction of habitat requirements of *Azolla*  
45  
46 *filiculoides* (Lam.) in Anzali wetland, Iran. *Ecol Modell* 251:44–53.  
47  
48 <https://doi.org/10.1016/j.ecolmodel.2012.12.010>  
49  
50
- 51 Saghali M, Hoseini SM, Hosseini SA, Baqraf R (2014) Determination of heavy metal (Zn, Pb, Cd and Cr) concentration  
52 in benthic fauna tissues collected from the Southeast Caspian Sea, Iran. *Bull Environ Contam Toxicol* 92:57–  
53  
54 60. <https://doi.org/10.1007/s00128-013-1133-1>  
55  
56
- 57 Secieru D, Secieru A (2002) Heavy Metal Enrichment of Man-made Origin of Superficial Sediment on the Continental  
58  
59  
60  
61  
62  
63  
64  
65



Shelf of the North-western Black Sea. *Estuarine, Coastal and Shelf Science* 54:513–526.

<https://doi.org/10.1006/ecss.2000.0671>

Shahrban M, Etemad-Shahidi A (2010) Classification of the Caspian Sea coastal waters based on trophic index and numerical analysis. *Environ Monit Assess* 164:349–356. <https://doi.org/10.1007/s10661-009-0897-6>

Signa G, Calizza E, Costantini ML, Tramati C, Sporta Caputi S, Mazzola A, Rossi L, Vizzini S (2019) Horizontal and vertical food web structure drives trace element trophic transfer in Terra Nova Bay, Antarctica. *Environ Pollut* 246:772–781. <https://doi.org/10.1016/j.envpol.2018.12.071>

Sohrabi T, Ismail A, Nabavi MB (2010) Distribution and normalization of some metals in surface sediments from South Caspian Sea. *Bull Environ Contam Toxicol* 85:502–508. <https://doi.org/10.1007/s00128-010-0112-z>

Tabari S, Saravi SSS, Bandany GA, Dehghan A, Shokrzadeh M (2010) Heavy metals (Zn, Pb, Cd and Cr) in fish, water and sediments sampled from Southern Caspian Sea, Iran. *Toxicol Ind Health* 26:649–656. <https://doi.org/10.1177/0748233710377777>

Titlyanov EA, Kiyashko SI, Titlyanova TV, Huyen PV, Yakovleva IM (2011) Identifying nitrogen sources for macroalgal growth in variously polluted coastal areas of southern Vietnam. *Bot Mar* 54:367–376. <https://doi.org/10.1515/bot.2011.041>

Vesali Naseh MR, Karbassi A, Ghazaban F, Baghvand A (2012) Evaluation of heavy metal pollution in Anzali wetland, Guilan, Iran. *Iran J Toxicol* 5:565–576.

Villares R, Puente X, Carballeira A (2001) *Ulva* and *Enteromorpha* as indicators of heavy metal pollution. *Hydrobiologia* 462:221–232. <https://doi.org/10.1023/A:1013154821531>

Vizzini S, Savona B, Chi TD, Mazzola A (2005) Spatial variability of stable carbon and nitrogen isotope ratios in a Mediterranean coastal lagoon. *Hydrobiologia* 550:73–82. <https://doi.org/10.1007/s10750-005-4364-2>

Wang Y, Liu D, Richard P, Di B (2016) Selection of effective macroalgal species and tracing nitrogen sources on the different part of Yantai coast, China indicated by macroalgal  $\delta^{15}\text{N}$  values. *Sci Total Environ* 542:306–314. <https://doi.org/10.1016/j.scitotenv.2015.10.059>

Wolf-Welling TCW, Moerz T, Hillenbrand CD, Pudsey CJ, Cowan E, (2002) Data report: Bulk sediment parameters (CaCO<sub>3</sub>, TOC, and more than 63  $\mu\text{m}$ ) of Sites 1095, 1096, and 1011, and coarse-fraction analysis of Site 1095 (ODP Leg 178, western Antarctic Peninsula). In: Barker PF, Camerlenghi A, Acton GD, Ramsay ATS (eds), *Proceedings of the Ocean Drilling Program, Scientific Results*, pp. 1–19.

Zamani Hargalani F, Karbassi A, Monavari SM, Azar PA (2014) A novel pollution index based on the bioavailability of elements: a study on Anzali wetland bed sediments. *Environ Monit Assess* 186:2329–2348. <https://doi.org/10.1007/s10661-013-3541-4>



Ziarati P, Zendehtdel T, Bidgoli SA (2014) Nitrate content in drinking water in Gilan and Mazandaran Provinces, Iran. J Environ Anal Toxicol 4:1–5.

Zonn IS (2005) Environmental issues of the Caspian. In: Kosarev AN (ed), the Caspian sea environment, Berlin Heidelberg, Springer-Verlag, pp. 223-242.

1  
2  
3  
4  
5  
6  
7  
8  
9  
10  
11  
12  
13  
14  
15  
16  
17  
18  
19  
20  
21  
22  
23  
24  
25  
26  
27  
28  
29  
30  
31  
32  
33  
34  
35  
36  
37  
38  
39  
40  
41  
42  
43  
44  
45  
46  
47  
48  
49  
50  
51  
52  
53  
54  
55  
56  
57  
58  
59  
60  
61  
62  
63  
64  
65

1 **Tables**

2  
3 Table 1. Water parameters (mean  $\pm$  standard error) at various sampling sites in the Southern Caspian Sea. TN and TP  
4 indicate the concentration of dissolved Nitrogen and Phosphorus respectively.  
5  
6

7

Site	O <sub>2</sub> (mg/l)	TN (mg/l)	TP (mg/l)	pH	T (°C)
Anzali	10.6 $\pm$ 0.31	2.44 $\pm$ 0.08	0.68 $\pm$ 0.18	7.62 $\pm$ 0.04	25.05 $\pm$ 0.04
Hachirud	4.65 $\pm$ 0.96	4.19 $\pm$ 0.47	0.63 $\pm$ 0.34	8.30 $\pm$ 0.01	25.20 $\pm$ 0.12
Radio Darya	3.73 $\pm$ 0.96	4.49 $\pm$ 0.38	0.90 $\pm$ 0.27	8.17 $\pm$ 0.14	24.83 $\pm$ 0.10
Nowshahr	7.10 $\pm$ 0.20	3.22 $\pm$ 0.04	0.03 $\pm$ 0.003	7.75 $\pm$ 0.02	25.10 $\pm$ 0.04
Sisangan	6.10 $\pm$ 0.11	3.51 $\pm$ 0.09	0.04 $\pm$ 0.002	7.79 $\pm$ 0.01	24.96 $\pm$ 0.02

8  
9  
10  
11  
12  
13  
14  
15  
16  
17  
18  
19  
20  
21  
22  
23  
24  
25  
26  
27  
28  
29  
30  
31  
32  
33  
34  
35  
36  
37  
38  
39  
40  
41  
42  
43  
44  
45  
46  
47  
48  
49  
50  
51  
52  
53  
54  
55  
56  
57  
58  
59  
60  
61  
62  
63  
64  
65

Table 2. Average  $\pm$  standard error of element concentrations (in ppm) in sediment at various sampling sites in the Southern Caspian Sea. “Maximum” indicates the site (first letter of site name, as indicated in brackets) where the highest concentration of each element was recorded.

Element	Anzali (A)	Hachirud (H)	Radio Darya (R)	Nowshahr (N)	Sisangan (S)	Maximum
Al (I)	45315 $\pm$ 2235	15649 $\pm$ 554	11366 $\pm$ 490	42824 $\pm$ 242	37285 $\pm$ 1579	A
Ca (I)	98875 $\pm$ 2786	43989 $\pm$ 2584	26054 $\pm$ 883	90278 $\pm$ 4248	83869 $\pm$ 2390	A
Fe (II)	63213 $\pm$ 2111	91384 $\pm$ 5700	97957 $\pm$ 4364	40370 $\pm$ 2500	66721 $\pm$ 3367	R
Mg (I)	30500 $\pm$ 1766	16792 $\pm$ 680	9185 $\pm$ 475	26511 $\pm$ 1379	28838 $\pm$ 1738	A
Mn (II)	2214 $\pm$ 149	3447 $\pm$ 221	2970 $\pm$ 168	778 $\pm$ 46	1503 $\pm$ 83	H
Na (I)	9997 $\pm$ 373	2550 $\pm$ 72	1487 $\pm$ 52	9847 $\pm$ 260	8703 $\pm$ 307	A
Ti (I)	15740 $\pm$ 781	3622 $\pm$ 112	6316 $\pm$ 340	13890 $\pm$ 645	6846 $\pm$ 244	A
K (I)	10378 $\pm$ 324	1967 $\pm$ 113	1463 $\pm$ 74	11802 $\pm$ 439	9162 $\pm$ 441	N
S (III)	726 $\pm$ 27	461 $\pm$ 8	404 $\pm$ 16	415 $\pm$ 23	450 $\pm$ 22	A
P (III)	751 $\pm$ 30	812 $\pm$ 39	689 $\pm$ 39	634 $\pm$ 33	644 $\pm$ 31	H
Ba (I)	244 $\pm$ 12	87 $\pm$ 4	118 $\pm$ 5	267 $\pm$ 9	213 $\pm$ 10	N
Cr (II)	303 $\pm$ 14	699 $\pm$ 35	692 $\pm$ 23	169 $\pm$ 6	301 $\pm$ 16	H
V (II)	264 $\pm$ 12	811 $\pm$ 39	874 $\pm$ 28	94 $\pm$ 4	266 $\pm$ 9	R
Ni (II)	51 $\pm$ 2	76 $\pm$ 3	76 $\pm$ 7	40 $\pm$ 1	47 $\pm$ 2	H
Pb (II)	27 $\pm$ 1	61 $\pm$ 2	62 $\pm$ 3	27 $\pm$ 1	31 $\pm$ 1	R
Zn (II)	81 $\pm$ 3	253 $\pm$ 8	223 $\pm$ 6	44 $\pm$ 2	97 $\pm$ 6	H
Co (II)	25 $\pm$ 1	43 $\pm$ 2	41 $\pm$ 1	15 $\pm$ 1	22 $\pm$ 1	H
Cu (II)	23 $\pm$ 1	44 $\pm$ 2	26 $\pm$ 1	11 $\pm$ 1	14 $\pm$ 1	H

I, II, and III associated to each element indicate different groups in which metals were grouped according to the PCA analysis. A=Anzali, H = Hachirud, R= Radio Darya, N= Nowshahr, S= Sisangan.

Table 3. R values associated to linear correlations between elements. Grouping of metals is well reflected by positive correlations between elements of the same group, and by negative correlations between elements of two different groups.

	Al (I)	Ba (I)	Ca (I)	K (I)	Mg (I)	Na (I)	Ti (I)	Co (II)	Cr (II)	Cu (II)	Fe (II)	Mn (II)	Ni (II)	Pb (II)	V (II)	Zn (II)	P (III)	S (III)
Al (I)	-	0.96*	0.99*	0.99*	0.96*	0.99*	0.83	-0.92*	-0.96*	-0.70	-0.91*	-0.81	-0.94*	-0.99*	-0.97*	-0.96*	-0.40	0.52
Ba (I)		-	0.92*	0.98*	0.84	0.96*	0.87	-0.97*	-0.98*	-0.85	-0.94*	-0.90*	-0.96*	-0.97*	-0.97*	-0.99*	-0.60	0.36
Ca (I)			-	0.97*	0.98*	0.99*	0.78	-0.89*	-0.94*	-0.63	-0.89*	-0.76	-0.92*	-0.98*	-0.95*	-0.92*	0.55	-0.18
K (I)				-	0.92*	0.99*	0.82	-0.97*	-0.99*	-0.78	-0.96*	-0.89*	-0.98*	-0.99*	-0.99*	-0.99*	-0.52	0.37
Mg (I)					-	0.96*	0.66	-0.84	-0.88*	-0.56	-0.81	-0.70	-0.88*	-0.94*	-0.91*	-0.86	-0.26	0.55
Na (I)						-	0.80	-0.94*	-0.97*	-0.73	-0.92*	-0.84	-0.96*	-0.99*	-0.98*	-0.97*	-0.44	0.47
Ti (I)							-	-0.73	-0.78	-0.59	-0.77	-0.62	-0.72	-0.80	-0.76	-0.83	-0.28	0.61
Co (II)								-	0.99*	0.88*	0.96*	0.97*	0.99*	0.95*	0.98*	0.98*	0.69	-0.16
Cr (II)									-	0.84	0.97*	0.94*	0.99*	0.98*	0.99*	0.99*	0.61	-0.27
Cu (II)										-	0.76	0.93*	0.85	0.78	0.80	0.87	0.92*	0.06
Fe (II)											-	0.92*	0.96*	0.92*	0.97*	0.95*	0.55	-0.18
Mn (II)												-	0.95*	0.86	0.92*	0.93*	0.82	0.06
Ni (II)													-	0.97*	0.99*	0.98*	0.64	-0.21
Pb (II)														-	0.98*	0.98*	0.50	-0.44
V (II)															-	0.98*	0.56	-0.30
Zn (II)																-	0.63	-0.31
P (III)																	-	0.42
S (III)																		-

\*:  $p < 0.05$ . I, II, and III indicate different groups in which elements were grouped according to the PCA analysis.

Table 4. Average  $\pm$  standard error of metal concentrations (in ppm) for those metals included in the Sediment Quality

Guidelines (SQG)

Sediment SQG classification					
Threshold effect level (TEL); Non polluted (NP); Moderately polluted (MP); Heavily polluted (HP)					
Element	Site	ppm	TEL	Classification	Class
Cr	Anzali	303 $\pm$ 14	52.3	Cr < 25 Non-polluted	HP
	Hachirud	699 $\pm$ 35		25 $\leq$ Cr $\leq$ 75 Moderately polluted	HP
	Radio Darya	692 $\pm$ 23		Cr > 75 Heavily polluted	HP
	Nowshahr	169 $\pm$ 6			HP
	Sisangan	301 $\pm$ 16			HP
Cu	Anzali	23 $\pm$ 1	18.7	Cu < 25 Non-polluted	NP
	Hachirud	44 $\pm$ 2		25 $\leq$ Cu $\leq$ 50 Moderate polluted	MP
	Radio Darya	26 $\pm$ 1		Cu > 50 Heavily polluted	MP
	Nowshahr	11 $\pm$ 1			NP
	Sisangan	14 $\pm$ 1			NP
Ni	Anzali	51 $\pm$ 2	15.9	Ni < 20 Non-polluted	HP
	Hachirud	76 $\pm$ 3		20 $\leq$ Ni $\leq$ 50 Moderate polluted	HP
	Radio Darya	76 $\pm$ 3		Ni > 50 Heavily polluted	HP
	Nowshahr	40 $\pm$ 1			MP
	Sisangan	47 $\pm$ 2			MP
Pb	Anzali	27 $\pm$ 1	30.2	Pb < 40 Non-polluted	NP
	Hachirud	61 $\pm$ 3		40 $\leq$ Pb $\leq$ 60 Moderate polluted	HP
	Radio Darya	62 $\pm$ 3		Pb > 60 Heavily polluted	HP
	Nowshahr	27 $\pm$ 1			NP
	Sisangan	31 $\pm$ 1			NP
Zn	Anzali	81 $\pm$ 3	124.0	Zn < 90 Non-polluted	NP
	Hachirud	253 $\pm$ 8		90 $\leq$ Zn $\leq$ 200 Moderate polluted	HP
	Radio Darya	223 $\pm$ 6		Zn > 200 Heavily polluted	HP
	Nowshahr	44 $\pm$ 2			NP
	Sisangan	97 $\pm$ 6			MP

Table 5. Descriptive statistics of metal concentrations (in ppm) measured in macroalgae along the Iranian coast of the Caspian Sea. Superscript letters above maximum values indicate the algal species where the maximum was observed. Samples belonging to the genus *Spyrogira* were excluded since with the lowest metal concentrations.

	Ca	Mg	Fe	Al	P	K	Mn	Zn	Ti	Cu	Cr	V	Ni	Co
Minimum	15378	1493	756	886	352.0	217.0	32.8	28.9	20.9	11.5	1.7	0.01	1.1	0.01
1 <sup>st</sup> Quartile	18026	2176	1119	1245	386.5	290.8	51.6	40.8	25.4	15.2	2.0	2.4	2.1	0.1
Median	20990	2508	1862	1744	445.5	353.5	77.8	51.3	27.7	17.7	2.5	2.8	2.5	0.5
Mean	21025	2522	1755	1750	503.5	426.6	75.3	56.5	37.9	26.7	3.2	2.7	2.6	0.6
3 <sup>rd</sup> Quartile	23982	2720	2203	2266	582.0	544.8	98.8	70.6	32.0	20.7	2.9	3.3	3.0	0.9
Maximum	27304 <sup>a</sup>	3898 <sup>a</sup>	3354 <sup>b</sup>	2697 <sup>b</sup>	942.0 <sup>b</sup>	860.0 <sup>b</sup>	113.10 <sup>b</sup>	93.8 <sup>b</sup>	153.8 <sup>b</sup>	78.5 <sup>a</sup>	12.2 <sup>b</sup>	6.1 <sup>b</sup>	4.6 <sup>b</sup>	1.9 <sup>a</sup>

a= *Sargassum*, b= *Enteromorpha*.

## Figure legends

1  
2 **Fig. 1** Map of the study area. **(a)** General view of the Iranian coast of the Caspian Sea, including the Gilan and  
3 Mazandaran Provinces. **(b)** Focus of the Gilan Province showing the sampling site of Anzali. **(c)** Focus of the  
4 Mazandaran Province showing the sampling sites of Hachirud, Radio Darya, Nowshahr and Sisangan  
5  
6  
7  
8  
9

10 **Fig. 2** Bar plots of mean ( $\pm$ standard error)  $\delta^{15}\text{N}$  values in macroalgae at different sampling sites. Isotopic thresholds  
11 denoting different sources and levels of anthropogenic N pollution are indicated in the background of the image.  
12 ‘inorganic’ pollution:  $\delta^{15}\text{N} < 3\text{‰}$ , ‘non-impacted’:  $3\text{‰} \leq \delta^{15}\text{N} \leq 6\text{‰}$ , ‘moderate organic’ pollution:  $6\text{‰} < \delta^{15}\text{N} \leq 9\text{‰}$ ,  
13 ‘high’ organic pollution:  $\delta^{15}\text{N} > 9\text{‰}$   
14  
15  
16  
17  
18  
19

20 **Fig. 3** Linear regressions between  $\delta^{15}\text{N}$  (‰) values in macroalgae against dissolved Nitrogen (TN, mg/l) in water **(a)**,  
21 and Oxygen concentration (mg/l) against  $\delta^{15}\text{N}$  (‰) in macroalgae **(b)**.  
22  
23  
24  
25  
26  
27  
28  
29  
30  
31  
32  
33  
34  
35  
36  
37  
38  
39  
40  
41  
42  
43  
44  
45  
46  
47  
48  
49  
50  
51  
52  
53  
54  
55  
56  
57  
58  
59  
60  
61  
62  
63  
64  
65

1  
2  
3  
4  
5  
6  
7  
8  
9  
10  
11  
12  
13  
14  
15  
16  
17  
18  
19  
20  
21  
22  
23  
24  
25  
26  
27  
28  
29  
30  
31  
32  
33  
34  
35  
36  
37  
38  
39  
40  
41  
42  
43  
44  
45  
46  
47  
48  
49  
50  
51  
52  
53  
54  
55  
56  
57  
58  
59  
60  
61  
62  
63  
64  
65

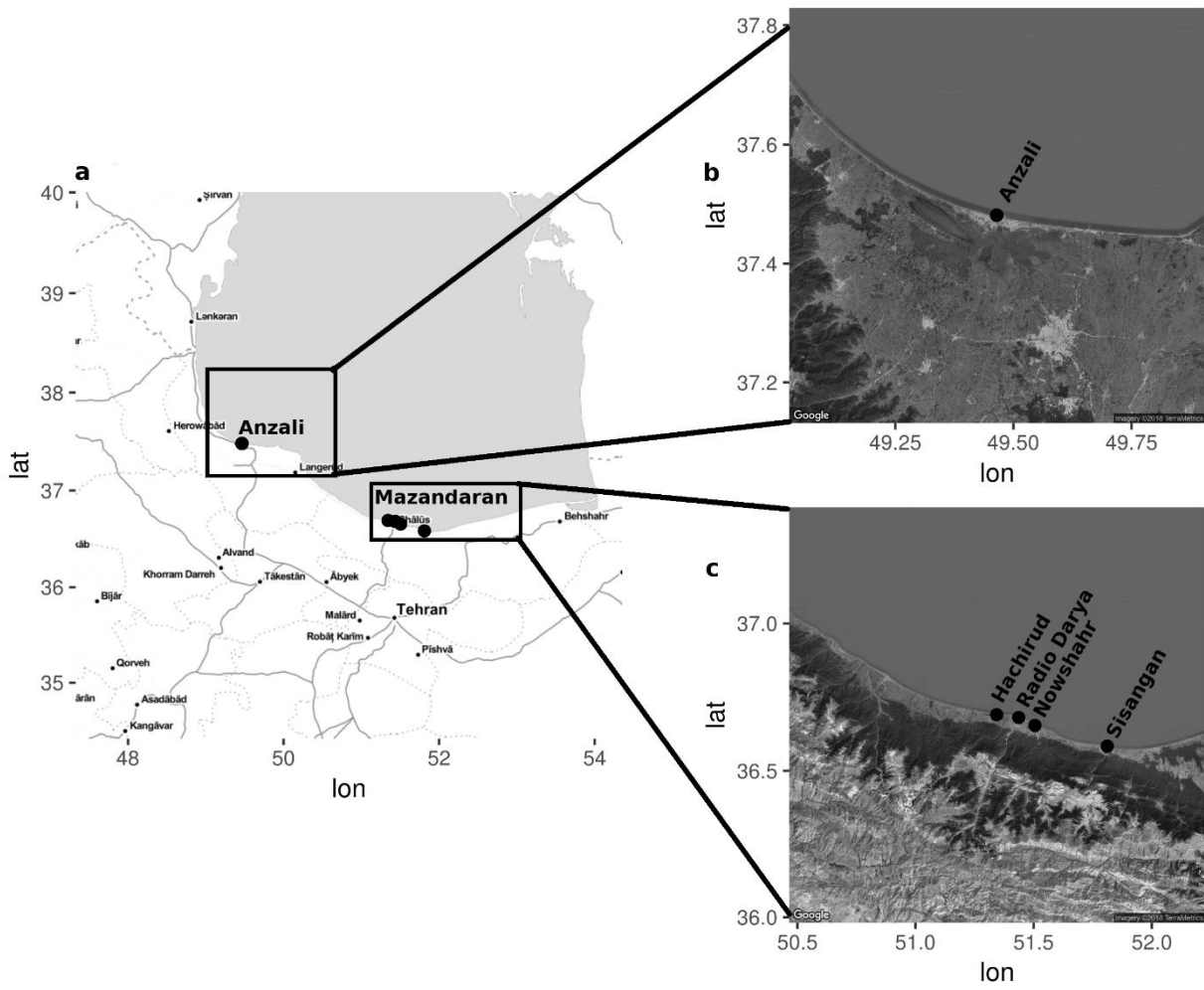


Fig. 1



1  
2  
3  
4  
5  
6  
7  
8  
9  
10  
11  
12  
13  
14  
15  
16  
17  
18  
19  
20  
21  
22  
23  
24  
25  
26  
27  
28  
29  
30  
31  
32  
33  
34  
35  
36  
37  
38  
39  
40  
41  
42  
43  
44  
45  
46  
47  
48  
49  
50  
51  
52  
53  
54  
55  
56  
57  
58  
59  
60  
61  
62  
63  
64  
65

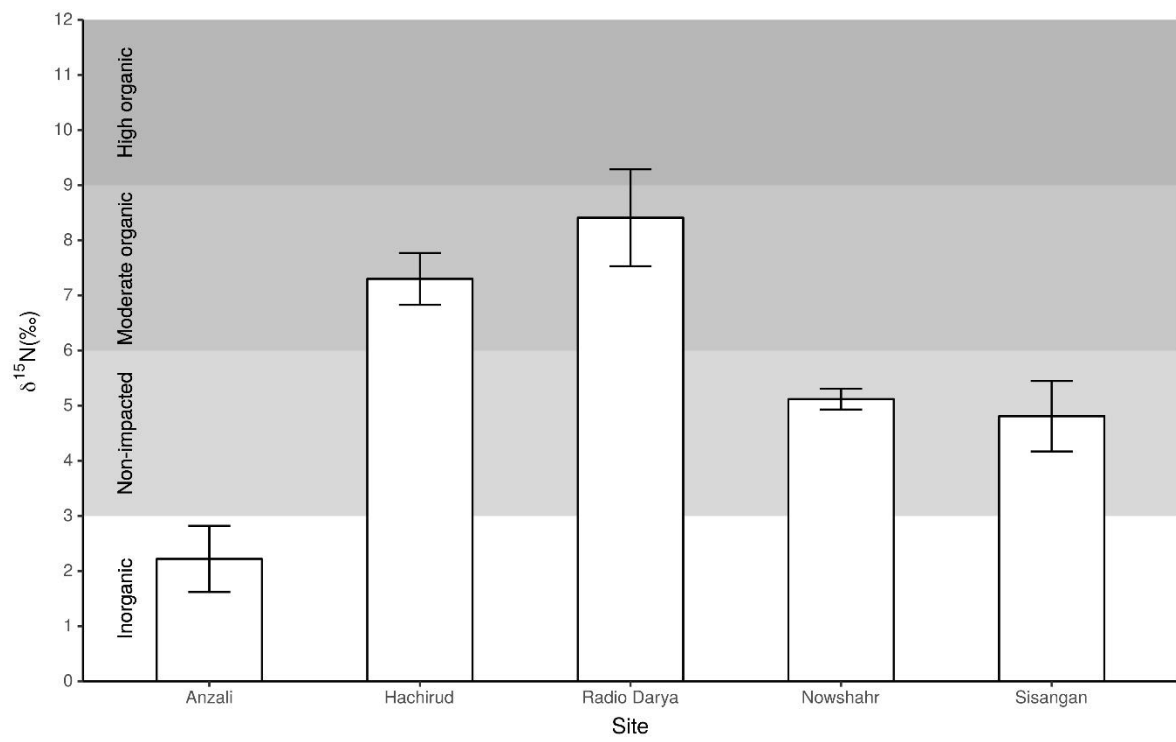


Fig. 2

1  
2  
3  
4  
5  
6  
7  
8  
9  
10  
11  
12  
13  
14  
15  
16  
17  
18  
19  
20  
21  
22  
23  
24  
25  
26  
27  
28  
29  
30  
31  
32  
33  
34  
35  
36  
37  
38  
39  
40  
41  
42  
43  
44  
45  
46  
47  
48  
49  
50  
51  
52  
53  
54  
55  
56  
57  
58  
59  
60  
61  
62  
63  
64  
65

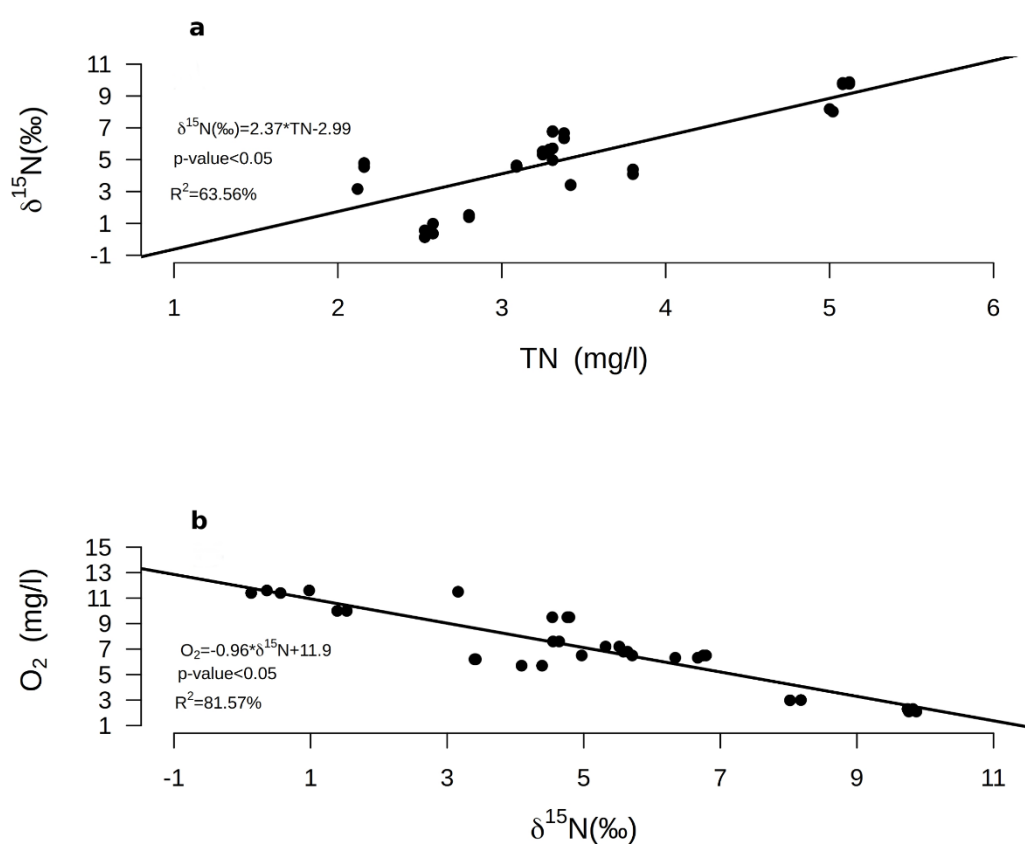
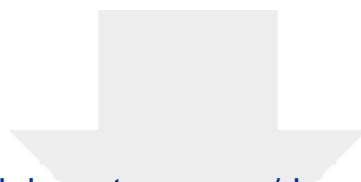


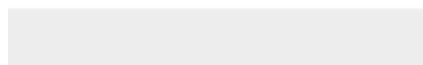
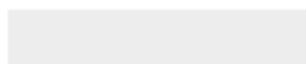
Fig. 3



[Click here to access/download](#)

**Supplementary Material**

Cover Letter\_Costantini et al\_EnvSciPolRes.pdf



## Chapter 4

### **Isotopic biomonitoring of N pollution in rivers embedded in complex human landscapes**

Calizza, Edoardo<sup>a,b</sup>, Favero, Federica<sup>a</sup>, Rossi, David<sup>c</sup>, Careddu, Giulio<sup>a</sup>,  
**Fiorentino, Federico<sup>a</sup>**, Sporta Caputi, Simona<sup>a,\*</sup>, Rossi, Loreto<sup>a,b</sup>,  
Costantini, Maria Letizia<sup>a,b</sup>.

<sup>a</sup> Department of Environmental Biology, Sapienza University of Rome, via dei Sardi 70, 00185 Rome, Italy

<sup>b</sup> CoNISMa, piazzale Flaminio 9, 00196 Rome, Italy

<sup>c</sup> CNR-Water Research Institute, Research Area RM1, via Salaria Km 29.300 C.P.10, 00015 Monterotondo (RM), Italy

**Corresponding Author:** [simona.sportacaputi@uniroma1.it](mailto:simona.sportacaputi@uniroma1.it) (S. Sporta Caputi)

Manuscript published in *Science of the Total Environment*



# Isotopic biomonitoring of N pollution in rivers embedded in complex human landscapes

E. Calizza<sup>a,b</sup>, F. Favero<sup>a</sup>, D. Rossi<sup>c</sup>, G. Careddu<sup>a</sup>, F. Fiorentino<sup>a</sup>, S. Sporta Caputi<sup>a,\*</sup>, L. Rossi<sup>a,b</sup>, M.L. Costantini<sup>a,b</sup>

<sup>a</sup> Department of Environmental Biology, Sapienza University of Rome, via dei Sardi 70, 00185 Rome, Italy

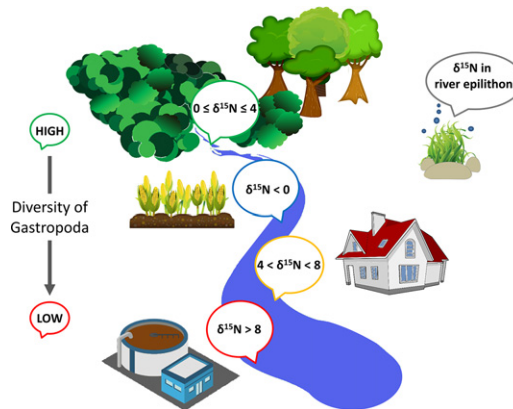
<sup>b</sup> CoNISMa, piazzale Flaminio 9, 00196 Rome, Italy

<sup>c</sup> CNR-Water Research Institute, Research Area RM1, via Salaria km 29.300 C.P.10, 00015 Monterotondo, RM, Italy

## HIGHLIGHTS

- A novel approach for the biomonitoring of N pollution in rivers is presented.
- Stable isotopes in river biota, land use and drainage in watersheds were analysed.
- $\delta^{15}\text{N}$  in epilithon reflected localised and diffuse N inputs of organic and inorganic origin.
- Dislocation of pollution sources and their dispersion along rivers were identified.
- N pollution affected abundance, richness and  $\beta$  diversity of freshwater gastropods.

## GRAPHICAL ABSTRACT



## ARTICLE INFO

### Article history:

Received 1 August 2019

Received in revised form 9 December 2019

Accepted 10 December 2019

Available online 11 December 2019

Editor: Ouyang Wei

### Keywords:

Stable isotopes

Mediterranean rivers

Epilithon

Snails

Land use

Multiple pollution sources

## ABSTRACT

The dynamic and hierarchical structure of rivers, together with disruption of the natural river continuum by human activities, makes it difficult to identify and locate sources of nutrient pollution affecting receiving waters and observe its dispersion, thus impairing monitoring efforts. The identification of reliable indicators of anthropogenic nitrogen inputs in catchments is therefore key to achieving effective management of polluted rivers. We tested the capacity of N isotopic signatures ( $\delta^{15}\text{N}$ ) of epilithon and snails to provide useful indications of organic and inorganic anthropogenic N inputs in three Mediterranean rivers differing in terms of surrounding land use and physicochemical conditions. We used a combined approach based on (i) analysis of nutrient concentrations in water, (ii) CORINE land cover classification and drainage patterns in catchments and (iii) isotopic analysis of river biota to verify whether isotopic variations were indicative of anthropic activities in the watershed, the associated alteration of water quality, and the consequent impact on snail abundance and diversity.

Variation in the  $\delta^{15}\text{N}$  of epilithon within and between rivers reflected localised and diffuse N inputs from inorganic and organic sources. Negative epilithon  $\delta^{15}\text{N}$  values ( $<0\%$ ) indicated inorganic pollution from agriculture. Values between 4‰ and 8‰ and those above 8‰ respectively indicated moderate organic pollution from urban areas, and high organic pollution, mostly from waste waters. The diversity and abundance of snails decreased with increasing water pollution. While their isotopic variations reflected between-river differences, they failed to indicate within-river variations in anthropogenic N inputs, since the proportion of epilithon in their diet varied along the rivers. Concluding, epilithon was a reliable indicator of anthropogenic N sources across a wide range of

\* Corresponding author at: Department of Environmental Biology, Sapienza University of Rome, via dei Sardi 70, 00185 Rome, Italy.

E-mail address: [simona.sportacaputi@uniroma1.it](mailto:simona.sportacaputi@uniroma1.it) (S. Sporta Caputi).

nutrient concentrations and anthropogenic inputs, and the proposed approach allowed us to determine the nature of nitrogen pollutants, their sources, location and dispersion along rivers embedded in complex human landscapes.

© 2019 Elsevier B.V. All rights reserved.

## 1. Introduction

Anthropic activities affecting lotic ecosystems, in combination with the geomorphology of catchment areas, can result in rivers with localised and/or diffuse disturbance that impairs water quality and disrupts the natural river continuum (di Lascio et al., 2013; Vannote et al., 1980; Winemiller et al., 2011; Woodward and Hildrew, 2002; Zeug et al., 2009). In anthropised landscapes, agriculture and urbanisation are the dominant sources of nitrogen loading to surface waters (Anderson and Cabana, 2006; Cole et al., 2004; Dalu et al., 2019; De Brabandere et al., 2007). Such inputs affect rivers and the receiving coastal waters (Bentivoglio et al., 2016; Ouyang et al., 2014; Rossi et al., 2018), increasing the risk of eutrophication, algal blooms, fish kills and habitat and biodiversity loss (Caporn et al., 2014; Le Moal et al., 2019; Vander Zanden et al., 2005). The most common anthropic N inputs in rivers are fertilisers, livestock manure and urban wastewater. Nevertheless, the dynamic and complex nature of rivers, as well as their dependence on external factors including land use and climatic factors (Álvarez-Cabria et al., 2016; Poole, 2002; Vannote et al., 1980; Ward, 1989; Woodward and Hildrew, 2002), makes it difficult to identify the nature and location of nutrient sources and to determine their dispersion, impairing management efforts. The identification of a reliable indicator of anthropogenic nutrient sources and dispersion is thus essential to effective river management aimed at the reduction of nutrient load and the implementation and monitoring of mitigation measures. In aquatic systems, isotopic analyses of nitrogen ( $\delta^{15}\text{N}$ ) are increasingly used to detect and distinguish between N inputs affecting surface waters (Bentivoglio et al., 2016; Dailer et al., 2010; di Lascio et al., 2013; Fiorentino et al., 2017; Jona-Lasinio et al., 2015; Orlandi et al., 2014; Rossi et al., 2018). Indeed, synthetic fertilisers display lower  $\delta^{15}\text{N}$  values than natural N sources (Dailer et al., 2010; Heaton, 1986; Kendall, 1998; Mayer et al., 2002; Y. Wang et al., 2016), while N inputs derived from animal manure and wastewater display higher values (Fiorentino et al., 2017; Jona-Lasinio et al., 2015; Kendall, 1998; Orlandi et al., 2017). Accordingly, N isotopic analysis has been successfully applied in coastal (Calizza et al., 2015a; Dailer et al., 2010; Orlandi et al., 2014; Rossi et al., 2018; Viana and Bode, 2013), transitional (Jona-Lasinio et al., 2015) and lentic waters (Fiorentino et al., 2017) to provide reliable bioindicators of anthropogenic N inputs, mostly based on aquatic algae (Dailer et al., 2010; Orlandi et al., 2017). However, while preliminary evidence of the applicability of isotopic monitoring to rivers exists (Bentivoglio et al., 2016; di Lascio et al., 2013), isotope-based methods for the systematic biomonitoring of river courses and mapping of nitrogen pollution have not yet been developed.

Given its ubiquity, tolerance of a wide range of conditions, quick response to changes and low tendency to drift, epilithon has been considered a good indicator of water quality in rivers (Burns and Ryder, 2001; Fernandes et al., 2019; T. Wang et al., 2016). Like macroalgae, algae in the biofilm matrix are able to assimilate N directly from the water and store excess N in their tissues (Bentivoglio et al., 2016; Fiorentino et al., 2017). Because of this characteristic and because species composition has no influence on isotopic signature (Fiorentino et al., 2017; MacLeod and Barton, 1998), epilithon is believed to reflect the availability and isotopic composition of N sources in lotic ecosystems. It also represents a nutrient source for higher trophic levels. Thus, given that the isotopic signatures of consumers reflect those of their food sources (Calizza et al., 2015a, 2015b, 2018; Carrozzo et al., 2014; Post, 2002; Rossi et al., 2015), animals feeding mainly on epilithon (e.g. gastropods)

could represent useful indicators of nitrogen pollutant transfer along food chains (Bentivoglio et al., 2016; Mancinelli and Vizzini, 2015).

The aim of this study was to develop a new, widely applicable bio-monitoring approach to N pollution in rivers. To achieve this, we (i) assessed the variation of  $\delta^{15}\text{N}$  in epilithon and snails in three geographically close Mediterranean rivers characterised by differing levels of anthropisation in their catchment areas, and (ii) tested their reliability as bioindicators of anthropogenic nutrient pollution of organic and inorganic origin. The three rivers are the main contributors in a complex mosaic of anthropogenic inputs discharged into a coastal area used for tourism, fishing and fish farming (Cicala et al., 2019; Rossi et al., 2018). Discerning the anthropogenic inputs carried by each river is thus essential for effective river management and mitigation of pollution, which is hard to characterise once mixed and diluted in coastal waters.

Isotopic signatures were compared both between rivers and along each river. We analysed land use and drainage patterns in catchment areas (Bentivoglio et al., 2016; Calizza et al., 2016; Fiorentino et al., 2017), and we assessed the capacity of  $\delta^{15}\text{N}$  in epilithon and snails to provide useful spatial information about allochthonous N inputs and to distinguish between the nature and origin of N sources. Specifically, we tested the hypothesis that the  $\delta^{15}\text{N}$  values of epilithon and snails increased in the presence of organic inputs and decreased in the presence of inorganic inputs along upstream-downstream sampling transects, reflecting variations in land use and N concentration in waters (Bentivoglio et al., 2016; Fiorentino et al., 2017; Jona-Lasinio et al., 2015; Rossi et al., 2018). In addition, to understand whether and to what extent water pollution affected snails, a key component of river ecosystems (Wallace and Webster, 1996, and literature cited therein), the abundance and diversity of Gastropoda between and along rivers were compared.

## 2. Materials and methods

### 2.1. Study area

The study was carried out in the hinterland of the Gulf of Gaeta ( $41^{\circ}15' \text{ N } 13^{\circ}40' \text{ E}$ ), on the west coast of Central Italy in the Mediterranean Sea. The Gulf is delimited to the North-West by the town of Sperlonga and to the South-East by the Garigliano river estuary and it is characterised by varying levels and density of anthropogenic pressure (Careddu et al., 2015, 2017; Orlandi et al., 2014; Rossi et al., 2018). This study examined the three main river systems discharging directly into the Gulf, whose catchment areas were affected by contrasting human activities: the Itri, the Capodacqua Santa Croce (hereafter: Santa Croce) and the Garigliano (Fig. 1).

Under the Köppen-Geiger climate classification (Köppen, 1936; Beck et al., 2018), this area is characterised by a temperate climate with hot-dry summers (Csa) and average rainfall amounting to  $1036.9 \pm 66.1$  mm/year in 2012–2018 (source: Centro Funzionale Regionale, Lazio Region; data prior to 2012 are not available for the study area). On average, rainfall was highest in November ( $155.8 \pm 4.2$  mm/month) and lowest in June ( $31.4 \pm 1.6$  mm/month). Data are expressed as mean  $\pm$  standard error. Due to their geographical proximity (15 km maximum linear distance between river mouths), mean rainfall in the three catchment areas is highly similar. Specifically, mean annual rainfall amounted to  $938.99 \pm 77.19$  mm for the Itri,  $1162.89 \pm 99.20$  mm for the Santa Croce and  $1008.90 \pm 88.19$  mm for the Garigliano. Rainfall data are from monitoring stations near upstream sites in each river.



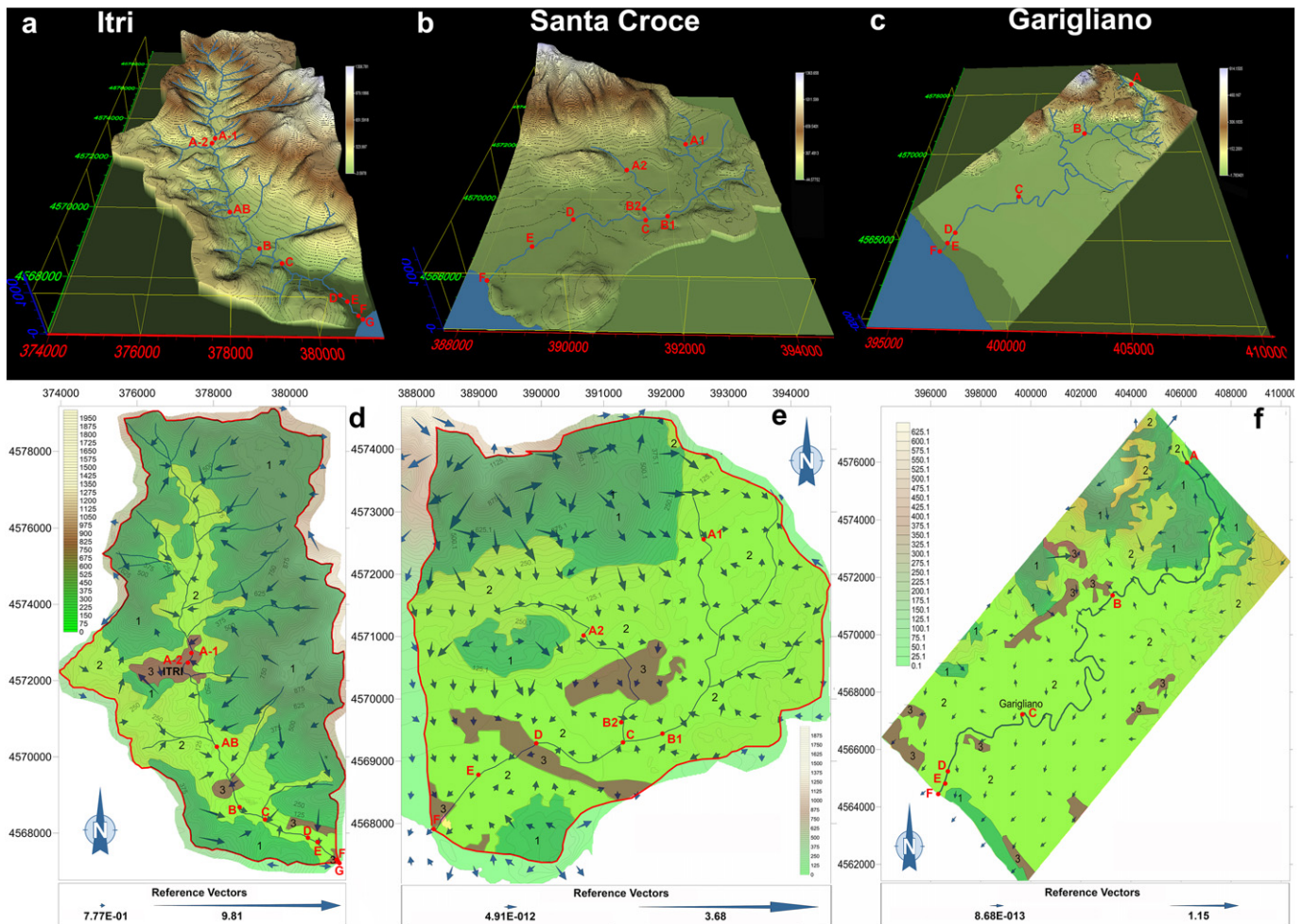


**Fig. 1.** Panels a–c: 3D maps showing the location of sampling sites in the three rivers, the geographical coordinates (x, y) and the altitude above sea level (z, from green to dark brown and white). Sites are listed in alphabetic order from upstream to downstream, and the most downstream site indicates the river mouth. Panels d–f: superimposed maps of catchment area (red line), digital elevation model, land use and drainage direction/intensity (arrow orientation/length) for the three rivers. Three main classes have been identified: (1) Natural areas (i.e. woods) in dark green; (2) Agricultural areas (i.e. permanent and semi-permanent crops) in light green; (3) Artificial areas (i.e. urban areas) in brown.

The river Itri rises in the Aurunci Mountains. It is 13 km long and drains an area of 55 km<sup>2</sup>. The river crosses the city of Itri and flows into the Gulf of Gaeta near the beach of Vindicio (Formia). The river outflow decreases in summer and is affected on a daily basis by a wastewater treatment plant (WWTP) in its upstream reach. In the absence of rainfall, the WWTP flow rate is estimated to be 5–10 L/s.

The river Santa Croce originates from the Capodacqua spring at the foot of the Aurunci Mountains (Spigno Saturnia). It is 10 km long and drains an area of 40 km<sup>2</sup>. The river crosses the towns of Spigno Saturnia, Minturno and, near the mouth, Formia. Its mean flow rate is 1000 ± 300 L/s (maximum 2500 L/s, in winter, and minimum 500 L/s, in summer). A secondary river branch 3.5 km long, crossing an area consisting mainly of farmland, flows into the main channel of the river in its upstream reach. To differentiate between the two upstream branches, in the text we will refer to them as 'main' and 'secondary'.

The river Garigliano starts at the confluence of the rivers Liri and Gari. The Liri-Garigliano is 158 km long with a catchment area of 5020 km<sup>2</sup>, which makes it the sixth largest river basin in Italy. The mean flow rate is estimated to be 120000 L/s. The river represents the main direct source of freshwaters in the Gulf of Gaeta, and its nutrient and organic matter inputs affect the quality of surface coastal waters and biodiversity and food web structure in marine communities (Careddu et al., 2015, 2017; Cicala et al., 2019; Rossi et al., 2018).

To determine the intensity and direction of drainage into each river, a detailed digital elevation model was created (Bentivoglio et al., 2016;

Calizza et al., 2016; Rossi et al., 2019). The 3D model was generated by digitising regional technical maps. Where missing data and topographic inaccuracies could have affected interpolation, field campaigns with GPS equipment were conducted to correct and update the morphology and river courses. Kriging interpolation methods were used to obtain contour maps. Specific 3D software was used to: 1) model the morphology, 2) calculate the surface area, and 3) evaluate terrain slope, terrain aspect, profile and plan curvature (Calizza et al., 2016; Rossi et al., 2019).

## 2.2. Field sampling

Within each river, a set of sampling sites was selected, reflecting variation in land use and hydromorphology within the catchment areas (Bentivoglio et al., 2016). In detail, eight sites were selected for the Santa Croce, nine sites for the Itri and six sites for the Garigliano, the longest river (Fig. 1a–c). Due to its extension, the Garigliano river basin straddles two different climate classes, i.e. “temperate no dry season-hot summer” (class: Cfa) in its upstream and intermediate sectors and “temperate dry-hot summer” (class: Csa) in its lowland sector (Köppen-Geiger climate classification system, Köppen, 1936). Thus, to avoid the potential confounding effects of the contrasting climatic conditions, we focused on the stretches of the three rivers included in the Csa class, which generally characterises Mediterranean coastal areas. For the Itri and the Santa Croce, this included the whole river course, while for the Garigliano it included the last 25 km, characterised by

more homogenous land use and drainage patterns than the other two (see Results).

Samplings were performed monthly from May to July 2014. In these months, agriculture and tourism in the river catchments peaked, as generally observed in coastal Mediterranean areas (Aguzzi et al., 2012). Thus, sampling during these months allowed us to test the ability of isotopic variations in epilithon and snails to provide information on a range of anthropogenic N inputs potentially affecting the three rivers (Fiorentino et al., 2017).

In each sampling site, we collected epilithon and snails, its main primary consumers. Epilithon was sampled by carefully scraping  $3 \times 3$  cm patches from three submerged rocks per site collected 10 m apart from each other. Impurities were gently removed from the vegetal component of the samples, which was separated from macrobenthic fauna. To avoid desiccation, samples were stored in sterile and refrigerated plastic containers before being transferred to the laboratory. Snails were sampled with a hand net (0.5 mm mesh size) by sampling 10 randomly chosen rocks of similar size in the proximity of the rocks selected for the collection of epilithon. The samples were then transferred in refrigerated plastic bags to the laboratory, where the contents were carefully sorted and separated. Samples of epilithon were checked again under a stereoscope to further remove impurities. All snails were counted and identified at the genus or species level and stored before isotopic analysis. In addition, dead leaves of the most representative local plant species were sampled from the riparian belt, together with undifferentiated detritus from the riverbed, in order to characterise the isotopic signatures of the snails' potential allochthonous food sources.

Physicochemical parameters including pH, temperature (in °C), turbidity (measured as total suspended solids, TSS, in ppm), dissolved oxygen (DO, in mg/L) were measured at all sampling sites with a multiparametric probe (Hanna instruments HI9829). Aliquots of water (1.5 L) were also collected at each site and analysed for their nutrient concentrations (i.e.  $\text{NO}_3^-$ ,  $\text{NO}_2^-$ ,  $\text{NH}_4^+$ , Total Dissolved Nitrogen-TDN,  $\text{PO}_4^-$ , Cl). Nutrient concentrations in water were assessed by Ionic Chromatography using a DIONEX system (ICS-90, Dionex Sunnyvale, CA, USA).

### 2.3. Stable isotope analysis

All samples were stored at  $-80^\circ\text{C}$  for at least 24 h before analysis. After freeze-drying, all samples were homogenised to a fine powder using a ball mill (Mini-Mill Fritsch Pulverisette 23; Fritsch Instruments, Idar-Oberstein, Germany). Snails were manually deprived of their shell and only soft tissues were considered for isotopic analyses. Samples were weighed into tin capsules with an electronic balance and analysed for SIA by continuous flow mass spectrometer (IsoPrime100, Isoprime Ltd., Cheadle Hulme, UK) coupled with an elemental analyser (Elementar Vario Micro-Cube, Elementar Analysensysteme GmbH, Germany). Each sample was analysed in two replicates, and isotopic signatures were expressed in  $\delta$  units ( $\delta^{15}\text{N}$ ;  $\delta^{13}\text{C}$ ) as the per mil (‰) difference with respect to standards:

$\delta X (\text{‰}) = [(R_{\text{sample}} - R_{\text{standard}})/R_{\text{standard}}] \times 10^3$ , where X is  $^{13}\text{C}$  or  $^{15}\text{N}$  and R is the corresponding ratio of heavy to light isotopes ( $^{13}\text{C}/^{12}\text{C}$  or  $^{15}\text{N}/^{14}\text{N}$ ). The reference materials used were the international Vienna PeeDee Belemnite (PDB) standard for carbon and atmospheric nitrogen ( $\text{N}_2$ ) for nitrogen. Measurement errors were found to be typically smaller than 0.05‰.

### 2.4. Data analysis

Differences in  $\delta^{15}\text{N}$  values among sampling sites were tested by one-way ANOVA and Tukey HSD test post hoc comparisons. Levene's test for variances was used to test differences among rivers in the variance of the  $\delta^{15}\text{N}$  values of epilithon and snails. The relationship between  $\delta^{15}\text{N}$  and both the physicochemical parameters (i.e. T, pH, DO, turbidity)

and the dissolved N forms was determined by multiple linear regression analyses. The correlation between snail and epilithon  $\delta^{15}\text{N}$  values was tested with a bivariate linear model. Pearson statistical significance was evaluated at  $\alpha = 0.05$ .

For epilithon, we considered  $\delta^{15}\text{N}$  values between 0‰ and 4‰ to be indicative of the absence of anthropogenic N inputs. This range derived from previous observations of unimpacted conditions (Kohzu et al., 2009; Pastor et al., 2014; Peterson et al., 1993) and was compared to values obtained in a reference site (Site A1 on the Santa Croce) located upstream of any anthropogenic pollution source based on land use and drainage patterns in the watershed. Thus, we categorised four impact classes:  $\delta^{15}\text{N} < 0\text{‰}$  (inorganic impact);  $0\text{‰} \leq \delta^{15}\text{N} \leq 4\text{‰}$  (absence of impact);  $4\text{‰} < \delta^{15}\text{N} \leq 8\text{‰}$ : (moderate organic impact); and  $\delta^{15}\text{N} > 8\text{‰}$  (high organic impact). CORINE Land Cover was used to classify the areas surrounding the rivers.

Isotopic mixing models were applied to the  $\delta^{15}\text{N}$  of snails, organic detritus and epilithon in order to quantify the proportional contribution ( $f$ ) of each of the two potential food sources to the N assimilated by snails at each sampling site, in accordance with the formula:

$$\delta^{15}\text{N}_{\text{snail}} = f_{\text{epilithon}} * \delta^{15}\text{N}_{\text{epilithon}} + f_{\text{detritus}} * \delta^{15}\text{N}_{\text{detritus}}$$

where  $f_{\text{epilithon}} + f_{\text{detritus}} = 1$ .

Using two endmembers in the mixing model, this formula provides  $f$  values with no uncertainty (Post, 2002). Based on the literature (Calizza et al., 2017; McCutchan et al., 2003), a trophic enrichment factor (i.e. the expected difference in isotopic signatures between trophic levels due to the metabolism of consumers) of 2.3‰ was applied.

Snail species diversity was expressed by the Shannon diversity index (Hs). For each river, the similarity of snail assemblages (SIMPER analysis based on the Bray-Curtis similarity index) and snail  $\beta$  diversity were also calculated in order to quantify the variation of snail species across sampling sites (Whittaker, 1960). Hs values were compared across rivers using a bootstrap procedure available in the Past 3.0 software package (Costantini et al., 2018).

Data in the text are reported as mean  $\pm$  standard error (s.e.). At the river scale, we refer to the mean and s.e. of sampling site values. At the sampling-site scale, we refer to the mean and s.e. of the values of the three consecutive monthly samplings.

## 3. Results

### 3.1. Land use and anthropic activities

The CORINE Land Cover inventory identified three main land-use classes for the areas surrounding the sampling sites: Woodlands (in class 1: Wooded and natural areas); Crops (in class 2: Farmland and permanent or semi-permanent crops); and Urban areas (in class 3: Artificial and urban areas) (Fig. 1). The Itri was characterised by extensive woodland (covering 80% of the catchment area), with smaller percentages characterised by agricultural areas (15%), and urbanised areas (5%). The wooded areas were mainly found on the relatively steep terrain characterising the external portion of the catchment, while agricultural areas were in the narrow river valley. Thus, the sampling sites were subject mainly to the influence of classes 2 (Permanent or semi-permanent crops) and 3 (Urban areas). The upstream sites A1 and A2 were directly affected by discharge from the wastewater treatment plant, while the intermediate sites were potentially affected by the town of Itri and the downstream sites were surrounded by agricultural areas (CORINE class 2).

Agricultural and natural areas accounted for 95% of the catchment area of the Santa Croce (30% natural, 65% agricultural and 5% urbanised areas). Specifically, natural areas influenced the headwaters of the main river branch (site A1), while both natural areas and permanent crops influenced site A2, on the secondary upstream branch. Permanent crops were identified around sites B1, C, D and E, while sites B2 and F were



under the influence of urban areas. On the Garigliano, agricultural areas accounted for 90% of the catchment area of the river stretch investigated, natural wooded areas 8% and urbanised areas only 2%. Specifically, sites A and B received direct runoff from woodland and site D from an urban area, while the others were located within extensive agricultural areas.

### 3.2. Water temperature, turbidity and N concentration

In the Itri, temperature (on average  $21.10 \pm 0.39$  °C) and turbidity ( $342.50 \pm 42.74$  ppm) did not vary across sampling sites (Table S1, one-way ANOVA,  $F < 1.5$  and  $p > 0.05$  for both). In contrast,  $\text{NO}_3^-$  concentrations ( $2.92 \pm 0.53$  mg/L) and Total Dissolved Nitrogen (TDN,  $5.96 \pm 1.05$  mg/L) were lower downstream from the WWTP (one-way ANOVA,  $F > 4.8$ ,  $p < 0.01$  in both cases) (Tables 1 and S1).

In the Santa Croce, temperature ( $16.00 \pm 0.64$  °C) and turbidity ( $266.62 \pm 32.54$  ppm) did not vary along the river (one-way ANOVA,  $F = 2.7$ ,  $p > 0.05$ ), but they differed between the 'main' and the 'secondary' upstream branches (Table 1, *t*-test,  $t > 4.3$ ,  $p < 0.01$  for both). Similarly,  $\text{NO}_3^-$  ( $0.46 \pm 0.11$  mg/L) and TDN ( $0.71 \pm 0.20$  mg/L) concentrations were lower in the 'main' than in the 'secondary' branch (Table 1), although the differences were not statistically significant ( $p > 0.05$  for both). Both parameters ( $\text{NO}_3^-$  and TDN) increased from upstream to downstream (Table 1 and Table S1, one-way ANOVA,  $F > 3.7$ , and  $p < 0.05$  for both).

In the Garigliano, temperature ( $18 \pm 0.27$  °C), turbidity ( $358.03 \pm 2.33$  ppm) and TDN ( $0.95 \pm 0.07$  mg/L) did not vary among sites (Tables 1 and S1, one-way ANOVA,  $p$  always  $> 0.05$ ). By contrast,  $\text{NO}_3^-$  ( $0.71 \pm 0.03$  mg/L) was higher downstream (Table 1, one-way ANOVA,  $F = 4.7$ ,  $p = 0.01$ ).

### 3.3. Isotopic variation in epilithon

#### 3.3.1. Variations within each river

In the Itri, epilithon  $\delta^{15}\text{N}$  values (on average  $8.16 \pm 0.35\%$ ) were lower downstream from the WWTP (Table 1, one-way ANOVA,  $F = 6.9$ ,  $p < 0.001$ ), with the lowest values in the intermediate section of the river (Fig. 2). Accordingly, sites A1, A2, D and F were included in

the high organic impact class, while sites AB, B, C and E were included in the moderate organic impact class (Table 1).

In the Santa Croce, the  $\delta^{15}\text{N}$  of epilithon (on average  $1.92 \pm 0.43\%$ ) differed between the 'main' and 'secondary' upstream branches ( $1.63 \pm 0.74\%$  and  $6.23 \pm 1.61\%$  respectively) (Table 1 and Fig. 2, one-way ANOVA,  $F$  values = 43.52,  $p < 0.001$ ). With the exception of site C, at the confluence of the two upstream branches, the upstream and intermediate sections of the main channel were not impacted (Table 1). Downstream, inorganic impact was detected at site E, where the river crossed a permanently cultivated area (Table 1). In the urban area (i.e. site F, at the river mouth), organic inputs were probably mixed with inorganic inputs from the cultivated area, as indicated by intermediate  $\delta^{15}\text{N}$  values and high N concentrations in the water (Tables 1 and S1).

In the Garigliano, the  $\delta^{15}\text{N}$  of epilithon ( $7.90 \pm 0.33\%$ ) did not vary significantly along the river (one-way ANOVA,  $p > 0.05$ ), remaining near the boundary between the moderate organic (sites B, C, D and F) and high organic (sites A and E) impact classes (Table 1 and Fig. 2).

Within each river, the  $\delta^{15}\text{N}$  of epilithon was correlated with neither physicochemical parameters (T, pH, DO and turbidity; multiple linear regression models, Itri:  $F = 1.95$ ,  $p = 0.30$ ; Santa Croce:  $F = 1.16$ ,  $p = 0.46$ ; Garigliano:  $F = 8.29$ ,  $p = 0.25$ ) nor the concentrations of the various forms of dissolved N (Itri:  $F = 0.66$ ,  $p = 0.65$ ; Santa Croce:  $F = 0.63$ ,  $p = 0.67$ ; Garigliano:  $F = 2.80$ ,  $p = 0.42$ ) (see also Table S2 for associated linear regression statistics).

#### 3.3.2. Comparison of $\delta^{15}\text{N}$ between rivers and nutrient concentrations between impact classes

Mean epilithon  $\delta^{15}\text{N}$  did not differ between the Itri and the Garigliano (one-way ANOVA post hoc Tukey Test,  $p > 0.05$ ), while it was lower in the Santa Croce (one-way ANOVA post hoc Tukey Test,  $p < 0.001$ ) (Fig. 2). The variance ( $\sigma^2$ ) of  $\delta^{15}\text{N}$  values differed between rivers, being lower in the Garigliano ( $\sigma^2 = 3.4\%$ ) than the Itri ( $\sigma^2 = 7.2\%$ ) and the Santa Croce ( $\sigma^2 = 12.0\%$ ) (Levene's test,  $p < 0.05$ ).

Pooling data from all three rivers, a significant positive correlation was observed between  $\text{NO}_3^-$  (the dominant dissolved N form) concentrations in water and the  $\delta^{15}\text{N}$  of epilithon ( $y = 2.59x + 2.88$ ,  $r = 0.48$ ,  $p < 0.05$ ). The intercept of the model was within the non-impacted isotopic range (i.e. between 0‰ and 4‰).

**Table 1**

$\text{NO}_3^-$  concentration in water (the dominant dissolved N form),  $\delta^{15}\text{N}$  of epilithon (E.) and snails (S.) measured at different sites within three rivers. "-" indicates that snails were not found at that site. km indicates the distance of each site from the river mouth, while "Epilithon in diet" represents the % contribution of epilithon to the diet of snails. HO (high organic,  $\delta^{15}\text{N} > 8\%$ ), MO (moderate organic,  $4\% < \delta^{15}\text{N} \leq 8\%$ ), NI (not impacted  $0\% \leq \delta^{15}\text{N} \leq 4\%$ ), and INO (inorganic,  $\delta^{15}\text{N} < 0\%$ ) indicate different impact classes to which each site has been assigned according to the  $\delta^{15}\text{N}$  value observed in epilithon. MIX indicates the mixing of inorganic and organic inputs.

River	Site	km	$\text{NO}_3^-$ (mg/l)	$\delta^{15}\text{N}$ E. (‰)	$\delta^{15}\text{N}$ S. (‰)	Epilithon in diet	Impact class
Itri	A1	7.3	$5.33 \pm 0.41$	$8.25 \pm 1.78$	$6.66 \pm 0.48$	47%	HO
	A2	7.0	$5.20 \pm 0.36$	$12.57 \pm 0.79$	$7.92 \pm 0.43$	40%	HO
	AB	4.5	$2.31 \pm 0.60$	$4.30 \pm 1.31$	$7.16 \pm 0.34$	100%	MO
	B	2.2	$0.82 \pm 0.23$	$7.92 \pm 0.59$	$7.50 \pm 0.39$	34%	MO
	C	0.7	$1.94 \pm 0.57$	$7.45 \pm 0.67$	-	-	MO
	D	0.4	$2.00 \pm 0.26$	$9.14 \pm 0.28$	$7.96 \pm 0.47$	58%	HO
	E	0.2	$2.10 \pm 0.35$	$7.97 \pm 0.72$	-	-	MO
	F	0.1	$1.43 \pm 0.13$	$8.93 \pm 1.99$	$3.92 \pm 0.23$	9%	HO
	G	0.0	$1.30 \pm 0.42$	$7.44 \pm 0.43$	$4.50 \pm 0.31$	19%	MO
	A1	8.2	$0.17 \pm 0.09$	$0.89 \pm 0.05$	$1.93 \pm 0.40$	100%	NI
Santa Croce	B1	3.8	$0.20 \pm 0.12$	$2.37 \pm 0.27$	$5.40 \pm 0.24$	30%	NI
	A2	6.9	$0.38 \pm 0.10$	$4.62 \pm 0.51$	$6.05 \pm 0.20$	54%	MO
	B2	3.6	$0.24 \pm 0.11$	$7.84 \pm 2.19$	$9.44 \pm 0.84$	86%	MO
	C	3.3	$0.17 \pm 0.07$	$4.21 \pm 0.23$	$5.48 \pm 0.39$	31%	MO
	D	1.3	$0.77 \pm 0.16$	$2.28 \pm 0.39$	$4.61 \pm 0.11$	93%	NI
	E	0.6	$0.93 \pm 0.12$	$-3.75 \pm 0.40$	$4.14 \pm 0.24$	14%	INO
	F	0.0	$0.84 \pm 0.15$	$1.84 \pm 0.73$	$4.44 \pm 0.13$	66%	MIX
	A	25.4	$0.65 \pm 0.14$	$8.58 \pm 0.35$	$6.43 \pm 1.27$	27%	HO
Garigliano	B	17.3	$0.62 \pm 0.13$	$5.76 \pm 0.16$	$7.87 \pm 0.35$	94%	MO
	C	5.6	$0.71 \pm 0.16$	$7.94 \pm 0.73$	$8.51 \pm 0.76$	68%	MO
	D	0.8	$0.73 \pm 0.11$	$7.59 \pm 0.64$	$6.49 \pm 0.50$	33%	MO
	E	0.5	$0.89 \pm 0.15$	$9.43 \pm 0.36$	$6.77 \pm 0.71$	71%	HO
	F	0.0	$0.94 \pm 0.21$	$7.54 \pm 0.53$	$6.32 \pm 0.94$	69%	MO

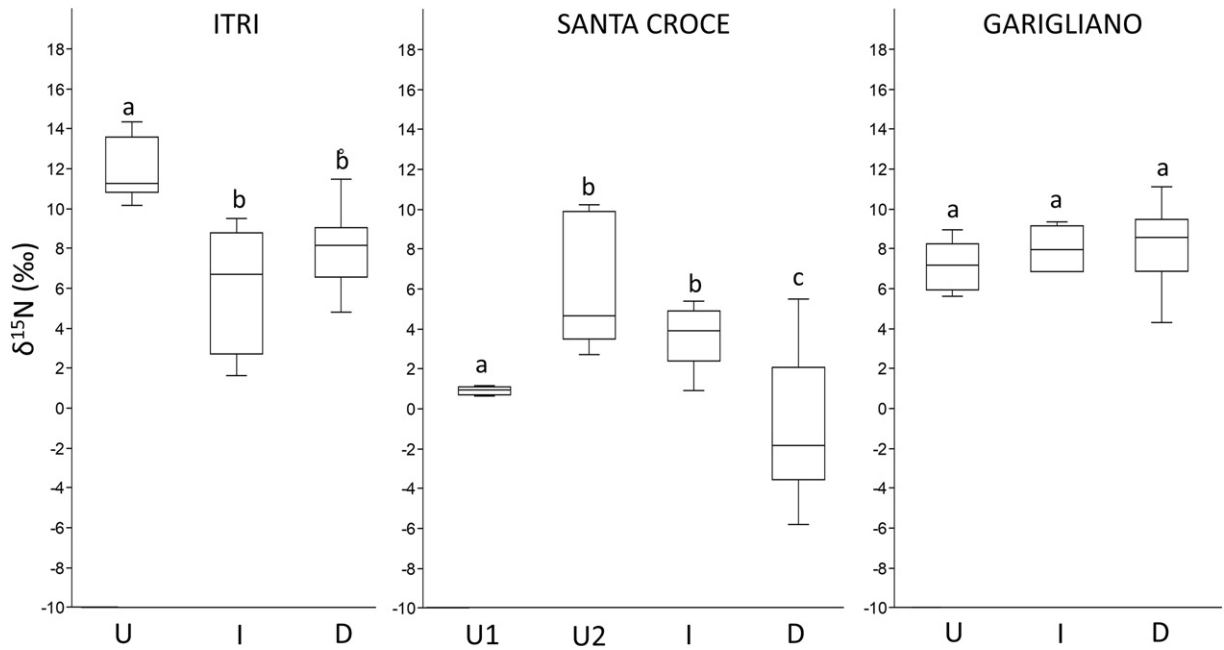


**Fig. 2.** Isotopic values of epilithon in the upstream (U), intermediate (I) and downstream (D) sections of each river. In the Santa Croce, the 'main' (U1) and 'secondary' (U2) upstream branches of the river are shown separately. Different superscript letters indicate significant differences within each river (one-way ANOVA and post-hoc comparisons,  $p < 0.05$ ).

Furthermore, the concentrations of  $\text{PO}_4^-$  and Cl were positively correlated with those of  $\text{NO}_3^-$  ( $r = 0.98$ ,  $p < 0.0001$ , and  $r = 0.46$ ,  $p < 0.05$  respectively).

Significant differences in the concentration of dissolved N forms,  $\text{PO}_4^-$  and Cl were observed between sites assigned to different impact classes (Fig. 3 and Table S1). For all the nutrients analysed, the non-impacted and the highly organic impacted sites showed the lowest and the highest concentrations respectively (Fig. 3; Kruskal-Wallis test,  $H_c$  at least = 9.5,  $p$  always  $< 0.05$ ). Cl concentration was low in the inorganic impacted and non-impacted sites, while it was high in the moderately and highly organic impacted sites (Fig. 3).

### 3.4. Isotopic variations in snails

In total, 1681 snails belonging to 10 genera were sampled. Both the biodiversity (as number of genera) and the abundance of the snails were higher in the Santa Croce and lower in the Itri (Table 2). *Bithynia* and *Physa* dominated the snail assemblages in the Garigliano and the Itri respectively, while several taxa were found at relatively high densities in the Santa Croce (Table 2). Accordingly, the Shannon diversity index (Hs),  $\beta$  diversity and % dissimilarity between sites of snail assemblages were higher in the Santa Croce and lower in the Itri (Table 2). Differences in snail diversity remained at the sampling site and river scale (Table 2).

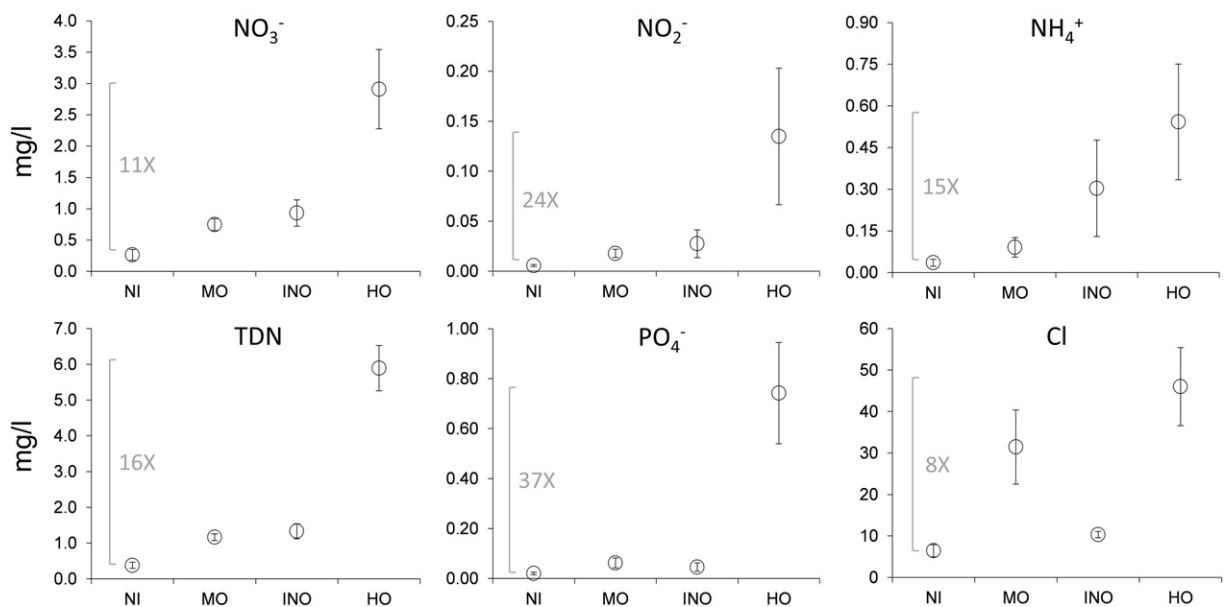


**Fig. 3.** Mean ( $\pm$  s.e.) river water concentrations of N forms,  $\text{PO}_4^-$  and Cl measured in sites assigned to different impact classes on the basis of epilithon  $\delta^{15}\text{N}$  values (NI: not impacted  $0\% \leq \delta^{15}\text{N} \leq 4\%$ ; MO: moderate organic impact,  $4\% < \delta^{15}\text{N} \leq 8\%$ ; INO: inorganic impact,  $\delta^{15}\text{N} < 0\%$ ; HO: high organic impact,  $\delta^{15}\text{N} > 8\%$ ). Grey bars and numbers indicate the ratio between the mean concentrations observed in the high organic impact class and the non-impacted class.

**Table 2**

Abundance and diversity of Gastropoda in the three rivers. Mean and c.v. refer to the mean abundance of snails and its coefficient of variation across sampling sites. % refers to the percentage of dissimilarity in snail assemblage between sites explained by each genus within each river (SIMPER analysis).  $\beta$  diversity measures the species turn-over across sites according to Whittaker (1960). "Hs site" refers to the Shannon diversity of snail assemblages measured at each site (Mann-Whitney pairwise comparisons, different superscript letters imply a significant difference for  $p < 0.05$ ), while "Hs river" refers to their Shannon diversity measured considering the overall abundance of each genus within each river (Bootstrap pairwise comparisons, different superscript letters imply a significant difference for  $p < 0.05$ ).

Genus	Itri			Santa Croce			Garigliano		
	mean	c. v.	%	mean	c. v.	%	mean	c. v.	%
<i>Bythinella</i>	1.7	2.4	9.3	84.3	2.1	29.8	0.4	1.4	2.8
<i>Potamopyrgus</i>	0.5	1.7	6.0	55.9	2.2	21.6	0.4	1.4	2.8
<i>Teodoxus</i>	0.0	–	–	33.9	1.9	18.4	0.2	2.2	2.8
<i>Emmericia</i>	0.0	–	–	20.3	2.3	12.9	0.0	–	–
<i>Bithynia</i>	0.0	–	–	10.6	1.4	4.5	12.4	1.6	45.6
<i>Ancylus</i>	0.2	2.4	2.3	5.4	2.4	3.7	2.2	1.7	17.1
<i>Planorbis</i>	0.0	–	–	1.9	2.2	0.6	0.0	–	–
<i>Lymnea</i>	0.0	–	–	0.6	2.6	0.4	0.0	–	–
<i>Physa</i>	12.8	1.3	46.9	0.1	2.6	0.1	0.0	–	–
<i>Valvata</i>	0.0	–	–	0.1	2.6	0.1	4.2	2.0	13.6
$\beta$ diversity	1.3			1.8			1.5		
Dissimilarity	64.4%			92.2%			84.4%		
	0.4			1.1			0.8		
Hs site	$\pm 0.1^a$			$\pm 0.2^b$			$\pm 0.2^{ab}$		
Hs river	$1.2^a$			$2.1^b$			$1.6^c$		

The mean  $\delta^{15}\text{N}$  values of snails differed between rivers, being lower in the Santa Croce ( $\delta^{15}\text{N} = 5.20 \pm 0.24\text{‰}$ ) than the Itri ( $\delta^{15}\text{N} = 6.83 \pm 0.26\text{‰}$ ) and the Garigliano ( $\delta^{15}\text{N} = 7.22 \pm 0.28\text{‰}$ ) (one-way ANOVA post hoc Tukey Test,  $p < 0.001$ ). Overall,  $\delta^{15}\text{N}$  values were not related to the concentrations of the different N forms in water, either when considered together (multiple linear regression,  $F = 2.7$ ,  $p = 0.13$ ) or in isolation ( $p$  always  $>0.05$ ). Within each river, isotopic variance ( $\sigma^2$ ) was lower in snails (2.1 in the Itri, 4.2 in the Santa Croce and 0.9 in the Garigliano) than epilithon (F test for equal variances,  $F$  at least = 2.85,  $p$  at least  $<0.05$ ).

Pooling data from all three rivers, the  $\delta^{15}\text{N}$  of snails and epilithon were positively correlated ( $r = 0.59$ ,  $p < 0.01$ ). However, the  $\delta^{15}\text{N}$  of snails and epilithon were related in the Santa Croce ( $r = 0.76$ ,  $p < 0.05$ ) but not in the Itri and Garigliano ( $p > 0.05$  for both) when the rivers were considered singly. Indeed, N assimilation from epilithon by snails varied greatly, showing evident mixing with organic detritus ( $\delta^{15}\text{N}$  of detritus: Itri:  $0.93 \pm 0.21\text{‰}$ , Santa Croce:  $2.72 \pm 0.61\text{‰}$ , Garigliano:  $2.48 \pm 0.10\text{‰}$ ) (Table 1). Overall, epilithon accounted for  $54.0 \pm 0.1\%$  of snail diets.

## 4. Discussion

### 4.1. Epilithon

This study provides experimental evidence of the usefulness of epilithon  $\delta^{15}\text{N}$  as an indicator of anthropogenic nitrogen pollution in rivers. Furthermore, it allows us to relate increasing levels of N pollution to decreasing abundance and diversity of freshwater gastropods, a key macroinvertebrate group promoting nutrient transfer and productivity in river food webs (Calizza et al., 2013; Wallace and Webster, 1996).

The sampling was carried out during the late spring-early summer period, allowing us to test the effectiveness of epilithon and snail  $\delta^{15}\text{N}$  in recording the diverse anthropogenic N inputs potentially affecting the rivers at a time when anthropic activities in the catchment areas are at their peak. Accordingly, the variation of  $\delta^{15}\text{N}$  in epilithon within and between rivers reflected localised and diffuse N inputs of both organic and inorganic origin, consistent with human activities in the catchment areas and nutrient concentrations in the waters.

The lack of correlation between  $\delta^{15}\text{N}$  and temperature, pH, turbidity and dissolved oxygen in the waters indicates that epilithon signatures were not influenced by physical factors, as previously demonstrated in lentic waters (Fiorentino et al., 2017). In contrast, the significant correlation between  $\text{NO}_3^-$  (the most abundant dissolved N form) and  $\delta^{15}\text{N}$  in epilithon suggests that organic anthropogenic inputs dominated N loading in the three rivers. This is consistent with (i) the organic N pollution recorded in coastal waters affected by the studied rivers (Careddu et al., 2015; Orlandi et al., 2014; Rossi et al., 2018), and (ii) the expected disproportionately higher contribution to N loading of the human population (64.6% of the total affecting surface waters in the Gulf of Gaeta) compared to inputs from agriculture (11.5%) and industrial activities (7.0%) (Aguzzi et al., 2012).

Previous studies have used stable isotopes of nitrogen to examine the role of epilithon and biofilm in aquatic food webs (Bentivoglio et al., 2016; Costantini et al., 2014; di Lascio et al., 2013), and their metabolism has been used as a measure of river ecosystem function (Bunn et al., 1999; Burns and Ryder, 2001). However, unlike lakes (Fiorentino et al., 2017), transitional waters (Jona-Lasinio et al., 2015) and marine coastal waters (Calizza et al., 2015a; Costanzo et al., 2001; Dailer et al., 2010; Orlandi et al., 2014; Rossi et al., 2018), no experimental test of  $\delta^{15}\text{N}$  variations in the biota as a reliable indicator of anthropogenic pressure is available for rivers. The combined approach based on the description of land use, drainage patterns in watersheds and isotopic variation in epilithon was key to determining the sources of nitrogen inputs along the rivers (i.e. natural, urban, agriculture, WWTP), and their dispersion downstream. The marked variations in isotopic signatures made it possible to discriminate between moderate and high organic impact (indicated by  $\delta^{15}\text{N}$  values higher than 4‰ and 8‰ respectively) in comparison to non-impacted conditions, reflecting differences in dissolved N concentration (Fiorentino et al., 2017; Jona-Lasinio et al., 2015). In addition, the lowest isotopic variance was observed in the Garigliano, although the river stretch investigated was longer than the other rivers. This suggests that differences in the spatial scale investigated did not affect the isotopic variations observed within each river.

Previous studies indicate that the  $\delta^{15}\text{N}$  of epilithon in unpolluted rivers varies from  $-0\text{‰}$  to  $-4\text{‰}$  (Kohzu et al., 2009; Pastor et al., 2014; Peterson et al., 1993). This is consistent with values measured in this study in the reference site, which was located upstream of any potential anthropogenic input, and with values expected from the linear regression between  $\delta^{15}\text{N}$  in epilithon and  $\text{NO}_3^-$  in water in the absence of anthropogenic  $\text{NO}_3^-$  inputs. In addition, high  $\delta^{15}\text{N}$  values indicating N input of organic origin were observed near the WWTP. In contrast,  $\delta^{15}\text{N}$  values were lower 2.5 km downstream from the plant, suggesting that inputs were diluted, as also indicated by decreasing N concentration. Both  $\delta^{15}\text{N}$  and  $\text{NO}_3^-$  were higher at sites close to the river mouth, in association with the urbanisation affecting the lowland stretch of the rivers. Localised inputs were also identified by negative  $\delta^{15}\text{N}$  values, indicative of inorganic pollution, and were associated with sites surrounded by permanent crops. However, in some cases we cannot exclude that the  $\delta^{15}\text{N}$  in epilithon could be affected by a local mix of N sources, including organic inputs from the urban area and inorganic inputs flowing downstream from agriculture-affected sites (Orlandi et al., 2017). This hypothesis is supported by the ability of epilithon to integrate N inputs from a range of sources (Fiorentino et al., 2017). In this case, the combined analysis of land use, N concentration in water and  $\delta^{15}\text{N}$  values was key to discriminating between a mix of pollution sources (indicated by high N concentration) and the absence of pollution impact.

When comparing nutrient pollution among sites belonging to different impact classes a posteriori, the level of impact as determined on the basis of  $\delta^{15}\text{N}$  values in epilithon reflected nutrient concentrations in waters. This demonstrates that the proposed isotopic thresholds for impact classes actually reflect significant changes in water quality due to anthropic activities. The low Cl and  $\text{PO}_4$  concentrations characterising the inorganic impact class further support the hypothesis that negative

$\delta^{15}\text{N}$  values in epilithon reliably reflected inorganic inputs from agriculture (Bentivoglio et al., 2016; Orlandi et al., 2017). Indeed, as a substance commonly used for water disinfection, Cl is expected to be present in urban waters, but not waters from cultivated lands, where chlorination and salinisation of soils are not desired outcomes. In parallel, it has been calculated that 73.9% of the total  $\text{PO}_4^-$  input affecting surface waters in the Gulf area derives from the human population, compared to only 3.7% from agriculture and 3.1% from industrial activities (Aguzzi et al., 2012).

#### 4.2. Snails

The diversity and abundance of Gastropoda varied between rivers, both decreasing with increasing overall N pollution. Water pollution also decreased  $\beta$  diversity. This suggests a negative and homogenising effect of anthropogenic inputs on the spatial structure of river biodiversity.

While the mean isotopic differences between rivers reflected what was observed for epilithon, the  $\delta^{15}\text{N}$  of snails within each river showed lower isotopic variability and less correspondence with land use. This suggests that at a finer spatial scale (i.e. upstream-downstream variations), snails were not able to provide a reliable description of anthropogenic N inputs affecting the river course. At this scale, we lost important information obtained from the isotopic analysis of epilithon, including the organic pollution measured downstream from the discharge of waste waters and the inorganic drainage associated with permanent crops.

Previous studies have shown that  $\delta^{15}\text{N}$  in snails reflects  $\delta^{15}\text{N}$  in epilithon (Bentivoglio et al., 2016; Kohzu et al., 2009), providing information on N pollution transfer across trophic levels. Here, while anthropogenic pollution affected snail diversity, the non-exclusive use of epilithon by snails may explain the observed isotopic mismatch between the two trophic levels. Indeed, snails indiscriminately fed on both epilithon and organic detritus, thus mixing the isotopic signatures of these two food sources in their tissues. Organic detritus, mainly composed of terrestrial plant species, can be redistributed along the river course over long distances by wind and currents, and therefore may not reflect local conditions (Bentivoglio et al., 2016).

#### 4.3. Concluding remarks

The innovative aspect of this study lies in combining land use and drainage pattern analysis with stable isotope analysis in epilithon and snails not only to determine the nature of nitrogen pollutants, but also as an indicator of the entry point of nitrogen pollutants along rivers embedded in complex landscapes. In this context, epilithon was a reliable indicator of anthropogenic sources of nitrogen in riverine systems across a wide range of nutrient concentrations and anthropogenic inputs. Isotopic bioindication provided reliable results at both the catchment area scale (within-river comparisons) and the landscape scale (between-river comparisons), the two monitoring scales providing different but complementary information. In the first case, we were able to identify the location of nitrogen inputs, their nature and their dispersion type. In the second case, we were able to compare the rivers with reference to the mean and variance of isotopic signatures measured within each water body, which represented a good indicator of input variability, consistent with the description of anthropic activities. Notably, considering the complexity of lotic systems and the close link between them and land use in the surrounding areas, this method proved to be efficient and broadly reproducible. Indeed, given the ubiquity of epilithon and snails in aquatic systems, this approach should also be applicable in non-Mediterranean flowing waters.

#### Credit authorship contribution statement

**E. Calizza:** Conceptualization, Writing - original draft, Writing - review & editing, Investigation, Data curation. **F. Favero:** Writing - original draft, Writing - review & editing, Investigation. **D. Rossi:** Visualization, Writing - review & editing, Formal analysis. **G. Careddu:** Writing - review & editing, Investigation, Formal analysis. **F. Fiorentino:** Writing - review & editing, Investigation, Formal analysis. **S. Sporta Caputi:** Writing - review & editing, Investigation, Visualization. **L. Rossi:** Funding acquisition, Supervision, Conceptualization, Writing - review & editing. **M.L. Costantini:** Funding acquisition, Supervision, Conceptualization, Writing - original draft, Writing - review & editing.

#### Declaration of competing interest

The authors declare that they have no known competing financial interests or personal relationships that could have appeared to influence the work reported in this paper.

#### Acknowledgements

This work was supported by Latina Provincial Administration (Project: SAMOBIS), and Sapienza University of Rome (Progetti di ricerca di Ateneo-L. Rossi and M.L. Costantini). We are grateful to ARPA Lazio-Latina Section for the analysis of water samples. George Metcalf reviewed the English text.

#### Appendix A. Supplementary data

Supplementary data to this article can be found online at <https://doi.org/10.1016/j.scitotenv.2019.136081>.

#### References

- Aguzzi, L., Bianco, I., Cortese, M., Monfrinotti, M., Perna, V., Sangiorgi, V., 2012. Stato dell'ambiente marino costiero del Golfo di Gaeta (LT) dieci anni di monitoraggio: 2001–2011. Report/Acqua\_01 (Report\_2012\_SLT.SRS.RI\_01 ARPALAZIO).
- Álvarez-Cabria, M., Barquín, J., Peñas, F.J., 2016. Modelling the spatial and seasonal variability of water quality for entire river networks: relationships with natural and anthropogenic factors. *Sci. Total Environ.* 545–546, 152–162. <https://doi.org/10.1016/j.scitotenv.2015.12.109>.
- Anderson, C., Cabana, G., 2006. Does  $\delta^{15}\text{N}$  in river food webs reflect the intensity and origin of N loads from the watershed? *Sci. Total Environ.* 367, 968–978. <https://doi.org/10.1016/j.scitotenv.2006.01.029>.
- Beck, H.E., Zimmermann, N.E., McVicar, T.R., Vergopolan, N., Berg, A., Wood, E.F., 2018. Present and future Köppen-Geiger climate classification maps at 1-km resolution. *Scientific Data* 5, 180214. <https://doi.org/10.1038/sdata.2018.214>.
- Bentivoglio, F., Calizza, E., Rossi, D., Carlino, P., Careddu, G., Rossi, L., Costantini, M.L., 2016. Site-scale isotopic variations along a river course help localize drainage basin influence on river food webs. *Hydrobiologia* 770, 257–272. <https://doi.org/10.1007/s10750-015-2597-2>.
- Bunn, S.E., Davies, P.M., Mosisch, T.D., 1999. Ecosystem measures of river health and their response to riparian and catchment degradation. *Freshw. Biol.* 41, 333–345. <https://doi.org/10.1046/j.1365-2427.1999.00434.x>.
- Burns, A., Ryder, D.S., 2001. Potential for biofilms as biological indicators in Australian riverine systems. *Ecol. Manag. Restor.* 2, 53–64. <https://doi.org/10.1046/j.1442-8903.2001.00069.x>.
- Calizza, E., Rossi, L., Costantini, M.L., 2013. Predators and resources influence phosphorus transfer along an invertebrate food web through changes in prey behaviour. *PLoS One* 8, e65186.
- Calizza, E., Aktan, Y., Costantini, M.L., Rossi, L., 2015a. Stable isotope variations in benthic primary producers along the Bosphorus (Turkey): a preliminary study. *Mar. Pollut. Bull.* 97, 535–538. <https://doi.org/10.1016/j.marpolbul.2015.05.016>.
- Calizza, E., Costantini, M.L., Rossi, L., 2015b. Effect of multiple disturbances on food web vulnerability to biodiversity loss in detritus-based systems. *Ecosphere* 6, 1–20.
- Calizza, E., Costantini, M.L., Rossi, D., Pasquali, V., Careddu, G., Rossi, L., 2016. Stable isotopes and digital elevation models to study nutrient inputs in high-arctic lakes. *Rend. Lincei* 27, 191–199. <https://doi.org/10.1007/s12210-016-0515-9>.
- Calizza, E., Costantini, M.L., Careddu, G., Rossi, L., 2017. Effect of habitat degradation on competition, carrying capacity, and species assemblage stability. *Ecol. Evol.* 7, 5784–5796.
- Calizza, E., Careddu, G., Caputi, S.S., Rossi, L., Costantini, M.L., 2018. Time- and depth-wise trophic niche shifts in Antarctic benthos. *PLoS One* 13, e0194796.
- Caporn, S.J.M., Carroll, J.A., Dise, N.B., Payne, R.J., 2014. Impacts and indicators of nitrogen deposition in moorlands: results from a national pollution gradient study. *Ecol. Indic.* 45, 227–234. <https://doi.org/10.1016/j.ecolind.2014.04.019>.



- Careddu, G., Costantini, M.L., Calizza, E., Carlino, P., Bentivoglio, F., Orlandi, L., Rossi, L., 2015. Effects of terrestrial input on macrobenthic food webs of coastal sea are detected by stable isotope analysis in Gaeta gulf. *Estuar. Coast. Shelf Sci.* 154, 158–168. <https://doi.org/10.1016/j.ecss.2015.01.013>.
- Careddu, G., Calizza, E., Costantini, M.L., Rossi, L., 2017. Isotopic determination of the trophic ecology of a ubiquitous key species – the crab *Liocarcinus depurator* (Brachyura: Portunidae). *Estuar. Coast. Shelf Sci.* 191, 106–114. <https://doi.org/10.1016/j.ecss.2017.04.013>.
- Carrozzo, L., Potenza, L., Carlino, P., Costantini, M.L., Rossi, L., Mancinelli, G., 2014. Seasonal abundance and trophic position of the Atlantic blue crab *Callinectes sapidus* Rathbun 1896 in a Mediterranean coastal habitat. *Rendiconti Lincei* 25, 201–208.
- Cicala, D., Calizza, E., Careddu, G., Fiorentino, F., Sporta Caputi, S., Rossi, L., Costantini, M.L., 2019. Spatial variation in the feeding strategies of Mediterranean fish: flatfish and mullet in the Gulf of Gaeta (Italy). *Aquat. Ecol.*, 1–13 in press. <https://doi.org/10.1007/s10452-019-09706-3>.
- Cole, M.L., Valiela, I., Kroeger, K.D., Tomasky, G.L., Cebrian, J., Wigand, C., McKinney, R.A., Grady, S.P., Carvalho da Silva, M.H., 2004. Assessment of a  $\delta^{15}\text{N}$  isotopic method to indicate anthropogenic eutrophication in aquatic ecosystems. *J. Environ. Qual.* 33, 124–132. <https://doi.org/10.2134/jeq2004.1240>.
- Costantini, M.L., Calizza, E., Rossi, L., 2014. Stable isotope variation during fungal colonisation of leaf detritus in aquatic environments. *Fungal Ecol.* 11, 154–163.
- Costantini, M.L., Carlino, P., Calizza, E., Careddu, G., Cicala, D., Sporta Caputi, S., Fiorentino, F., Rossi, L., 2018. The role of alien fish (the centrarchid *Micropterus salmoides*) in lake food webs highlighted by stable isotope analysis. *Freshw. Biol.* 63, 1130–1142.
- Costanzo, S.D., O'Donohue, M.J., Dennison, W.C., Loneragan, N.R., Thomas, M., 2001. A new approach for detecting and mapping sewage impacts. *Mar. Pollut. Bull.* 42, 149–156. [https://doi.org/10.1016/S0025-326X\(00\)00125-9](https://doi.org/10.1016/S0025-326X(00)00125-9).
- Dailer, M.L., Knox, R.S., Smith, J.E., Napier, M., Smith, C.M., 2010. Using  $\delta^{15}\text{N}$  values in algal tissue to map locations and potential sources of anthropogenic nutrient inputs on the island of Maui, Hawai'i, USA. *Mar. Pollut. Bull.* 60, 655–671. <https://doi.org/10.1016/j.marpolbul.2009.12.021>.
- Dalu, T., Wasserman, R.J., Magoro, M.L., Froneman, P.W., Weyl, O.L., 2019. River nutrient water and sediment measurements inform on nutrient retention, with implications for eutrophication. *Sci. Total Environ.* 684, 296–302. <https://doi.org/10.1016/j.scitotenv.2019.05.167>.
- De Brabandere, L., Frazer, T.K., Montoya, J.P., 2007. Stable nitrogen isotope ratios of macrophytes and associated periphyton along a nitrate gradient in two subtropical, spring-fed streams. *Freshw. Biol.* 52, 1564–1575. <https://doi.org/10.1111/j.1365-2427.2007.01788.x>.
- di Lascio, A., Rossi, L., Carlino, P., Calizza, E., Rossi, D., Costantini, M.L., 2013. Stable isotope variation in macroinvertebrates indicates anthropogenic disturbance along an urban stretch of the river Tiber (Rome, Italy). *Ecol. Indic.* 28, 107–114. <https://doi.org/10.1016/j.ecolind.2012.04.006>.
- Fernandes, G., Aparicio, V.C., Bastos, M.C., De Gerónimo, E., Labanowski, J., Prestes, O.D., Zanella, R., dos Santos, D.R., 2019. Indiscriminate use of glyphosate impregnates river epilithic biofilms in southern Brazil. *Sci. Total Environ.* 651, 1377–1387. <https://doi.org/10.1016/j.scitotenv.2018.09.292>.
- Fiorentino, F., Cicala, D., Careddu, G., Calizza, E., Jona-Lasinio, G., Rossi, L., Costantini, M.L., 2017. Epilithon  $\delta^{15}\text{N}$  signatures indicate the origins of nitrogen loading and its seasonal dynamics in a volcanic Lake. *Ecol. Indic.* 79, 19–27. <https://doi.org/10.1016/j.ecolind.2017.04.007>.
- Heaton, T.H.E., 1986. Isotopic studies of nitrogen pollution in the hydrosphere and atmosphere: a review. *Chem. Geol.* 59, 87–102. [https://doi.org/10.1016/0168-9622\(86\)90059-X](https://doi.org/10.1016/0168-9622(86)90059-X).
- Jona-Lasinio, G., Costantini, M.L., Calizza, E., Pollice, A., Bentivoglio, F., Orlandi, L., Careddu, G., Rossi, L., 2015. Stable isotope-based statistical tools as ecological indicator of pollution sources in Mediterranean transitional water ecosystems. *Ecol. Indic.* 55, 23–31. <https://doi.org/10.1016/j.ecolind.2015.03.006>.
- Kendall, C., 1998. Tracing nitrogen sources and cycling in catchments. In: Kendall, C., McDonnell, J.J. (Eds.), *Isotope Tracers in Catchment Hydrology*. Elsevier, Amsterdam, pp. 519–576. <https://doi.org/10.1016/B978-0-444-81546-0.50023-9>.
- Kohzu, A., Tayasu, I., Yoshimizu, C., Maruyama, A., Kohmatsu, Y., Hyodo, F., Onoda, Y., Igeta, A., Matsui, K., Nakano, T., Wada, E., Nagata, T., Takemon, Y., 2009. Nitrogen-stable isotopic signatures of basal food items, primary consumers and omnivores in rivers with different levels of human impact. *Ecol. Res.* 24, 127–136. <https://doi.org/10.1007/s11284-008-0489-x>.
- Köppen, W., 1936. Das geographische system der climate. In: Köppen, W., Geiger, R. (Eds.), *Handbuch der Klimatologie*. Gebrüder Borntraeger, Berlin, p. 44.
- Le Moal, M., Gascuel-Oudou, C., Ménesguen, A., Souchon, Y., Étrillard, C., Levain, A., Moatar, F., Pannard, A., Souchu, P., Lefebvre, A., Pinay, G., 2019. Eutrophication: a new wine in an old bottle? *Sci. Total Environ.* 651, 1–11. <https://doi.org/10.1016/j.scitotenv.2018.09.139>.
- MacLeod, N.A., Barton, D.R., 1998. Effects of light intensity, water velocity, and species composition on carbon and nitrogen stable isotope ratios in periphyton. *Can. J. Fish. Aquat. Sci.* 55, 1919–1925. <https://doi.org/10.1139/f98-075>.
- Mancinelli, G., Vizzini, S., 2015. Assessing anthropogenic pressures on coastal marine ecosystems using stable CNS isotopes: state of the art, knowledge gaps, and community-scale perspectives. *Estuar. Coast. Shelf Sci.* 156, 195–204. <https://doi.org/10.1016/j.ecss.2014.11.030>.
- Mayer, B., Boyer, E.W., Goodale, C., Jaworski, N.A., van Breemen, N., Howarth, R.W., Seitzinger, S., Billen, G., Lajtha, K., Nadelhoffer, K., Van Dam, D., Hetling, L.J., Nosal, M., Paustian, K., 2002. Sources of nitrate in rivers draining sixteen watersheds in the northeastern U.S.: isotopic constraints. *Biogeochemistry* 57, 171–197. <https://doi.org/10.1023/A:1015744002496>.
- McCutchan, J.H., Lewis, W.M., Kendall, C., McGrath, C.C., 2003. Variation in trophic shift for stable isotope ratios of carbon, nitrogen, and sulfur. *Oikos* 102, 378–390. <https://doi.org/10.1034/j.1600-0706.2003.12098.x>.
- Orlandi, L., Bentivoglio, F., Carlino, P., Calizza, E., Rossi, D., Costantini, M.L., Rossi, L., 2014.  $\delta^{15}\text{N}$  variation in *Ulva lactuca* as a proxy for anthropogenic nitrogen inputs in coastal areas of Gulf of Gaeta (Mediterranean Sea). *Mar. Pollut. Bull.* 84, 76–82. <https://doi.org/10.1016/j.marpolbul.2014.05.036>.
- Orlandi, L., Calizza, E., Careddu, G., Carlino, P., Costantini, M.L., Rossi, L., 2017. The effects of nitrogen pollutants on the isotopic signal ( $\delta^{15}\text{N}$ ) of *Ulva lactuca*: microcosm experiments. *Mar. Pollut. Bull.* 115, 429–435. <https://doi.org/10.1016/j.marpolbul.2016.12.051>.
- Ouyang, W., Song, K., Wang, X., Hao, F., 2014. Non-point source pollution dynamics under long-term agricultural development and relationship with landscape dynamics. *Ecol. Indic.* 45, 579–589. <https://doi.org/10.1016/j.ecolind.2014.05.025>.
- Pastor, A., Riera, J.L., Peipoch, M., Cañas, L., Ribot, M., Gacia, E., Martí, E., Sabater, F., 2014. Temporal variability of nitrogen stable isotopes in primary uptake compartments in four streams differing in human impacts. *Environ. Sci. Technol.* 48, 6612–6619. <https://doi.org/10.1021/es405493k>.
- Peterson, B., Fry, B., Deegan, L., Hershey, A., 1993. The trophic significance of epilithic algal production in a fertilized tundra river ecosystem. *Limnol. Oceanogr.* 38, 872–878. <https://doi.org/10.4319/lo.1993.38.4.0872>.
- Poole, G.C., 2002. Fluvial landscape ecology: addressing uniqueness within the river discontinuum. *Freshw. Biol.* 47, 641–660. <https://doi.org/10.1046/j.1365-2427.2002.00922.x>.
- Post, D.M., 2002. Using stable isotopes to estimate trophic position: models, methods, and assumptions. *Ecology* 83, 703–718. [https://doi.org/10.1890/0012-9658\(2002\)083\[0703:USITET\]2.0.CO;2](https://doi.org/10.1890/0012-9658(2002)083[0703:USITET]2.0.CO;2).
- Rossi, L., di Lascio, A., Carlino, P., Calizza, E., Costantini, M.L., 2015. Predator and detritivore niche width helps to explain biocomplexity of experimental detritus-based food webs in four aquatic and terrestrial ecosystems. *Ecol. Complex.* 23, 14–24.
- Rossi, L., Calizza, E., Careddu, G., Rossi, D., Orlandi, L., Jona-Lasinio, G., Aguzzi, L., Costantini, M.L., 2018. Space-time monitoring of coastal pollution in the Gulf of Gaeta, Italy, using  $\delta^{15}\text{N}$  values of *Ulva lactuca*, landscape hydromorphology, and Bayesian Kriging modelling. *Mar. Pollut. Bull.* 126, 479–487. <https://doi.org/10.1016/j.marpolbul.2017.11.063>.
- Rossi, D., Romano, E., Guyennon, N., Rainaldi, M., Ghergo, S., Mecali, A., Parrone, D., Taviani, S., Scala, A., Perugini, E., 2019. The present state of Lake Bracciano: Hope and despair. *Rendiconti Lincei. Scienze Fisiche e Naturali* 30 (1), 83–91. <https://doi.org/10.1007/s12210-018-0733-4>.
- Vander Zanden, M.J., Vadeboncoeur, Y., Diebel, M.W., Jepsen, E., 2005. Primary consumer stable nitrogen isotopes as indicators of nutrient source. *Environ. Sci. Technol.* 39, 7509–7515. <https://doi.org/10.1021/es050606t>.
- Vannote, R.L., Minshall, G.W., Cummins, K.W., Sedell, J.R., Cushing, C.E., 1980. The river continuum concept. *Can. J. Fish. Aquat. Sci.* 37, 130–137. <https://doi.org/10.1139/f80-017>.
- Viana, I.G., Bode, A., 2013. Stable nitrogen isotopes in coastal macroalgae: geographic and anthropogenic variability. *Sci. Total Environ.* 443, 887–895. <https://doi.org/10.1016/j.scitotenv.2012.11.065>.
- Wallace, J.B., Webster, J.R., 1996. The role of macroinvertebrates in stream ecosystem function. *Annu. Rev. Entomol.* 41, 115–139.
- Wang, Y., Liu, D., Richard, P., Di, B., 2016. Selection of effective macroalgal species and tracing nitrogen sources on the different part of Yantai coast, China indicated by macroalgal  $\delta^{15}\text{N}$  values. *Sci. Total Environ.* 542, 306–314.
- Wang, T., Xu, Z., Li, Y., Liang, M., Wang, Z., Hynds, P., 2016. Biofilm growth kinetics and nutrient (N/P) adsorption in an urban lake using reclaimed water: a quantitative baseline for ecological health assessment. *Ecol. Indic.* 71, 598–607. <https://doi.org/10.1016/j.ecolind.2016.07.046>.
- Ward, J.V., 1989. The four-dimensional nature of lotic ecosystem. *J. N. Benthol. Soc.* 8, 2–8.
- Whittaker, R.H., 1960. Vegetation of the Siskiyou Mountains, Oregon and California. *Ecol. Monogr.* 30, 279–338. <https://doi.org/10.2307/1943563>.
- Winemiller, K.O., Hoetinghaus, D.J., Pease, A.A., Esselman, P.C., Gbanaador, D., Carrera, E., Payne, J., 2011. Stable isotope analysis reveals food web structure and watershed impacts along the fluvial gradient of a Mesoamerican coastal river. *River Res. Appl.* 27, 791–803. <https://doi.org/10.1002/rra.1396>.
- Woodward, G., Hildrew, A.G., 2002. Food web structure in riverine landscapes. *Freshw. Biol.* 47, 777–798. <https://doi.org/10.1046/j.1365-2427.2002.00908.x>.
- Zeug, S.C., Peretti, D., Winemiller, K.O., 2009. Movement into floodplain habitats by gizzard shad (*Dorosoma cepedianum*) revealed by dietary and stable isotope analyses. *Environ. Biol. Fish.* 84, 307–314. <https://doi.org/10.1007/s10641-008-9438-3>.

## Chapter 5

**New analytical protocol for the classification of nitrogen inputs in lakes based on epilithic  $\delta^{15}\text{N}$  indicator.**

**Fiorentino, Federico<sup>a</sup>**, Jona Lasinio, Giovanna<sup>b</sup>, Careddu, Giulio<sup>a</sup>, Spota Caputi, Simona<sup>a</sup>, Rossi, Loreto<sup>a,c</sup>, Calizza, Edoardo <sup>a,c,\*</sup>, Costantini, Maria Letizia<sup>a,c</sup>

<sup>a</sup> Department of Environmental Biology, Sapienza University of Rome, Via dei Sardi 70, Rome, Italy, 00185 Rome, Italy

<sup>b</sup> Department of Statistical Sciences, Sapienza University of Rome, P.le Aldo Moro 5, 00185 Rome, Italy

<sup>c</sup> CoNISMa -Consorzio Nazionale Interuniversitario per le Scienze del Mare, Piazzale Flaminio 9, 00100 Rome, Italy

**Corresponding Author:** calizza.edoardo@uniroma1.it (E. Calizza)

Manuscript to be submitted to *Ecological Indicators*

Manuscript Number:

Title: New analytical protocol for the classification of Nitrogen inputs in lakes based on epilithic  $\delta^{15}\text{N}$

Article Type: Research paper

Keywords: Nitrogen input; Environmental monitoring; Lacustrine ecosystem; Epilithon; Stable isotope analysis; Bayesian modelling

Corresponding Author: Dr. Edoardo Calizza, Ph.D.

Corresponding Author's Institution: Sapienza, University of Rome

First Author: Federico Fiorentino, Ph.D. candidate

Order of Authors: Federico Fiorentino, Ph.D. candidate; Giovanna Jona Lasinio, Full Professor; Giulio Careddu, Post Doc; Simona Sporta Caputi; Loreto Rossi, Full Professor; Edoardo Calizza, Ph.D.; Maria Letizia Costantini, Associate Professor

Abstract: Nitrogen inputs in aquatic ecosystems are increasing and climate change is likely to exacerbate cultural eutrophication. The recovery of aquatic ecosystem functionality requires strenuous efforts and entails considerable costs. Therefore, the development of early warning ecological indicators that can help arrest the phenomenon in its early stages is highly desirable. Stable isotope analysis of Nitrogen in algal primary producers has proved useful in determining the origins of Nitrogen inputs in several marine and freshwater ecosystems. Nitrogen signatures are often assigned to impact or non-impact classes by comparing the Nitrogen signature of samples with the Nitrogen signature ranges of potential sources, which can hinder objective ecological evaluation when sample signatures are close to the upper/lower boundaries of source ranges. To overcome this problem, we obtained the Nitrogen signatures of the epilithic associations collected in the littoral zone of Lake Bracciano (Central Italy), covering a pre-drought (2015-2016) and ongoing drought (2017-2019) period. The Bayesian Gaussian Mixture Model determined four probability distributions, each associated with a Nitrogen impact class, and assigned the observed epilithic signatures to the most appropriate classes. Application of the approach at various spatial and temporal scales allowed us to compare the pre-drought and ongoing drought Nitrogen input dynamics. At each spatial and temporal scale, we observed differences in the input dynamics arising from the side effects of the drought on human activities, which were reflected in changes in the probability of Nitrogen signatures belonging to one or the other impact class. Based on the probability of samples belonging to one of the impact classes, the proposed analytical protocol provided a useful tool for prioritizing specific management measures in areas affected by specific Nitrogen inputs. Moreover, with a few recalibrations, the model proposed for Lake Bracciano can be extended to other contexts.







## Ecological Indicators

Dear Editor in Chief and Editorial Board,

please find enclosed the manuscript entitled: 'New analytical protocol for the classification of Nitrogen inputs in lakes based on epilithic  $\delta^{15}\text{N}$ ' by Federico Fiorentino et al., which we wish to submit for publication. In this study, we provide an analytical protocol for the classification of Nitrogen inputs in terms of the Nitrogen isotopic signature ( $\delta^{15}\text{N}$ ) and through Bayesian Gaussian Mixture Model. By this modeling approach we were able to estimate four well separated normal densities, each one associated with a Nitrogen input class ('inorganic', 'non impacted', 'moderate organic' and 'high organic'). The proposed analytical protocol provides a rather unambiguous classification of the Nitrogen inputs and allows highlighting their spatial and temporal shifts. The protocol helps environmental scientists in prioritizing sampling areas and management actions, acting conservative for ecologically/economically important zones, and its results are easy informative tools for stakeholders. Moreover, the entire protocol can be properly calibrated to be extended to other aquatic ecosystems.

The main text contains 3 tables and 6 figures. The manuscript has not been submitted to other Journals or Books before and is not considered for publication elsewhere.

On behalf of all Authors,

Your Sincerely

The Corresponding Author

*Edoardo Calizza*

Department of Environmental Biology, Sapienza University of Rome

A handwritten signature in purple ink that reads 'Edoardo Calizza'.

## Highlights

- A robust analytical protocol for the epilithic  $\delta^{15}\text{N}$  analysis is proposed
- Bayesian model identifies probability distributions for Nitrogen input classes
- Changes of Nitrogen inputs occur during drought at different space and time scales
- Two areas of Lake Bracciano are affected by persistent anthropic Nitrogen inputs

1 **New analytical protocol for the classification of Nitrogen inputs in lakes based**  
2 **on epilithic  $\delta^{15}\text{N}$**

3  
4 Federico Fiorentino<sup>a</sup>, Giovanna Jona Lasinio<sup>b</sup>, Giulio Careddu<sup>a</sup>, Simona Sporta Caputi<sup>a</sup>, Loreto  
5 Rossi<sup>a,c</sup>, Edoardo Calizza<sup>a,c,\*</sup>, Maria Letizia Costantini<sup>a,c</sup>

6  
7 <sup>a</sup>Department of Environmental Biology, Sapienza University of Rome, Via dei Sardi 70, Rome,  
8 Italy, 00185 Rome, Italy

9 <sup>b</sup>Department of Statistical Sciences, Sapienza University of Rome, P.le Aldo Moro 5, 00185 Rome,  
10 Italy

11 <sup>c</sup>CoNISMa -Consorzio Nazionale Interuniversitario per le Scienze del Mare, Piazzale Flaminio 9,  
12 00100 Rome, Italy

13 \* **Corresponding Author:** [edoardo.calizza@uniroma1.it](mailto:edoardo.calizza@uniroma1.it)

14  
15 **Abstract**

16 Nitrogen inputs in aquatic ecosystems are increasing and climate change is likely to exacerbate  
17 cultural eutrophication. The recovery of aquatic ecosystem functionality requires strenuous efforts  
18 and entails considerable costs. Therefore, the development of early warning ecological indicators  
19 that can help arrest the phenomenon in its early stages is highly desirable. Stable isotope analysis of  
20 Nitrogen in algal primary producers has proved useful in determining the origins of Nitrogen inputs  
21 in several marine and freshwater ecosystems. Nitrogen signatures are often assigned to impact or  
22 non-impact classes by comparing the Nitrogen signature of samples with the Nitrogen signature  
23 ranges of potential sources, which can hinder objective ecological evaluation when sample  
24 signatures are close to the upper/lower boundaries of source ranges. To overcome this problem, we  
25 obtained the Nitrogen signatures of the epilithic associations collected in the littoral zone of Lake  
26 Bracciano (Central Italy), covering a pre-drought (2015-2016) and ongoing drought (2017-2019)

27 period. The Bayesian Gaussian Mixture Model determined four probability distributions, each  
28 associated with a Nitrogen impact class, and assigned the observed epilithic signatures to the most  
29 appropriate classes. Application of the approach at various spatial and temporal scales allowed us to  
30 compare the pre-drought and ongoing drought Nitrogen input dynamics. At each spatial and  
31 temporal scale, we observed differences in the input dynamics arising from the side effects of the  
32 drought on human activities, which were reflected in changes in the probability of Nitrogen  
33 signatures belonging to one or the other impact class. Based on the probability of samples belonging  
34 to one of the impact classes, the proposed analytical protocol provided a useful tool for prioritizing  
35 specific management measures in areas affected by specific Nitrogen inputs. Moreover, with a few  
36 recalibrations, the model proposed for Lake Bracciano can be extended to other contexts.

37

### 38 **Keywords**

39 Nitrogen input; Environmental monitoring; Lacustrine ecosystem; Epilithon; Stable isotope  
40 analysis; Bayesian modelling

41

42

### 43 **1. Introduction**

44 A major challenge in the environmental monitoring of lacustrine ecosystems is the detection of  
45 stressors before they produce a substantial reduction of the water body's ecological status  
46 (McCormick and Cairns, 1994; Singh et al., 2013). Restoring a compromised ecosystem requires a  
47 complex mixture of scientific and social interactions, it is expensive, and it takes time (Hilderbrand  
48 et al., 2005; Hobbs, 2007). The development of 'early warning' ecological indicators (Dale and  
49 Beyeler, 2001) is thus highly desirable.

50 Among the anthropic pressures that affect aquatic ecosystems, cultural eutrophication caused by  
51 Nitrogen inputs from untreated wastewater discharges, manure and chemical fertilizers (Hayes et

52 al., 2015; Maberly et al., 2002; Paerl et al., 2014; Schmale et al., 2019) favours algal blooms and  
53 impairs aquatic ecosystem structure and functioning (He et al., 2019; Le Moal et al., 2019; Paerl  
54 2017). In addition to anthropic inputs, these phenomena can be ‘boosted’ by climate change (Delpla  
55 et al., 2009). Specifically, in the Mediterranean area, long dry periods, interrupted by extreme and  
56 time-concentrated rainfall events, are expected to increase (Pal et al., 2004; Spinoni et al., 2018).  
57 During a drought, soil leaching is reduced, meaning that nutrients tend to accumulate and do not  
58 immediately enter water bodies (Hayes et al., 2015; van Vliet and Zwolsman, 2008). However,  
59 when heavy rainfall occurs, nutrients are mobilized from the soil and released in considerable  
60 amounts (Delpla et al., 2009; Greaver et al., 2016; Hayes et al., 2015), potentially exceeding the  
61 buffering capacity of aquatic vegetation (Dong et al., 2014; Kosten et al., 2009) and the water  
62 body’s capacity for N removal (Greaver et al., 2016). On the other hand, in the case of agricultural  
63 and/or wastewater loadings that eventually enter the water body despite the low rainfall, drought  
64 can potentially cause their concentrations to rise as a result of the reduced water volume (Brusewitz  
65 et al., 2017; van Vliet and Zwolsman, 2008). Coupled with higher water temperatures, these high  
66 amounts of nutrients, especially Nitrogen, favour algal blooms (Paerl et al., 2016 and literature cited  
67 therein). Chemical analysis of Nitrogen concentrations in the water column is affected by dilution  
68 and biotic assimilation (Dailer et al., 2010; Gartner et al., 2002; Hadwen et al., 2005; Kaminski et  
69 al., 2018), and does not provide information on the origin (‘biological’ vs. ‘chemical’) of the inputs.  
70 Stable Isotope Analysis (SIA) is a widely employed technique relevant to several aspects of  
71 ecological and environmental research, including the detection of N sources (Careddu et al., 2017;  
72 Cicala et al., 2019; Rossi et al., 2019; Titlyanov et al., 2011; von Schiller et al., 2009). Indeed, the  
73 differing origins of Nitrogen inputs (‘biological’ or ‘chemical’) are reflected in their  $^{15}\text{N}:^{14}\text{N}$  ratios  
74 (Orlandi et al., 2017). Macroalgae in marine and brackish ecosystems (Jona Lasinio et al., 2015;  
75 Orlandi et al., 2014; Rossi et al., 2018) and epilithic associations in freshwater ecosystems  
76 (Bentivoglio et al., 2016; Fiorentino et al., 2017, Pastor et al., 2014) directly take up Nitrogen from  
77 the water column, and thus reflect the origin of the N input in the water body (Jones et al., 2004),

78 since their isotopic fractionation is small or null (Dailer et al., 2010; Orlandi et al., 2017). Despite  
79 the growing use of aquatic primary producer  $\delta^{15}\text{N}$  signatures in N input monitoring, to our  
80 knowledge, a robust determination of the probability distributions of algal and epilithon  $\delta^{15}\text{N}$  values  
81 within the ‘inorganic’, ‘non-impacted’, ‘moderate organic’ and ‘high organic’ signature ranges  
82 (Fiorentino et al., 2017) is still lacking. For this reason, the assignment of a given  $\delta^{15}\text{N}$  value to a  
83 specific impact class, for values close to the boundaries between neighbouring ranges, is  
84 problematic. In order to improve classification, ensuring samples are placed in the most likely  
85 impact class, determining the probability distributions associated with each class is thus necessary.  
86 Specifically, substantial improvement can be obtained with ranges adjacent to the ‘non-impacted’  
87 class, providing useful suggestions for effective management and, when the algal  $\delta^{15}\text{N}$  signature  
88 classification returns equal membership probability for two classes, indicating the required focus of  
89 further investigations.

90 In order to model the distributions within the  $\delta^{15}\text{N}$  impact classes and improve  $\delta^{15}\text{N}$  as an N  
91 indicator, we used two different datasets based on the epilithon of Lake Bracciano. The first dataset  
92 covers a pre-drought period (2015-2016) and the second corresponds to a drought (2017-2019) that  
93 affected the lake (Rossi et al., 2019) and caused variations in N inputs.

94 The field data covering the 2015-2019 period were combined with evidence from the scientific  
95 literature (Dailer et al., 2010; Jona Lasinio et al., 2015, Lapointe and Bedford, 2007) in order to  
96 estimate: 1) in a Bayesian framework, the posterior probability distribution of each Nitrogen impact  
97 class (Jona Lasinio et al., 2015), 2) the probability of each observation belonging to each impact  
98 class and 3) the potential changes in classification during the interval 2015-2019, which includes a  
99 period of drought. In these analyses, we considered various spatial and time scales.

100

## 101 **2. Materials and methods**

### 102 *2.1 Study area*



103 Lake Bracciano is a sub-circular oligo-mesotrophic volcanic lake (Bolpagni et al., 2016;  
104 Mastrantuono et al., 2008), located 32 Km Northwest of Rome (Italy). It has a surface area of  $\approx 57$   
105  $\text{Km}^2$ , a perimeter of  $\approx 32$  Km, an elevation of  $\approx 163$  m a.s.l, a maximum depth of  $\approx 165$  m and a  
106 theoretical renewal time of 137 years (Ferrara et al. 2002). It has a catchment area of  $147.483 \text{ Km}^2$   
107 with 24 sub-basins and a small number of low-flow springs (Rossi et al., 2019). Rainfall is the main  
108 water source for the lake and the groundwater system is able to buffer only short dry periods  
109 (Taviani and Henriksen, 2015). The lake is part of the Bracciano-Martignano regional park and is  
110 the main drinking water reservoir for the city of Rome (Rossi et al., 2019). There is a wide range of  
111 human activities around the water body, with agriculture mostly located in the North-Eastern zone  
112 and leisure activities mostly located in the Western and North-Western zones. Three major towns  
113 (Anguillara Sabazia, Bracciano and Trevignano Romano) face directly on to the lake. Despite the  
114 presence of a sewer system that prevents the discharge of wastewaters into the water body, local  
115 organic and inorganic inputs arising from human activities not connected to the sewer system have  
116 been recorded (Fiorentino et al., 2017; Mastrantuono and Mancinelli, 2005). Currently, the lake is  
117 threatened by invasions of alien species (Costantini et al., 2018), falling water levels (Mastrantuono  
118 and Mancinelli, 2005; Rossi et al., 2019; Taviani and Henriksen, 2015), reduction in aquatic  
119 vegetation (Mastrantuono et al., 2008) and loss of N removal capacity (Rossi et al., 2019).  
120 In order to take account of drought (Rossi et al., 2019) and the effects of low rainfall on aquatic  
121 ecosystems (Greaver et al., 2016; Paerl et al., 2016), we performed a sampling campaign over a  
122 longer period (2017-2019) than our previous study (2015-2016; Fiorentino et al., 2017).  
123 Specifically, we sought to highlight potential changes in epilithic  $\delta^{15}\text{N}$  signatures as a result of  
124 falling water levels. In order to model the distributions of  $\delta^{15}\text{N}$  impact classes, a Hierarchical  
125 Bayesian Gaussian Mixture Model (Marin and Robert, 2014) was used to obtain a probabilistic  
126 description of epilithic  $\delta^{15}\text{N}$  signatures in the two different periods.

127

128 *2.2 Field and laboratory procedures*

129 Samples of epilithon were collected in accordance with the procedure described in Fiorentino et al.  
130 (2017) from April 2017 to April 2019 from fourteen sites around the lake perimeter (Fig. 1). Eleven  
131 sites replicated those of a previous study (Fiorentino et al., 2017). The sampling dates and sites are  
132 described in the Supplementary materials (Table S1 and Table S2). Epilithic samples were  
133 conserved at -80°C and then freeze-dried for 24 hours. The samples were pulverized to a fine and  
134 homogenous powder with a ball mill (Fritsch Mini-Mill Pulverisette 23 with a zirconium oxide  
135 ball). For each epilithic sample, two replicates ( $2.8 \pm 0.2$  mg) were sub-sampled and placed in ultra-  
136 pure tin capsules and analyzed using an Elementar Vario Micro-Cube elemental analyser (Elementar  
137 Analysensysteme GmbH, Germany) coupled with an IsoPrime100 isotope mass ratio spectrometer  
138 (Isoprime Ltd., Cheadle Hulme, UK). The Nitrogen signatures were obtained in accordance with  
139 Ponsard and Arditì (2000) and expressed as per mil deviations (‰) from the international standard  
140 (atmospheric N<sub>2</sub>). The internal laboratory standard was IAEA-600 Caffeine. Measurement errors  
141 were found to be typically smaller than  $\pm 0.05\%$ .

142

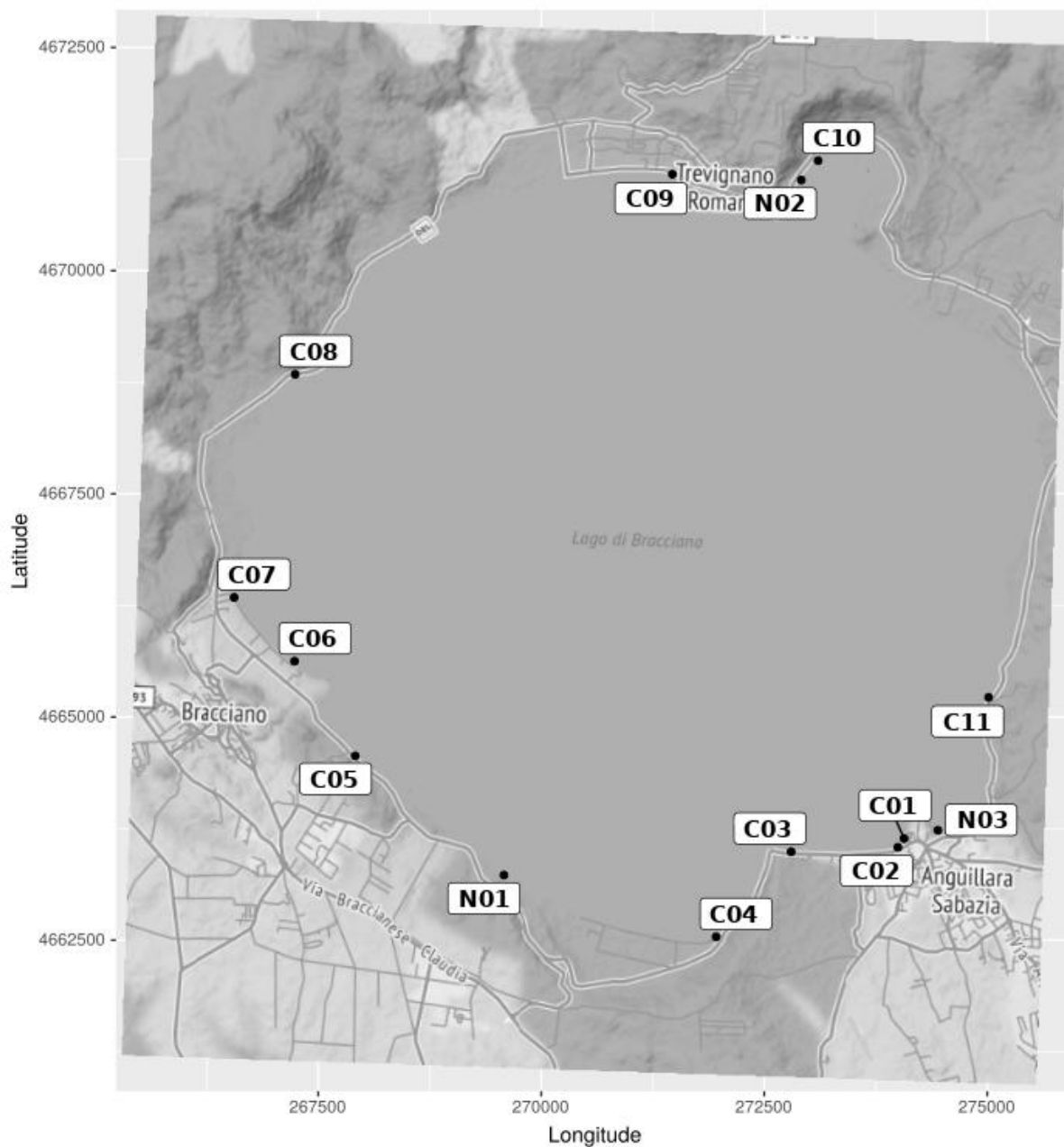


**Fig. 1.** Sampling sites along the shore of Lake Bracciano in the 2017-2019 campaign. Sites labelled with the letter ‘C’ were sampled in both the 2015-2016 and 2017-2019 campaigns. Sites labelled with the letter ‘N’ were sampled in the 2017-2019 campaign alone.

143

144 *2.3 Statistical analysis*

145 *2.3.1 The classification model*

146 The classification model (a Bayesian Mixture Model) was estimated with reference to the mean  
 147 epilithic  $\delta^{15}\text{N}$  values at each sampling site and on each sampling date (hereafter referred as ‘raw  
 148 data’) of the 2015-2016 campaign. The model is a finite mixture of k Gaussian densities (letters in

149 bold indicate vectors), one for each group. This is a convex combination

150  $f(\mathbf{X}|k, \mathbf{p}, \boldsymbol{\theta}) = \sum_{j=1}^k p_j f(\mathbf{X}|\theta_j)$ , where  $\mathbf{X} = (x_1, \dots, x_n)$  is a set of identically distributed

151 observations,  $k$  is the number of groups,  $f(\mathbf{X}|\theta_j)$  is a Gaussian density function,  $p_j$  is the probability

152 of belonging to the  $j^{\text{th}}$ -group, with the constraint  $\sum_{j=1}^k p_j = 1$  (so each observation has to be

153 included in at least one group, Marin and Robert, 2014) and  $\theta_j$  is the set of parameters (mean and

154 variance) of the Gaussian distribution in the  $j^{\text{th}}$ -group. In a Bayesian setting it is necessary to specify

155 a set of prior distributions describing prior knowledge of the group parameters. For any set of such

156 prior distributions  $\pi(\boldsymbol{\theta}, \mathbf{p})$ , the joint posterior distribution of the parameters and the probabilities of

157  $(\boldsymbol{\theta}, \mathbf{p})$ , given the observations and the impact classes, can be written as

158  $\pi(\boldsymbol{\theta}, \mathbf{p}|\mathbf{X}, \mathbf{z}) \propto [\prod_{i=1}^n p_{z_i} f(x_i|\theta_{z_i})] \pi(\boldsymbol{\theta}, \mathbf{p})$ . In this formulation, each  $x_i$  is associated with a label  $z_i$

159 that represents the group to which  $x_i$  belongs. Thus, given the set of  $p_j$ , we can write

160  $z_i|\mathbf{p} \sim M_k(p_1, \dots, p_k)$ , where  $M_k$  is a discrete distribution describing the clusters, and

161  $X_i|z_i, \boldsymbol{\theta} \sim f(\cdot|\theta_{z_i})$ . This approach simplifies both the model and its estimation.

162 We assumed four groups, each associated to a normal density and these densities differing only in

163 their means. For computational reasons, we chose to model normal distributions using their

164 precision (the inverse of variance  $\tau = 1/\sigma^2$ ), and we assumed equal precision across groups.

165 In our study, the following prior distribution settings were chosen:

166  $\mathbf{p} \sim \text{Dirichlet}(1,1,1,1)$ ,  $\boldsymbol{\theta} = (\mu_j, \tau, \tau_\varepsilon)$ ,  $\mu_j \sim N(m_j, \tau)$  and  $\tau, \tau_\varepsilon \sim \text{Gamma}(a, b)$ .

167 The choice of a Dirichlet distribution (1,1,1,1) for  $p$  assumes that there are four groups and all the

168 groups have a probability of  $1/k$  to be found, where  $k = 4$  (Arima et al., 2013). The means of the

169 prior distributions of  $m_j$  were considered to represent the central values of the ‘inorganic’, ‘non-

170 impacted’, ‘moderate organic’ and ‘high organic’ classes (-0.1‰, 4.5‰, 7.7‰ and 11‰). The

171 distributions of  $\tau$  and  $\tau_\varepsilon$  were assigned modes of around 5 (resulting in a variance for each group of

172 0.2), allowing for wide variance of the prior distribution ( $\sigma_\varepsilon^2 = 1/\tau_\varepsilon$ ) ( $a = 2, b = 0.2$ ). Estimation

173 of the model, which was implemented in JAGS (Plummer, 2003), required the use of the Monte

174 Carlo Markov Chain (MCMC) algorithm. We used two chains of 250,000 iterations and the first  
 175 50,000 were discarded as burnin. For each chain, one in ten samples was kept for the inference to  
 176 reduce samples autocorrelation. Model estimation convergence was assessed by visually inspecting  
 177 the MCMC traces and calculating convergence statistics (Potential Scale Reduction Factor and  
 178 effective sample size, Gelman and Rubin, 1992). Due to possible asymmetry in the posterior  
 179 distributions, 95% credibility intervals were calculated as Highest Posterior Density intervals (HPD,  
 180 Lee, 1997). The estimated model (Fig. 2A) makes it possible to classify any new  $\delta^{15}\text{N}$  value by  
 181 computing the probability of it belonging to each class.

182 Site classification was based on raw data. The probability of belonging to each impact class (Fig.  
 183 2A) was computed for each  $\delta^{15}\text{N}$  value of the sampling sites analyzed during each survey (2015-  
 184 2019). Each  $\delta^{15}\text{N}$  signature was then assigned to the class returning the highest probability of  
 185 belonging to it. For sites sampled in both surveys, in order to detect potential input shifts between  
 186 surveys, the results of the classification were compared. For each site and for each Nitrogen input  
 187 class, we computed the mean of these probabilities over time and used it to determine the overall  
 188 classification of the site.

189

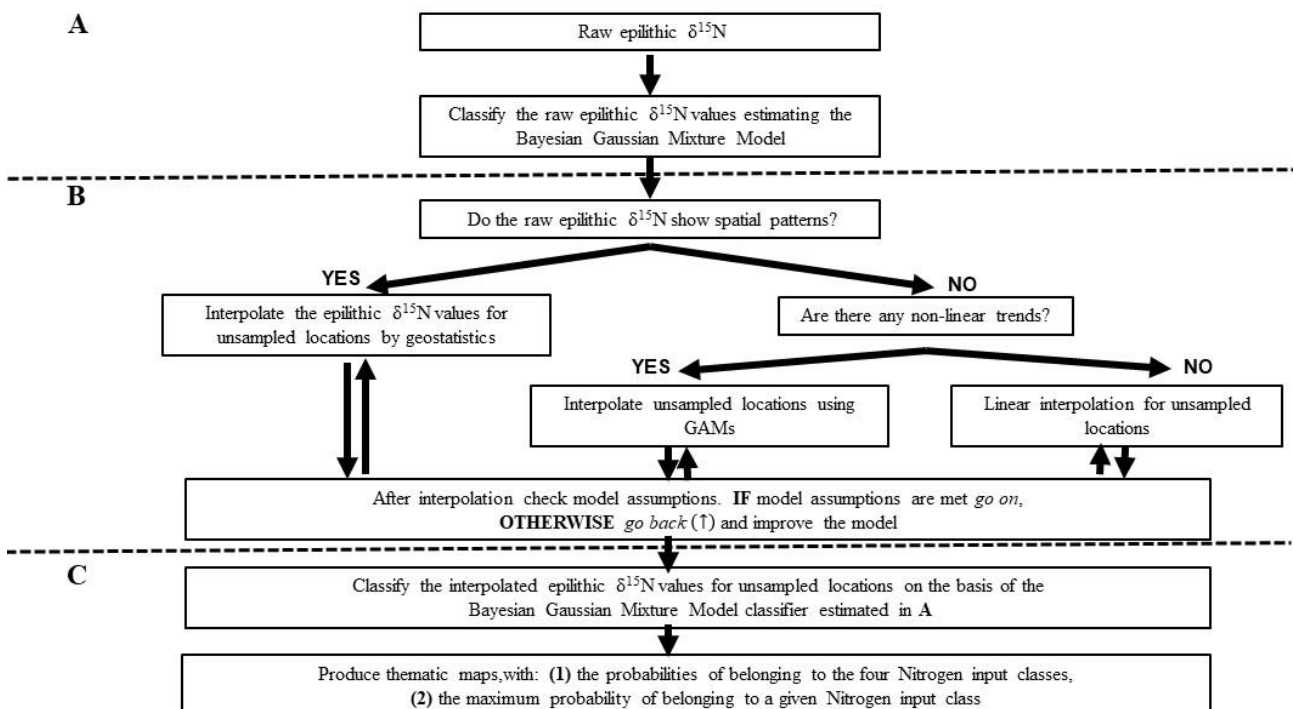


**Fig. 2.** Workflow for the assignment of epilithic  $\delta^{15}\text{N}$  signatures to the most probable Nitrogen impact class. In panel **A** the raw data are used to estimate the Normal probability distributions of the impact classes in accordance with the Bayesian Mixture Model. In panel **B** the raw data are checked for spatial patterns. If spatial patterns emerge, the most appropriate way to estimate the  $\delta^{15}\text{N}$  values of unsampled locations is geostatistics. Otherwise the data should be checked for non-linear trends (Generalized Additive Models, GAMs). If there are not non-linear trends nor spatial patterns, the data can be processed using Linear Models. In any case, whatever model has been estimated, model assumptions must be met, otherwise a model improvement is necessary. In panel **C**, the estimated epilithic  $\delta^{15}\text{N}$  values of a region are classified in accordance with the results of the Bayesian Mixture Model in **A**, and the probabilities of belonging to each Nitrogen input class can be plotted to produce thematic maps of the regions.

### 190 2.3.2 Classification model validation

191 To validate the classification model, we ran it with different subsets of the available raw data (see  
192 Supplementary materials), seeking to understand which time window allowed the ‘best’ estimate of  
193 the four distributions. In other words, we wanted to find four well-separated classes, each described  
194 by a Gaussian distribution. Specifically, the model was run five times, using the raw data from the  
195 first sampling campaign (2015-2016), the raw data from the second sampling campaign without the  
196 2019 sampling (2017-2018), the raw data from the 2019 sampling date alone, the raw data for the  
197 period 2015-2018 and the raw data for the period 2015-2019. Once the convergence issues had been  
198 solved, running the model with all the data (2015-2019) returned very similar results to running it  
199 with the 2015-2018 data, while models run with the 2017-2018 or 2019 data returned very poor  
200 behaviour (asymmetric mean distributions, overlapping HPDs). The models based on data from  
201 2015-2016 and 2015-2018 readily converged. Once convergence was achieved, in order to choose  
202 the final reference time scale we considered a) the shape of the four class mean distributions  
203 (unimodal symmetric is preferred), b) the highest posterior density of the class means (checking that  
204 they were well separated), c) variance estimates and d) overall class separation. As a reference time  
205 scale we chose the 2015-2016 period as the results were stable, the classes well separated and the

206 distribution unimodal and symmetric. Details of the results of the validation procedure are given in  
207 the Supplementary materials (Fig. S1, Fig. S2, Fig. S3 and Table S3).

208

### 209 *2.3.3 Generalized Additive Model (GAM) and classification*

210 To obtain the epilithic  $\delta^{15}\text{N}$  values for unsampled locations (Aalto et al., 2013) and to classify them  
211 according to the proposed protocol (Fig. 2B and Fig. 2C), Generalized Additive Models, GAM,  
212 (Zuur et al., 2007, 2009) were estimated (one for each survey). The  $\delta^{15}\text{N}$  values were modelled as a  
213 function of a bivariate thin-plate spline including the geographical coordinates (Fig. 2B). The  
214 normality of residuals was checked using the Shapiro-Wilks test and their homoscedasticity was  
215 checked visually (Wood, 2017).

216 The estimated epilithon  $\delta^{15}\text{N}$  values from the 2015-2016 and 2017-2019 sampling campaigns were  
217 then classified (Fig. 2C) using the procedure described in 2.3.1 for the sampling sites. To check for  
218 possible changes between the campaigns in the classification in the littoral zone, the average  
219 probability of belonging to a class was computed and compared across sampling dates. In addition,  
220 single samplings and samplings made before and after the drought were compared. All the statistical  
221 analyses were performed using open-source R software (R Core Team, 2019), the GAM was  
222 estimated using the mgcv R package (Wood, 2011), and the R2jags package (Su and Yajima, 2015)  
223 was used to run JAGS within R (JAGS and R codes are available as Supplementary materials).

224

## 225 **3. Results**

### 226 *3.1 Exploratory data analysis*

227 In both 2015-2016 and 2017-2019, the mean ( $\pm$  SD)  $\delta^{15}\text{N}$  value of epilithon in the littoral zone  
228 varied. Information on 2015-2016 is available in Fiorentino et al. (2017) while the 2017-2019 data  
229 are shown in Table 1. For classification of the unprocessed data, we considered the following four  
230 Nitrogen impact classes (Fiorentino et al. 2017): ‘inorganic’ ( $\delta^{15}\text{N} < 3\text{‰}$ ), ‘non-impacted’ ( $3\text{‰} \leq$   
231  $\delta^{15}\text{N} \leq 6\text{‰}$ ), ‘moderate organic’ ( $6\text{‰} < \delta^{15}\text{N} \leq 9\text{‰}$ ) and ‘high organic’ ( $\delta^{15}\text{N} > 9\text{‰}$ ). Based on the



232 unprocessed data, in 2017-2019 one site (C01, Anguillara Sabazia) was affected by moderate  
 233 organic inputs, with values only slightly above the upper boundary of the ‘non-impacted’ class  
 234 ( $\delta^{15}\text{N} = 6.31\text{‰}$  on average). Another two sites, C10 (outside Trevignano Romano) and C11 (outside  
 235 Anguillara Sabazia), were on average in the inorganic class ( $\delta^{15}\text{N} = 2.47\text{‰}$  and  $\delta^{15}\text{N} = 2.65\text{‰}$   
 236 respectively). Since in each of these sites epilithic  $\delta^{15}\text{N}$  was close to the limit of the corresponding  
 237 Nitrogen impact class, classification of the unprocessed data based on mean values alone could not  
 238 be considered robust.

239

Site	Mean $\pm$ SD	Unprocessed classification
C01	6.31 $\pm$ 1.42‰	MO
C02	3.68 $\pm$ 1.48‰	NI
C03	4.08 $\pm$ 1.75‰	NI
C04	3.59 $\pm$ 2.16‰	NI
N01	4.53 $\pm$ 1.72‰	NI
C05	5.75 $\pm$ 2.08‰	NI
C06	4.81 $\pm$ 1.80‰	NI
C07	5.33 $\pm$ 1.34‰	NI
C08	4.69 $\pm$ 2.29‰	NI
C09	4.60 $\pm$ 1.18‰	NI
N02	4.65 $\pm$ 1.12‰	NI
C10	2.47 $\pm$ 1.25‰	INO
C11	2.65 $\pm$ 1.48‰	INO
N03	4.66 $\pm$ 2.00‰	NI

240

241 **Table 1** Mean epilithon  $\delta^{15}\text{N}$  values ( $\pm$  standard deviations) from the 2017-2019 sampling campaign and classification  
 242 based on unprocessed data (MO = ‘moderate organic’, NI = ‘non-impacted’, INO = ‘inorganic’).

243

244 *3.2 Model estimation*

245 The Hierarchical Bayesian Mixture Model estimated on the basis of the raw epilithic  $\delta^{15}\text{N}$  data from  
 246 2015-2016 returned the means of the four normal densities associated with the impact classes, in  
 247 addition to the variance and its 95% HPD [ respectively, 2.37, 95% HPD: (0.02; 2.50)] (Fig. 3A,  
 248 Table 2). The classes were clearly separated (Fig. 3B) and the data were easily classified with little  
 249 uncertainty.

250

251

252

253

CLASS	HPD Lower (2.5%)	Mean	HPD Upper (97.5%)
<i>Inorganic</i>	-0.60‰	0.73‰	3.32‰
<i>Non-impacted</i>	3.10‰	4.30‰	5.70‰
<i>Moderate organic</i>	6.33‰	7.15‰	8.08‰
<i>High organic</i>	9.97‰	11.04‰	11.96‰

**Table 2** Bayesian Mixture Model results for the raw data  $\delta^{15}\text{N}$  from 2015-2016. For each impact Normal distribution (CLASS), the lower HPD (2.5%), mean and higher HPD (97.5%) are shown.

254

255

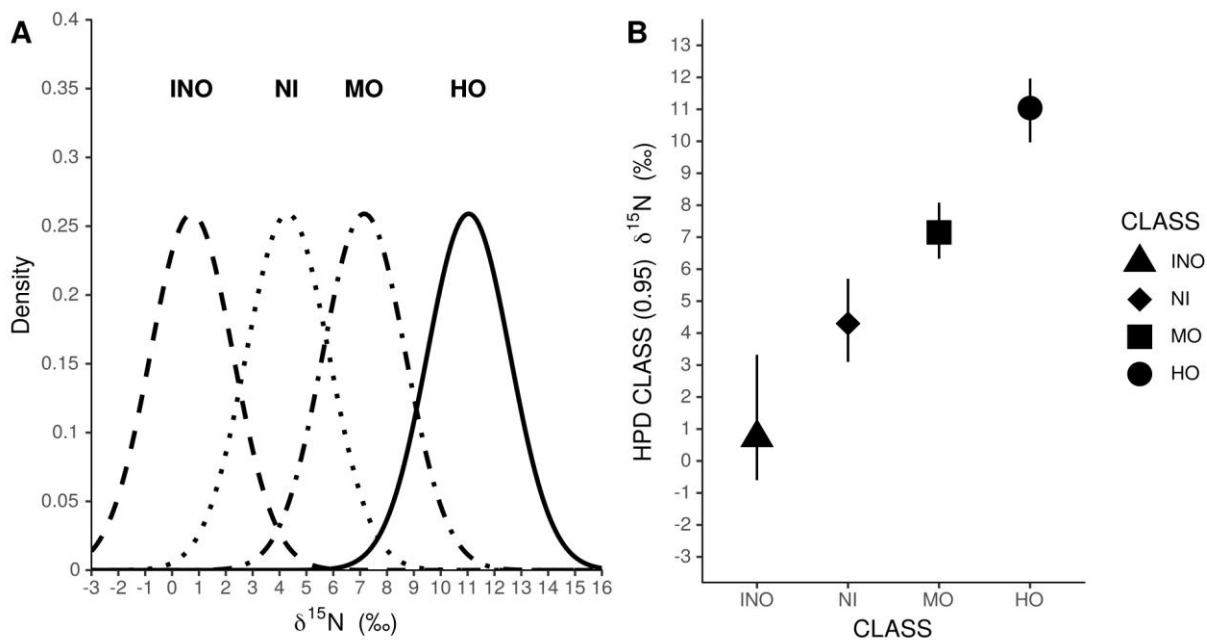


**Fig. 3.** (A) Densities of the four Nitrogen impact classes. (B) Highest Posterior Density (vertical line) and mean (shapes) of each impact class. Each shape represents a specific  $\delta^{15}\text{N}$  signature class (INO = ‘inorganic’, NI = ‘non-impacted’, MO = ‘moderate organic’, HO = ‘high organic’).

256

257 3.2.1 Classification of sites

258 The proposed classification model allowed us to identify changes in eleven sampling sites  
259 monitored in two sampling periods (Fig. 4).

260 On average, during 2017, we observed a decrease in ‘moderate organic’ inputs. By contrast, in  
261 Spring and Early Summer 2018, eight of the eleven sites were characterized by ‘moderate organic’  
262 inputs (C01, C02, C03, C04, C05, C06, C07 and C09). ‘Inorganic’ sites were more frequent in  
263 2017-2019 than the preceding period, affecting half the sites by Spring 2019.

264

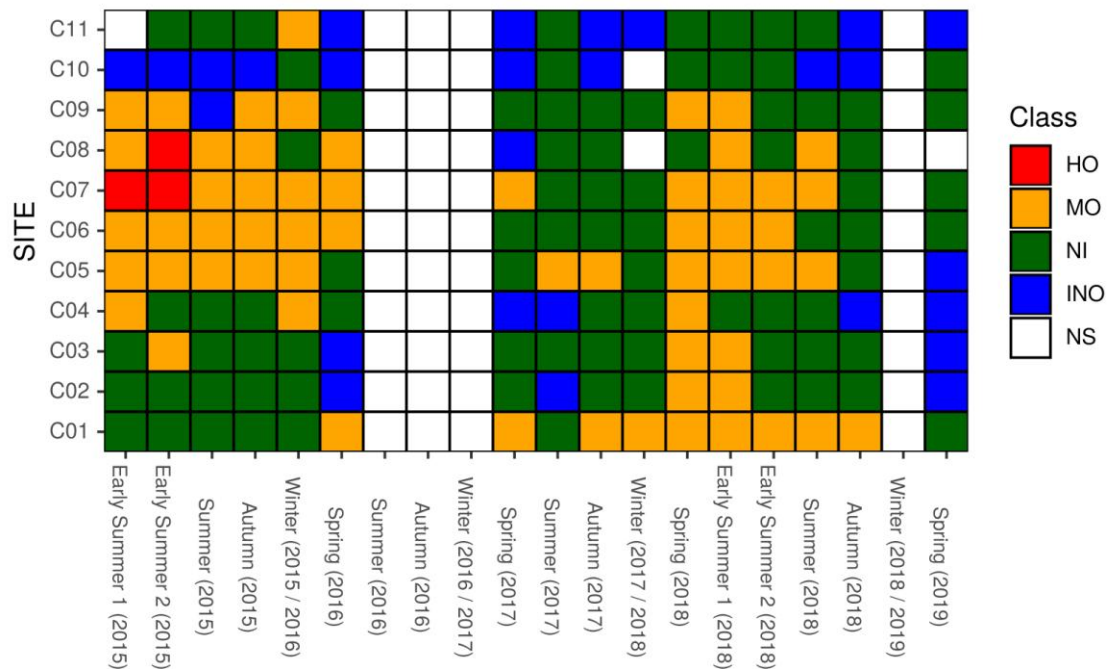


**Fig. 4.** Plot of the site classification in the time frame considered. Colours represent Nitrogen impact classes (NS = ‘not sampled’, INO = ‘inorganic’, NI = ‘non-impacted’, MO = ‘moderate organic’, HO = ‘high organic’). White squares represent missing data.

265

266 In accordance with the proposed classification approach, the exposure of each sampling site to the  
267 various Nitrogen input sources was also evaluated in terms of the overall mean probability of the  
268 site belonging to each of the impact classes in 2015-2019 (Table 3). As a whole, more than half the

269 sampling sites considered were most likely to belong to the ‘non-impacted’ class and all of these are  
 270 located in the Southern and Northern areas.

271

Site	P (Inorganic)	P (Non-impacted)	P (Moderate Organic)	P (High Organic)
C01	0.03	0.49	0.45	0.03
C02	0.28	0.57	0.14	0.00
C03	0.18	0.56	0.26	0.00
C04	0.25	0.51	0.24	0.00
C05	0.06	0.33	0.57	0.04
C06	0.07	0.39	0.49	0.05
C07	0.03	0.35	0.45	0.17
C08	0.10	0.40	0.40	0.10
C09	0.10	0.56	0.34	0.01
C10	0.54	0.43	0.03	0.00
C11	0.37	0.51	0.12	0.00

**Table 3** Mean overall (2015-2019) probability (P) of each site belonging to the four Nitrogen impact classes

272

273

### 274 3.2.2 GAM estimate for unsampled sites and classifications at different temporal scales

275 Epilithic  $\delta^{15}\text{N}$  values were estimated for unsampled locations using GAM models. The deviance  
 276 explained by the GAM models (Supplementary materials, Table S4) ranged from a minimum of  
 277 35.3% (Early Summer 2 2018) to a maximum of 83.2% (Spring 2016). A significant spatial effect  
 278 on epilithic  $\delta^{15}\text{N}$  was detected for both sampling periods, except for Winter 2017-2018 (F-value =  
 279 2.08, p-value = 0.08). The residuals of the estimated models were normally distributed (Shapiro-  
 280 Wilks test, p-value >0.05) and homoschedastic.

281 All interpolated  $\delta^{15}\text{N}$  values (hereafter referred as ‘points’) were classified using the procedure  
 282 described in 2.3.1 and assigned to the class to which they had the highest probability of belonging.  
 283 Here we show the assignment to classes of the interpolated  $\delta^{15}\text{N}$  values from the Spring surveys  
 284 2016 to 2019 (Fig. 5 and Table S5).

285

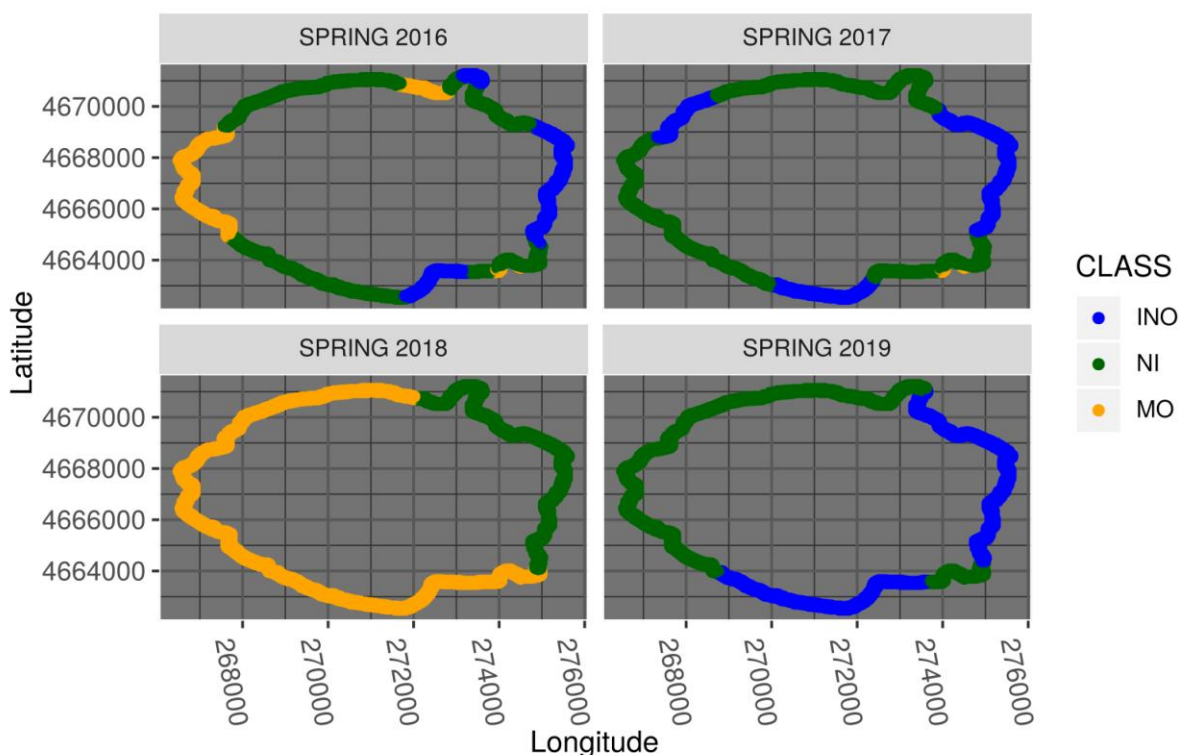


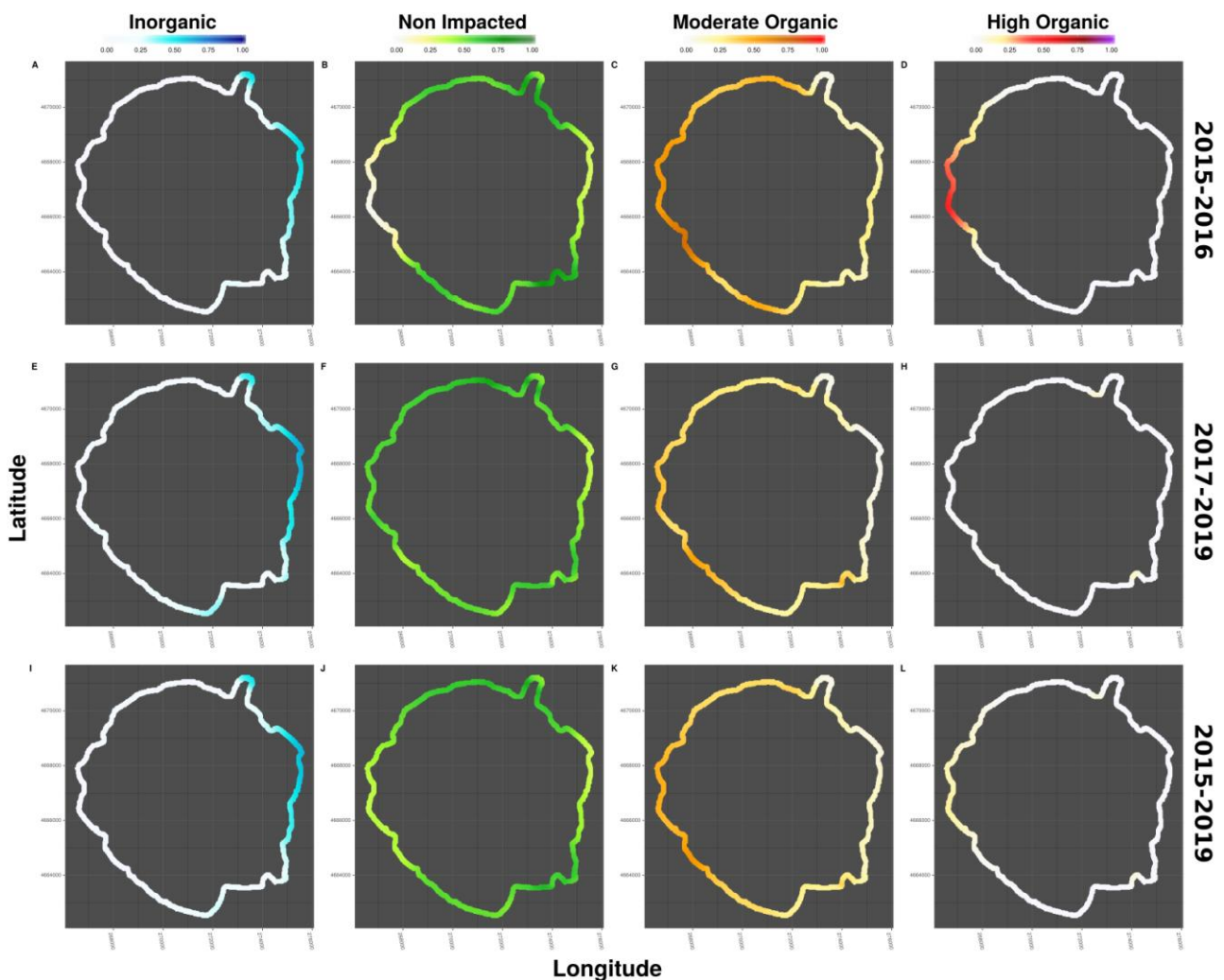
**Fig. 5.** Plot of the classified GAM estimates for spring in each year. Different colours represent different classes (INO = ‘inorganic’, NI = ‘non-impacted’, MO = ‘moderate organic’)

286

287 With respect to 2016, 45.53% of the interpolated points changed classification in 2017: the ‘non-  
 288 impacted’ points in 2017 mostly derived from what had previously been ‘moderate organic’ points,  
 289 while the ‘inorganic’ points were more numerous in 2017, mostly deriving from what had  
 290 previously been ‘non-impacted’ points (Table S5). Comparing 2017 and 2018, 83.89% of the  
 291 interpolated points changed classification. We observed a general shift from ‘non-impacted’ to  
 292 ‘organic’, while the ‘inorganic’ class was not observed. In 2019, 92.3% of the points changed  
 293 classification relative to 2018. Many points that had been ‘moderate organic’ became ‘non-  
 294 impacted’ and ‘inorganic’, but a considerable percentage of ‘non-impacted’ points moved to the  
 295 ‘inorganic’ class.

296 On an annual scale, the classifications showed that in 2015-2016 the Western and South-Western  
 297 zones had a high average probability of belonging to the ‘moderate organic’ class (Fig. 6C),  
 298 whereas the Northern and the Southern zones had a high average probability of belonging to the

299 'non-impacted' class (Fig. 6B). By contrast, the Eastern zone and a narrow Northern area, close to  
 300 the town of Trevignano Romano, were in the 'inorganic' class (Fig. 6A).  
 301 In 2017-2019 (Fig. 6E-H), the Northern and Southern areas still had a high average probability of  
 302 belonging to the 'non-impacted' class (Fig. 6F), while 'inorganic' inputs persisted in the East (Fig.  
 303 6E) and the 'moderate organic' class was dominant in a narrow zone in the South-West (Fig. 6G).  
 304 Comparison between the two periods (Table S6) highlights the general stability of the classified  
 305 points. Indeed,  $\approx 77\%$  of the total points maintained the same classification. About 21% of points  
 306 changed from 'moderate organic' to 'non-impacted' in 2017-2019. Thus, considering the entire  
 307 period, on average, the lake was likely to be affected by 'moderate organic' and 'inorganic' inputs  
 308 on the West and East sides respectively (Fig. 6K and Fig. 6I), whereas the remaining areas were  
 309 likely to be unaffected by human-derived Nitrogen inputs (Fig. 6J).  
 310



311

312

**Fig. 6.** Mean probability of the lake shore belonging to each of the four Nitrogen impact classes during the first sampling campaign (**A-D**), second sampling campaign (**E-H**) and entire time period considered (**I-L**).

313 **4. Discussion**

314 In this study, we addressed three main research questions, the first two concerning the creation of an  
315 effective classification tool for epilithic  $\delta^{15}\text{N}$  values: (1) estimation of the probability distributions  
316 associated with the Nitrogen impact classes and (2) assignment of the  $\delta^{15}\text{N}$  signatures to the most  
317 appropriate classes. The third research question concerned (3) shifts in impact class as a result of  
318 drought.

319

320 *4.1 The model*

321 These crucial issues were solved by means of the proposed protocol. Indeed, identifying impact  
322 classes and assigning data to classes are standard practice in environmental monitoring as they  
323 reduce judgment subjectivity (Bhagowati and Ahamad, 2019; Costanzo et al., 2005; Jona Lasinio et  
324 al., 2017). The Bayesian procedure allowed us to base the definition of classes on quantitative prior  
325 information and thus to produce an unambiguous final classification. The estimated probability of  
326 belonging to a specific class provided a rigorous quantitative tool with which to evaluate the  
327 uncertainty associated with class membership. Thanks to this approach, the impact ranges in the  
328 lake can be clearly depicted on the basis of epilithic  $\delta^{15}\text{N}$  signatures.

329 Fiorentino et al. (2017) published an updated land-use map of Lake Bracciano that allowed us to  
330 verify the consistency of this  $\delta^{15}\text{N}$ -based classification with the observed input sources. In the North  
331 and North-eastern zones, Corine Land Cover data (Copernicus Land Monitoring Service) was  
332 consistent with the ‘inorganic’ classification resulting from the epilithic signatures, which indicated  
333 that the potential anthropogenic Nitrogen inputs (Fig. S4) were mainly derived from agricultural  
334 activities. The ‘moderate’ and ‘high organic’ Nitrogen inputs found in the West, in particular at the  
335 northern end of the recreational area on the shore near the town of Bracciano where there are no

336 farms or cultivated fields, were associated with intense tourism and leisure activities. This result  
337 suggested that tourism is the main local source of Nitrogen inputs on this side of the lake and  
338 confirmed the usefulness of epilithic  $\delta^{15}\text{N}$  signatures as an ecological indicator able to detect the  
339 dominant Nitrogen sources (Fiorentino et al., 2017).

340 Regarding the statistical modelling, the Mixture Model classifier based on the Bayesian framework  
341 represented the most consistent theoretical approach. The model considered a convex combination  
342 of a finite number of  $k$  densities, which in our case were four Gaussian densities (Scrucca et al.,  
343 2016), each with its own specific weight. For each observation, the model returned the probability  
344 of belonging to each class. Following the Maximum Likelihood approach (Scrucca et al., 2016), it  
345 was not possible to identify the ‘high organic’ class, as only a small percentage of the observed  $\delta^{15}\text{N}$   
346 values were above 9‰. On the other hand, ignoring the ‘high organic’ class produced a bimodal  
347 ‘moderate organic’ distribution. Furthermore, not considering the ‘high organic’ impact class might  
348 lead to a large human-derived organic input being incorrectly assessed (Risk et al., 2009), which in  
349 turn would lead to unsuitable policy decisions. The Bayesian approach solved the problem by  
350 allowing us to add (a priori) information on the class centers and the variability of the associated  
351 Normal distributions solving estimation/identification issues. The four distributions differed clearly  
352 in terms of their means and were well separated. The uncertainty of the distribution means was  
353 measured using the 95% highest posterior density intervals (HPD), which highlighted only one  
354 small overlap between the ‘inorganic’ HPD upper bound and the ‘non-impacted’ HPD lower bound.  
355 These intersections were expected because the change between classes is naturally smooth, as we  
356 have already observed (Fiorentino et al., 2017).

#### 357

#### 358 *4.2 Effects of the drought*

359 Some areas of Lake Bracciano are known to undergo seasonal variation as an effect of tourism and  
360 agricultural activities (Fiorentino et al., 2017). The former induces oscillation between ‘non-  
361 impacted’ and ‘moderate organic’ classes, and the latter between ‘non-impacted’ and ‘inorganic’



362 classes. Changes in the probability of belonging to these classes thus probably reflect fluctuations in  
363 human activities around the water body. The proposed classification approach answered our  
364 question concerning potential spatial variation in terms of Nitrogen impact class. These shifts  
365 occurred during the drought and were of variable magnitude, being seen at local, seasonal, and  
366 whole-lake annual scales. At local and seasonal scales, in 2017 the lake was characterized by the  
367 absence, for most of the sampling sites, of ‘moderate organic’ inputs due to the fall in tourism  
368 (Calizza et al., 2017). With the mitigation-of the drought, ‘moderate organic’ inputs were recorded  
369 but for a shorter period than in the past. In 2017-2019 the ‘inorganic’ inputs were no longer limited  
370 to a few sampling sites as in the previous years, although the total absence of these agriculture-  
371 related inputs during Spring-Summer 2018 can be seen as the effect of the drought. In contrast, the  
372 absence of tourism-related ‘organic’ inputs and the presence of ‘inorganic’ inputs in Spring 2019  
373 may be related to the intense rainfall (Fiorentino et al., 2017; Agenzia Regionale per lo Sviluppo e  
374 l’Innovazione dell’Agricoltura del Lazio, ARSIAL 2019). Local changes were reflected in inter-  
375 annual differences at the whole-lake scale. Over time, an increasing percentage of the interpolated  
376 points changed class, resulting in shifts in the spatial distribution of both ‘organic’ and ‘inorganic’  
377 inputs.

378

#### 379 *4.3 $\delta^{15}N$ classification at the local and whole-lake scale as an informative tool for monitoring and* 380 *planning*

381 In the context of environmental monitoring and planning, our lake classifications are useful  
382 informative tools. At the local scale, the mean probabilities of belonging to each of the impact  
383 classes highlighted: (i) sites that are mainly ‘non-impacted’ and (ii) sites that are mainly affected by  
384 human-related Nitrogen inputs. At the whole-lake scale, the mean probabilities of belonging to each  
385 impact class showed spatial separation of the two types of human-induced Nitrogen inputs.  
386 Specifically, the ‘moderate organic’ and ‘inorganic’ classes and the corresponding Nitrogen inputs  
387 affected distinct areas, confirming the differing nature of the influences on opposite sides of the

388 lake, i.e. tourism (on the West side) and agriculture (on the East side). In areas adjacent to the town  
389 of Trevignano Romano, the stability of its ‘non-impacted’ status explains the recent ‘blue flag’ of  
390 excellence (Foundation for Environmental Education, FEE 2018) awarded to the town’s beach. On  
391 the other hand, a stable presence in one of the impacted classes suggests persistent inputs. Such  
392 stability can be useful for concentrating sampling efforts, prioritizing improvements to the  
393 wastewater collection system and planning mitigation strategies. Finally, despite our model being  
394 developed for a specific lacustrine ecosystem, studies in other aquatic ecosystems have found  
395 similar macroalgal and epilithic  $\delta^{15}\text{N}$  signatures, indicating human-derived organic (Bentivoglio et  
396 al., 2016; DeBruyn and Rasmussen 2002, Fry et al., 2011; Wang et al., 2016) and inorganic  
397 (Bentivoglio et al., 2016; Derse et al., 2007; Wang et al., 2016) Nitrogen inputs. It is thus likely that  
398 only a few re-calibrations will be required for this bioindication system to be adopted more widely.

399

## 400 **5. Conclusions**

401 Our empirical modelling approach improves the use of epilithic  $\delta^{15}\text{N}$  signatures as an ecological  
402 indicator of human-related Nitrogen inputs. Indeed, it provides a probabilistic and statistically  
403 robust operating protocol for assigning specific epilithic  $\delta^{15}\text{N}$  signatures to appropriate classes and  
404 running comparisons at various spatial and temporal scales.

405 The switch from classification based on raw epilithic  $\delta^{15}\text{N}$  data to the probabilistic protocol not only  
406 represents a solid basis for planning environmental monitoring programmes, but also helps  
407 environmental scientists to prioritize the location and timing of management measures based on the  
408 probability of belonging to specific Nitrogen impact classes. For ecologically and economically  
409 important littoral zones, probabilistic classification provides information on potential threats even at  
410 low probabilities of exposure. Lastly, this is an effective method for informing stakeholders,  
411 because not only does the protocol return simple thematic maps, but it also expresses shifts between  
412 classes as percentages and degrees of exposure to anthropic Nitrogen inputs as probabilities.

413

414 *Acknowledgements*

415 We thank George Metcalf for revising the English text. This research was supported by PNRA,  
416 projects: PNRA-2015/AZ1.01-M.L. Costantini, and PNRA16\_00291-L. Rossi

417 Giovanna Jona Lasinio was partially supported by the PRIN2015 project entitled “Environmental  
418 processes and human activities: capturing their interactions via statistical methods (EPHASTAT)”  
419 funded by MIUR – Italian Ministry of University and Research.

420

421

422 **Funding**

423 This research was supported by PNRA, projects: PNRA-2015/AZ1.01-M.L. Costantini, and  
424 PNRA16\_00291-L. Rossi

425 Giovanna Jona Lasinio was partially supported by the PRIN2015 project entitled “Environmental  
426 processes and human activities: capturing their interactions via statistical methods (EPHASTAT)”  
427 funded by MIUR – Italian Ministry of University and Research.

428

429  
430  
431  
432  
433  
434  
435  
436  
437  
438  
439  
440  
441  
442  
443  
444  
445  
446  
447  
448  
449  
450  
451  
452  
453  
454  
455  
456  
457  
458  
459  
460  
461  
462  
463  
464  
465  
466  
467  
468  
469  
470  
471  
472

## References

- Aalto, J., Pirinen, P., Heikkinen, J., Venäläinen, A., 2013. Spatial interpolation of monthly climate data for Finland: comparing the performance of kriging and generalized additive models. *Theor. Appl. Climatol.* 112, 99–111. <https://doi.org/10.1007/s00704-012-0716-9>
- Arima, S., Basset, A., Jona Lasinio, G., Pollice, A., Rosati, I., 2013. A hierarchical Bayesian model for the ecological status classification of lagoons. *Ecol. Model.* 263, 187-195.
- ARSIAL,2019  
<http://www.arsial.it/portalearsial/agrometeo/D3.asp?anno=16&codice=RM05SPE&misura=8>  
(accessed 10/30/2019)
- Bentivoglio, F., Calizza, E., Rossi, D., Carlino, P., Careddu, G., Rossi, L., Costantini, M.L., 2016. Site-scale isotopic variations along a river course help localize drainage basin influence on river food webs. *Hydrobiologia* 770, 257-272.
- Bhagowati, B., Ahamad, K.U., 2019. A review on lake eutrophication dynamics and recent developments in lake modeling. *Ecohydrol. Hydrobiol.* 19, 155-166.
- Bolpagni, R., Laini, A., Azzella, M.M., 2016. Short- term dynamics of submerged aquatic vegetation diversity and abundance in deep lakes. *Appl. Veg. Sci.* 19, 711- 723.
- Bruesewitz, D.A., Hoellein, T.J., Mooney, R.F., Gardner, W.S., Buskey, E.J., 2017. Wastewater influences nitrogen dynamics in a coastal catchment during a prolonged drought: Nitrogen dynamics from river to estuary. *Limnol. Oceanogr.* 62, S239–S257. <https://doi.org/10.1002/lno.10576>
- Calizza, E., Fiorentino, F., Careddu, G., Rossi, L., Costantini, M.L., 2017. Lake water quality for human use and tourism in Central Italy (Rome). *WIT Trans. Ecol. Environ.* 216, 229-236.
- Careddu, G., Calizza, E., Costantini, M.L., Rossi, L., 2017. Isotopic determination of the trophic ecology of a ubiquitous key species–The crab *Liocarcinus depurator* (Brachyura: Portunidae). *Estuar. Coast. Shelf Sci.*, 191, 106-114.
- Cicala, D., Calizza, E., Careddu, G., Fiorentino, F., Sporta Caputi, S., Rossi, L., Costantini, M.L., 2019. Spatial variation in the feeding strategies of Mediterranean fish: flatfish and mullet in the Gulf of Gaeta (Italy). *Aquat. Ecol.*, 1-13. <https://doi.org/10.1007/s10452-019-09706-3>
- Copernicus Land Monitoring Service <https://land.copernicus.eu/pan-european/corine-land-cover>.  
(Accessed 05/14/2019)
- Costantini, M.L., Carlino, P., Calizza, E., Careddu, G., Cicala, D., Sporta Caputi, S., Fiorentino, F., Rossi, L., 2018. The role of alien fish (the centrarchid *Micropterus salmoides*) in lake food webs highlighted by stable isotope analysis. *Freshw. Biol.* 63, 1130-1142.
- Costanzo, S.D., Udy, J., Longstaff, B., Jones, A., 2005. Using nitrogen stable isotope ratios ( $\delta^{15}\text{N}$ ) of macroalgae to determine the effectiveness of sewage upgrades: changes in the extent of sewage plumes over four years in Moreton Bay, Australia. *Mar. Pollut. Bull.* 51, 212-217.
- Dailer, M.L., Knox, R.S., Smith, J.E., Napier, M., Smith, C.M., 2010. Using  $\delta^{15}\text{N}$  values in algal tissue to map locations and potential sources of anthropogenic nutrient inputs on the island of Maui, Hawai ‘i, USA. *Mar. Pollut. Bull.* 60, 655-671.
- Dale, V.H., Beyeler, S.C., 2001. Challenges in the development and use of ecological indicators. *Ecol. Indic.* 1, 3-10.
- DeBruyn, A.M., Rasmussen, J.B., 2002. Quantifying assimilation of sewage- derived organic matter by riverine benthos. *Ecol. Appl.* 12, 511-520.

- 473 Delpla, I., Jung, A.V., Baures, E., Clement, M., Thomas, O., 2009. Impacts of climate change on  
474 surface water quality in relation to drinking water production. *Environ. Int.* 35, 1225–1233.  
475 <https://doi.org/10.1016/j.envint.2009.07.001>
- 476 Derse, E., Knee, K.L., Wankel, S.D., Kendall, C., Berg, C.J., Paytan, A., 2007. Identifying sources  
477 of nitrogen to Hanalei Bay, Kauai, utilizing the nitrogen isotope signature of macroalgae.  
478 *Environ. Sci. Technol.* 41, 5217-5223.
- 479 Dong, J., Yang, K., Li, S., Li, G., Song, L., 2014. Submerged vegetation removal promotes shift of  
480 dominant phytoplankton functional groups in a eutrophic lake. *J. Environ. Sci.* 26, 1699–  
481 1707. <https://doi.org/10.1016/j.jes.2014.06.010>
- 482 FEE, Foundation for Environmental Education (2018). <https://www.fee.global/> (accessed  
483 07/30/2019)
- 484 Ferrara, O., Vagaggini, D., Margaritora, F.G., 2002. Zooplankton abundance and diversity in lake  
485 Bracciano, Latium, Italy. *J. Limnol.* 61, 169–175.
- 486 Fiorentino, F., Cicala, D., Careddu, G., Calizza, E., Jona Lasinio, G., Rossi, L., Costantini, M.L.,  
487 2017. Epilithon  $\delta^{15}\text{N}$  signatures indicate the origins of nitrogen loading and its seasonal  
488 dynamics in a volcanic Lake. *Ecol. Indic.* 79, 19-27.
- 489 Fry, B., Rogers, K., Barry, B., Barr, N., Dudley, B., 2011. Eutrophication indicators in the Hutt  
490 River Estuary, New Zealand. *N. Z. J. Mar. Freshwater Res.* 45, 665-677.
- 491 Gartner, A., Lavery, P., Smit, A.J., 2002. Use of  $\delta^{15}\text{N}$  signatures of different functional forms of  
492 macroalgae and filter-feeders to reveal temporal and spatial patterns in sewage dispersal. *Mar.*  
493 *Ecol. Prog. Ser.* 235, 63–73. <https://doi.org/10.3354/meps235063>
- 494 Gelman, A., Rubin, D.B., 1992. Inference from iterative simulation using multiple sequences. *Stat.*  
495 *Sci.* 7, 457-472.
- 496 Greaver, T.L., Clark, C.M., Compton, J.E., Vallano, D., Talhelm, A.F., Weaver, C.P., Band, L.E.,  
497 Baron, J.S., Davidson, E.A., Tague, C.L., Felker-Quinn, E., Lynch, J.A., Herrick, J.D., Liu, L.,  
498 Goodale, C.L., Novak, K.J., Haeuber, R.A., 2016. Key ecological responses to nitrogen are  
499 altered by climate change. *Nat. Clim. Chang.* 6, 836–843.  
500 <https://doi.org/10.1038/nclimate3088>
- 501 Hadwen, W.L., Bunn, S.E., Arthington, A.H., Mosisch, T.D., 2005. Within-lake detection of the  
502 effects of tourist activities in the littoral zone of oligotrophic dune lakes. *Aquat. Ecosyst.*  
503 *Health Manag.* 8, 159–173. <https://doi.org/10.1080/14634980590953211>
- 504 Hayes, N.M., Vanni, M.J., Horgan, M.J., Renwick, W.H., 2015. Climate and land use interactively  
505 affect lake phytoplankton nutrient limitation status. *Ecology* 96, 392–402.  
506 <https://doi.org/10.1890/13-1840.1>
- 507 He, R., Yang, X., Gassman, P.W., Wang, G., Yu, C., 2019. Spatiotemporal characterization of  
508 nutrient pollution source compositions in the Xiaohong River Basin, China. *Ecol. Indic.* 107,  
509 105676. <https://doi.org/10.1016/j.ecolind.2019.105676>
- 510 Hilderbrand, R. H., Watts, A. C., Randle, A.M., 2005. The myths of restoration ecology. *Ecol. Soc.*  
511 10,19.
- 512 Hobbs, R.J., 2007. Setting effective and realistic restoration goals: key directions for research.  
513 *Restor. Ecol.* 15, 354-357.
- 514 Jona Lasinio, G., Costantini, M.L., Calizza, E., Pollice, A., Bentivoglio, F., Orlandi, L., Careddu, G.,  
515 Rossi, L., 2015. Stable isotope-based statistical tools as ecological indicator of pollution sources in  
516 Mediterranean transitional water ecosystems. *Ecol. Indic.* 55, 23–31.  
517 <http://dx.doi.org/10.1016/j.ecolind.2015.03.006>.

- 519 Jona Lasinio, G., Tullio, M.A., Ventura, D., Ardizzone, G., Abdelahad, N., 2017. Statistical  
520 analysis of the distribution of infralittoral *Cystoseira* populations on pristine coasts of four  
521 Tyrrhenian islands: Proposed adjustment to the CARLIT index. *Ecol. Indic.* 73, 293-301.
- 522 Jones, R.I., King, L., Dent, M.M., Maberly, S.C., Gibson, C.E., 2004. Nitrogen stable isotope  
523 ratios in surface sediments, epilithon and macrophytes from upland lakes with differing  
524 nutrient status. *Freshw. Biol.* 49, 382-391.
- 525 Kaminski, H.L., Fry, B., Warnken, J., Pitt, K.A., 2018. Stable isotopes demonstrate the effectiveness  
526 of a tidally-staged sewage release system. *Mar. Pollut. Bull.* 133, 233–239.  
527 <https://doi.org/10.1016/j.marpolbul.2018.05.020>
- 528 Kosten, S., Lacerot, G., Jeppesen, E., da Motta Marques, D., van Nes, E.H., Mazzeo, N., Scheffer,  
529 M., 2009. Effects of submerged vegetation on water clarity across climates. *Ecosystems* 12,  
530 1117–1129. <https://doi.org/10.1007/s10021-009-9277-x>
- 531 Lapointe, B.E., Bedford, B.J., 2007. Drift rhodophyte blooms emerge in Lee County, Florida,  
532 USA: evidence of escalating coastal eutrophication. *Harmful Algae* 6, 421-437.
- 533 Lee, P.M., 1997. *Bayesian statistics: an introduction*. Arnold Publication.
- 534 Le Moal, M., Gascuel-Oudou, C., Ménesguen, A., Souchon, Y., Étrillard, C., Levain, A., Moatar, F.,  
535 Pannard, A., Souchu, P., Lefebvre, A., Pinay, G., 2019. Eutrophication: A new wine in an old  
536 bottle?. *Sci. Total Environ.* 651, 1-11.
- 537 Maberly, S.C., King, L., Dent, M.M., Jones, R.I., Gibson, C.E., 2002. Nutrient limitation of  
538 phytoplankton and periphyton growth in upland lakes. *Freshw. Biol.* 47, 2136-2152.
- 539 Marin, J.-M., Robert, C.P., 2014. Mixture Models, in: Marin, J-M, Robert, C.P. (Eds.), *Bayesian*  
540 *Essential with R*, second edition, Springer Texts in Statistics, pp. 173-206.
- 541 Mastrantuono, L., Mancinelli, T., 2005. Littoral invertebrates associated with aquatic plants and  
542 bioassessment of ecological status in Lake Bracciano (Central Italy). *J. Limnol.* 64, 43-53.
- 543 Mastrantuono, L., Solimini, A.G., Nöges, P., Bazzanti, M., 2008. Plant-associated invertebrates  
544 and hydrological balance in the large volcanic Lake Bracciano (Central Italy) during two  
545 years with different water levels, in Nöges, T., Eckmann, R., Kangur, K., Nöges, P.,  
546 Reinart, A., Roll, G., Simola, H., Viljanen, M. (Eds.), *European Large Lakes Ecosystem*  
547 *changes and their ecological and socioeconomic impacts*. Springer, Dordrecht, pp. 143-152.
- 548 McCormick, P.V., Cairns, J., 1994. Algae as indicators of environmental change. *J. Appl. Phycol.* 6,  
549 509-526.
- 550 Orlandi, L., Bentivoglio, F., Carlino, P., Calizza, E., Rossi, D., Costantini, M.L., Rossi, L., 2014.  
551  $\delta^{15}\text{N}$  variation in *Ulva lactuca* as a proxy for anthropogenic nitrogen inputs in coastal areas  
552 of Gulf of Gaeta (Mediterranean Sea). *Mar. Pollut. Bull.* 84, 76-82.
- 553 Orlandi, L., Calizza, E., Careddu, G., Carlino, P., Costantini, M.L., Rossi, L., 2017. The effects of  
554 nitrogen pollutants on the isotopic signal ( $\delta^{15}\text{N}$ ) of *Ulva lactuca*: microcosm experiments.  
555 *Mar. Pollut. Bull.* 115, 429-435.
- 556 Paerl, H.W., Hall, N.S., Peierls, B.L., Rossignol, K.L., 2014. Evolving paradigms and challenges in  
557 estuarine and coastal eutrophication dynamics in a culturally and climatically stressed  
558 world. *Estuaries Coasts* 37, 243-258.
- 559 Paerl, H.W., Gardner, W.S., Havens, K. E., Joyner, A.R., McCarthy, M.J., Newell, S.E., Qin, B.,  
560 Scott, J.T., 2016 Mitigating cyanobacterial harmful algal blooms in aquatic ecosystems  
561 impacted by climate change and anthropogenic nutrients. *Harmful Algae* 54, 213–222.  
562 <https://doi.org/10.1016/j.hal.2015.09.009>
- 563 Paerl, H.W., 2017. Controlling cyanobacterial harmful blooms in freshwater ecosystems. *Microb.*  
564 *Biotechnol.* 10, 1106–1110. <https://doi.org/10.1111/1751-7915.12725>

565

566

567

568

569

570

571

572

573

574

575

576

577

578

579

580

581

582

583

584

585

586

587

588

589

590

591

592

593

594

595

596

597

598

599

600

601

602

603

604

605

606

607

608

609

- Pal, J.S., Giorgi, F., Bi, X., 2004. Consistency of recent European summer precipitation trends and extremes with future regional climate projections. *Geophys. Res. Lett.* 31, L13202. <https://doi.org/10.1029/2004GL019836>
- Pastor, A., Riera, J.L., Peipoch, M., Cañas, L., Ribot, M., Gacia, E., Martí, E., Sabater, F., 2014. Temporal variability of nitrogen stable isotopes in primary uptake compartments in four streams differing in human impacts. *Environ. Sci. Technol.* 48, 6612–6619. <http://dx.doi.org/10.1021/es405493k>.
- Plummer, M., 2003. JAGS: a program for analysis of Bayesian graphical models using Gibbs sampling. *Proceedings of the 3rd International Workshop Distributed Statistical Computing (2003)*
- Ponsard, S., Ardití, R., 2000. What can stable isotopes ( $\delta^{15}\text{N}$  and  $\delta^{13}\text{C}$ ) tell about the food web of soil macro-invertebrates? *Ecology* 81, 852–864.
- R Core Team, 2019. R: A language and environment for statistical computing. R Foundation for Statistical Computing, Vienna, Austria. URL <https://www.R-project.org/>.
- Risk, M.J., Lapointe, B.E., Sherwood, O.A., Bedford, B.J., 2009. The use of  $\delta^{15}\text{N}$  in assessing sewage stress on coral reefs. *Mar. Pollut. Bull.* 58, 793-802.
- Rossi, L., Calizza, E., Careddu, G., Rossi, D., Orlandi, L., Jona Lasinio, G., Aguzzi, L., Costantini, M.L., 2018. Space-time monitoring of coastal pollution in the Gulf of Gaeta, Italy, using  $\delta^{15}\text{N}$  values of *Ulva lactuca*, landscape hydromorphology, and Bayesian Kriging modelling. *Mar. Pollut. Bull.* 126, 479-487.
- Rossi, L., Sporta Caputi, S., Calizza, E., Careddu, G., Oliverio, M., Schiaparelli, S., Costantini, M. L., 2019. Antarctic food web architecture under varying dynamics of sea ice cover. *Sci. Rep.* 9, 1-13. <https://doi.org/10.1038/s41598-019-48245-7>
- Rossi, D., Romano, E., Guyennon, N., Rainaldi, M., Ghergo, S., Mecali, A., Parrone, D., Taviani, S., Scala, A., Perugini, E., 2019. The present state of Lake Bracciano: hope and despair. *Rend. Lincei Sci. Fis. Nat.* 30, 83-91.
- Schmale, D.G., Ault, A.P., Saad, W., Scott, D.T., Westrick, J.A., 2019. Perspectives on Harmful Algal Blooms (HABs) and the Cyberbiosecurity of Freshwater Systems. *Front. Bioeng. Biotechnol.* 7, 128. <https://doi.org/10.3389/fbioe.2019.00128>
- Scrucca, L., Fop, M., Murphy, T.B., Raftery, A.E., 2016. mclust 5: clustering, classification and density estimation using Gaussian finite mixture models. *R J.* 8, 289-317.
- Singh, U.B., Ahluwalia, A.S., Sharma, C., Jindal, R., Thakur, R.K., 2013. Planktonic indicators: a promising tool for monitoring water quality (early-warning signals). *Eco. Environ. Cons.* 19, 793-800.
- Spinoni, J., Vogt, J.V., Naumann, G., Barbosa, P., Dosio, A., 2018. Will drought events become more frequent and severe in Europe?. *Int. J. Climatol.* 38, 1718-1736.
- Su, Y.-S., Yajima, M., 2015. R2jags: Using R to Run 'JAGS'. R package version 0.5-7. <https://CRAN.R-project.org/package=R2jags>
- Taviani, S., Henriksen, H.J., 2015. The application of a groundwater/surface-water model to test the vulnerability of Bracciano Lake (near Rome, Italy) to climatic and water-use stresses. *Hydrogeol. J.* 23, 1481-1498.
- Titlyanov, E. A., Kiyashko, S. I., Titlyanova, T. V., Van Huyen, P., Yakovleva, I. M., 2011. Identifying nitrogen sources for macroalgal growth in variously polluted coastal areas of southern Vietnam. *Bot. Mar.*, 54, 367-376. <https://doi.org/10.1515/bot.2011.041>



- 610 van Vliet, M.T.H., Zwolsman, J.J.G., 2008. Impact of summer droughts on the water quality of the  
611 Meuse river. *J. Hydrol.* 353, 1–17. <https://doi.org/10.1016/j.jhydrol.2008.01.001>
- 612 von Schiller, D., Martí, E., Riera, J.L., 2009. Nitrate retention and removal in Mediterranean  
613 streams bordered by contrasting land uses: a  $^{15}\text{N}$  tracer study. *Biogeosciences*, 6, 181–196.  
614 <https://doi.org/10.5194/bg-6-181-2009>
- 615 Wang, Y., Liu, D., Richard, P., Di, B., 2016. Selection of effective macroalgal species and tracing  
616 nitrogen sources on the different part of Yantai coast, China indicated by macroalgal  $\delta^{15}\text{N}$   
617 values. *Sci. Total Environ.* 542, 306-314.
- 618 Wood, S.N., 2011. Fast stable restricted maximum likelihood and marginal likelihood estimation of  
619 semiparametric generalized linear models. *J. R. Stat. Soc. Series B Stat. Methodol.* 73, 3-36.
- 620 Wood, S.N., 2017. *Generalized additive models: an introduction with R*. Chapman and Hall/CRC.
- 621 Zuur, A., Ieno, E.N., Smith, G.M., 2007. Beginner's guide to GAM with R, in: Zuur, A., Ieno, E.N.,  
622 Smith, G.M. (Eds.), *Analyzing Ecological Data*. Springer, Science & Business Media, pp.  
623 97–124. <http://dx.doi.org/10.1007/978-0-387-45972-1>.
- 624 Zuur, A.F., Ieno, E.N., Walker, N.J., Saveliev, A.A., Smith, G.M., 2009. Things are not always  
625 linear; additive modelling in: Zuur, A., Ieno, E.N., Walker, N., Saveliev, A.A., Smith, G.M.  
626 (Eds.), *Mixed Effects Models and Extensions in Ecology with R*. Springer, New York, pp. 35–  
627 69. <http://dx.doi.org/10.1007/978-0-387-87458-6>



## Supplementary material

### New analytical protocol for the classification of Nitrogen inputs in lakes based on epilithic $\delta^{15}\text{N}$

**Federico Fiorentino<sup>a</sup>, Giovanna Jona Lasinio<sup>b</sup>, Giulio Careddu<sup>a</sup>, Simona Sporta Caputi<sup>a</sup>, Loreto Rossi<sup>a,c</sup>, Edoardo Calizza<sup>a,c,\*</sup>, Maria Letizia Costantini<sup>a,c</sup>**

<sup>a</sup> Department of Environmental Biology, Sapienza University of Rome, Via dei Sardi 70, Rome, Italy, 00185 Rome, Italy

<sup>b</sup> Department of Statistical Sciences, Sapienza University of Rome, P.le Aldo Moro 5, 00185 Rome, Italy

<sup>c</sup> CoNISMa -Consorzio Nazionale Interuniversitario per le Scienze del Mare, Piazzale Flaminio 9, 00100 Rome, Italy

\* **Corresponding Author:** [calizza.edoardo@uniroma1.it](mailto:calizza.edoardo@uniroma1.it)

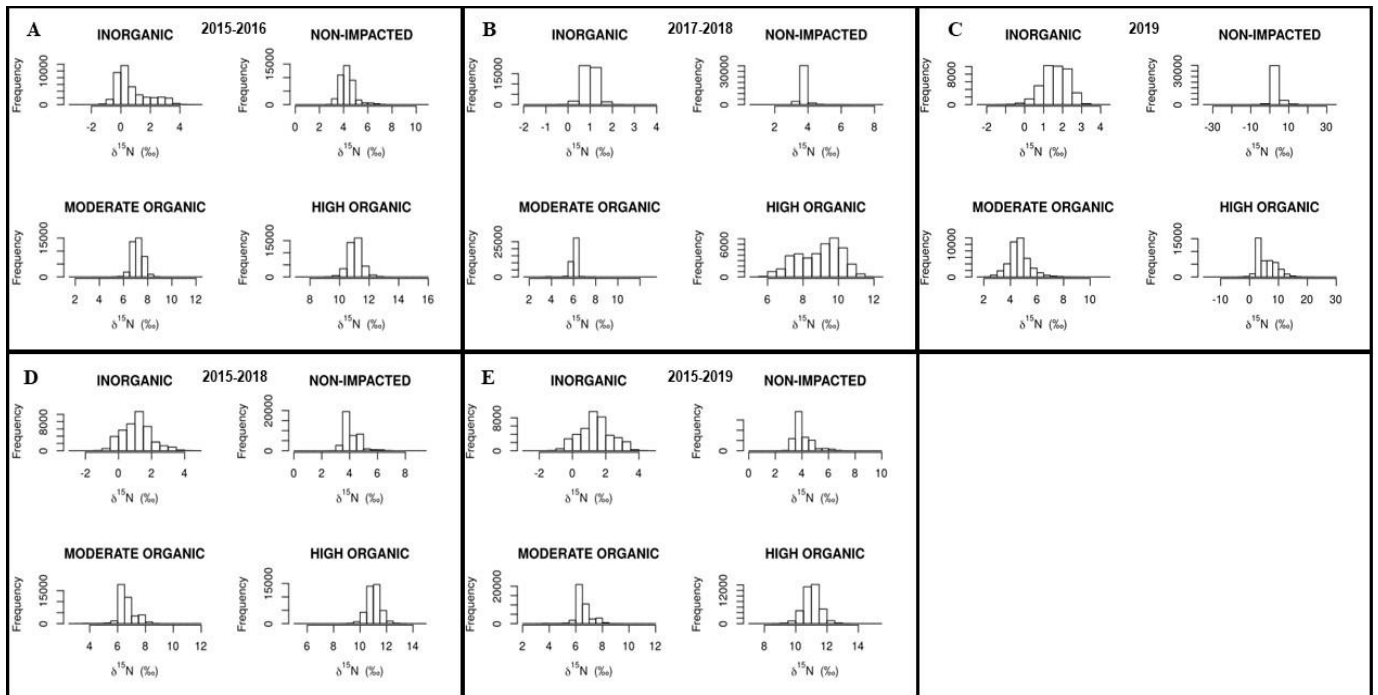


**Fig. S1.** Histograms of the Nitrogen impact class averages for the classification model ran with the: 2015-2016 (**A**) raw data only, 2017-2018 raw data (**B**), 2019 raw data (**C**), 2015-2018 period raw data (**D**) and 2015-2019 period raw data (**E**)

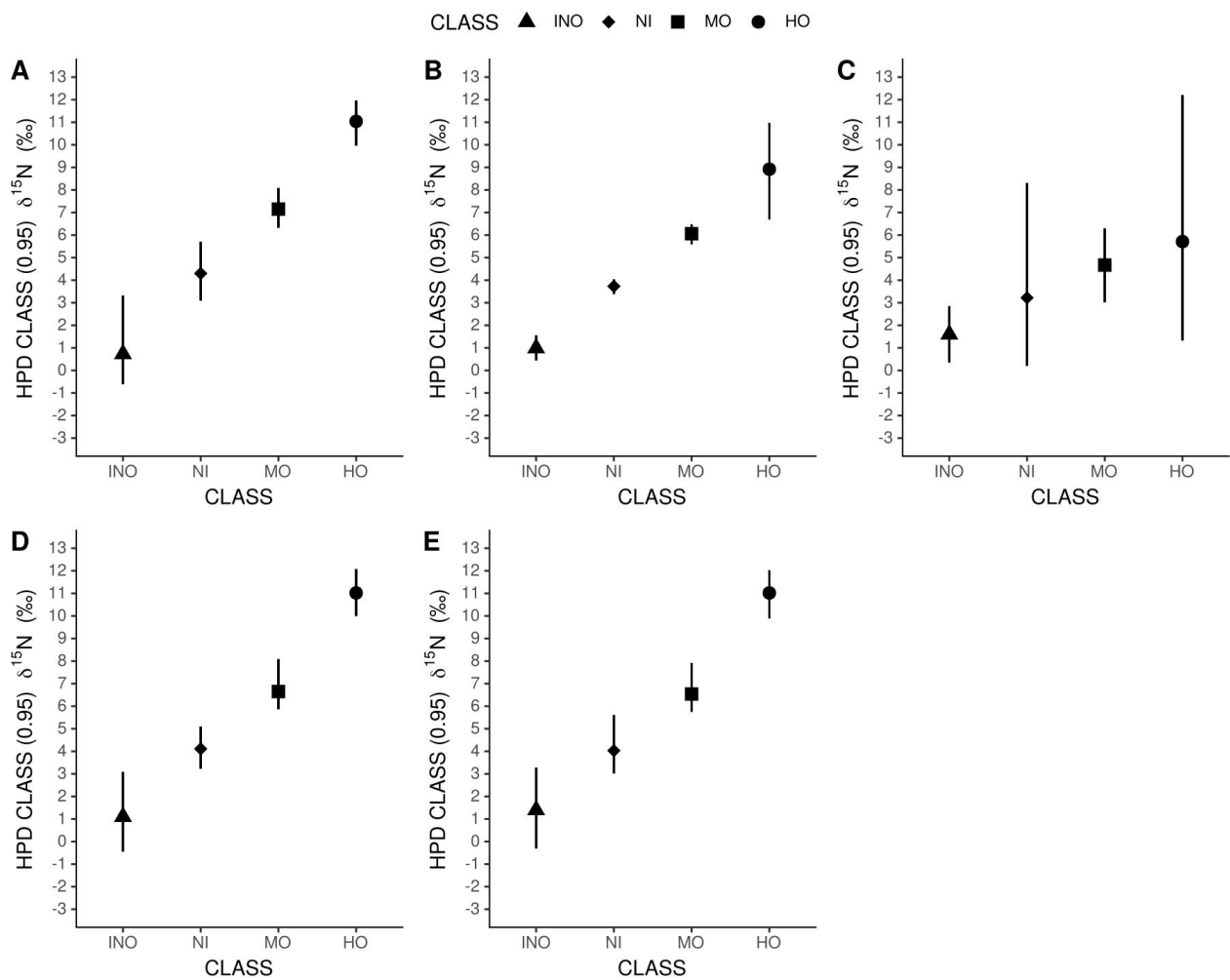


**Fig. S2.** Nitrogen impact classes HPD (95%) for the classification model ran with the: 2015-2016 (A) raw data only, 2017-2018 raw data (B), 2019 raw data (C), 2015-2018 period raw data (D) and 2015-2019 period raw data (E). Different shapes represent a specific  $\delta^{15}\text{N}$  signature classification (**triangles**=‘inorganic’, **rhombuses**=‘non-impacted’, **squares**=‘moderate organic’, **circles**=‘high organic’)

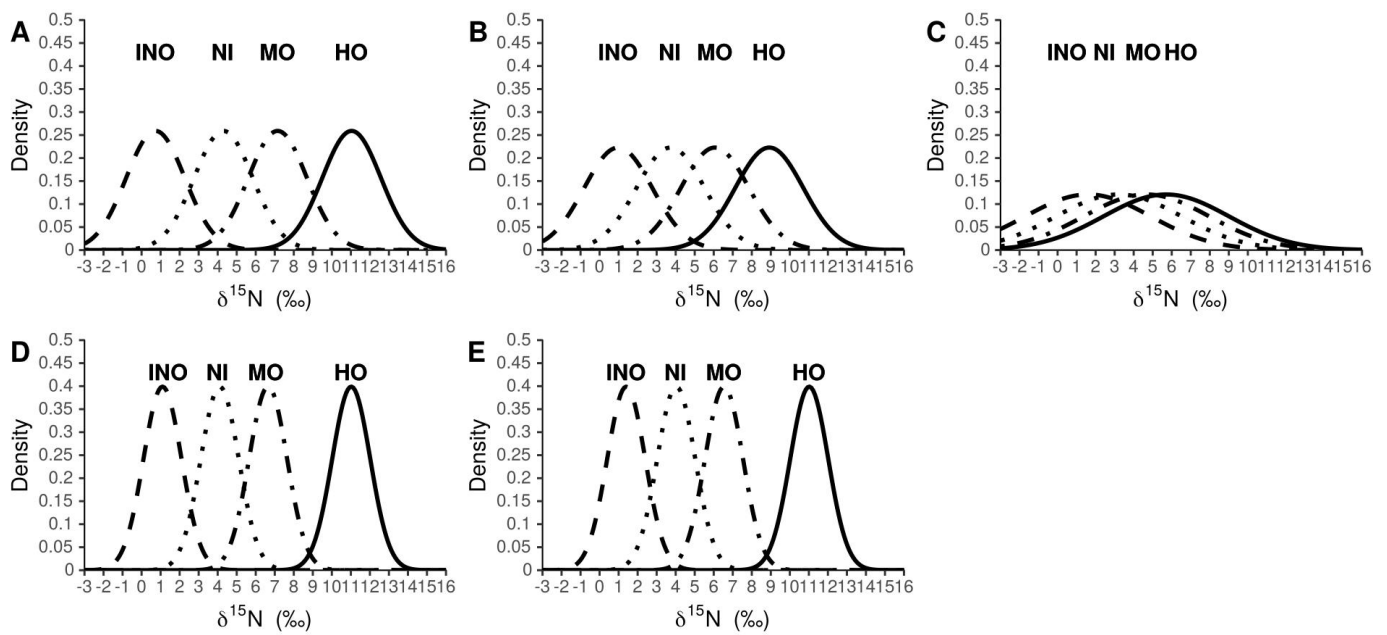


**Fig. S3.** Density of the Nitrogen impact classes with classification model ran with the: 2015-2016 classification (**A**), 2017-2018 classification (**B**), 2019 classification (**C**), 2015-2018 classification (**D**) and 2015-2019 classification (**E**).

Different lines represent different Nitrogen impact classes.

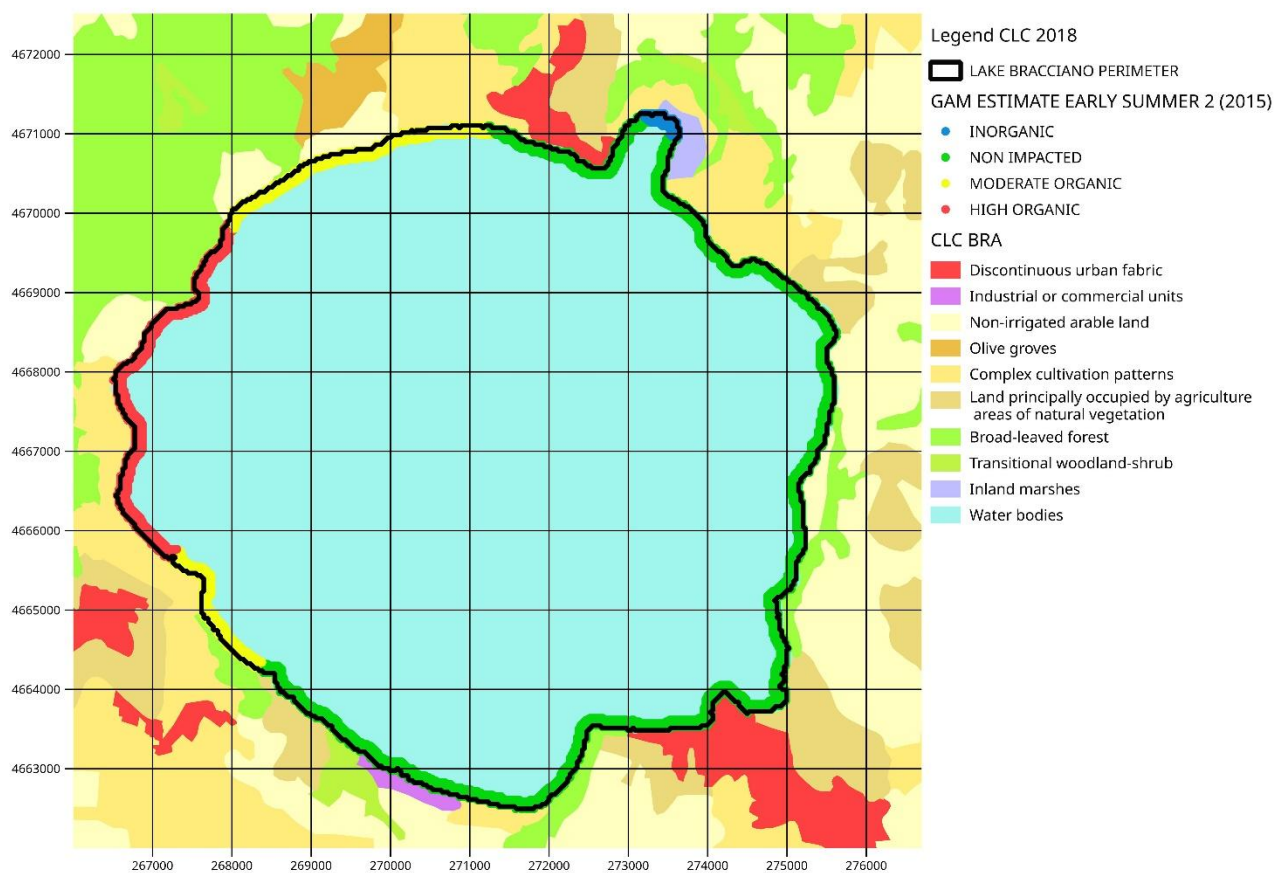


**Fig. S4.** Corine Land Cover (2018) of the area surrounding the water body of Lake Bracciano (the black line indicates the lake perimeter) and GAM estimate for the Early Summer 2 (2015) sampling date (Fiorentino et al., 2017). Here, for simplicity, GAM estimated values were categorized according with the unprocessed  $\delta^{15}\text{N}$  epilithic signature classification proposed in our previous work (Fiorentino et al., 2017).

**Table S1** Sampling dates for the 2015-2019 surveys.

<b>Survey</b>	<b>Sampling date</b>	<b>Month</b>
2015-2016	Early Summer 1 2015	June 2015
2015-2016	Early Summer 2 2015	June 2015
2015-2016	Summer 2015	July 2015
2015-2016	Autumn 2015	September 2015
2015-2016	Winter 2015-2016	December 2015
2015-2016	Spring 2016	March 2016
2017-2019	Spring 2017	April 2017
2017-2019	Summer 2017	July 2017
2017-2019	Autumn 2017	(12/5) December 2017
2017-2019	Winter 2017-2018	February 2018
2017-2019	Spring 2018	May 2018
2017-2019	Early Summer 1 2018	June 2018
2017-2019	Early Summer 2 2018	July 2018
2017-2019	Summer 2018	July 2018
2017-2019	Autumn 2018	September 2018
2017-2019	Spring 2019	April 2019

**Table S2** Table reports the eleven sampling sites in common between the two surveys.

<b>2015-2016 survey</b>	<b>2017-2019 survey</b>
S01	C01
S02	C02
S03	C03
S04	C04
S08	C05
S09	C06
S10	C07
S12	C08
S14	C09
S16	C10
S19	C11

**Table S3** Table of the estimated variance of the Nitrogen classes by different raw data subsets.

<b>Raw data subset</b>	<b><math>\sigma^2</math></b>
2015-2016 only	2.37
2017-2018 only	3.22
2019 only	11.11
2015-2018	1.00
2015-2019	1.00



**Table S4** Table of the GAM models results. The first column reports the survey time frame, the second the sampling date, the third reports the estimated intercept and the thin-plate spline (TPS), the fourth the t-value for the intercept and the F-value for the spline, the fifth the p-value for the intercept and for the spline, the sixth the explained deviance by the GAM models.

<b>Survey</b>	<b>Sampling date</b>	<b>Intercept TPS</b>	<b>t-value F-value</b>	<b>p-value</b>	<b>Dev. explained</b>
(2015-2016)	Early Summer 1 (2015)	6.52 ± 0.17 s(long.,lat.)	38.19 15.68	<0.05 <0.05	76.7%
(2015-2016)	Early Summer 2 (2015)	6.74 ± 0.18 s(long.,lat.)	36.24 17.75	<0.05 <0.05	79.4%
(2015-2016)	Summer (2015)	5.48 ± 0.31 s(long.,lat.)	17.42 5.00	<0.05 <0.05	49.4%
(2015-2016)	Autumn (2015)	4.90 ± 0.23 s(long.,lat.)	21.23 5.23	<0.05 <0.05	66%
(2015-2016)	Winter (2015/2016)	5.14 ± 0.22 s(long.,lat.)	23.68 3.85	<0.05 <0.05	57.8%
(2015-2016)	Spring (2016)	4.41 ± 0.16 s(long.,lat.)	27.45 12.48	<0.05 <0.05	83.2%
(2017-2019)	Spring (2017)	4.18 ± 0.23 s(long.,lat.)	18.01 5.02	<0.05 <0.05	70.1%
(2017-2019)	Summer (2017)	3.53 ± 0.18 s(long.,lat.)	19.36 6.37	<0.05 <0.05	78.6%
(2017-2019)	Autumn (2017)	4.04 ± 0.16 s(long.,lat.)	25.29 8.85	<0.05 <0.05	79.3%
(2017-2019)	Winter (2017/2018)	4.27 ± 0.18 s(long.,lat.)	23.72 2.08	<0.05 0.08	48.2%
(2017-2019)	Spring (2018)	6.16 ± 0.14 s(long.,lat.)	44.00 4.03	<0.05 <0.05	54.5%
(2017-2019)	Early Summer 1 (2018)	5.69 ± 0.12 s(long.,lat.)	48.86 11.64	<0.05 <0.05	81.1%
(2017-2019)	Early Summer 2 (2018)	5.60 ± 0.21 s(long.,lat.)	26.92 2.36	<0.05 <0.05	35.3%
(2017-2019)	Summer (2018)	4.72 ± 0.22 s(long.,lat.)	21.42 3.18	<0.05 <0.05	51.8%
(2017-2019)	Autumn (2018)	3.45 ± 0.17 s(long.,lat.)	20.62 5.74	<0.05 <0.05	75%
(2017-2019)	Spring (2019)	2.78 ± 0.12 s(long.,lat.)	22.32 6.38	<0.05 <0.05	62.6%

**Table S5** Comparison of Spring interpolated surfaces in 2016, 2017,2018 and 2019. Percentage values.

<b>Classification Spring 2017</b>				
		<b>Inorganic</b>	<b>Non-impacted</b>	<b>Moderate organic</b>
<b>Classification Spring 2016</b>	<b>Inorganic</b>	18.27	6.83	0.00
	<b>Non-impacted</b>	15.97	35.46	0.40
	<b>Moderate organic</b>	1.96	20.37	0.74
<b>Classification Spring 2018</b>				
		<b>Non-impacted</b>	<b>Moderate organic</b>	
<b>Classification Spring 2017</b>	<b>Inorganic</b>	19.54	16.66	
	<b>Non-impacted</b>	14.97	47.69	
	<b>Moderate organic</b>	0.00	1.14	
<b>Classification Spring 2019</b>				
		<b>Inorganic</b>	<b>Non-impacted</b>	
<b>Classification Spring 2018</b>	<b>Non-impacted</b>	26.74	7.77	
	<b>Moderate organic</b>	19.25	46.24	

**Supplementary Material\_JAGS CODE**

**[Click here to download Supplementary Material: JAGS CODE.txt](#)**

**Supplementary Material\_R CODE**

[Click here to download Supplementary Material: R CODE.txt](#)

**Declaration of interests**

The authors declare that they have no known competing financial interests or personal relationships that could have appeared to influence the work reported in this paper.

The authors declare the following financial interests/personal relationships which may be considered as potential competing interests:

JAGS code

```
model {
  # Likelihood:
  for( i in 1 : N ) {
    y[i] ~ dnorm( mu[i] , tauy )
    mu[i] <- muOfClust[ clust[i] ]
    clust[i] ~ dcat( pClust[1:Nclust] )
  }
  # Prior:
  tau~dgamma(2,0.2)
  tauy~dgamma(2,0.2)
  for ( clustIdx in 1: Nclust ) {

    muOfClust[clustIdx] ~ dnorm( m[clustIdx] , tau )
  }
  pClust[1:Nclust] ~ ddirch( onesRepNclust )
}
```

R code

```
# load required packages #

require(R2jags)
require(xtable)
require(DescTools)
require(coda)

# X is a one column data.frame with the observed epilithic d15N #

# Bayesian Gaussian Mixture Model #

Nclust=4 # number of clusters #
y = X
clust = rep(NA,length(y))
N=length(y)
clust[which.min(y)]=1 # smallest value assigned to cluster 1#
clust[which.max(y)]=4 # highest value assigned to cluster 4#

# dataList is a list with the data elements to be passed to the JAGS model #

dataList = list(
  y = y , # observed d15N signature for the model estimation #
  N = length(y) , # number of the observed data #
  Nclust = Nclust , #number of the clusters #
  clust = clust ,
  #vector of length equal to N. In this vector, all the positions are NA
  #except for the positions corresponding to the smallest and largest values
  #in y #
  onesRepNclust = rep(1,Nclust), # hyper parameters of the Dirichlet
  #distribution used as prior distribution for the clusters labels in the
  #JAGS model #
  m=c(a, b ,c ,d) # replace a,b,c,d with the mean of the Gaussian prior
  #distributions associated to the means of the Nclust=4 clusters #
)

partosave<-c("clust","tau","tauy","muOfClust","pClust") # which parameters
# need to be saved #

# check that the JAGS code is in your working directory #
# fit the model #

fit=jags(data=dataList,parameters.to.save=partosave,
  n.chain=2, # number of markov chains that will be used for
  #estimation #
  n.iter=250000, # iterations #
  n.thin=10, # retain every 10 observations to reduce autocorrelation
  #in the saved chains #
  n.burnin=50000, # discard n.burnin observations before start saving
  #samples to ensure that the chains are close to convergence #
  jags.seed=56789, # simulations seed set for replicability #
```

```

    model.file="replace_with_JAGS_model_filename.txt") # name of the
JAGS model file #

#create a pdf where traces of Markov chains are saved #
pdf("model_traces.pdf")
traceplot(fit,ask=F)
dev.off()

#save summary of the model and convergence checks (That and neff)#

print(xtable(round(fit$BUGSoutput$summary,3),digits =
3),file="model_summary.tex")

# extract tau, to build the point estimates of the precisions (and then of
the variances) of clusters distributions and the residuals#

tau.sim=fit$BUGSoutput$sims.matrix[,grep("tau",colnames(fit$BUGSoutput$sims
s.matrix))] #samples
tau.sim=round(tau.sim,digits=2)
tau.hat=apply(tau.sim,2,Mode) # tau mode i.e. the maximum a posteriori
estimate #

## we build the variances as well#
var.sim<-tau.sim
var.sim[,1]<-1/tau.sim[,1]
var.sim[,2]<-1/tau.sim[,2]
var.hat<-apply(var.sim,2,Mode)
## standard deviation of the clusters
sd_clusters<-sqrt(var.hat[1])
# plot tau #

par(mfrow=c(1,2)) # two plots per page #
apply(tau.sim,2,hist) # histograms for the precisions#
apply(var.sim,2,hist) # histograms for the variances#
#extract averages of clusters#

mu<-
fit$BUGSoutput$sims.matrix[,grep("muOfClust",colnames(fit$BUGSoutput$sims.
matrix))]
mu.hat<-apply(mu,2,mean) #posterior means as point estimation #

#plot mu #
par(mfrow=c(2,2)) # four plots per page #
apply(mu,2,hist) # histograms for the clusters means #

par(mfrow=c(1,1)) # one plot per page #

#compute the HPD using the coda package#

Mean1<-mcmc(mu,start=1,end=5000,thin=1)
Mean1<-mcmc.list(Mean1)

```



```

hpd.mean<-HPDinterval(Mean1,prob = 0.95) # 95% highest posterior density
intervals for the clusters means
## 95% highest posterior density intervals for the precisions and the
variances

hpd.tau<-
HPDinterval(mcmc.list(mcmc(tau.sim,start=1,end=5000,thin=1)),prob=0.95)

Hpdvar<-HPDinterval(mcmc.list(mcmc(var.sim,start=1,end=5000,thin=1)))

# return the probabilities of belonging for observed/ new data according
to the estimated model. It uses a for loop #

# K is a one column data.frame with observed epilithic d15N #

obs_new_data<-matrix(K,ncol=1) #matrix of the data to be classified #

clust.fit.prob<-matrix(0,nrow=length(obs_new_data),4)
# matrix to save the membership probabilities to each Nitrogen impact
class for each new observation. Each column of the matrix represents a
Nitrogen impact class #

# variable2 is a convenience variable to temporary store values associated
to the i-th row #
# the dnorm function returns the density of a value according to a Normal
distribution identified by its mean (mean) and standard deviation (sd) ###
see the R help for details#
# mu.hat[j] (j=1,2,3,4) is the mean of the Normal distribution associated
to the jth Nitrogen impact class #
# sd_clusters is the standard deviation of the Normal distributions of the
Nitrogen impact classes #

### Membership probabilities computation ###

# each element of variable2 is the Gaussian density computed at the i-th
observation for each Nitrogen impact class #
# the j-th cluster membership probability of the i-th observation is
obtained as the ratio between variable2[j] and the sum over j of all
elements in variable2.

# the probabilities of membership to each Nitrogen impact class are then
stored in the i-th row of the clust.fit.prob matrix #

# the following loop runs through the rows (i) of the obs_new_data matrix
#
for(i in 1:nrow(obs_new_data)){
  variable2=c(dnorm(obs_new_data[i],mean=mu.hat[1],sd=sd_clusters),
             dnorm(obs_new_data[i],mean=mu.hat[2],sd=sd_clusters),

```

```
        dnorm(obs_new_data[i],mean=mu.hat[3],sd=sd_clusters),
        dnorm(obs_new_data[i],mean=mu.hat[4],sd=sd_clusters))
    clust.fit.prob[i,]=matrix(variable2/sum(variable2))
```

```
}
```

```
# to visualize
```

```
head(clust.fit.prob)
```

```
heatmap(clust.fit.prob,Colv=NA)
```

## Discussion

Nitrogen inputs in aquatic ecosystems showed a dramatic increase in the last two decades (Glibert, 2017; Howart, 2008), with consequent ecosystem services losses, threats for ecosystem stability and for human interests and health (Le Moal et al., 2019; Paerl et al., 2016; Yao et al., 2018). Despite the management efforts, a notable percentage of the aquatic ecosystems are currently affected by nutrient inputs (Carvalho et al., 2019). The recovery and the preventions of these ecosystems is highly dependent on the identification of such nutrient input origins (organic vs inorganic). The Nitrogen stable isotopes analysis, applied to macroalgae and epilithic associations, has proven to be effective for this purpose in several marine and a few fluvial ecosystems (Bentivoglio et al., 2016; Jona-Lasinio et al., 2015; Orlandi et al., 2014; Pastor et al., 2014; Rossi et al., 2018), turning into advantage the assimilation, from the aquatic medium, of Nitrogen into the biotic samples (Gartner et al., 2002; Kaminski et al., 2018). For freshwater and land locked ecosystems, however, there was a general lack of researches on the applicability of this methodology on their environmental monitoring. All the case studies of this dissertation contributed for filling up this notable gap. The split of the macroalgae/epilithic  $\delta^{15}\text{N}$  signatures in four categories ('inorganic', 'non-impacted', 'moderate organic' and 'high organic') allowed us to highlight wide/narrow, organically/inorganically or non-impacted areas. In all the study cases, epilithic and macroalgal signatures revealed the occurrence of industrial fertilizer Nitrogen inlets into the water bodies due to the presence of agricultural activities. The principal cause for these Nitrogen inputs in Lake Bracciano were the rainfalls that leached the agricultural fields (diffuse sources), whereas diffuse sources in the Caspian Sea were associated to the 'White River' (Sefi- Rud) input transport along its lowland  $\approx 55$  Km long stretch, which crosses heavily cultivated areas. For the Santa Croce river, the 'inorganic' inputs represent a minor threat to the water body, compared to the wide organic inputs recorded, affecting only one sampling site.

In parallel, the epilithic and macroalgal Nitrogen signatures, in all the water bodies, recorded the typical traces of organic inputs. In Lake Bracciano and Caspian Sea, the  $\delta^{15}\text{N}$  organic signatures were attributed to the touristic activities due to their high concentrations in the most popular touristic areas. For Lake Bracciano, the touristic derivation of these high epilithic  $\delta^{15}\text{N}$  signatures (which fell up to the 'high organic' range) were confirmed by the strong seasonality of the phenomenon. In fact, the higher organic  $\delta^{15}\text{N}$  values corresponded to the Summer season (June-July 2015) with a peak (after a public holiday, 29<sup>th</sup> June, for the entire municipality of Rome) correlated the incomes of parking meters.

In the Iranian Caspian Sea, the macroalgal  $\delta^{15}\text{N}$  signatures were related to the total dissolved inorganic Nitrogen concentration. This positive linear relationship, coupled with a decrease of the dissolved Oxygen concentrations in anthropic-derived Nitrogen impacted areas, confirmed the concerns of the water quality of the Caspian Sea due to the cultural eutrophication (Sadeghi et al., 2013). The ‘moderate’ and ‘high organic’ inputs are dominant in the three studied rivers, affecting more than  $\frac{3}{4}$  of the sampling sites as a result of the persistent effects of the wastewater treatment plant and urban Nitrogen loadings.

Except in rivers, there were also areas non-affected by human derived Nitrogen inputs. These ‘non-impacted’ signatures, in the two land locked ecosystems, highlighted how the management of human activities buffered the inlets of the human-related Nitrogen inputs.

In Lake Bracciano, the non-homogenous distribution of human activities around the water body and their seasonal magnitudes played a major role for the input dynamics. In fact, different areas switched between ‘non-impacted’- ‘moderate organic’ and ‘non-impacted’ – ‘inorganic’ monodimensional classes (Chapter 1), with epilithic  $\delta^{15}\text{N}$  values, sometimes, close to the upper/lower boundaries of consecutive classes. This aspect represents an issue both in the objective assignment of an epilithic signature to the most appropriate Nitrogen impact class and in the ecological interpretation of the classification results. The Bayesian Gaussian Mixture Model solved both these aspects. The model estimated four Gaussian distributions, each one associated to a previously recognized class (Chapter 1) and returned the probabilities of belonging of the ‘raw’ epilithic  $\delta^{15}\text{N}$  signature for each Nitrogen impact class, so the most appropriate class is the class with the highest probability of belonging. Moreover, model results can act as an early warning signal for the cultural eutrophication when there is equiprobability between ‘non-impacted’ and ‘inorganic’ or ‘moderate organic’ classes or when human-related impact classes have non zero probabilities to affect ecologically or economically important zones, so further environmental monitoring can be more specifically planned. A second advantage provided by the robust assignment of the epilithic  $\delta^{15}\text{N}$  signatures to specific classes is the possibility to follow the temporal dynamics of the class at different spatial scales and produce thematic maps for the probability of belonging to different Nitrogen impact classes. From these analyses emerged that the human-related Nitrogen input dynamics changed as a side effect of the drought. At sampling site (across seasons) and at entire perimeter (across vernal seasons in different years) there were: (i) a significant reduction of the ‘moderate organic’ class (2017) and (ii) an increase of the ‘inorganic’ class. These results, for the ‘moderate organic’ class, can be explained in terms of tourism decrease compared with the previous observations (Chapter 1), whereas the ‘inorganic’ inputs can be explained as an

increase of industrial fertilizers use in surrounding areas.

The studies presented in this thesis showed that the algal  $\delta^{15}\text{N}$  signature is a flexible tool for the environmental monitoring of Nitrogen inputs affecting the fluvial and land locked ecosystems. Notably, the  $\delta^{15}\text{N}$  signature ranges were coherent in discriminating the human derived origins of the inputs (organic vs inorganic) despite: **(1)** the differences in biotic samples (epilithon and macroalgae), **(2)** the morphological differences and **(3)** the different magnitude of human pressures. For all the water bodies, it is advisable to increase the sampling efforts in areas impacted by human-derived Nitrogen inputs and proceed, for Lake Bracciano, an update of the wastewater collecting system, for the Iranian Caspian Sea littoral zone, to increase the number of such wastewater plants (Abadi et al., 2018) and for the three Central Italian rivers, to manage the urban and wastewater treatment plant organic Nitrogen inputs. The wide applicability of this Nitrogen input indicator is further enhanced by the determination of the probability distribution, that represent a more robust approach for the assignment of tight/wide areas to the most appropriate Nitrogen impact class compared to the monodimensional ranges. The analytical protocol proposed in Chapter 5, allows the prioritization for more detailed analyses or specific interventions based on class probability of belonging at different space-time scales. Furthermore, the protocol is an easier method to inform stakeholders, because it not only returns simple thematic maps, but it also expresses the shifts among classes as percentages and the exposures to the anthropic Nitrogen inputs as probabilities. Lastly, the coherence among the observed field data of oligo-mesotrophic and eutrophic ecosystems, as well as the similarity with the observed macroalgae and epilithic  $\delta^{15}\text{N}$  signatures in scientific literature (Bentivoglio et al., 2016; DeBruyn and Rasmussen 2002; Derse et al., 2007; Fry et al., 2011; Wang et al., 2016), suggests that the proposed protocol can be extended to other aquatic ecosystems. Considering the notable percentages of water bodies still affected by cultural eutrophication (Carvalho et al., 2019) and the increasing trend in human-derived Nitrogen loadings (Glibert, 2017; Howart, 2008), the proven ability of the epilithic/macroalgal  $\delta^{15}\text{N}$  signature to properly discriminate, in different aquatic ecosystems, the origins of the human-related Nitrogen inputs at different spatial and temporal scales, can substantially contribute to the cultural eutrophication management. Therefore, it can be considered to add this informative biomonitoring tool to the environmental monitoring legislation and to add it to the standard protocols, as already happens in Australia for the marine coastal areas monitoring (Costanzo et al., 2001, 2005).

## References

- Abadi, M., Zamani, A., Parizanganeh, A., Khosravi, Y., Badiee, H., 2018. Heavy metals and arsenic content in water along the southern Caspian coasts in Iran. *Environ. Sci. Pollut. Res.* 25, 23725–23735. <https://doi.org/10.1007/s11356-018-2455-7>
- Baccetti, N., Bellucci, V., Bernabei, S., Bianco, P., Braca, G., Bussetini, M., Cascone, C., Ciccacese, L., D'Antoni, S., Grignetti, A., Lastoria, A., Mandrone, S., Mariani, S., Silli, V., Venturelli, S., 2017. Analisi e valutazione dello stato ambientale del Lago di Bracciano riferito all'estate 2017. Rapporto ISPRA, 18.
- Bentivoglio, F., Calizza, E., Rossi, D., Carlino, P., Careddu, G., Rossi, L., Costantini, M.L., 2016. Site-scale isotopic variations along a river course help localize drainage basin influence on river food webs. *Hydrobiologia* 770, 257–272. <https://doi.org/10.1007/s10750-015-2597-2>
- Bhagowati, B., Ahamad, K.U., 2019. A review on lake eutrophication dynamics and recent developments in lake modeling. *Ecohydrol. Hydrobiol.* 19, 155–166. <https://doi.org/10.1016/j.ecohyd.2018.03.002>
- Bolpagni, R., Laini, A., Azzella, M.M., 2016. Short-term dynamics of submerged aquatic vegetation diversity and abundance in deep lakes. *Appl. Veg. Sci.* 19, 711–723. <https://doi.org/10.1111/avsc.12245>
- Bruesewitz, D.A., Hoellein, T.J., Mooney, R.F., Gardner, W.S., Buskey, E.J., 2017. Wastewater influences nitrogen dynamics in a coastal catchment during a prolonged drought: Nitrogen dynamics from river to estuary. *Limnol. Oceanogr.* 62, S239–S257. <https://doi.org/10.1002/lno.10576>
- Careddu, G., Costantini, M.L., Calizza, E., Carlino, P., Bentivoglio, F., Orlandi, L., Rossi, L., 2015. Effects of terrestrial input on macrobenthic food webs of coastal sea are detected by stable isotope analysis in Gaeta Gulf. *Estuar., Coast. Shelf Sci.* 154, 158–168. <https://doi.org/10.1016/j.ecss.2015.01.013>
- Careddu, G., Calizza, E., Costantini, M.L., Rossi, L., 2017. Isotopic determination of the trophic ecology of a ubiquitous key species – The crab *Liocarcinus depurator* (Brachyura: Portunidae). *Estuar. Coast. Shelf Sci.* 191, 106–114. <https://doi.org/10.1016/j.ecss.2017.04.013>
- Carré, C., Meybeck, M., Esculier, F., 2017. The Water Framework Directive's “percentage of surface water bodies at good status”: unveiling the hidden side of a “hyperindicator.” *Ecol. Indic.* 78, 371–380. <https://doi.org/10.1016/j.ecolind.2017.03.021>
- Carvalho, L., Mackay, E.B., Cardoso, A.C., Baattrup-Pedersen, A., Birk, S., Blackstock, K.L., Borics, G., Borja, A., Feld, C.K., Ferreira, M.T., Globevnik, L., Grizzetti, B., Hendry, S., Hering, D., Kelly, M., Langaas, S., Meissner, K., Panagopoulos, Y., Penning, E., Rouillard, J., Sabater, S., Schmedtje, U., Spears, B.M., Venohr, M., van de Bund, W., Solheim, A.L., 2019. Protecting and restoring Europe's waters: An analysis of the future development needs of the Water Framework Directive. *Sci. Total Environ.* 658, 1228–1238.

<https://doi.org/10.1016/j.scitotenv.2018.12.255>

- Cicala, D., Calizza, E., Careddu, G., Fiorentino, F., Sporta Caputi, S., Rossi, L., Costantini, M. L., 2019. Spatial variation in the feeding strategies of Mediterranean fish: flatfish and mullet in the Gulf of Gaeta (Italy). *Aquat. Ecol.*, 1-13 (in press).  
<https://doi.org/10.1007/s10452-019-09706-3>
- Cole, M.L., Valiela, I., Kroeger, K.D., Tomasky, G.L., Cebrian, J., Wigand, C., McKinney, R.A., Grady, S.P., Carvalho da Silva, M.H., 2004. Assessment of a  $\delta^{15}\text{N}$  isotopic method to indicate anthropogenic eutrophication in aquatic ecosystems. *J. Environ. Qual.* 33, 124. <https://doi.org/10.2134/jeq2004.1240>
- Costantini, M.L., Carlino, P., Calizza, E., Careddu, G., Cicala, D., Caputi, S.S., Fiorentino, F., Rossi, L., 2018. The role of alien fish (the centrarchid *Micropterus salmoides*) in lake food webs highlighted by stable isotope analysis. *Freshw. Biol.* 63, 1130–1142. <https://doi.org/10.1111/fwb.13122>
- Costanzo, S. D., O'donohue, M. J., Dennison, W. C., Loneragan, N. R., Thomas, M. (2001). A new approach for detecting and mapping sewage impacts. *Mar. Pollut. Bull.*, 42, 149-156.
- Costanzo, S. D., Udy, J., Longstaff, B., Jones, A. (2005). Using nitrogen stable isotope ratios ( $\delta^{15}\text{N}$ ) of macroalgae to determine the effectiveness of sewage upgrades: changes in the extent of sewage plumes over four years in Moreton Bay, Australia. *Mar. Pollut. Bull.*, 51, 212-217.
- Dadar, Maryam, Adel, M., Saravi, H.N., Dadar, Mozhgan, 2016. A comparative study of trace metals in male and female Caspian kutum (*Rutilus frisii kutum*) from the southern basin of Caspian Sea. *Environ. Sci. Pollut. Res.* 23, 24540–24546.  
<https://doi.org/10.1007/s11356-016-6871-2>
- Dailer, M.L., Knox, R.S., Smith, J.E., Napier, M., Smith, C.M., 2010. Using  $\delta^{15}\text{N}$  values in algal tissue to map locations and potential sources of anthropogenic nutrient inputs on the island of Maui, Hawai'i, USA. *Mar. Pollut. Bull.* 60, 655–671.  
<https://doi.org/10.1016/j.marpolbul.2009.12.021>
- Dale, V.H., Beyeler, S.C., 2001. Challenges in the development and use of ecological indicators. *Ecol. Indic.* 1, 3–10. [https://doi.org/10.1016/S1470-160X\(01\)00003-6](https://doi.org/10.1016/S1470-160X(01)00003-6)
- DeBruyn, A. M., Rasmussen, J. B., 2002. Quantifying assimilation of sewage-derived organic matter by riverine benthos. *Ecol. Appl.*, 12, 511-520.
- de Mora, S., Sheikholeslami, M.R., Wyse, E., Azemard, S., Cassi, R., 2004. An assessment of metal contamination in coastal sediments of the Caspian Sea. *Mar. Pollut. Bull.* 48, 61–77. [https://doi.org/10.1016/S0025-326X\(03\)00285-6](https://doi.org/10.1016/S0025-326X(03)00285-6)
- Delpla, I., Jung, A.-V., Baures, E., Clement, M., Thomas, O., 2009. Impacts of climate change on surface water quality in relation to drinking water production. *Environ. Int.* 35, 1225–1233. <https://doi.org/10.1016/j.envint.2009.07.001>

- Derse, E., Knee, K. L., Wankel, S. D., Kendall, C., Berg, C. J., Paytan, A., 2007. Identifying sources of nitrogen to Hanalei Bay, Kauai, utilizing the nitrogen isotope signature of macroalgae. *Environ. Sci. Technol.* 41, 5217-5223.
- Dodds, W.K., Smith, V.H., 2016. Nitrogen, phosphorus, and eutrophication in streams. *Inland Waters* 6, 155–164. <https://doi.org/10.5268/IW-6.2.909>
- Dong, J., Yang, K., Li, S., Li, G., Song, L., 2014. Submerged vegetation removal promotes shift of dominant phytoplankton functional groups in a eutrophic lake. *J. Environ. Sci.* 26, 1699–1707. <https://doi.org/10.1016/j.jes.2014.06.010>
- Fry, B., Rogers, K., Barry, B., Barr, N., Dudley, B., 2011. Eutrophication indicators in the Hutt River Estuary, New Zealand. *N. Z. J. Mar. Freshw. Res.* 45, 665-677.
- Gartner, A., Lavery, P., Smit, A.J., 2002. Use of  $\delta^{15}\text{N}$  signatures of different functional forms of macroalgae and filter-feeders to reveal temporal and spatial patterns in sewage dispersal. *Mar. Ecol. Prog. Ser.* 235, 63–73. <https://doi.org/10.3354/meps235063>
- Glibert, P.M., 2017. Eutrophication, harmful algae and biodiversity — Challenging paradigms in a world of complex nutrient changes. *Mar. Pollut. Bull.* 124, 591–606. <https://doi.org/10.1016/j.marpolbul.2017.04.027>
- Greaver, T.L., Clark, C.M., Compton, J.E., Vallano, D., Talhelm, A.F., Weaver, C.P., Band, L.E., Baron, J.S., Davidson, E.A., Tague, C.L., Felker-Quinn, E., Lynch, J.A., Herrick, J.D., Liu, L., Goodale, C.L., Novak, K.J., Haeuber, R.A., 2016. Key ecological responses to nitrogen are altered by climate change. *Nat. Clim. Chang.* 6, 836–843. <https://doi.org/10.1038/nclimate3088>
- Hadwen, W.L., Bunn, S.E., Arthington, A.H., Mosisch, T.D., 2005. Within-lake detection of the effects of tourist activities in the littoral zone of oligotrophic dune lakes. *Aquat. Ecosyst. Health Manag.* 8, 159–173. <https://doi.org/10.1080/14634980590953211>
- Hayes, N.M., Vanni, M.J., Horgan, M.J., Renwick, W.H., 2015. Climate and land use interactively affect lake phytoplankton nutrient limitation status. *Ecology* 96, 392–402. <https://doi.org/10.1890/13-1840.1>
- Hosseini, S.M., Sobhanardakani, S., Navaei, M.B., Kariminasab, M., Aghilinejad, S.M., Regenstein, J.M., 2013. Metal content in caviar of wild Persian sturgeon from the southern Caspian Sea. *Environ. Sci. Pollut. Res.* 20, 5839–5843. <https://doi.org/10.1007/s11356-013-1598-9>
- Howarth, R.W., 2008. Coastal nitrogen pollution: A review of sources and trends globally and regionally. *Harmful Algae* 8, 14–20. <https://doi.org/10.1016/j.hal.2008.08.015>
- Irankehah, S., Soudi, M.R., Gharavi, S., 2016. Ex situ study of *Enterococcus faecalis* survival in the recreational waters of the southern coast of the Caspian Sea. *Iran J. Microbiol.* 8, 101–107.



ISTAT, 2018. <http://demo.istat.it/pop2018/index.html>. Accessed 28/06/2019

Jelodar, A.H., Rad, H.A., Navaiynia, B., Zazouli, M.A., 2012. Heavy metal ions adsorption by suspended particle and sediment of the Chalus River, Iran. *Afr. J. Biotechnol.* 11, 628-634–634. <https://doi.org/10.5897/AJB09.902>

Jona-Lasinio, G., Costantini, M.L., Calizza, E., Pollice, A., Bentivoglio, F., Orlandi, L., Careddu, G., Rossi, L., 2015. Stable isotope-based statistical tools as ecological indicator of pollution sources in Mediterranean transitional water ecosystems. *Ecol. Indic.* 55, 23–31. <https://doi.org/10.1016/j.ecolind.2015.03.006>

Jones, A.B., O'Donohue, M.J., Udy, J., Dennison, W.C., 2001. Assessing ecological impacts of shrimp and sewage effluent: biological indicators with standard water quality analyses. *Estuar. Coast. Shelf Sci.* 52, 91–109. <https://doi.org/10.1006/ecss.2000.0729>

Jones, R.I., King, L., Dent, M.M., Maberly, S.C., Gibson, C.E., 2004. Nitrogen stable isotope ratios in surface sediments, epilithon and macrophytes from upland lakes with differing nutrient status. *Freshw. Biol.* 49, 382–391. <https://doi.org/10.1111/j.1365-2427.2004.01194.x>

Kaminski, H.L., Fry, B., Warnken, J., Pitt, K.A., 2018. Stable isotopes demonstrate the effectiveness of a tidally-staged sewage release system. *Mar. Pollut. Bull.* 133, 233–239. <https://doi.org/10.1016/j.marpolbul.2018.05.020>

Katzenberg, MA (2008). Stable Isotope Analysis: A Tool for Studying Past Diet, Demography, and Life History, in M. A. Katzenberg, A. L. Grauer (Eds.), 2008. *Biological Anthropology of the Human Skeleton*, Wiley-Liss, pp. 305-327

Kendall, C., Elliot, E. M., Wankel, S. D., 2007. Tracing anthropogenic inputs of nitrogen to ecosystems. In Michener, R. H., Lajtha, K. (Eds.) *Stable isotopes in Ecology and Environmental Science*, Blackwell Publishing, pp. 375-449

Kosten, S., Lacerot, G., Jeppesen, E., da Motta Marques, D., van Nes, E.H., Mazzeo, N., Scheffer, M., 2009. Effects of submerged vegetation on water clarity across climates. *Ecosystems* 12, 1117–1129. <https://doi.org/10.1007/s10021-009-9277-x>

Lapointe, B.E., Bedford, B.J., 2007. Drift rhodophyte blooms emerge in Lee County, Florida, USA: evidence of escalating coastal eutrophication. *Harmful Algae* 6, 421-437.

Le Moal, M., Gascuel-Oudou, C., Ménesguen, A., Souchon, Y., Étrillard, C., Levain, A., Moatar, F., Pannard, A., Souchu, P., Lefebvre, A., Pinay, G., 2019. Eutrophication: a new wine in an old bottle? *Sci. Total Environ.* 651, 1–11. <https://doi.org/10.1016/j.scitotenv.2018.09.139>

- Maberly, S.C., King, L., Dent, M.M., Jones, R.I., Gibson, C.E., 2002. Nutrient limitation of phytoplankton and periphyton growth in upland lakes. *Freshw. Biol.* 47, 2136–2152. <https://doi.org/10.1046/j.1365-2427.2002.00962.x>
- Mastrantuono, L., Mancinelli, T., 2005. Littoral invertebrates associated with aquatic plants and bioassessment of ecological status in Lake Bracciano (Central Italy). *J. Limnol.* 64, 43–53. <https://doi.org/10.4081/jlimnol.2005.43>
- Mastrantuono, L., Solimini, A.G., Nöges, P., Bazzanti, M., 2008. Plant-associated invertebrates and hydrological balance in the large volcanic Lake Bracciano (Central Italy) during two years with different water levels, in: Nöges, T., Eckmann, R., Kangur, K., Nöges, P., Reinart, A., Roll, G., Simola, H., Viljanen, M. (Eds.), *European Large Lakes Ecosystem Changes and Their Ecological and Socioeconomic Impacts, Developments in Hydrobiology*. Springer Netherlands, pp. 143– 152. [https://doi.org/10.1007/978-1-4020-8379-2\\_17](https://doi.org/10.1007/978-1-4020-8379-2_17)
- Orlandi, L., Bentivoglio, F., Carlino, P., Calizza, E., Rossi, D., Costantini, M.L., Rossi, L., 2014.  $\delta^{15}\text{N}$  variation in *Ulva lactuca* as a proxy for anthropogenic nitrogen inputs in coastal areas of Gulf of Gaeta (Mediterranean Sea). *Mar. Pollut. Bull.* 84, 76–82. <https://doi.org/10.1016/j.marpolbul.2014.05.036>
- Orlandi, L., Calizza, E., Careddu, G., Carlino, P., Costantini, M.L., Rossi, L., 2017. The effects of nitrogen pollutants on the isotopic signal ( $\delta^{15}\text{N}$ ) of *Ulva lactuca*: Microcosm experiments. *Mar. Pollut. Bull.* 115, 429–435. <https://doi.org/10.1016/j.marpolbul.2016.12.051>
- Paerl, H.W., 2017. Controlling cyanobacterial harmful blooms in freshwater ecosystems. *Microb. Biotechnol.* 10, 1106–1110. <https://doi.org/10.1111/1751-7915.12725>
- Paerl, H.W., Hall, N.S., Peierls, B.L., Rossignol, K.L., 2014. Evolving paradigms and challenges in estuarine and coastal eutrophication dynamics in a culturally and climatically stressed world. *Estuaries Coasts* 37, 243–258. <https://doi.org/10.1007/s12237-014-9773-x>
- Paerl, H.W., Gardner, W.S., Havens, K.E., Joyner, A.R., McCarthy, M.J., Newell, S.E., Qin, B., Scott, J.T., 2016. Mitigating cyanobacterial harmful algal blooms in aquatic ecosystems impacted by climate change and anthropogenic nutrients. *Harmful Algae*, 54, 213–222. <https://doi.org/10.1016/j.hal.2015.09.009>
- Pastor, A., Riera, J.L., Peipoch, M., Cañas, L., Ribot, M., Gacia, E., Martí, E., Sabater, F., 2014. Temporal variability of Nitrogen stable isotopes in primary uptake compartments in four streams differing in human impacts. *Environ. Sci. Technol.* 48, 6612–6619. <https://doi.org/10.1021/es405493k>
- Pimentel, D., Berger, B., Filiberto, D., Newton, M., Wolfe, B., Karabinakis, E., Clark, S., Poon, E., Abbett, E., Nandagopal, S., 2004. Water resources: agricultural and environmental issues. *BioScience* 54, 909–918. <https://doi.org/10.1641/0006-123>

- Rossi, D., Romano, E., Guyennon, N., Rainaldi, M., Ghergo, S., Mecali, A., Parrone, D., Taviani, S., Scala, A., Perugini, E., 2019. The present state of Lake Bracciano: hope and despair. *Rend. Fis. Acc. Lincei* 30, 83–91. <https://doi.org/10.1007/s12210-018-0733-4>
- Rossi, L., Calizza, E., Careddu, G., Rossi, D., Orlandi, L., Jona-Lasinio, G., Aguzzi, L., Costantini, M.L., 2018. Space-time monitoring of coastal pollution in the Gulf of Gaeta, Italy, using  $\delta^{15}\text{N}$  values of *Ulva lactuca*, landscape hydromorphology, and Bayesian Kriging modelling. *Mar. Pollut. Bull.* 126, 479–487. <https://doi.org/10.1016/j.marpolbul.2017.11.063>
- Sadeghi, R., Zarkami, R., Sabetraftar, K., Van Damme, P., 2013. Application of genetic algorithm and greedy stepwise to select input variables in classification tree models for the prediction of habitat requirements of *Azolla filiculoides* (Lam.) in Anzali wetland, Iran. *Ecol. Modell.* 251, 44–53. <https://doi.org/10.1016/j.ecolmodel.2012.12.010>
- Sadeghi, R., Zarkami, R., Van Damme, P., 2017. Analyzing the occurrence of an invasive aquatic fern in wetland using data-driven and multivariate techniques. *Wetl. Ecol. Manag.* 25, 485–500. <https://doi.org/10.1007/s11273-017-9530-6>
- Smith, V. H., 2003 Eutrophication of freshwater and coastal marine ecosystems a global problem. *Environ. Sci. Poll. Res.*, 10, pp. 126-139
- Sohrabi, T., Ismail, A., Nabavi, M.B., 2010. Distribution and normalization of some metals in surface sediments from South Caspian Sea. *Bull. Environ. Contam. Toxicol.* 85, 502–508. <https://doi.org/10.1007/s00128-010-0112-z>
- Spinoni, J., Vogt, J. V., Naumann, G., Barbosa, P., Dosio, A., 2018. Will drought events become more frequent and severe in Europe?. *Int. J. Climatol.* 38, 1718-1736.
- Sulzman, E. W. (2007). Stable isotope chemistry and measurement: a primer. In: Michener, R., Lajtha, K. (Eds.) *Stable isotopes in ecology and environmental science*. Blackwell Publishing, pp. 1-18
- Taviani, S., Henriksen, H.J., 2015. The application of a groundwater/surface-water model to test the vulnerability of Bracciano Lake (near Rome, Italy) to climatic and water-use stresses. *Hydrogeol. J.* 23, 1481–1498. <https://doi.org/10.1007/s10040-015-1271-0>
- Troia, A., Azzella, M.M., 2013. *Isoëtes sabatina* (IsoëtaceaeLycopodiophyta), a new aquatic species from central Italy. *Plant Biosyst.* 147, 1052–1058. <https://doi.org/10.1080/11263504.2013.782902>
- van Vliet, M.T.H., Zwolsman, J.J.G., 2008. Impact of summer droughts on the water quality of the Meuse river. *J. Hydrol.* 353, 1–17. <https://doi.org/10.1016/j.jhydrol.2008.01.001>

- Vinçon-Leite, B., Casenave, C., 2019. Modelling eutrophication in lake ecosystems: A review. *Sci. Total Environm.* 651, 2985–3001.  
<https://doi.org/10.1016/j.scitotenv.2018.09.320>
- Vörösmarty, C.J., McIntyre, P.B., Gessner, M.O., Dudgeon, D., Prusevich, A., Green, P., Glidden, S., Bunn, S.E., Sullivan, C.A., Liermann, C.R., Davies, P.M., 2010. Global threats to human water security and river biodiversity. *Nature* 467, 555–561.  
<https://doi.org/10.1038/nature09440>
- Voulvoulis, N., Arpon, K.D., Giakoumis, T., 2017. The EU Water Framework Directive: From great expectations to problems with implementation. *Sci. Total Environm.* 575, 358–366. <https://doi.org/10.1016/j.scitotenv.2016.09.228>
- Wang, Y., Liu, D., Richard, P., Di, B., 2016. Selection of effective macroalgal species and tracing nitrogen sources on the different part of Yantai coast, China indicated by macroalgal  $\delta^{15}\text{N}$  values. *Sci. Total Environm.* 542, 306–314.  
<https://doi.org/10.1016/j.scitotenv.2015.10.059>
- Xu, H., Paerl, H.W., Qin, B., Zhu, G., Gao, G., 2010. Nitrogen and phosphorus inputs control phytoplankton growth in eutrophic Lake Taihu, China. *Limnol. Oceanogr.* 55, 420–432. <https://doi.org/10.4319/lo.2010.55.1.0420>
- Yao, X., Zhang, Y., Zhang, L., Zhou, Y., 2018. A bibliometric review of nitrogen research in eutrophic lakes and reservoirs. *J. Environm. Sci.* 66, 274–285.  
<https://doi.org/10.1016/j.jes.2016.10.022>

